A COMPREHENSIVE STUDY ON CYCLOIRIDATED 1-ARYLALKYLAMINE AND IMINE COMPLEXES

NANYANG TECHNOLOGICAL UNIVERSITY
SINGAPORE

THE CHEMISTRY OF CYCLOMETALATION
A COMPREHENSIVE STUDY ON CYCLOIRIDATED 1-ARYLALKYLAMINE AND IMINE COMPLEXES

CHEN HOUGUANG JEREMY

2018

CHEN HOUGUANG JEREMY

SCHOOL OF PHYSICAL AND MATHEMATICAL SCIENCES

2018

The Chemistry of Cyclometalation

A Comprehensive Study on Cycloiridated 1-Arylalkylamine and Imine Complexes

Chen Houguang Jeremy
(*B.Sc.(Hon), Nanyang Technological University*)

School of Physical and Mathematical Sciences

A thesis submitted to the Nanyang Technological University
in partial fulfillment of the requirement for the degree of
Doctor of Philosophy

2018

ABSTRACT

As fundamental ligand frameworks within the field of cyclometalation, the 1-arylalkylamine and imine motifs have a widespread presence as cyclometalating ligands for an extensive number of transition metal elements. In the thesis, we investigate the outcome of cycloiridation of various 1-arylalkylamine and imine ligands with $[IrCp^*Cl_2]_2$. A good balance of steric factors within the organic scaffold was found to be vital for the formation and stability of *amino*-derived iridacycles. While excessive steric hindrance would lead to numerous side reactions affording an assortment of byproducts, the lack of steric bulk within the amine ligands would lead to an internal oxidation to its imine functionality within the cyclometalated ring. Investigations into the failed cyclization procedure revealed a consistent competing pathway leading to either a strained ring system or an iminium species. The postulated intermediates can then readily undergo hydrolysis to provide a *N*-dealkylated amine moiety and a carbonyl compound. Optically-active cycloiridated complexes from successful direct *ortho*-metalation procedures were characterized for its conformational lock and evaluated for its efficiency in the catalytic asymmetric hydrogen transfer reaction. Lastly, we examine the crystallographic structures of the synthesized iridacycles to gain insights into their bonding.

ACKNOWLEDGEMENTS

As I progress to the next stage of life after Ph.D. studies, feelings of sweet and bitterness came as I recall the seven years I had (including two and a half years from my undergraduate days) in this very group. The journey has been awesome, and there are many people whom I must thank for their support and encouragements over the years.

First and foremost, I would like to express my gratitude to my supervisor, Professor Leung Pak-Hing. Without his support, whether research or otherwise, I would have not come so far to where I am today. His motivation, patience and cheerfulness has kept me going strong over the ups and downs in the course of my Ph.D. studies. I also truly appreciate the scientific freedom he has granted to me, which left me with a satisfying and enriching learning experience.

My gratitude also extends to my co-supervisor, Dr. Sumod A. Pullarkat, for his continual support, guidance, encouragement and patience with me throughout these years. His door was always open to us, providing much support, and the occasional chats, whenever we needed it. Your advice, whether research or otherwise, will always be invaluable to me.

Next, I would like to specifically show my gratitude to Jonathan Wong, who have shared my successes, failures and frustrations over research and life. Your advice and assistance over these years has been extremely invaluable. I will also always recall our extremely fun early days when we took over from each other between lessons and having no idea what experiment we are conducting in the lab.

I would also like to extend my appreciation to my three mentors who have taught me many things in the research lab: Dr. Jeanette Yap, for her freedom to Jonathan and me to explore anything we wanted; Dr. Xu Chang, for the fundamental lab skills she has taught me; and Dr. Chen Ke, for the small little things we can do to improve our skills.

Next, I would like to thank my former and current lab mates – Dr. Yang Xiangyuan, Dr. Kennard Gan, Dr. Li Binbin, Wenjia, Esther, Christina, Xirui, Sadeer, Wee Shan, László, David and Ce Qing – for their great company, warmest friendship and unselfish assistance in one way or another. I also cannot forget Dr. Ng Yong Xiang, Dr. Feny, Melody, Odelia and Jia Sheng for their company, encouragement and days of laughter.

Special mention goes to my students – Ronald, Jeffery, Meldon and Yuet Wan – for their friendship, patience, encouragements and support to my work. Whilst most of your projects did not proceed very well under me, the times spent with you guys (and gal) was extremely fun and memorable. All of you have been great friends, and lab without any of you would be unbearable. I also cannot forget my six poly kids – Aisyah, Natasha, Sharifah, Galvin, Hong Ming and Jun Cong – whom, together with Jonathan, shared many great moments inside and outside lab in the early days of my research life.

My appreciation is also extended to Ai Hua from the Teaching Lab, Dr. Li Yongxin, Ee Ling, Keith, Joanne and Wen Wei from the Central Facilities Lab, Wee Jian and Wilson from the Chemical Store, as well as Celine, Lynette, Susan, Clemence, Janice Low, David, Yean Chin and Si Yun from the administrative offices, for their assistance in teaching, technical, logistical and administrative support respectively.

My deepest gratitude goes to Nanyang Technological University and the School of Physical and Mathematical Sciences for their utmost support into our research and scholarship for my Ph.D. studies.

Special thanks to Dr. Mihaiela Stuparu for allowing me to be Chief Teaching Assistant for two semesters which have provided me with learning opportunities to coordinate the lab course with you. It has also been an extremely fun, although sometimes stressful, time working with the laboratory staff, teaching assistants and students. To the CBC graduating batch of 2016/2017 and 2017/2018, I thank all of you in making my teaching journey an enjoyable one.

To my family, I would like to thank them, especially my parents, for their endless support, encouragement, confidence and trust in me for the past 30 years. Without them, the completion of my study would not be possible.

Last, but not least, I would like to thank my good friends – Emily, Lay Peng, Kun Tat, Peiwen, Wen Jun, Wen Xiang, Yihuan and Zhen Jie – for their listening ear, especially over the constant failures of my research work, encouragements, support and invaluable advice over these years.

Chen Houguang Jeremy

Nanyang Technological University, 2018

TABLE OF CONTENTS

NOMENCLATURE

The nomenclature used throughout the thesis conforms to the format adopted by Chemical Abstracts (Chemical Abstracts, 13th Collective Index, Index Guide, 1992-1996).

ABBREVIATIONS AND SYMBOLS

Ac	acetyl
acac	acetylacetonate
Anal.	combustion elemental analysis
Ar	aryl group
b.p.	boiling point
br	broad
Bu	butyl
ca.	about (Latin: *circa*)
calcd.	calculated
$CDCl_3$	chloroform-*d*
CD_2Cl_2	dichloromethane-d_2
cod	1,5-cyclooctadiene
conc.	concentrated
conversn	conversion
Cp	cyclopentadienyl
Cp*	1,2,3,4,5-pentamethylcyclopentadienyl
Cy	cyclohexyl

de	diastereomeric excess
dm	decimeter
d	doublet
deg	degree(s)
dmso	dimethyl sulfoxide
E	donor moiety
ee	enantiomeric excess
equiv.	equivalence
ESI	electrospray ionization
Et	ethyl
etc.	and the rest (Latin: *et cetera*)
g	gram(s)
h	hour(s)
Hz	hertz
i.e.	that is (Latin: *id est*)
^{i}Pr	isopropyl
L	neutral ligand
M	metal
m	multiplet
m.p.	melting point
m	*meta*
Me	methyl
Mes	mesityl

Mes*	supermesityl (^{t}Bu$_3$(C$_6$H$_2$))
min	minute(s)
mL	milliliter
mmol	millimole
n	straight chain
NMR	nuclear magnetic resonance
NOE	nuclear overhauser effect
NOESY	nuclear overhauser effect spectroscopy
o	*ortho*
p	*para*
Ph	phenyl
Piv	pivalyl (^{t}BuC(=O))
Py	pyridine
ppm	parts per million
q	quartet
R	substituent
R	right absolute configuration (Latin: *rectus*)
rac	racemic
ROESY	rotating frame nuclear overhauser effect spectroscopy
S	left absolute configuration (Latin: *sinister*)
s	singlet
sep	septet
t	triplet

tfa	trifluoroacetic acid
^{t}Bu	*tert*-butyl
temp	temperature
thf	tetrahydrofuran
UV	ultraviolet
X	anionic ligand
Å	ångström
δ	chemical shift
L	left (Latin: *laevus*)
κ^n	polydentate chelate with *n* ligating atoms attached to a coordination center
μ	bridging
°	degree(s)
°C	degrees Celsius / degrees centigrade
$[\alpha]_D$	specific rotation measured at sodium D line (589 nm)

LIST OF FIGURES

CHAPTER 1

CHAPTER 2

CHAPTER 3

CHAPTER 4

LIST OF SCHEMES

CHAPTER 1

CHAPTER 2

CHAPTER 3

LIST OF TABLES

CHAPTER 1

CHAPTER 2

CHAPTER 3

CHAPTER 4

REPRODUCTION OF CONTENT

- Content from **CHAPTER 3** and its relevant experimental data was adapted with permission from Chen, H. J.; Teo, R. H. X.; Li, Y.; Pullarkat, S. A. and Leung, P.-H. *Organometallics* **2018**, *37*, 99-106 (DOI: 10.1021/acs.organomet.7b00760). Copyright © 2018 American Chemical Society).

CHAPTER 1
The Chemistry of Cyclometalation

ABSTRACT

The formal definition to cyclometalation and its related complexes are presented. The chapter then concentrates onto ligand-directed cyclometalation and outlines it principles, concepts and history. Recent developments into the cyclometalation chemistry of palladium, platinum, ruthenium and iridium will also be discussed. Delving into the synthetic utility of these species, we will look into their roles as building blocks, resolving agents, reactive intermediates and catalysts. The chapter will end with research interest of the group, leading to the research objectives of the thesis.

Keywords: Cyclometalation / *ortho*-Metalation / Metallacycles / Cyclometalated Complexes / Coordination Complexes

1.1 The Field of Cyclometalation

Cyclometalation, in its simplest sense, is the cyclization of a metal center to provide a heterocyclic ring with at least one metal center within the system. The definition is broad, with cyclometalation chemists belonging to three main schools of thought – carbometallacycles, ligand-directed metallacycles and donor-type metallacycles.

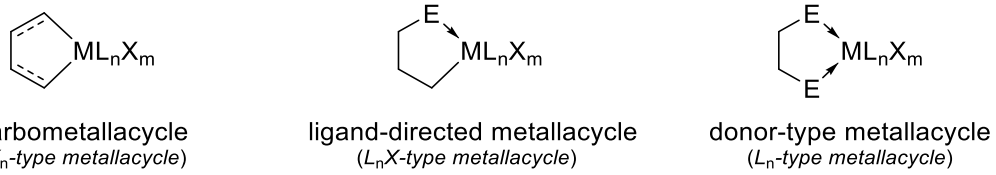

carbometallacycle (*X*$_n$*-type metallacycle*) | ligand-directed metallacycle (*L*$_n$*X-type metallacycle*) | donor-type metallacycle (*L*$_n$*-type metallacycle*)

Figure 1.1. Classes of five-membered bidentate cyclometalated complexes (M = metal center, E = donor moiety, L = neutral ligand, X = anionic ligand).

Carbometallacycle is a X_n-type cyclometalated complex in which the metal center is directly bonded to at least two anionic carbon atoms within a ring. The compound is generally produced from the oxidative coupling of two π ligands, commonly alkenes or alkynes, to the metal center. In this process, the metal transfers its electrons to the π^* orbital of the multiple bond, effectively cleaving the π bond between the atoms of the π ligands and forming a new σ bond between the coordinated hydrocarbons to provide the metallacycle.

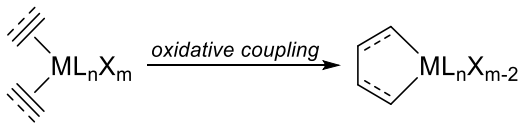

Scheme 1.1. Formation of a five-membered carbometallacycle *via* oxidative coupling mechanism.

The L_nX-type ligand-directed metallacycle involves the metal atom within the heterocyclic complex to be directly bonded to at least one neutral donor ligand and an anionic carbon atom within the same cyclic system. As indicative from its term, the ligand directs the metal center to its point of activation (based on proximity) prior to cyclization. Several modes of activation exist, and these will be covered in greater detail in subsequent sections.

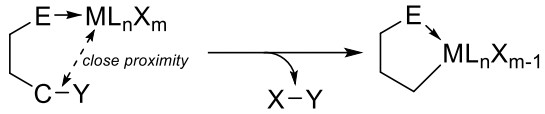

Scheme 1.2. Formation of a five-membered ligand-directed metallacycle.

Lastly, the L_n-type donor-type metallacycle presents the simplest access to these cyclometalated systems. In these compounds, the metal center is datively bonded to at least two adjoining neutral donor ligands affording a metallacyclic complex upon coordination.

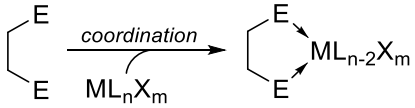

Scheme 1.3. Formation of a five-membered donor-type metallacycle *via* coordination.

The diverse classification of cyclometalation and its associated concepts brings much challenge upon discussion of the entire field. As such, the thesis will narrow down the field of study and attention will be placed on ligand-directed metallacycles. It should also be noted, from this point, that all terminologies relating to *cyclometalation* would only refer to *ligand-directed cyclometalation*.

1.2 Classification of Cyclometalated Complexes

Cyclometalated complexes can be generalized into two main categories – bidentate *LX*-type metallacycles and terdentate L_2X pincer-type complexes. Other modes of coordination also exist, but the two classes embody majority of these compounds.

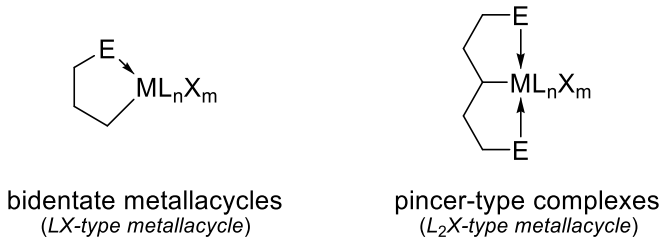

Figure 1.2. Two main classes of five-membered cyclometalated complexes.

The bidentate *LX*-type metallacycle is complexed by at least one set of *LX* ligand consisting of a neutral donor moiety and an anionic carbon center within the ring. The metallacyclic system can exist as monomers, dimers, bis-cyclometalated or tris-cyclometalated complexes. These species can also be found in neutral, cationic or anionic forms.

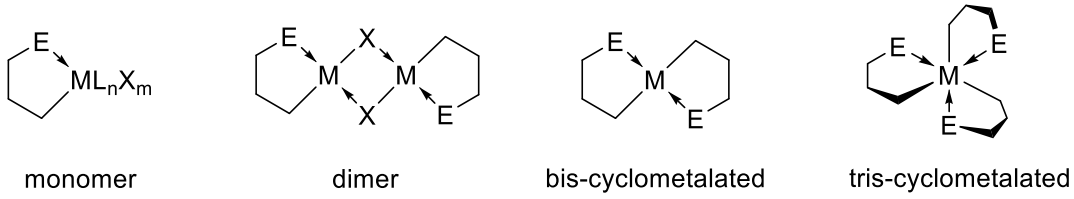

Figure 1.3. Types of five-membered bidentate *LX* cyclometalated complexes.

The L_2X pincer-type cyclometalated complexes can be identified by its characteristic terdentate *ECE* ligand motif in which its coordination mode to the metal center resembles a crab supporting the metal atom with its pincers. Depending on the nature of the metal, the species can exist as monomers or bis-cyclometalated complexes, although the former is more prevalent. Similar to its bidentate counterparts, the compounds can also exist in neutral, cationic or anionic forms.

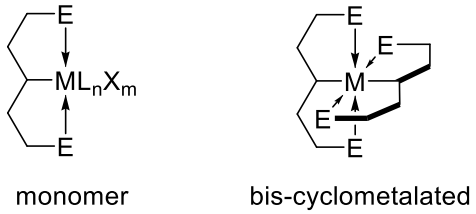

Figure 1.4. Types of five-membered terdentate L_2X pincer-type cyclometalated complexes.

1.3 Historical Overview

The development of cyclometalation chemistry was marked by several distinctive phases.

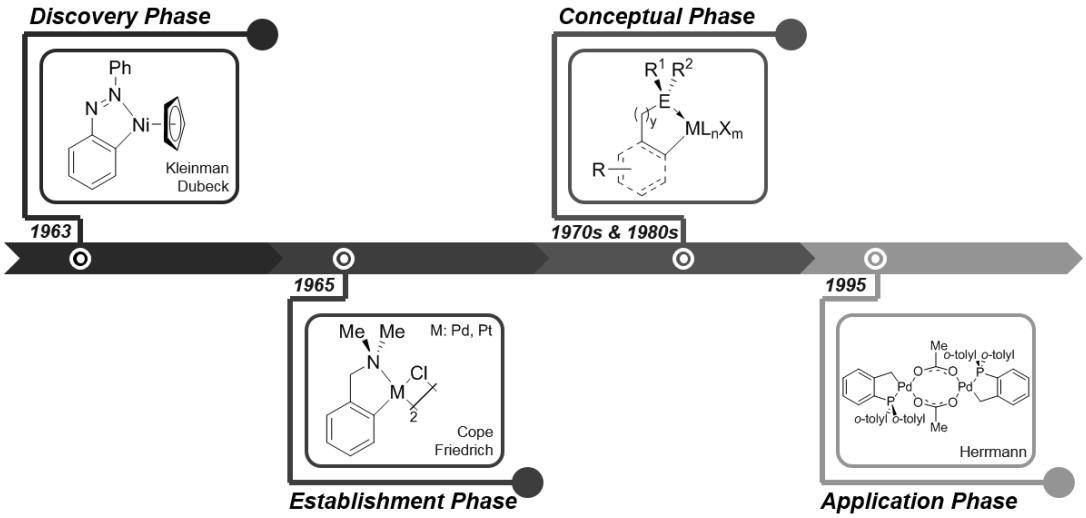

Figure 1.5. Milestones of cyclometalation chemistry.

The first phase – *discovery* – involved the first documented cyclometalated complex by Kleinman and Dubeck in 1963.[1] In the experiment, azobenzene and nickelocene were reacted to afford a diamagnetic air-stable five-membered *ortho*-metalated complex. At the time of publication, the metal center was believed to be coordinated to the N=N π bond instead of the lone electron pair at nitrogen. However, with the establishment of cyclometalation concepts years later, the structure was refined to its current form.[2]

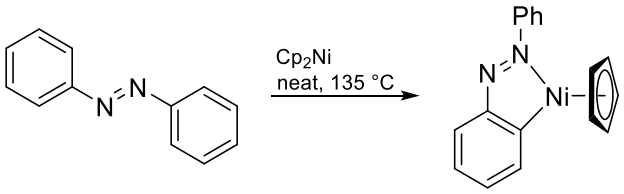

Scheme 1.4. First documented cyclometalation reaction.

The *establishment* phase affirmed the fundamental coordination modes of cyclometalated complexes. In an observation by Cope and Siekman in 1965, it was first suggested that the metallacycles generated from azobenzene and salts of palladium or platinum were coordinated to the metal center *via* the lone electron pair at the *azo* moiety (rather than the N=N π bond of the same functionality).[3]

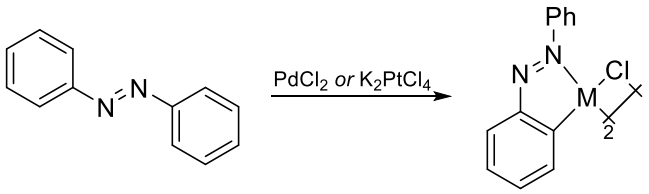

Scheme 1.5. Cyclometalation of azobenzene by palladium or platinum salts (M = Pd, Pt).

Basic framework to the concepts of cyclometalation were also laid with the expansion of scope to amine ligands during the same period. Cope and Friedrich performed numerous *ortho*-metalation reactions with benzylamine and its derivatives and determined several conditions for cyclometalation to be favorable.[4] These conditions included the need for substituted donor moiety, activated aromatic ring system and a five-centered transition state. It should, however, be noted that these limitations would slowly be overcome during the *conceptual* phase of cyclometalation chemistry.

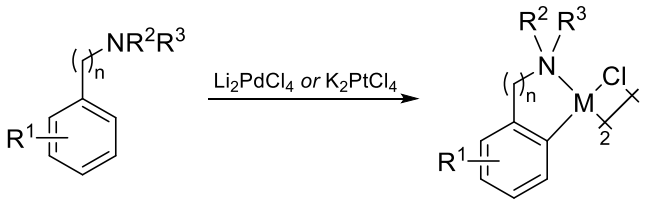

		Pd	Pt			Pd	Pt
n=1	R^1=H, R^2=R^3=Me	95%	28%	n=1	R^1=4-OMe, R^2=R^3=Me	50%	-
n=1	R^1=R^2=H, R^3=Me	0%	0%	n=1	R^1=3,5-OMe, R^2=R^3=Me	66%	-
n=1	R^1=R^2=R^3=H	0%	0%	n=2	R^1=H, R^2=R^3=Me	0%	-
n=1	R^1=4-NO_2, R^2=R^3=Me	0%	0%	n=3	R^1=H, R^2=R^3=Me	0%	-

Scheme 1.6. Cyclometalation of benzylamine and its derivatives by palladium or platinum salts (M = Pd, Pt).

The groundwork laid by Cope and Friedrich led to an explosion of research dedicated to the chemistry of cyclometalation in the 1970s and 1980s – the *conceptual* phase. Works into the field expanded the scope of cyclometalation to other transition metal elements and ligand motifs. These assisted in laying the principles of cyclometalation chemistry that is known today.

As the concepts of cyclometalation developed, the thirst for applications of these complexes begin to emerge. However, other than the optical resolution of pnictogenic compounds, the uses of metallacycles did not really take off until 1995 when Herrmann[5] developed a novel palladacycle that was robust for the catalytic Heck reaction. Since then, applications of cyclometalated complexes have expanded greatly with efforts dedicated to the fields of catalysis (as reactive intermediates[6] and as catalysts[7]), photoluminescence[8] and biomedical drug research[9].

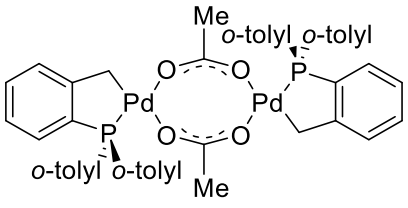

Figure 1.6. Herrmann catalyst.

1.4 Principles of Cyclometalation

The cyclometalation reaction is governed by two main sequential processes: (a) the coordination of the neutral donor ligand to the metal center, and (b) the intramolecular activation of the C–Y bond (Y = H or leaving group) directed by the coordinated species. In the first step, electron densities between the donor moiety and the metal center are redistributed to increase the propensity of the transition metal element to activate bonds. Furthermore, substituents near or at the donor atom compress the internal angles between neighboring groups bringing the metal center closer to the point of activation facilitating cyclization.[10] Thereafter, the second process takes over with the metal center activating the C–Y bond through one of the many mechanistic pathways of cyclometalation.

The success of a cyclometalation procedure depends on a series of electronic and steric factors. The overall process is now well-understood and involves all components within the cyclometalation reaction.

1.4.1 Effects of Metal Precursors in Cyclometalation

Since the first stage of the cyclometalation process involves the dative bonding of the neutral donor moiety to the metal center, the metal precursor must have a vacant site within the coordination sphere of the central atom prior to cyclometalation.[11] In addition, anionic ligands within the metal precursor must readily dissociate to give way to the carbanion moiety.[12] These criteria, thus, limit the classes of precursors[11] that can be utilized for cyclometalation to: (a) dimeric metal complexes that can exist as monomers in solution or upon coordination by the donor moiety, (b) metal complexes with labile ligands, and (c) "*-ate"* complexes in which the anionic ligand can be easily displaced by a neutral donor ligand.

Table 1.1. Classes of metal precursors for cyclometalation.

dimeric metal complexes[a]	**metal complexes with labile ligands**	***"-ate"* complexes**[b]
$[M(cod)Cl_2]_2$	$Ir(PPh_3)_2H_5$	M_2PdCl_4
$[MCp^*Cl_2]_2$	$PdCl_2(NCMe)_2$	M_2PtCl_4
$[RuCl_2(cymene)]_2$	$PtCl_2(SEt_2)_2$	M_3IrCl_6
	$Ru(dmso)_4Cl_2$	

[a]M = rhodium (Rh) and iridium (Ir). [b]M = lithium (Li), sodium (Na) and potassium (K).

1.4.2 Effects of Neutral Donor Ligands in Cyclometalation

In numerous instances prior to cyclometalation, a coordinated species with two units of the cyclometalating ligand is usually observed upon mixing of the said ligand with the metal precursor in solution. One of the neutral ligand pair then dissociates, providing a complex with a vacant coordination site, invoking the activation of the C–Y bond to provide the desired metallacycle.[12]

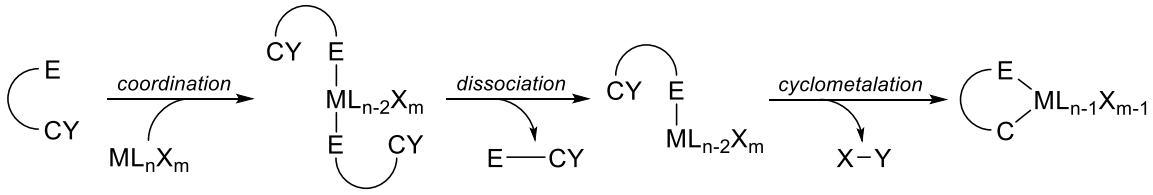

Scheme 1.7. Coordination modes prior to cyclometalation.

Differing donor heteroatoms and its substituents can impact cyclometalation due to differences in bonding character at the donor site. In an example, when the amine functionality of *N*,*N*-dimethylbenzylamine was replaced by its phosphine and arsine counterparts, the cyclometalated analogues could not be attained when reacted with [Na_2PdCl_4] under similar conditions.[13] The unsuccessful attempt was rationalized to be due to the inability of the doubly ligated neutral donors to discharge one of the cyclometalating ligands from the coordination sphere to provide a vacant site for *ortho*-metalation.

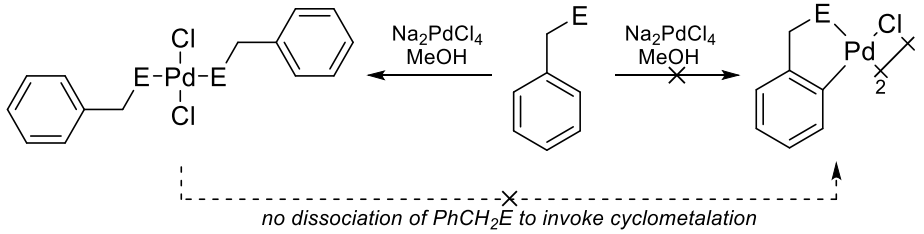

Scheme 1.8. Attempted cyclopalladation with dimethylbenzylphosphine and dimethylbenzylarsine (E = PMe_2, $ArMe_2$).

Substituents at the donor heteroatom can also either promote or hinder cyclometalation. In the case of amine donors, larger *N*-alkyl substituents were found to have weaker metal-ligand bond than that to its *N*-methyl counterpart.[14] The weakening of the coordination bond was postulated to be due to greater shielding of the lone electron pair

at the nitrogen atom by the substituents. It should also be noted that the propensity to cyclometalate decreases in order of tertiary, secondary and primary benzylamines.[3] A proposal for this observation involved the difficulty to dissociate a unit of the amine ligand from the bis-amine complex.[12] Since primary amines bind more strongly to the metal center (on steric grounds), it is less likely to dissociate and, thus, more inert towards cyclometalation. Phosphine ligands seemed to thrive when bulkier substituents were introduced.[15] It was postulated that the increased steric bulk expands the cone angle of the phosphine leading to a longer coordinate bond. This would allow the dissociation of a phosphine moiety from the bis-phosphine complex to effect the cyclometalation process.[11]

Generically, the probability of success in cyclometalation can be predicted from the principles of hard-soft acid-base (HSAB) theory.[16] As a general guide, hard donor ligands, such as amines and alkoxides, favor high-valent transition metal elements, whereas softer donor groups, in the case of phosphines and thioethers, have preference for low-valent electron-rich metal centers.[11] It should, however, be noted that the principles are only guidelines since hard-soft mismatches are not uncommon.[11]

1.4.3 Effects of the Carbon Nature in Cyclometalation

The nature of the carbon atom that is to be activated plays a significant role in cyclometalation. In general, it is widely accepted that the cyclometalation procedure has a preference for the activation of C_{sp2}–H bond than its sp^3-carbon counterpart.[17] This is surprising since the former bond is stronger than the latter due to greater *s* character. However, thermodynamic stability pushed for the stronger sp^2-carbon–metal bond due to its better orbital overlap between the sp^2-carbanion moiety and the metal center. Furthermore, kinetic considerations favored the unsaturated C=C bond for its more efficient coordinative ability to its aliphatic C–C bond counterpart.[18]

In the instance when activation of aliphatic hydrocarbons is observed, the ease of C–H bond activation of the saturated carbon atoms was found to decrease in the order of primary-, secondary- and tertiary-carbon centers on the basis of steric grounds.[19]

1.4.4 Effects of Chelate Ring Size in Cyclometalation

A quick review of literature on cyclometalation would reveal most cyclometalated systems existing in a five-membered configuration.[11, 20] Although metallacycles of other chelate ring sizes can be synthesized and isolated, it seemed that there is a tendency for cyclometalation to favor these five-membered systems when given a choice between several modes of activation. In an example, 8-ethylquinoline was treated with $Pd(OAc)_2$, and subsequently LiCl, to afford a five-membered palladacycle.[21] The result was surprising since primary carbon centers were known to be more readily metalated than secondary carbon centers. Similarly, structurally-analogous products were observed for the cycloplatination of di-*tert*-butyl(*o*-ethylphenyl)phosphine with *trans*-$[PtCl_2(NCPh)_2]_2$.[22]

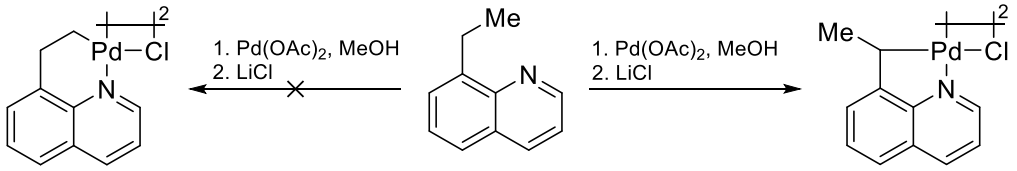

Scheme 1.9. Cyclopalladation of 8-ethylquinoline.

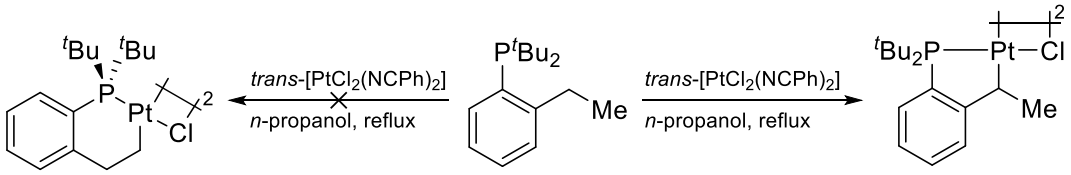

Scheme 1.10. Cycloplatination of di-*tert*-butyl(*o*-ethylphenyl)phosphine.

Computational studies disclosed smaller ring strain and significantly higher ring formation energies in five-membered cyclostannated systems compared to their six- and four-membered counterparts.[23] This could provide some insights into the regioselectivity of cyclometalation reactions.

Nonetheless, although prevalent in nature, it is difficult to unquestionably predict the resulting chelating ring size of the metallacycle when more than one mode of activation exists in the ligand framework.

1.4.5 Effects of Substituents on Non-Donor Group in Cyclometalation

Substituents along the expected organometallic ring can influence cyclometalation. As indicated earlier, these substituents could reduce the internal angles between adjacent groups to bring the metal center closer to the C–Y bond for easier activation. The phenomenon is known as Thorpe-Ingold effect or *gem*-dialkyl effect, and it mainly influences the formation of small ring systems.[10]

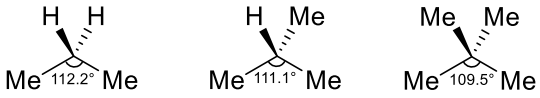

Figure 1.7. Thorpe-Ingold effect exemplified by substituted propane.

Its effects in cyclometalation can be illustrated in the *ortho*-palladation of benzylamine and its derivatives.[4, 24] When the *α*-position of *N*-methylbenzylamine was replaced with an alkyl group (R^1=Me *or* ^{t}Bu), the cyclometalation procedure proceeded affording its respective metallacycles, with the bulkier *tert*-butyl derivative attained in higher yields. On the other hand, less cyclopalladated complex were attained when the primary amine analogue (R^1=^{t}Bu, R^2=H) was utilized for the cyclization process. It is also worth recalling that the *ortho*-metalation procedure do not proceed if the ligands were benzylamine or *N*-methylbenzylamine.[4]

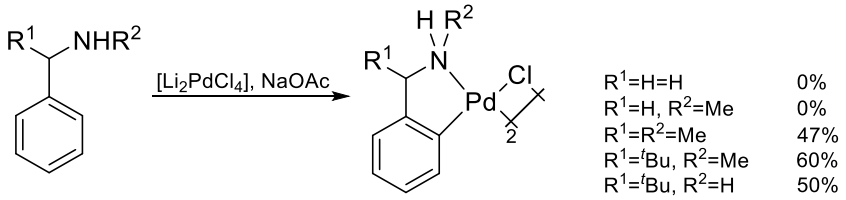

Scheme 1.11. Effect of substituents on cyclopalladation of benzylamine.

1.4.6 Effects of the C–Y Bond in Cyclometalation

Depending on the identity of Y within the ligand motif, the regioselectivity of the cyclometalation procedure can be affected.

When Y = H, C–H bond activation is generally dependent on the aforementioned principles. However, due to the complexity of the actual process, it is usually difficult to identify the factors that determine the regioselectivity within the cyclometalation reaction.[25]

On the other hand, when Y = leaving group (*i.e.* acetate, carbonate, halide, tosylate and triflate), the point of activation is usually regiospecific. The regioselectivity stems from the oxidative addition mechanism in which an electron-rich metal center inserts itself across a polarized bond. The functionality, thus, give rise to new possibilities to access synthetically-challenging and/or specific cyclometalated compounds.

1.4.7 Effects of Bases in Cyclometalation

In cases when Y = H, the cyclometalation procedure would depict a loss of proton from the ligand motif after cyclization. Depending on the metal precursor utilized for the protocol, the acidic byproducts could potentially affect the reaction, especially if the eliminated molecule is a strong acid. Base is, thus, typically added in most instances to overcome the issue.

Although some cyclometalation procedures have been shown to proceed in the absence of base, its necessity cannot be undermined in some cases. In one of the classic examples, the cyclopalladation of *N*,*N*-dimethylferrocenylmethylamine did not proceed in the absence of base.[26] This was surprising since the cyclopentadienyl ring within the ferrocene moiety was known to be more susceptible to electrophilic attack by the palladium center than its benzene counterpart.[27] Nonetheless, the cyclopalladated complex could be attained when sodium acetate was introduced into the reaction.[28] The role of the base in the reaction was further enhanced when Sokolov reported the synthesis of the same complex in enantioenriched forms with the salt of *N*-acetyl-L-valine.[29]

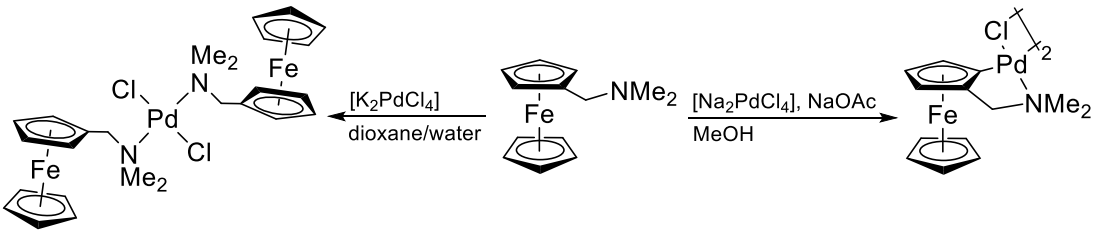

Scheme 1.12. Effect of base on cyclopalladation of *N*,*N*-dimethylferrocenylmethylamine.

Of the many bases that were utilized in cyclometalation, a single type of base stood out undoubtedly in its entirety – the *carboxylate* (RCO_2–) moiety. Well-known members of the family include the acetate (R = Me), trifloroacetic (R = CF_3) and pivalate (R = ^{t}Bu) anions and they are shown to initiate the ring-closing procedure through deprotonation of the activated C–H bond *via* a six-membered transition state upon coordination to a metal center.[30] Theoretical calculations have also been performed and they supported the dual role of the anion.[31]

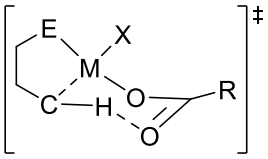

Figure 1.8. Proposed transition state for the carboxylate-assisted cyclometalation reaction.

1.5 Mechanisms of Cyclometalation Reactions

The activation of the C–Y bond is central to the formation of cyclometalated complexes. Three generally-accepted activation modes have been identified – *oxidative addition*, *electrophilic bond activation* and *σ-bond metathesis* – although the dividing line between these processes are usually not clear. There also exist two other mechanisms – *transmetallation* and *transcyclometalation* – although these processes are considered as special cases in the formation of cyclometalated complexes since they require a secondary metallacycle for the reaction.

1.5.1 Oxidative Addition

To put it simply, the oxidative addition of the C–Y bond by the metal involves the latter inserting itself across the C–Y σ bond. For the process to be successful, the metal must have an empty σ-type molecular orbital and an electron-rich high-energy molecular orbital in which electrons can be donated to the σ^* orbital of C–Y bond to initiate the bond cleavage process.[32] The pathway is, thus, nucleophilic and is favored by electron-rich metal centers.

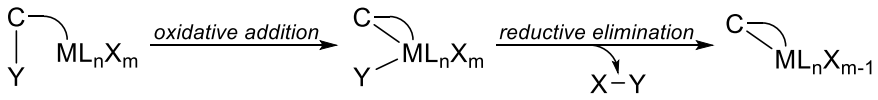

Scheme 1.13. Oxidative addition mechanism for cyclometalation.

In cases when Y = H, a metal-hydride (M–H) bond would be formed within the complex. The oxidation state of the metal center will also increase by two units, although reductive elimination (of molecule X–Y) may quickly proceed to return the metal center back to its original valency. Nonetheless, if the metal hydride intermediate could be isolated or detected in spectroscopic studies, one should be able to determine the process to undergo the oxidative addition mechanism.

In the instances when C–H bond activation could not be attained or is inaccessible, the C–Y (Y = leaving group; *i.e.* acetate, carbonate, halide, tosylate and triflate) moiety could replace the C–H bond for oxidative addition. Moreover, due to their electrophilic nature, the cyclometalation reaction is regioselective with the activation of the bond occurring only at the functionalized position.

1.5.2 Electrophilic Bond Activation

Under the electrophilic bond activation mechanistic pathway, cyclometalation is assisted by coordinated leaving groups or free bases in the reaction mixture.[12] Within this mechanism, metal hydride complexes do not form at any stage in this pathway. As such, there is no change to the oxidation number of the metal center upon cyclometalation.

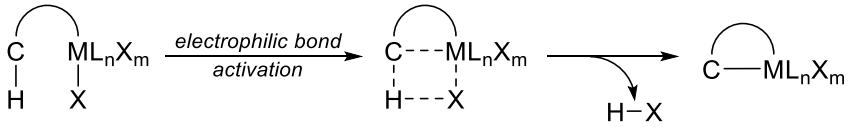

Scheme 1.14. General electrophilic bond activation mechanism for cyclometalation.

Two similar, but distinct, mechanisms are operated under this category – *electrophilic aromatic substitution* and *agostic C–H bond activation*.

The electrophilic aromatic substitution mechanism resembles its organic model. A Wheland intermediate is formed from the attack of the unsaturated bond to the electrophilic metal center. The close proximity of the anionic ligand and the proton on the arenium ion then allows an attack on the latter by the former to eliminate H–X from the molecule. It is also worth mentioning that a free base can deprotonate the said proton since aromaticity is the driving force for the reaction.

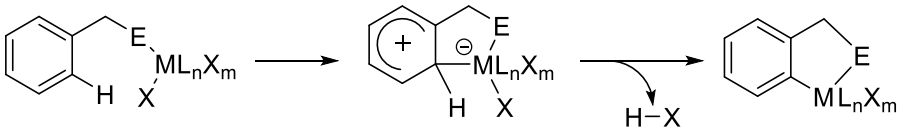

Scheme 1.15. Activation by electrophilic aromatic substitution.

The agostic C–H bond activation model, on the other hand, predicts agostic interactions from the initial phase of the mechanism.[30-31] The approach of the metal center to the C–H bond elongates the σ bond. Simultaneously, the anionic ligand or free base interacts with the proton of the extended C–H bond until it is sufficiently basic to deprotonate the latter, eliminating H–X from the molecule to yield the metallacycle.

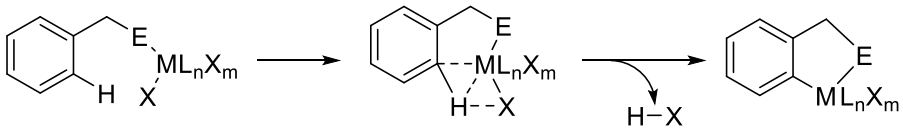

Scheme 1.16. Activation by agostic C–H bond activation.

A recent computation work by Harrison and Nielson involving more complex agostic interactions – *syndetic interactions* – should also be mentioned.[33] In their study for the cyclopalladation of 1-tetralone oxime with $[PdCl_4]^{2-}$, they discovered the donation of electron density from the C–H σ bond to the metal involved the *cis* and *trans* Pd–Cl σ* anti-bonding molecular orbitals instead of the metal *d* orbitals. In addition, the π-electron cloud of the aromatic system further enhanced the agostic donation to the same anti-bonding orbitals. Two smaller back-donation from the metal center to the C–H σ* orbitals were also observed.

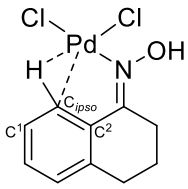

Table 1.2. Natural bond order (NBO) donations (kcal mol^{-1}) for 1-tetralone oxime complex.

	C_{ipso}–H σ	C_{ipso}–C^1 π	C_{ipso}–C^2 σ	Pd *d*
Pd–Cl σ* (*cis*)	10.0	6.5	0.4	–
Pd–Cl σ* (*trans*)	58.6	20.3	1.4	–
C_{ipso}–H σ*	–	–	–	4.9, 2.9

To generalize the concept, the authors plotted the more commonly-known cyclopalladation reaction of 8-methylquinoline in the same article.[33] The resulting complex indicated that one of the hydrogen atoms (H^2) within the methyl substituent has a longer C–H bond detailing an agostic interaction between the metal and the said bond. Similar donation and back-donation of electron densities into orbitals mentioned earlier were also recorded.

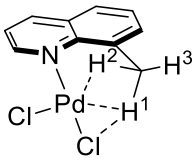

Table 1.3. Natural bond order (NBO) donations (kcal mol^{-1}) for 8-methylquinoline complex.

	C–H^1 σ	C–H^2 σ	C–H^3 σ	Pd *d*
Pd–Cl σ* (*cis*)	3.7	9.1	0.4	–
Pd–Cl σ* (*trans*)	16.6	44.0	1.5	–
C–H^2 σ*	–	–	–	6.0

1.5.3 σ-Bond Metathesis

Originally conceptualized for d^0 metal complexes which are usually high-valent and coordinately saturated, the σ-bond metathesis mechanism presents one of the pathways in which cyclometalation can proceed.[11] Diagrammatically, the activation mode seems to be similar to that of the electrophilic bond activation pathway. However, the process must involve a four-centered transition state.[34] Furthermore, the anionic ligand participating in the process is usually a carbanion instead of a leaving group.

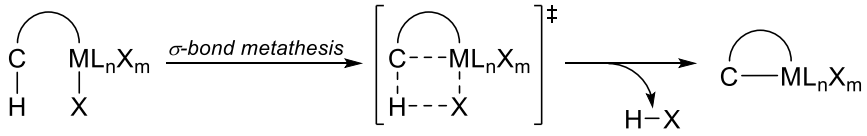

Scheme 1.17. σ-Bond metathesis mechanism for cyclometalation.

1.5.4 Transmetallation

The transmetallation procedure presents an effective method to obtain cyclometalated compounds. However, a separate metallacyclic system is a prerequisite for the mechanism to initialize. The ligand of interest must, thus, be susceptible to cyclometalation with a different metal center, usually lithium, magnesium or mercury, prior to the procedure. In most cases, the sacrificial complex can be obtained through C–Y bond activation mechanisms described earlier, direct metalation with elemental metal or its salts, or through metal-halogen exchange reactions. It should be noted that although the latter procedure generally does not require the directing group for metalation to take place, it was shown that the directing donor ligands could assist in the stabilization of the complex.

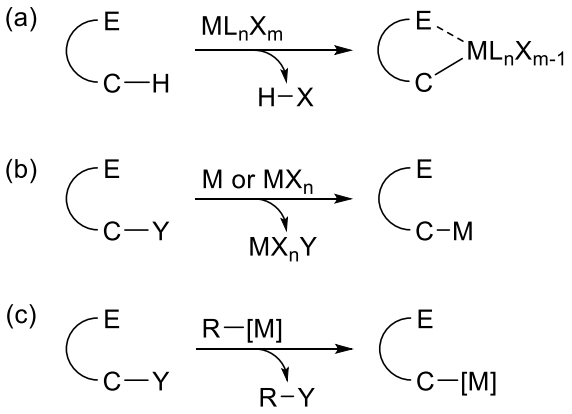

Scheme 1.18. Synthetic methods to sacrificial complexes: (a) ligand-directed cyclometalation, (b) direct metalation, and (c) metal-halogen exchange reactions.

By definition, transmetallation involves the transfer of ligand from one metal to another.[35] The procedure exist as an equilibrium, although it can shifted towards the complex of interest if the sacrificial metal is more electropositive.[36]

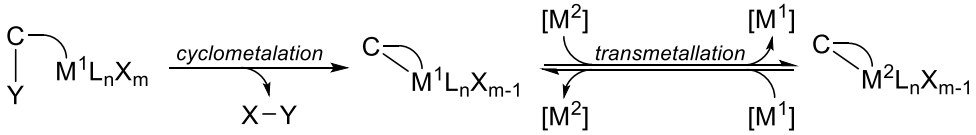

Scheme 1.19. Transmetallation mechanism for cyclometalation.

It is also worth mentioning that the transmetallation pathway can attain cyclometalated complexes with challenging ligand motif and difficult-to-cyclometalate metal centers. However, the procedure has its downsides with its non-atom economical approach, air- and moisture-sensitive intermediates and the occasional need for functionalized substrates.

1.5.5 Transcyclometallation

Like transmetallation, transcyclometallation requires another cyclometalated complex for the reaction to take place. In general, the procedure involves both bond forming and bond breaking processes at the metal-carbon bond. The sequence of the formation-cleavage process is important, and it determines the intermediate in the cyclometalation reaction.

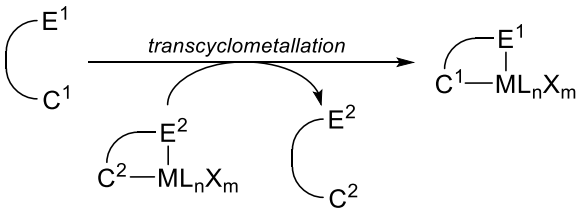

Scheme 1.20. General transcyclometallation mechanism for cyclometalation.

If the metal-carbon bond was cleaved prior to the formation of the new metal-carbon bond, the pathway will most likely proceed *via* an inorganic intermediate. In an example, the reaction between di-μ-acetatobis[2-[(dimethylamino)methyl]phenyl-*C,N*]dipalladium(II) and 2-phenylpyridine in acetic acid afforded the 2-phenylpyridine-derived palladacycle *via* a series of steps.[37] The first stage involved the decoordination and subsequent protonation of the amine moiety by the acid. This transformed the chelate into a monodentate carbanion complex which released a metal intermediate upon further protonolysis. The metal precursor can then undergo cyclometalation with the ligand of interest to offer the desired metallacycle. This method has also been shown to effectively attain cyclometalated complexes with arsenic[38] and selenium[39] donors, as well as C_{sp3}-coordinated[40] metallacycles.

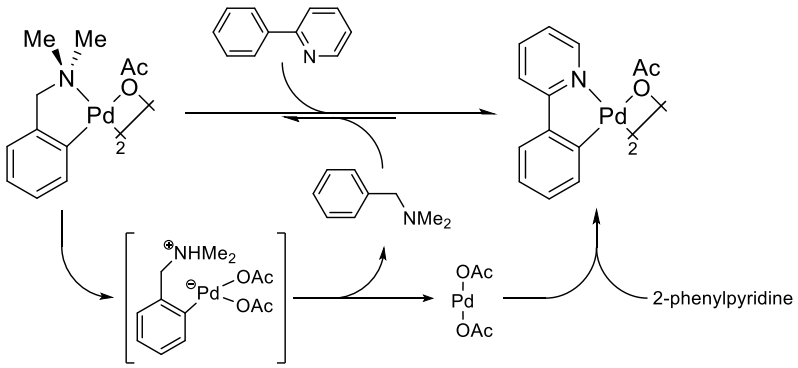

Scheme 1.21. Transcyclometallation of 2-phenylpyridine with di-μ-acetatobis[2-[(dimethyl-amino)methyl]phenyl-*C*,*N*]dipalladium(II).

On the other hand, the opposite pathway in which a new metal-carbon bond is formed after the cleavage of the initial metal-carbon bond proceeds *via* a diorgano-metal species. The reaction is driven by the more efficient coordinative ability of the new ligand motif to that of the original chelate. The pathway can be exemplified by the reaction of a *NCN*-pincer complex with 1,3-bis(diphenylphosphinomethyl)benzene to attain its corresponding *PCP*-pincer complex.[41] In the reaction, the labile arms of the *NCN*-pincer can exchange with the stronger bonding phosphine donors of 1,3-bis(diphenylphosphinomethyl)benzene to form a diorgano-metal complex. The C–H bond within the new ligand motif can then be activated and acidified to provide the *PCP*-pincer complex.

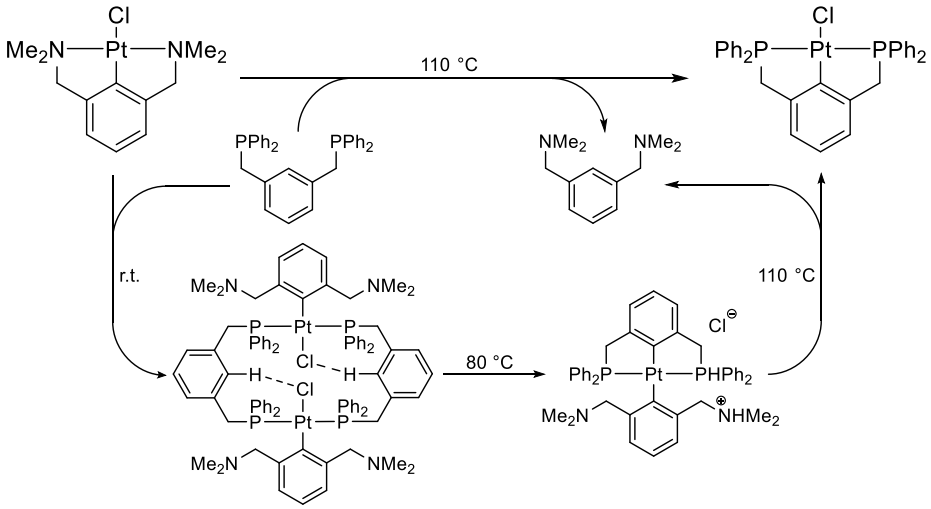

Scheme 1.22. Transcyclometallation of 1,3-bis(diphenylphosphinomethyl)benzene with *NCN*-platinum pincer complex.

1.6 Cyclometalated Complexes

Since its inception, a plethora of metallacycles have been synthesized and characterized. Figure 1.9 depicts the *d* block elements in which cyclometalated complexes have been reported.

GROUP									
3	4	5	6	7	8	9	10	11	12
44.956 Sc scandium 21	47.880 Ti titanium 22	50.941 V vanadium 23	51.996 Cr chromium 24	54.938 Mn manganese 25	55.847 Fe iron 26	58.933 Co cobalt 27	58.690 Ni nickel 28	63.546 Cu copper 29	65.390 Zn zinc 30
88.906 Y yttrium 39	91.224 Zr zirconium 40	92.906 Nb niobium 41	95.940 Mo molybdenum 42	(98.906) Tc technetium 43	101.070 Ru ruthenium 44	102.905 Rh rhodium 45	106.420 Pd palladium 46	107.868 Ag silver 47	112.411 Cd cadmium 48
138.905 La lanthanum 57	178.490 Hf hafnium 72	180.948 Ta tantalum 73	183.850 W tungsten 74	186.207 Re rhenium 75	190.200 Os osmium 76	192.220 Ir iridium 77	195.080 Pt platinum 78	196.966 Au gold 79	200.590 Hg mercury 80
(227) Ac actinium 89	(267) Rf rutherfordium 104	(268) Db dubnium 105	(269) Sg seaborgium 106	(270) Bh bohrium 107	(269) Hs hassium 108	(278) Mt meitnerium 109	(281) Ds darmstadtium 110	(281) Rg roentgenium 111	(283) Cn copernicium 112

Figure 1.9. Transition metal elements with reported cyclometalated complexes are shaded. Elements in darker grey will be discussed in greater detail in the thesis.

A comprehensive discussion on this massive pool of cyclometalated complexes would be overly voluminous and is beyond the scope of this thesis. As such, we will narrow down the study of these compounds to cyclometalated complexes of *palladium*, *platinum*, *ruthenium* and *iridium*. The former three represents the three most extensively used transition metal elements for cyclometalation, while the latter is an emerging field and is within the scope of discussion in the thesis. The review on the variants would cover significant aspects of each field, as well as recent research on the area.

1.6.1 Cyclopalladated Complexes

Undoubtedly, cyclopalladation presents one of the most extensively researched topic within the field of organopalladium chemistry.[20b] It is immensely versatile and is compatible with a wide variety of pnictogenic and chalcogenic ligands. Moreover, the predictable square-planar coordination mode of the d^8 complex allows electronic and steric modulations to be easily tailored through rational design of the ligand without significant modifications that may upset the cyclopalladation process.

Palladacycles has existed for slightly over half a century at the point of writing. Since the first-known cyclopalladated complex,[3] significant progress has been made over the years.

Of particular interest is the *ortho*-palladation of primary benzylamines due to its strong binding mode to the palladium center in the bis-amine complex.[12] The cyclopalladation was later achieved through the use of $Pd(acac)_2$ in lieu of $[Li_2PdCl_4]$.[42] A closer analogue to the palladacycle generated by Cope and Friedrich[4] was only achieved almost a decade later when the diiododiamine complex was treated with silver(I) tetrafluoroborate.[43] However, it should be noted that the procedure required the complex to be generated separately prior to *ortho*-palladation. It was then only in 1993 when a general protocol was established with $Pd(OAc)_2$ as the metal precursor.[44] Three main factors were postulated for the increased cyclometalation reactivity.[45] Firstly, the *acetato* ligand could enhance cyclometalation by activating the *ortho*-proton through a six-membered transition state. Next, the same anionic ligand can increase the electrophilicity of the palladium center, through its electron-withdrawing capabilities, making the latter more susceptible to attack by the aromatic ring. Lastly, the increased temperature may have facilitated easier dissociation of an amine moiety from the postulated bis-amine complex to initiate cyclometalation.

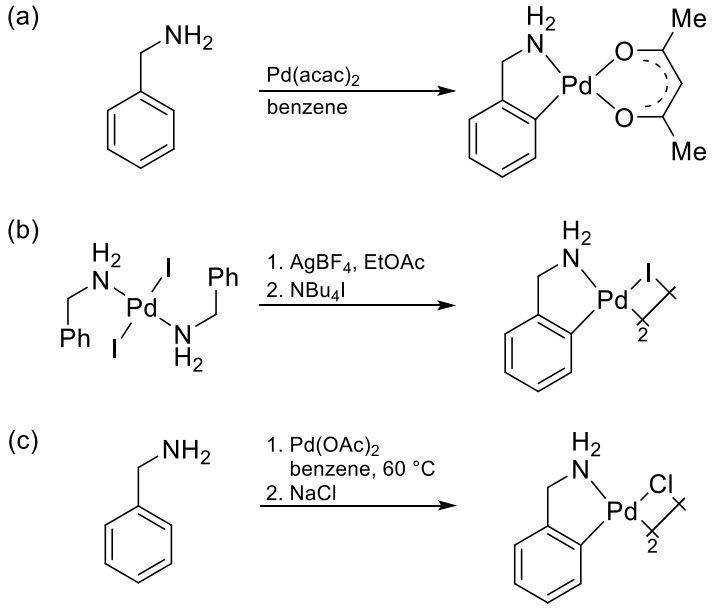

Scheme 1.23. Cyclopalladation of benzylamine with (a) $Pd(acac)_2$, (b) $AgBF_4$ and (c) $Pd(OAc)_2$.

The extension of nitrogen-based palladacycles to phosphapalladacycles also had an impact on the chemistry of cyclopalladation. While the nitrogenous congeners are versatile, the rich chemistry of the phosphorus atom allowed for greater structural manipulation (on both electronic and steric grounds).[46] The key difference between the cyclometalated systems lies with the phosphorus ligand being able to act as both σ-donor and π-acceptor.[47] The nitrogen-derived groups, on the other hand, are generally σ-donating.

Shaw synthesized one of the earliest reported phosphapalladacycles by treating *tert*-butyl-di-*o*-tolylphosphine and di-*tert*-butyl-*o*-tolylphosphine separately with $[Na_2PdCl_4]$ in refluxing methanol.[48] Between the two phosphines, the bulkier di-*tert*-butyl-*o*-tolylphosphine substrate was shown to cyclopalladate at a faster rate (a reflection of the Thorpe-Ingold effect). Its more well-known cyclometalated variant, di(μ-acetato)bis[*o*-(di-*o*-tolyl-phosphino)benzyl]-dipalladium(II), was only reported decades later when tri-*o*-tolylphosphine was successfully *ortho*-palladated with $Pd(OAc)_2$.[5]

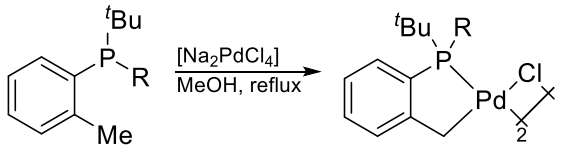

Scheme 1.24. Cyclopalladation of *tert*-butyl-di-*o*-tolylphosphine (R = *o*-tolyl) and di-*tert*-butyl-*o*-tolylphosphine (R = ^{t}Bu).

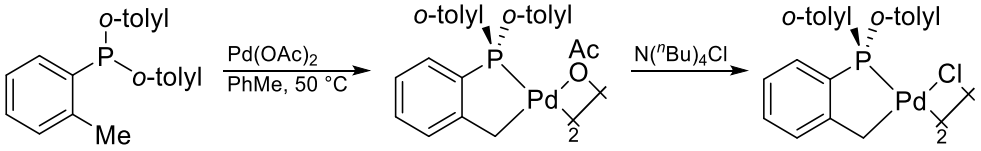

Scheme 1.25. Cyclopalladation of tri-*o*-tolylphosphine.

In another example, the sp^2-cyclometalated analogues were found to be more difficult to produce compared to its sp^3-counterparts. When *trans*-[$PdCl_2$(P(benzyl)$_2$(^{t}Bu))$_2$] and *trans*-[$PdCl_2$(P(benzyl)(^{t}Bu)$_2$)$_2$] was treated with sodium acetate, cyclopalladation proceeded, albeit sluggishly, when the reaction mixture was heated.[49] Once again, the bulkier phosphine ligand demonstrated greater potential for cyclization.

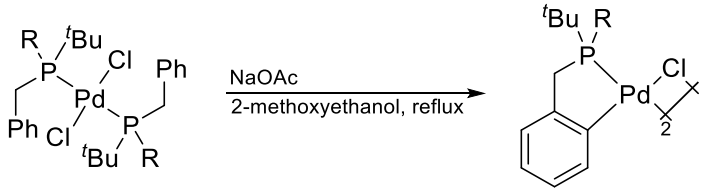

Scheme 1.26. Cyclopalladation of *trans*-[$PdCl_2$(benzyl)(R)(^{t}Bu)] (R = benzyl, ^{t}Bu).

A consistent challenge remains for the synthesis of phosphapalladacycles. Compared to the nitrogen donors, the phosphorus-coordinated palladium seems to be more indifferent towards C–H bond activation. Nonetheless, strategies have been refined and developed over the years and has now provided access to a huge collection of these compounds today.[50]

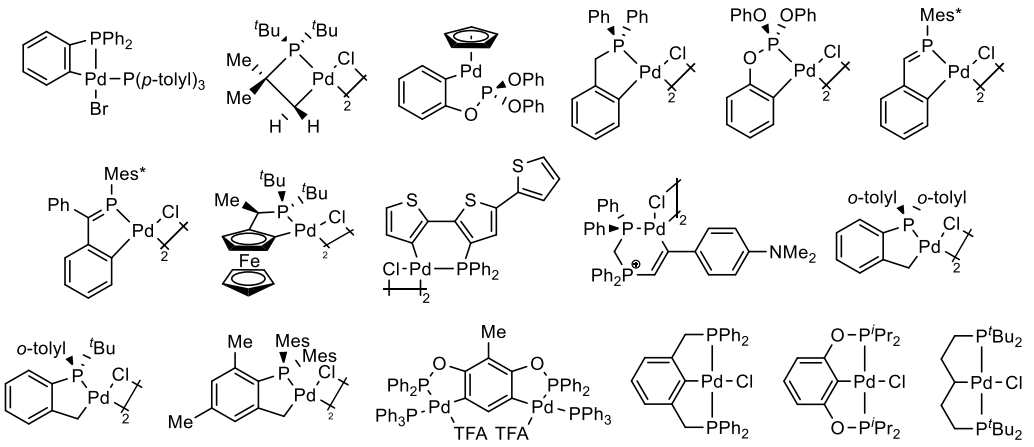

Figure 1.10. Selected examples of phosphapalladacycles.

Today, chiral palladacycles play significant roles in cyclopalladation chemistry. One of the earliest chiral cyclopalladated complex was the *N*,*N*-dimethyl-1-phenylethylamine palladacycle[51] as derived from the achiral variant[4] made by Cope and Friedrich in 1968. The optically-active palladacycle has since been refined to its alternate form by Wild[52] to enhance its effects in applications, particularly optical resolution protocols, through steric factors.

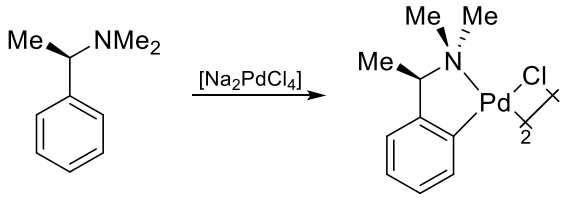

Scheme 1.27. Cyclopalladation of (*R*)-*N*,*N*-dimethyl-1-phenylethylamine.

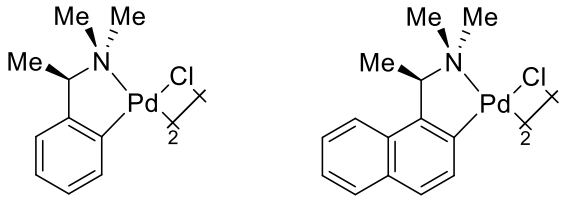

(Otsuka, 1971) (Wild, 1982)

Figure 1.11. Chiral cyclopalladated complexes with *N*,*N*-dimethyl-1-arylethylamine motifs.

An alternate access to these optically active palladacycles involved the chiral pool. Ligands can be modified or even used directly from the wide variety of optically-active amino acids and natural products for cyclopalladation. In one example, the salt of (*R*)-2-phenylglycine was utilized for the palladacyclic reaction.[53] Another experiment involved functionalizing L-(–)-fenchone to its oxime-derivative prior to cyclopalladation with $Pd(OAc)_2$.[54]

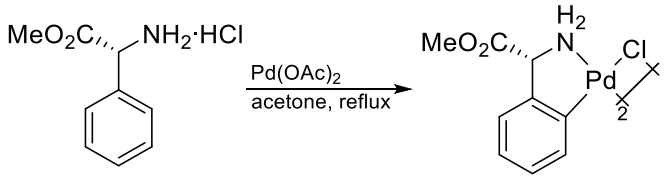

Scheme 1.28. Cyclopalladation of (*R*)-2-phenylglycine methyl ester hydrogen chloride.

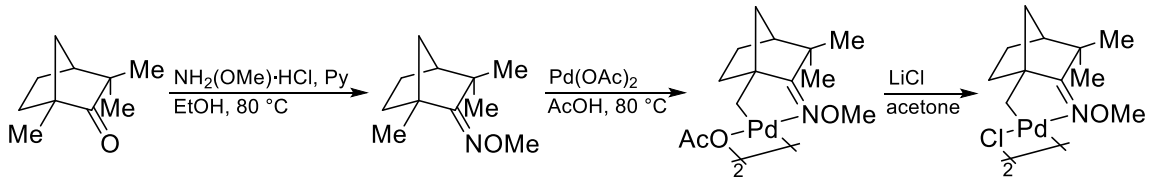

Scheme 1.29. Cyclopalladation of functionalized L-(–)-fenchone.

If the optically-active substrate is not naturally-occurring or commercially-available, the incorporation of chiral additives would be necessary for stereochemical induction. Alternatively, resolving agents can be introduced to afford diastereomers which can then be separated by physical means.

One might recall an earlier example where *N*,*N*-dimethylferrocenylmethylamine was cyclopalladated with $[Na_2PdCl_4]$ and a chiral carboxylate salt to afford an *ortho*-palladated complex with planar chirality.[29] The induction of stereochemical information was hypothesized to be effected by the optically-active carboxylate moiety which played dual role as ligand and base during the cyclometalation process. A similar ferrocenyl phosphine derivative, 2-(diphenylphosphino)phenylferrocene, was also synthesized *via* a similar method recently in 2009.[55] Recent theoretical calculations revealed an alternative mechanism involving *N*-acyl amino acids to the formation of the metallacycle.[56] The amino acid was theorized to chelate to the palladium center, with its *N*-acetyl moiety interacting with the C–H bond to invoke the activation process.

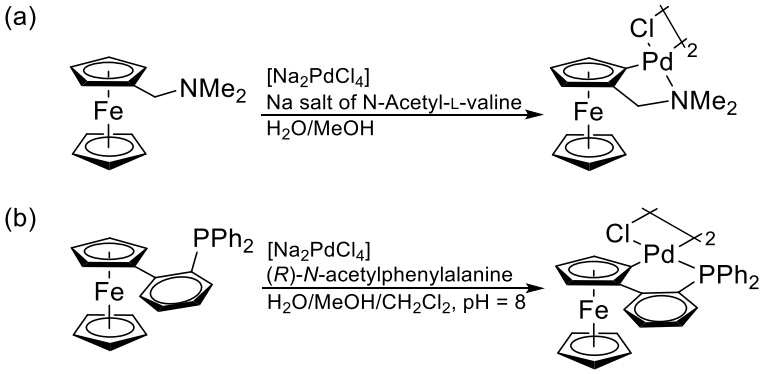

Scheme 1.30. Cyclopalladation of ferrocene ligands ((a) *N*,*N*-dimethylferrocenylmethylamine and (b) 2-(diphenylphosphino)phenylferrocene) with chiral amino acids.

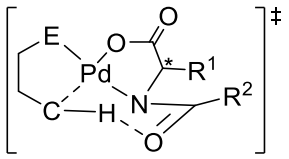

Figure 1.12. Proposed transition state for the chiral *N*-acyl amino acid-assisted cyclometalation reaction.

*P**-chiral cyclopalladated complexes can also be generated through optical resolution. In an extension to the phosphapalladacycle[48] synthesized by Shaw, Dunina demonstrated the resolution of the same racemic *ortho*-metalated complex[57] with the chiral salt of proline to afford the enantiopure palladacycles.

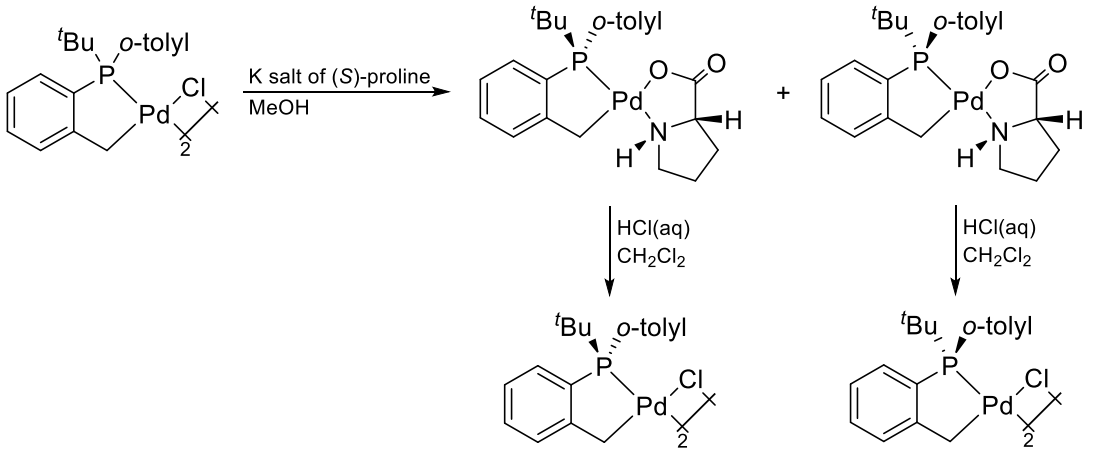

Figure 1.31. Resolution of di-μ-chloro-bis[2-(*tert*-butyl-*o*-tolylphosphine)benzyl-*C*,*P*]dipalladium(II) with potassium salt of (*S*)-proline.

Fast forward to the recent decade, new concepts to cyclometalation and structural motifs have emerged. We shall review some of the more interesting discoveries on the field.

The first discussion involved the C–H bond activation and subsequent cyclopalladation of the tertiary carbon center of a norbornane compound directed by an *exo-imino* ligand. The work originated from its application where the said bond can be functionalized with acetic anhydride.[58] It was then questioned if such activation mode was plausible with emphasis placed into proving the mode of activation through the isolation of its intermediate (a cyclopalladated complex). Careful manipulation of electronic factors led to the chelation of the aldoxime-derived salicylaldehyde to the palladium center, which then undergoes cyclopalladation upon addition of one equivalence of PPh_3.[59] The successful formulation was postulated to be driven by the dissociation of a single unit of the aldoxime-derived salicylaldehyde ligand from the bis-coordinated complex, initiated by the stronger coordinative ability of the phosphine moiety (to the oxime ligand), which led the said complex to proceed with intramolecular C–H bond activation to yield the desired metallacycle.[59]

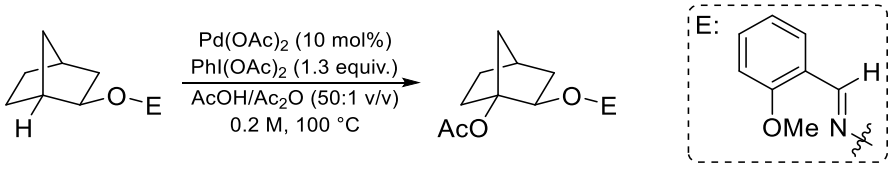

Scheme 1.32. Functionalization at tertiary carbon center of norbornane *via* ligand-directed C–H bond activation.

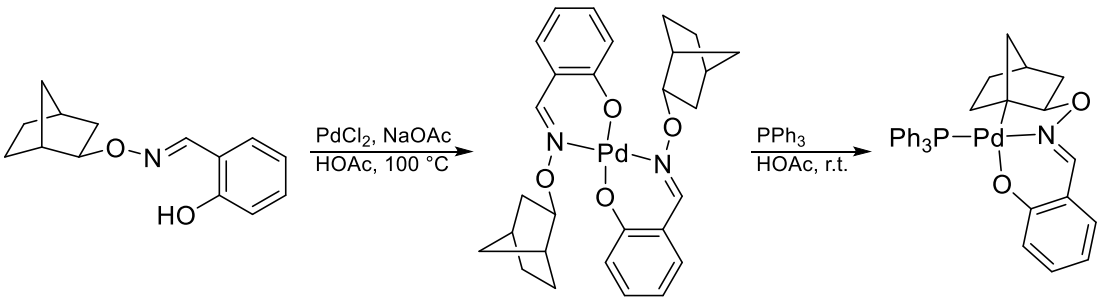

Scheme 1.33. Cyclopalladation of aldoxime-derived salicylaldehyde.

A novel class of C_{sp3}-phosphapalladacycle has emerged recently – the *triarylmethane* motif. In one of such derivatives, the ligand consists of a singly *ortho*-functionalized triphenylphosphine moiety that was joint to the methine center with two other tunable aryl substituents. The coordinated complex can undergo cyclopalladation upon treatment with KO^{t}Bu to yield the palladacycle.[60] Agostic C–H bond activation was predicted on the basis of its crystallographic study in which the said bond was found to interact closely with the palladium center or one of the phenyl moiety at the phosphorus center.

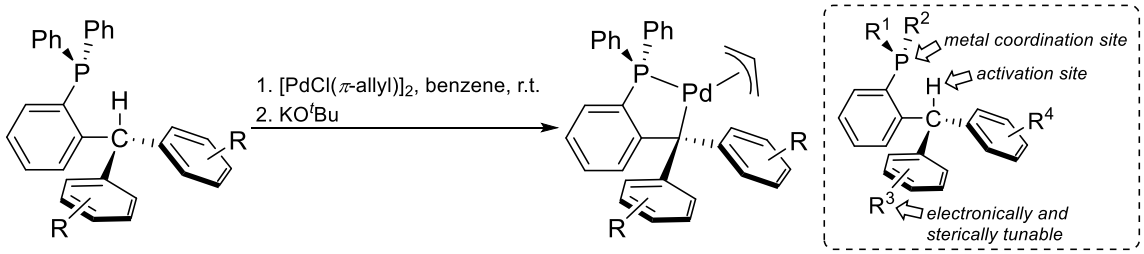

Scheme 1.34. Cyclopalladation of a triarylmethane motif (R = H, *p*-Me) with [PdCl(π-allyl)]$_2$.

Lastly, we discuss another novel class of cyclopalladated complex – the (aminomethyl)silylmethyl-derived cyclopalladated complex. Structurally, the compound resembles a carbon-based neopentylamine cyclopalladated complex. However, unlike its carbon analogue, the silicon atom adds depth to the chemistry by fulfilling two additional tasks: (a) stabilizing the α-metalated carbon centers through polarization effects, and (b) preventing unwanted β-elimination decomposition pathways.[61] The methylsilane moiety also further induces greater σ-donation of electron densities to the palladium center due to the carbanion's ability to bear a higher charge than a simple methyl substituent.[62] The metallacycle can be synthesized from 1-((methyldiphenylsilyl)methyl)piperidine as the starting material. However, unlike most of the aforementioned palladacycles, the functionalized methylsilane was unable to undergo ligand-directed C–H bond activation. To overcome the problem, the acidic proton of the α-methyl group was litiated with *tert*-butyllithium to provide an organolithium species, which can then be transmetallated with [$PdCl_2(SMe_2)_2$] to give the desired cyclopalladated complex.[61] It is also worth mentioning

that complex presents one of the largest difference in thermodynamic *trans* influence between two donors and their respective *trans* ligand among cyclopalladated complexes.[62]

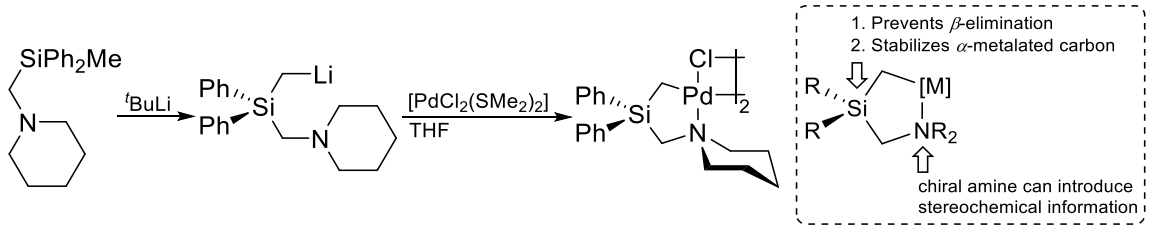

Scheme 1.35. Cyclopalladation of 1-((methyldiphenylsilyl)methyl)piperidine.

1.6.2 Cycloplatinated Complexes

Cycloplatination and cyclopalladation share a common beginning with their first cyclometalated azobenzene complex.[3] In many aspects, these two fields are strongly related and overlap significantly in their chemistry. Nonetheless, the two noble metals do differ to some extent in comparison. Firstly, the reduced electrophilicity of the platinum center decreases the scope of electrophilic bond activation.[11] As a result, cycloplatination can be only initiated by a smaller variety of substrates. Kinetically, the process was also observed to proceed more sluggishly than its lighter palladium congener.[63] Secondly, the increased softness of the metal provides greater stability at higher oxidation states. Such property adds the possibility of oxidative addition pathway to its arsenal of activation modes that is not possible with its palladium counterpart.[64]

Let us first look into the oxidative addition mechanism for cycloplatinated complexes. It was proposed that an equilibrium lies between the tricoordinate systems of $[PtMe_2(SMe_2)]$ and $[PtMe_2(E—C–Y)]$ due to their concentration dependence in the dissociation-association procedure.[65] The slower oxidative addition process then takes over for the $[PtMe_2(E—C–Y)]$ complex affording a pentacoordinated cycloplatinated complex, which subsequently rearranges to provide a compound with its Y moiety *trans* to the carbanion of the metallacycle.[66] The free SMe_2 ligand then quickly returns to the platinum center to afford the octahedral metallacycle.

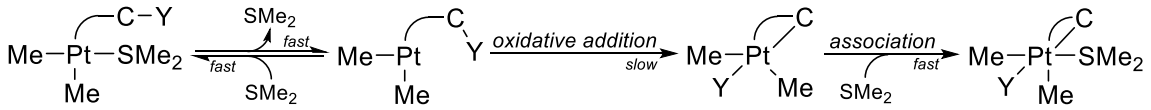

Scheme 1.36. General oxidative addition mechanism for cycloplatination.

Complexes that underwent the aforementioned pathway usually involved $[PtR_2(SMe_2)_2]$ and $[PtR_2(dmso)_2]$ (R = Me, Ph, Mes) as the platinum precursor. Its ligand motif also usually carries a polar C–Y bond to direct the oxidative addition procedure onto the said bond. In an example, *N*-benzyl-1-(2-bromophenyl)methanimine was cycloplatinated with $[PtMe_2(SMe_2)_2]$ to afford its respective metallacycle.[66] The complex was subsequently recrystallized and its position of the ligands within the coordination sphere confirmed by crystallographic studies. The method can also be utilized to obtain seven-membered platinacycles as shown in Scheme 1.37(b).[67]

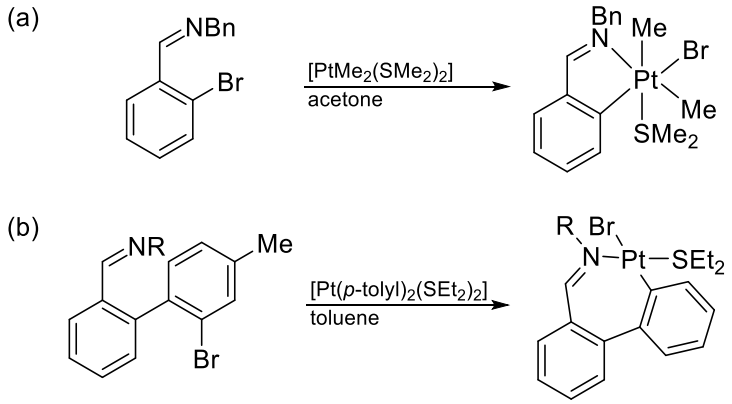

Scheme 1.37. Cycloplatination of *N*-benzylidenebenzylamine derivatives ((a) *N*-benzyl-1-(2-bromophenyl)methanimine and (b) 1-(2'-bromo-4'-methyl-[1,1'-biphenyl]-2-yl)-*N*-(4-chlorobenzyl)methanimine) (R = $CH_2(4\text{-}ClC_6H_4)$).

Although less common, the ligand-directed oxidative addition procedure can also occur for the C–H bond. In a recent example, 2-vinylpyridine can be cycloplatinated with $[PtMe_2(dmso)_2]$ in hot toluene to give a square planar platinacycle, with the loss of a methane fragment (possibly through reductive elimination from the octahedral complex).[68] The resultant complex reflected regioselectivity within the coordination sphere of the metal center with only one geometric isomer isolated from the reaction mixture. The preference of the isomer was theorized to be due to *trans* influence of the ligands with the dmso moiety

coordinating *trans* to the vinylic carbon. Lastly, it is worth mentioning that attempts were made to cycloplatinate ethylpyridine for comparison. However, the resulting coordinated complex failed to cyclize.

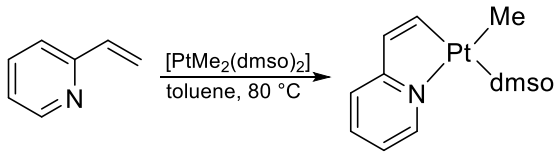

Scheme 1.38. Cycloplatination of 2-vinylpyridine with $[PtMe_2(dmso)_2]$.

The challenge to cyclopalladate primary amines[44] has long been solved since 1993. Its cycloplatination protocol, on the other hand, has only been generalized in the past decade.[63] Prior to this, there existed only one publication, to the best of our knowledge, in which cycloplatination of a primary amine derivative has been successful.[69] The procedure, however, only provided a low yield of 10% after five days at elevated temperatures.

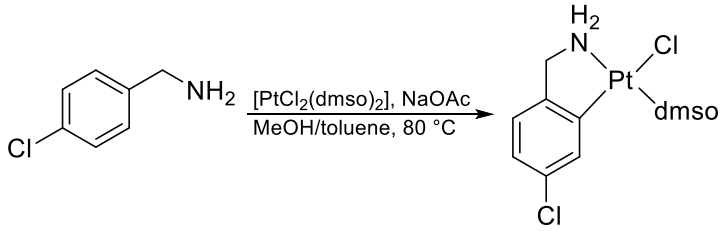

Scheme 1.39. Cycloplatination of 4-chlorobenzylamine.

The revised methodology[63] utilized a salt from the reaction between $[K_2PtCl_4]$ and hydroiodic acid, postulated to have formula $[K_2PtI_5]$, as the metal precursor for the cycloplatination procedure. The salt can then be reacted with the primary amine in refluxing solvent mixture of methanol and water to afford the amine-coordinated platinacycle. The complex can further undergo ligand exchange with other donor moieties, if required. It is noteworthy that the platinum salt bears a resemblance to separate entities of $[K_2PtI_4]$ and I_2. As such, an experiment involving only the primary amine and $[K_2PtI_4]$ was conducted at elevated temperatures. The reaction yielded a mixture of *trans* diamine complex, the desired platinacycle and significant amounts of platinum residue. It is also interesting to note that a methyl substituent exists at the α-carbon center which can promote

cyclometalation through Thorpe-Ingold effect. That being said, cycloplatination of the parent benzylamine by the aforementioned method has not been reported.

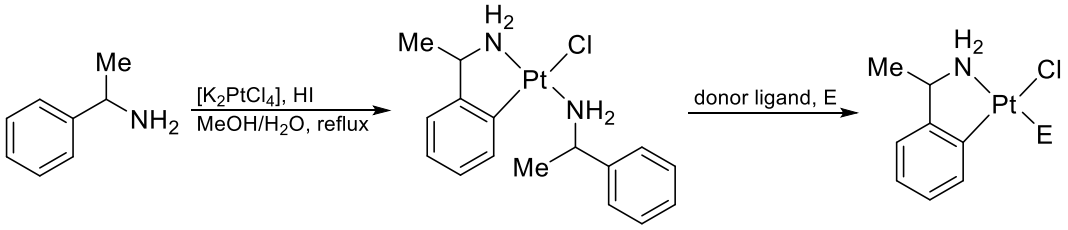

Scheme 1.40. Cycloplatination of 1-phenylethylamine.

Lastly, we discuss a special topic within cycloplatination – *rollover reactions*. The area was first discussed by Skapski and Young in 1985,[70] but has only recently regained its popularity over the past decade. The platinum-based rollover reaction began with the cycloplatination of 2,2'-bipyridine. In the case with most metals, a bipyridine moiety would coordinate to the metal center to provide a *N*,*N*-chelate complex. However, when the same reaction was performed with platinum precursor [$PtPh_2(dmso)_2$], the protocol returned an unexpected *C*,*N*-cycloplatinated complex in which one of the pyridine ring has seemed to "rollover" to allow the activation of a C–H bond. It should be noted that the concept was not unique to organoplatinum compounds, nor it was the first-known complex of this type.[71] However, the generation of these compounds were generally more difficult in other metals than that of platinum.

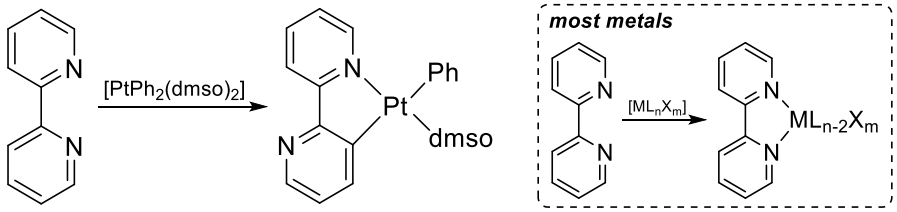

Scheme 1.41. Cycloplatination of 2,2'-bipyridine.

Minghetti later revealed in 1999 that the cyclometalation process can be pushed towards rollover type reactions if a substituent is present at the 6-position of the pyridine ring.[72] The reaction was also shown to be affected by its metal precursor with [K_2PtCl_4] and [$PtMeCl(SMe_2)_2$] delivering a *C*,*N*,*N*-platinacycle[73] and a *C*,*N*-rollover complex[72] respectively.

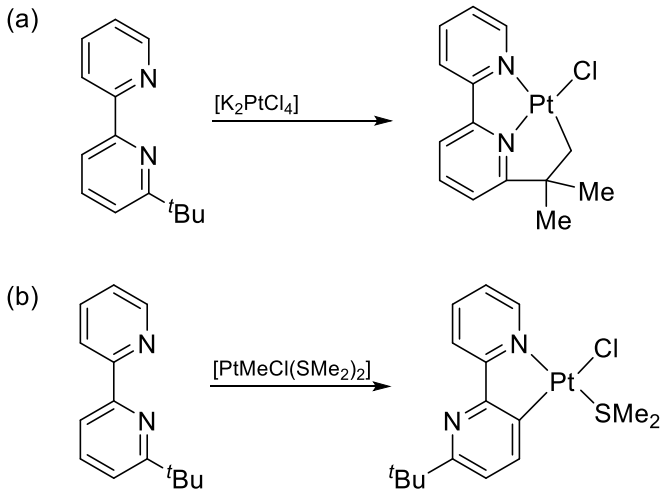

Scheme 1.42. Cycloplatination of 6-(tert-butyl)-2,2'-bipyridine by (a) $[K_2PtCl_4]$ and (b) $[PtMeCl(SMe_2)_2]$.

In the rollover cycloplatination of a chiral 2,2'-bipyridine pinene derivative, the reaction shed light into some mechanistic aspects of the reaction.[74] Firstly, the 6-substituted pyridine ring adds steric bulk to the dipyridine complex, tempting the platinum center to allow a rollover. Secondly, the more influential thermodynamic *trans* influence, caused by the methyl group, weakened the Pt–N bond pushing the pyridine ring away to influence the oxidative addition of the C–H bond for cyclometalation. It is also worth mentioning that the resultant complex was the first reported chiral variant of rollover cyclometalated complex.

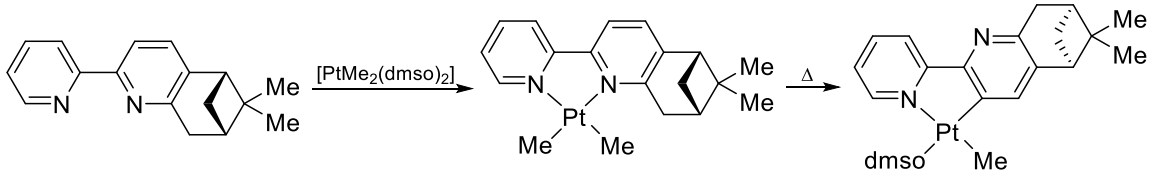

Scheme 1.43. Cycloplatination of a chiral 2,2'-bipyridine pinene derivative.

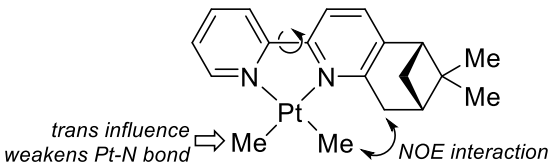

Figure 1.13. Ligand and substituent effects on rollover cyclometalation.

Electronic effects from the aromatic ring was also found to play a part in the rollover cyclometalation procedure. In a recent example in which a 5-substituted-2,2'-bipyridine ligand was complexed, it was revealed that an electronic-withdrawing trifluoromethane moiety at the substituted position would initiate the C–H bond activation process more readily than its methyl counterpart.[75] Two justifications were suggested for the observation: (a) electron density about the nitrogen were reduced due to the presence of electron-withdrawing group resulting in weaker coordination bond, and (b) a more efficient nucleophilic attack at the C–H bond by the metal center attributable to activation by the electron-withdrawing substituent.

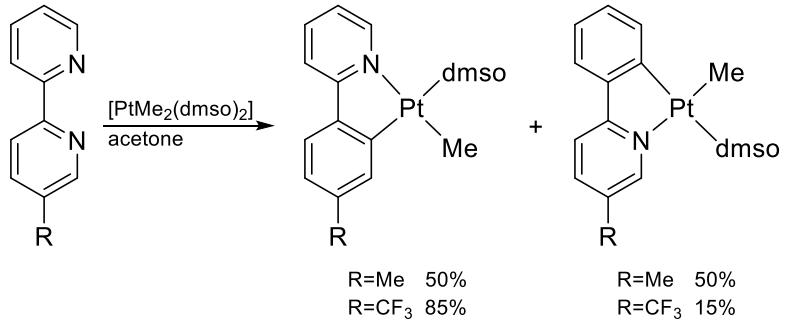

Scheme 1.44. Electronic effects on rollover cycloplatination.

1.6.3 Cycloruthenated Complexes

Although less fashionable than its palladium and platinum brethren, the study of cycloruthenation covers a broad scope within the field of cyclometalation. Unlike most transition metals elements in which little cyclometalating precursors exist, a diverse library of these compounds was available to effect cycloruthenation through bond activation pathways.[76] That being said, it is, thus, unsurprising that cycloruthenation has such a broad scope, with essentially all classes of cyclometalating ligands known to afford their respective ruthenacycles.[11]

The first-known cycloruthenated complex originated from the reaction between triphenylphosphite and $[Ru(PPh_3)_3HCl]$.[77] Through a simple ligand exchange protocol, its *phosphito*-complex can then readily undergo C–H bond activation to provide the octahedral *ortho*-ruthenated complex.

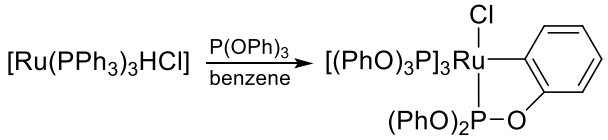

Scheme 1.45. First-known cycloruthenation protocol.

The discovery soon led to the cycloruthenation of triphenylphosphine from the same ruthenium precursor, although it was found that stoichiometric amounts of activated olefins were required to push for cyclization.[78] It was suggested that the precursor undergone a dehydrogenation protocol in the presence of an activated olefin to provide the four-membered ruthenacycle (and its hydrogenated product). Whilst the process was reversible, it should be noted that the metallacycle was not a key intermediate in the hydrogenation procedure.[79]

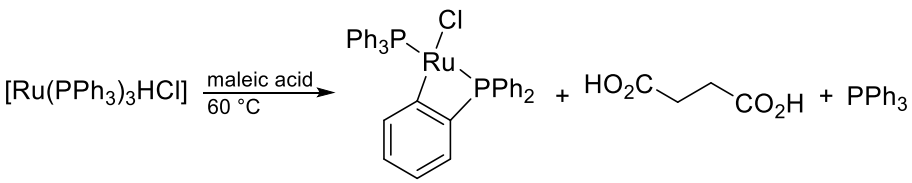

Scheme 1.46. Intramolecular cycloruthenation of $[Ru(PPh_3)_3HCl]$ activated by maleic acid.

Another variant of cycloruthenated compounds involved the carbonylchlorido-ruthenium precursors. Whilst it may seem that these polymeric complexes can sustain cyclometalation due to its available vacant sites, the precursor is rather inert and usually requires high temperatures to displace an additional carbonyl moiety to initiate the procedure. In an example, cycloruthenation of azobenzene with $[Ru(CO)_3Cl_2]_2$ provided only modest amounts of the desired ruthenacycle.[80] Further experimentation later revealed that the displacement of the carbonyl ligand could be favored if the reaction was conducted under neat conditions.[81]

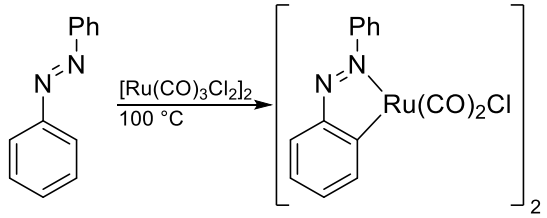

Scheme 1.47. Cycloruthenation of azobenzene.

It is worth mentioning that the complexes obtained from the aforementioned reaction exist as dimers. Given that each molecule contained four carbonyls and two *chlorido* moieties (in its dimeric form), it was proposed that the complex remained bridged to chlorine atoms with four possible configurations. Through infrared spectroscopy, Hiraki was able to account for two possible configurations (**A** and **B**) based on C≡O stretching vibrations of the isolated complex from the cycloruthenation of 1-phenylpyrazole with solvated $[Ru(CO)_2Cl_2]$.[82]

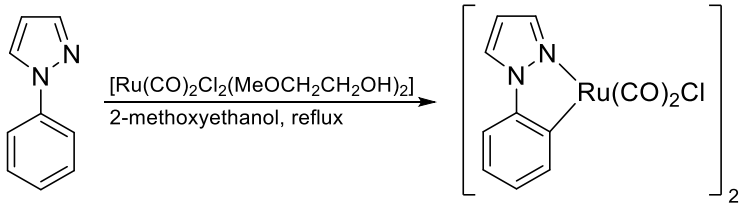

Scheme 1.48. Cycloruthenation of 1-phenylpyrazole.

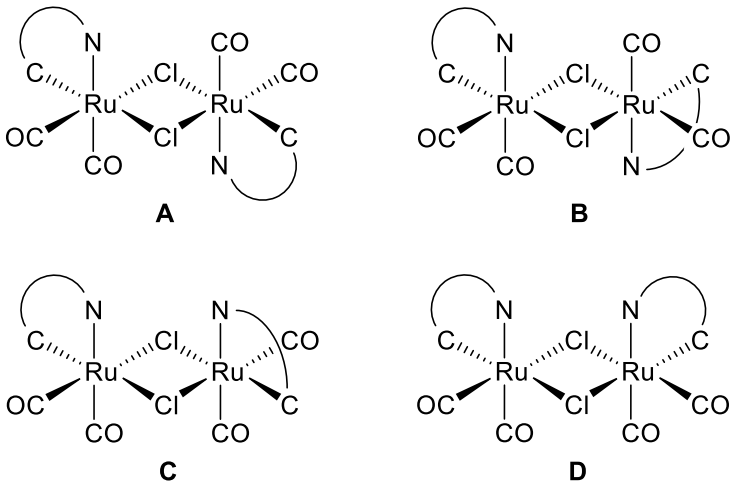

Figure 1.14. Possible configurations for carbonylchlorido-based ruthenacycles.

Recently, it was reported that planar prochiral ligands can undergo cycloruthenation with $[Ru(CO)_2Cl_2]_n$ polymer to provide their corresponding ruthenacycles. Whilst the reaction continued to provide a mixture of diastereomeric complexes, it was found that addition of monodentate ligands or chloride-containing salts would afford only one form of the product, indicative of some selectivity within the cycloruthenation process.[83]

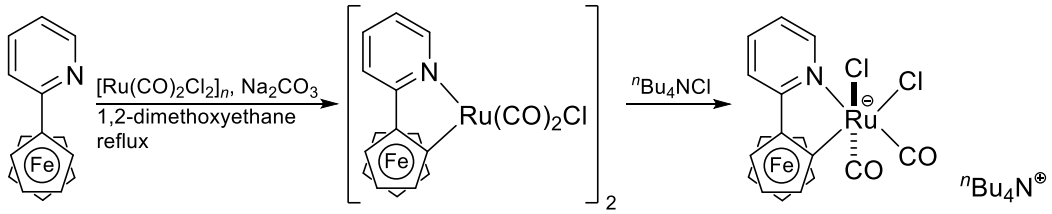

Scheme 1.49. Cycloruthenation of 2-ferrocenylpyridine.

A notable class of cycloruthenated complexes is its half-sandwich variants. Although octahedral in nature, these complexes exhibit a *pseudo*-tetrahedral geometry due to the engagement of a *polyhapto* aromatic entity bonding to three of its *facial* coordination sites. Additionally, the spectator ligand can influence the coordinative nature of its *trans* cyclometalating ligands through its electronic and steric effects.

Reported along with a variety of other piano-stool metallacycles,[84] the first ruthenacycle of this class was the azobenzene-based ruthenium(II) complex.[2b] Whilst the cyclometalation procedure proceeded, the reaction required irradiation with UV light to provide the compound in small quantities. With the intention to improve the protocol, the authors set out to cycloruthenate the same ligand with other η^5-Cp ruthenium precursors. The trial was successful providing the desired cyclometalated complex at elevated temperatures.[85] It was also pointed out that they observed the cyclization of the ruthenium precursor to provide a four-membered phosphine-based ruthenacycle upon heat treatment in the absence of the cyclometalating ligand.

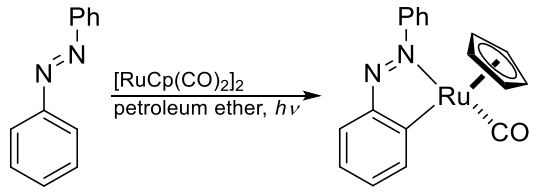

Scheme 1.50. Cycloruthenation of azobenzene.

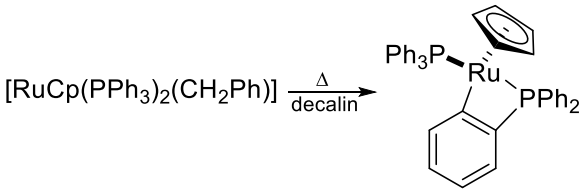

Scheme 1.51. Intramolecular cycloruthenation of $[RuCp(PPh_3)_2(CH_2Ph)]$.

Roundhill, in 1991, revealed that the abstraction of the *chlorido* ligand from the *pseudo*-tetrahedral precursor could facilitate cycloruthenation *via* an activated electron-deficient ruthenium species, as exemplified from the cyclization between triphenylphosphite and $[RuCp(PPh_3)_2Cl]$ in the presence of silver(I) triflate.[86] The process was later perfected by Pfeffer in which hexafluorophosphate salt was used in place of the light-sensitive silver(I) reagent for the cycloruthenation of *N*,*N*-dimethylbenzylamine.[87]

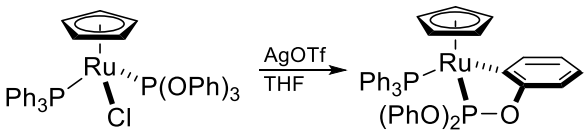

Scheme 1.52. Intramolecular cycloruthenation of [RuCp(PPh_3)($P(OPh)_3$)Cl] activated by AgOTf.

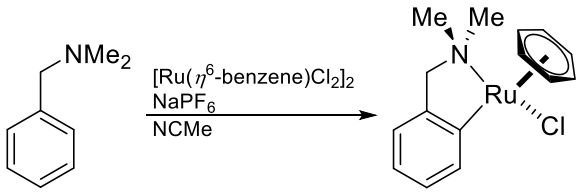

Scheme 1.53. Cycloruthenation of *N*,*N*-dimethylbenzyamine.

Since then, a collection of these *pseudo*-tetrahedral cycloruthenated complexes with varying donor groups have been developed *via* the aforementioned strategy.[88]

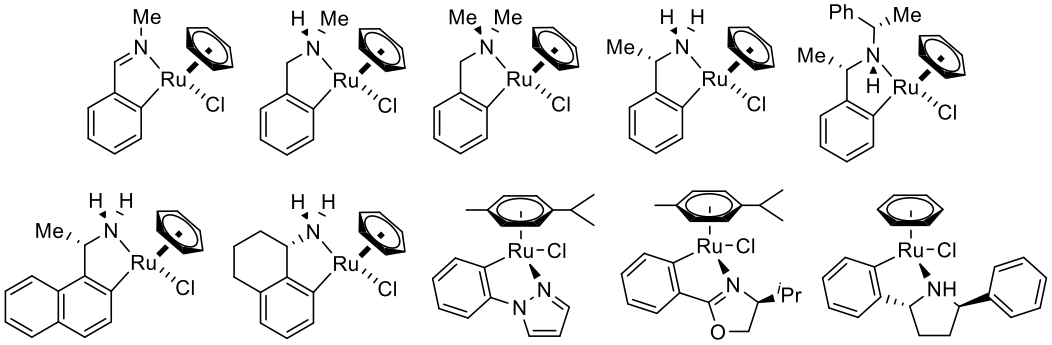

Figure 1.15. Selected examples of *pseudo*-tetrahedral cycloruthenated complexes.

Proceeding to some smaller, but important, recent developments within the field, Grubbs described the cycloruthenation of his second-generation Grubbs catalyst upon dissolution in methanol containing trace amounts of dichloromethane at room temperature. The reaction readily afforded the cycloruthenated compound with a reported loss of benzylidene moiety that originated from the carbene fragment of the ruthenium(II) complex.[89] Supporting the observation was a separate investigation in which the coordination of an unsaturated mesityl carbene to [$Ru(PPh_3)_3HCl$] resulted in the cyclometalation of the ligand to provide the structurally analogous cyclometalated Grubbs catalyst.[90]

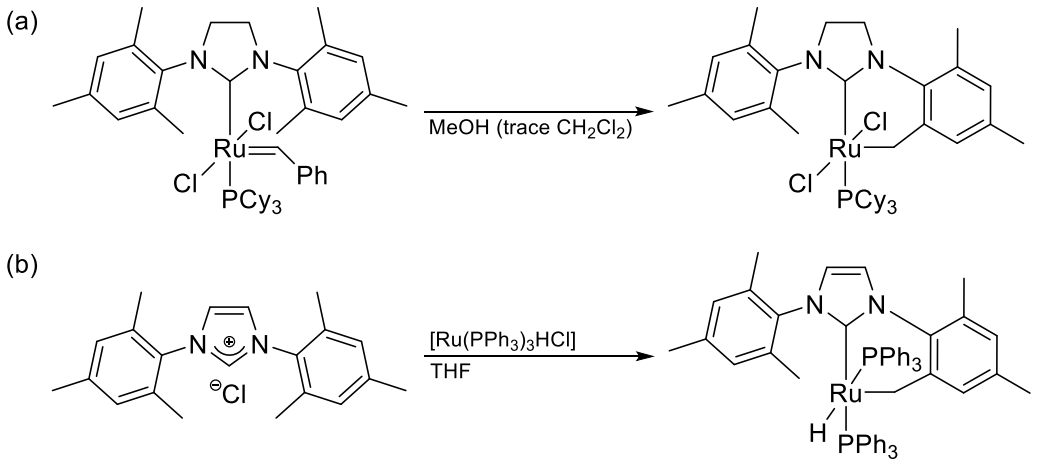

Scheme 1.54. Incidental cycloruthenation of (a) second-generation Grubbs catalyst and (b) *N*,*N*-bis(mesitylimidazolium).

Lastly, it is worth reporting a recent study on the reversibility of cyclometalation *via* hydrogenation under acidic conditions on a cycloruthenated complex.[91] A 2-phenylpyridine-based ruthenacycle was found to be able to undergo a reversible hydrogenation process to provide a complex with observable agostic C–H bond interaction at the ruthenium center. The compound was postulated to a key intermediate to the cyclometalation procedure and was supported by deuterium studies. Theoretical calculations further revealed a small intrinsic agostic interaction energy between the agostic and *ortho*-metalated species, indicative of an equilibrium between the complexes.

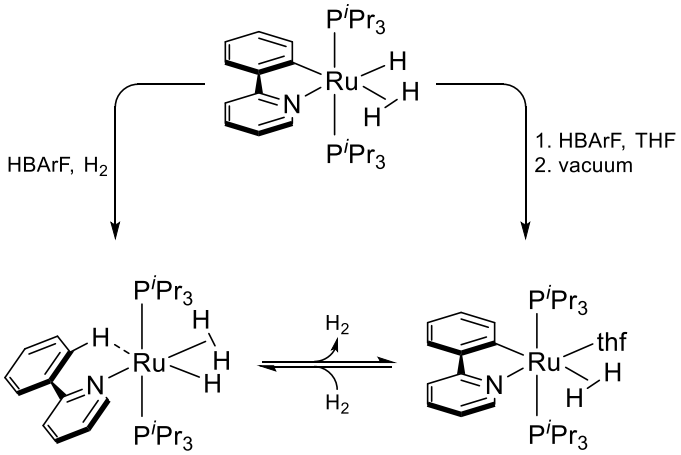

Scheme 1.55. Reversibility in the cycloruthenation of 2-phenylpyridine under acidic conditions.

1.6.4 Cycloiridated Complexes

Against the backdrop of cyclopalladation, cycloplatination and cycloruthenation, the contribution of cycloiridation to the field of cyclometalation is modest, although interest into the area was shown to have risen in recent years due to its exceptional capabilities in applications.[7b, 8a, 9a, 92]

One of the first iridacycle to be documented involved the intramolecular *ortho*-iridation of $[Ir(PPh_3)_3Cl]$.[93] Although the procedure may seem similar to that of its ruthenium counterpart[78] (as described earlier in the previous section), the four-membered cycloiridated species does not require the addition of activated olefins to initiate the cyclization process. The protocol can also be extended to its arsine and stibine derivatives, although these processes were reported to proceed more sluggishly.[94]

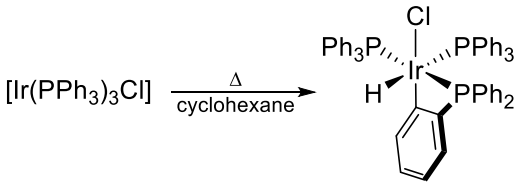

Scheme 1.56. First-known cycloiridation protocol.

Intermolecularly, a naphthalene-based five-membered cycloiridated complex can be obtained from reacting dimethyl(1-naphthyl)phosphine with iridium(III) chloride in refluxing acidified 2-methoxyethanol.[95] Treatment of the product with sodium acetate in the same boiling solvent would then yield its corresponding bis-cyclometalated compound. Interestingly, the tris-cycloiridated complex can only be obtained upon abstraction of the remaining *chlorido* ligand with silver(I) tetrafluoroborate.

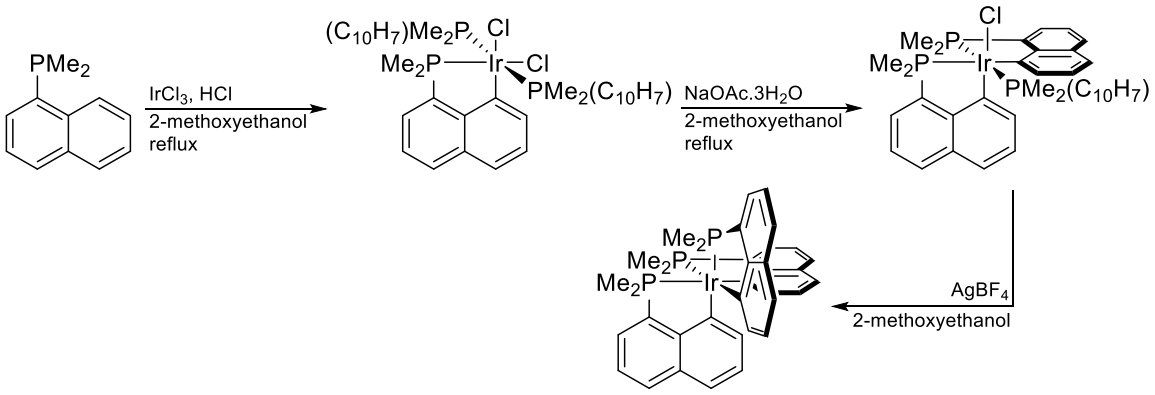

Scheme 1.57. Cycloiridation of dimethyl(1-naphthyl)phosphine.

One of the earliest nitrogen-containing cycloiridated complex was an *azo*-based iridacycle. The product was obtained incidentally from the addition of benzenediazonium tetrafluoroborate to Vaska's complex with the intention to attain an iridium(III) azolium salt. Instead, the reaction afforded an *azo*-iridacycle and an iridium-tetrazene complex.[96]

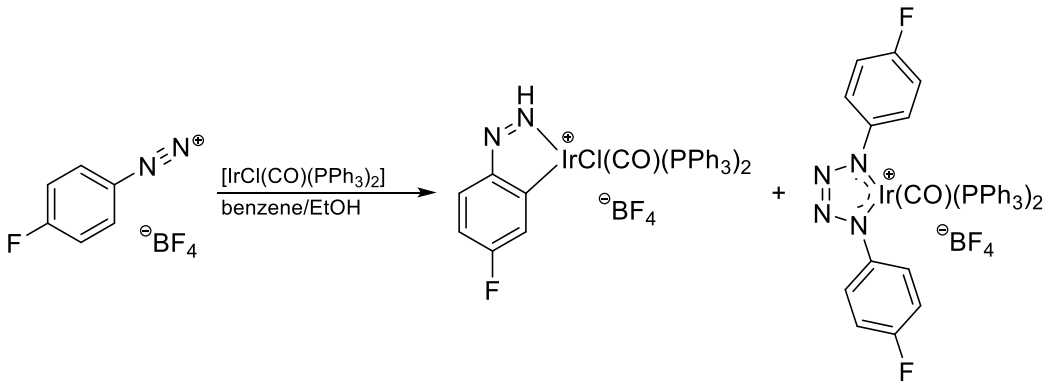

Scheme 1.58. Iridation of benzenediazonium tetrafluoroborate by Vaska's complex.

Similar to its phosphine derivatives, bis-cycloiridated nitrogen-based complexes can also be attained through direct cyclometalation with iridium precursors. In an example, *N*-phenylpyrazole can react with [$Na_3(IrCl_6)$] in boiling 2-methoxyethanol to provide its corresponding dimeric bis-chelated iridacycle.[97] However, unlike the phosphorus analogue, the mono-chelated species was not observable in the reaction mixture.

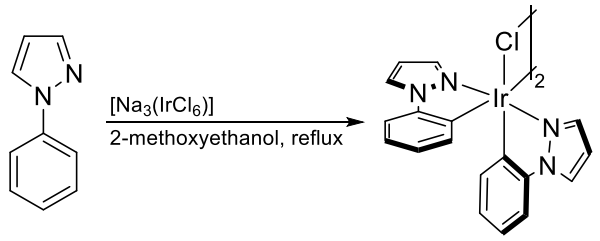

Scheme 1.59. Cycloiridation of *N*-phenylpyrazole.

In recent years, research into these bis-chelated iridium(III) systems have been widespread due to its diverse photo-physical applications.[8b] Whilst access to these compounds mostly remained the same with little variations to its reaction conditions, a myriad of these cycloiridated complexes with various conjugated cyclometalating ligand motif have since emerged and are shown in Figure 1.16.[98]

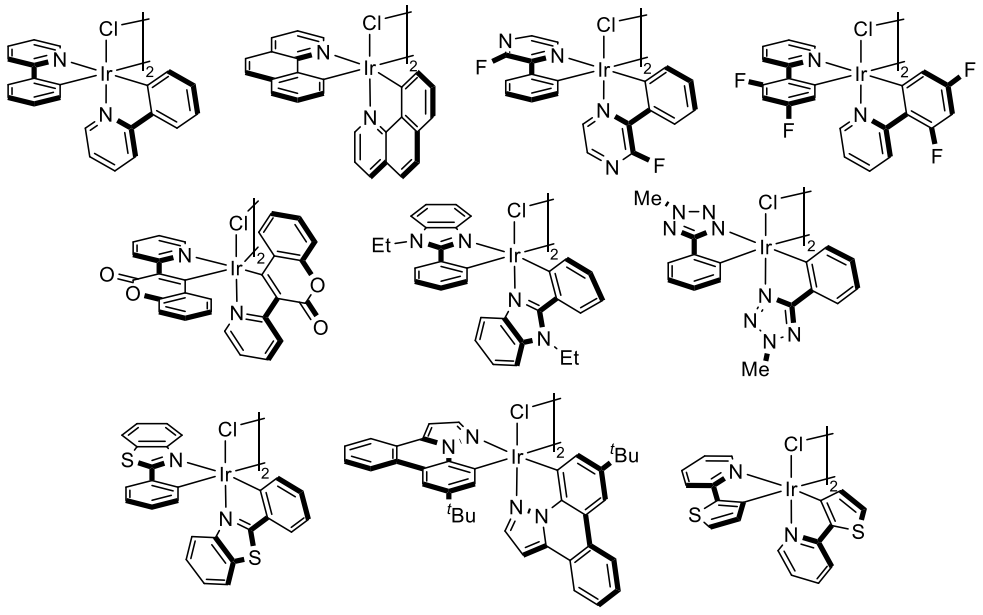

Figure 1.16. Selected examples of bis-chelated *C*,*N*-cycloiridated complexes.

Another emerging area in the chemistry of cycloiridation is the study of *pseudo*-tetrahedral iridacycles. Like its multi-chelated cycloiridated derivatives, the field only gained popularity recently due to its enhanced activity in applications, specifically as catalysts.[7b, 92, 99]

One of the key studies involving these complexes came from Beck who documented the cycloiridation of substituted 2-phenyl-4-*R*-5(4*H*)-oxazolone with $[IrCp^*Cl_2]_2$ in the presence of sodium acetate.[100] Whilst the procedure was successful in affording the desired iridacycles, it was not until half a decade later that Davies generalized the methodology to access cycloiridated amines and imines complexes.[101]

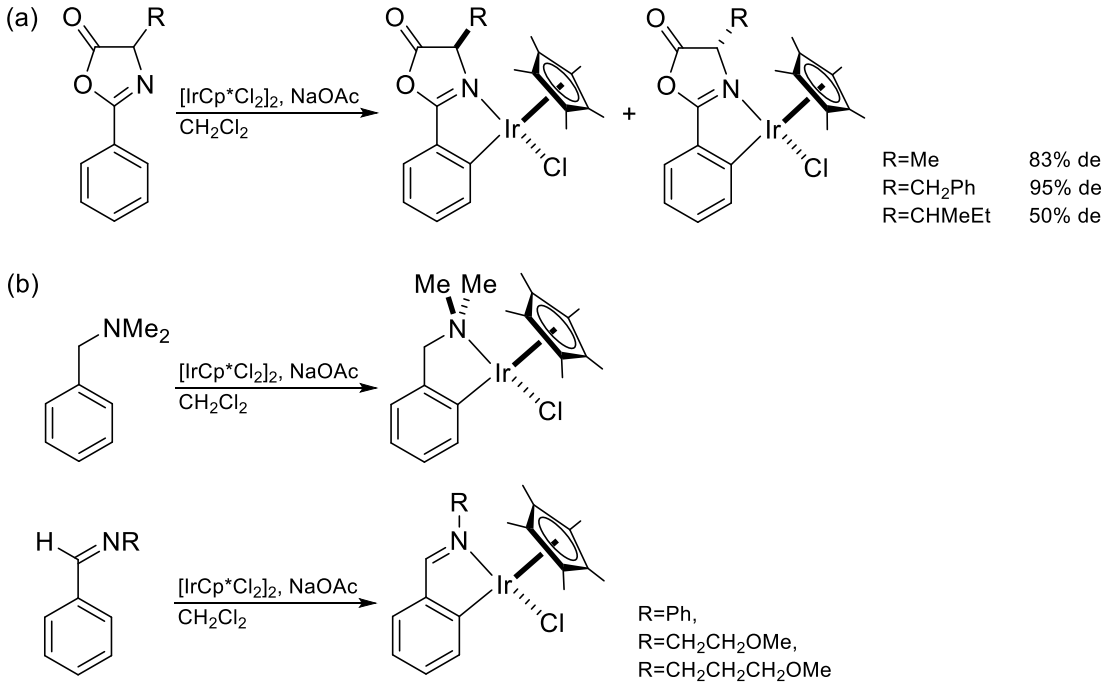

Scheme 1.60. Cycloiridation reactions performed by (a) Beck and (b) Davies.

A secondary method exists to access these piano-stool cycloiridated systems. The protocol was developed by Pfeffer and was based on his synthesis of structurally analogous ruthenacycles.[87] In this instance, abstraction of the chloride moiety by the potassium salt of hexafluorophosphate led to an activated cationic metal center for the initiation of the C–H bond activation process. In an example, *N*,*N*-dimethylbenzylamine was utilized for cycloiridation with $[IrCp^*Cl_2]_2$ in the presence of sodium hydroxide and potassium hexafluorophosphate.[88b] The desired metallacycle was obtained in excellent yields, although a cationic cycloiridated species was attained in the process. It should be noted that the neutral *chlorido* iridacycle can be easily attained if the product was washed in a solution of chloride ions.

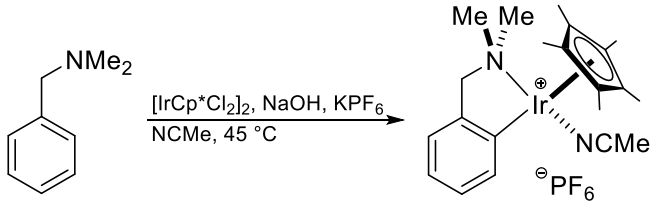

Scheme 1.61. Cycloiridation of *N*,*N*-dimethylbenzylamine *via* Pfeffer's protocol.

While both techniques afforded similar cycloiridated complexes, the mode of activation do differ slightly in nature. An obvious difference between the methods could be exemplified by the cycloiridation of (2*R*,5*R*)-2,5-diphenylpyrrolidine. In the case when the cyclometalating ligand was reacted *via* the activated cationic iridium(III) center, a mixture of the desired *ortho*-iridated product and oxidized pyrroline-derived metallacycle were obtained.[102] On the other hand, the chiral cycloiridated pyrrolidine complex could be solely attained when the same reaction was performed utilizing sodium acetate as base.[103]

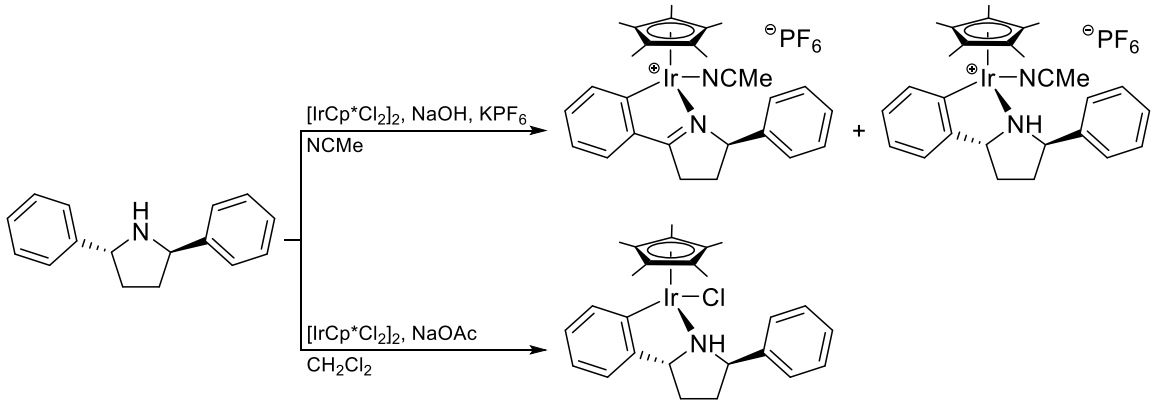

Scheme 1.62. Cycloiridation of (2*R*,5*R*)-2,5-diphenylpyrrolidine *via* Pfeffer's (top) and Davies' (bottom) protocol.

For half sandwich iridacycles that consist of a primary or secondary amine donor moiety, a separate class of Cp*-based cycloiridated complex was attainable. Simultaneous deprotonation at the nitrogen atom and abstraction of the *chloride* ligand by a strong base could result in an *amido* species with a *pseudo*-trigonal planar geometry. In an example, Ikariya treated an *ortho*-iridated 2-phenylpropyl-2-amine complex with potassium *tert*-butoxide to provide its corresponding *amido* iridacycle.[104] Whilst the species was long speculated to exist as an intermediate upon addition of a strong base, isolation of such class of complexes has only been achievable after the aforementioned study. It should be noted that the *amido*-type cycloiridation complexes were prone to acid hydrolysis which could return the iridacycle back to its neutral *amino*-variant. It is also worth mentioning that the complex has been identified to be the active species in the catalytic hydrogen transfer reaction.[104]

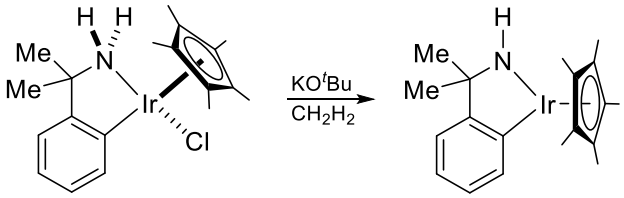

Scheme 1.63. Formation of *amido*-type cycloiridated complex from *amino*-derived iridacycle.

Last but not least, we discuss the piano-stool cyclometalated iridium(III) complexes of phosphinine. Müller recently reported the generation of κ^2-*C*,*P*-iridacycle from the reaction between 2,4,6-triphenylphosphinine and $[IrCp^*Cl_2]_2$ in the presence of sodium acetate.[105] Compared against the nitrogenous congeners described earlier in the section, the coordinated phosphinine complex did not undergo any conversion at room temperature. However, upon heating the reaction mixture, $^{31}P\{^1H\}$ NMR revealed clean conversion of complexed phosphinine to a new phosphorus-based compound – the cycloiridated phosphinine complex. It should also be noted that the pyridine counterpart does not undergo the cyclometalation reaction under identical reaction conditions to which the authors attributed it to kinetic stabilization by the 2-phenyl moiety on the phosphorus heterocycle to the iridium complex.

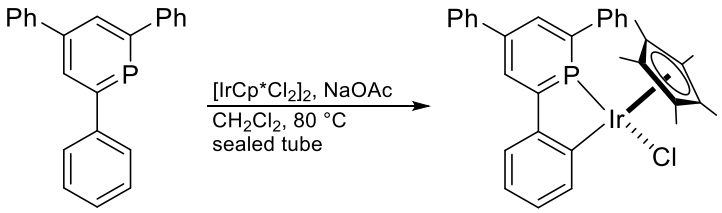

Scheme 1.64. Cycloiridation of 2,4,6-triphenylphosphinine.

1.7 Applications of Cyclometalation

Like the synthesis of its complexes, the boundaries to applications of cyclometalated complexes are virtually limitless. An exhaustive discussion into all applications of metallacycles is not possible and would be beyond the scope of the thesis. As such, we will begin the section with some of its humble beginnings, before proceeding to recent developments with regards to applications of these compounds.

1.7.1 Cyclometalated Complexes as Builders of Molecules

Upon ligation to the metal center, the nature of the coordinating donors within the cyclometalating ligand would be slightly altered due to the electron-withdrawing properties of the metal. The transfer of electron densities activates these groups allowing them to attack, or be attacked by external reagents under controlled environment, although, more often than not, the functionalization occurs *via* organometallic pathways initiated by the metal center. Due to this, the cyclometalated complex can act as a builder to bridge organic building blocks to the ligand framework with the intention to construct new or challenging molecules.

The reactions of organometallic complexes with coordinative donors including, but not limited to, carbon monoxide, olefins, alkynes, isocyanides and allenes, are well-documented in textbooks of organometallic chemistry.[106] As such, we will not delve into the fundamentals of these insertion reactions, but into the applications of these procedures in the total synthesis of complex molecules.

Another synthetic utility of metallacycles with regards to its role as builders can be seen from its use as an auxiliary to activate molecules for functionalization or for stereoinduction. Following the discussion of the former topic, we will take a look at an application of this class.

1.7.1.1 Synthesis of the Narwedine

A strategic plan to access narwedine, developed by Holton,[107] involved the prior synthesis of a norbelladine derivative which can be cyclopalladated to afford a pincer complex supported by a thioether and a tertiary amine moiety. While intramolecular palladation to attack the phenolate functionality failed with a variety of bases, treatment of the palladacycle with thalium(III) trifluoroacetate afforded the desired product (narwedine) upon hydrolysis. It was postulated that a number of rearrangement process proceeded prior to the formation of the natural product as shown in Scheme 1.65.

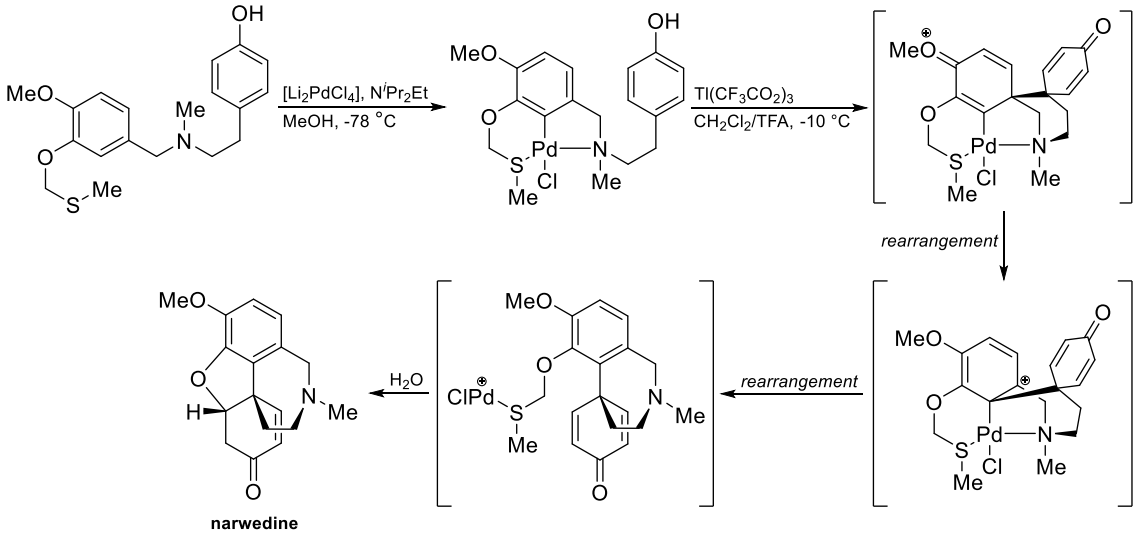

Scheme 1.65. Synthetic plan by Holton[107] to access narwedine.

1.7.1.2 Synthesis of the Core of Teleocidin B4

The synthesis of Teleocidin B4 core fragment by Sames[108] involved two palladacyclic intermediates in his synthetic strategy. The activation of the C_{sp3}–H bond directed by the methoxy and imine donors led to the first palladacycle which can be isolated in good yields. Transmetallation with a vinyl boronic acid derivative, followed by insertion, functionalized the sp^3-carbon center. The olefinic product was then cyclized through a formal hydroarylation process mediated by methanesulfonic acid. The resultant bicyclic compound was once again cyclopalladated, although carbon monoxide was inserted in this instance. It should be noted that a diastereomeric mixture was obtained at this point. Acidification of the metallacycles provided two racemic tricyclic precursors which was then separated and resolved at this stage. Further chemical manipulations would finally afford the desired core fragment.

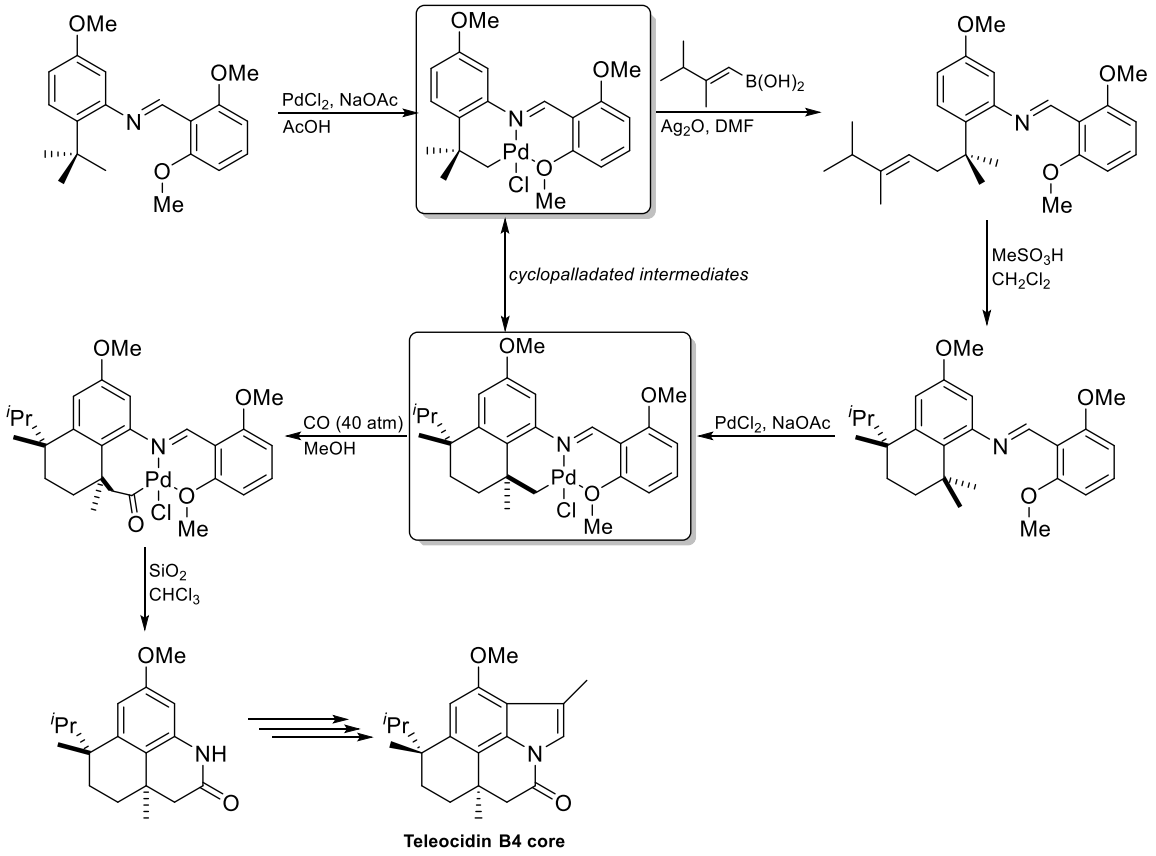

Scheme 1.66. Synthetic plan by Sames[108] to access the core of Teleocidin B4.

1.7.1.3 Chiral Cyclometalated Auxiliaries for Cycloaddition Reactions

One of the most common uses of metallacycles as auxiliaries involved stereoinduction in Diels-Alder [4+2]-cycloaddition reactions. Given the Lewis acidic nature of metal complexes, donor moieties bearing diene functionalities, such as phospholes, pyrroles, thiophenes or furans, can coordinate onto the vacant site within the metallacycle. The electron-deficient dienophile can then approach the coordinated heterocycle *via* the least sterically-hindered pathway to provide its enantioenriched Diels-Alder adduct.

The naphthalene-derived *N*,*N*-dimethyl-1-naphthylethylamine *ortho*-palladated complex is an interesting chiral auxiliary. The template is versatile, allowing adjustments to be made to control stereochemistries on the desired product through chemical treatment of the palladacycle. In an example, the phosphole-containing complex, without any alterations to the metallacycle, can proceed *via* an *endo* pathway with methyl acrylate as the dienophile.[109] However, upon abstraction of the halide moiety from the coordinated complex, the procedure progressed through an *exo* pathway for the same substrate.[110] It was proposed that the abstraction process allowed the coordination of the dienophile to the metal through its activating group. This resulted in an intramolecular cycloaddition process yielding the *exo*-adduct. Nonetheless, it is worth mentioning that both processes generated a phosphanorbornene species with four stereogenic centers. Lastly, to liberate the free ligand, the complex could be treated with potassium cyanide or 1,2-bis(diphenylphosphino)ethane to provide the free *C**,*P**-chiral bicyclic phosphine.

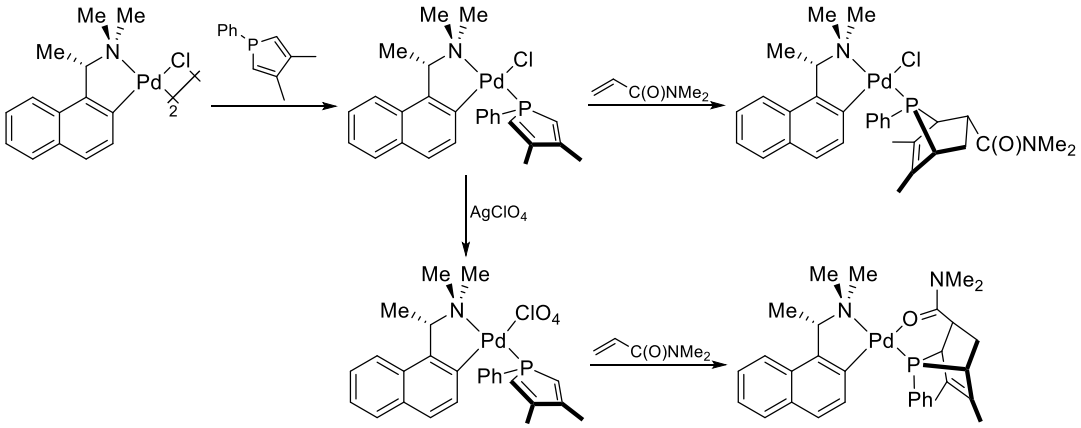

Scheme 1.67. Chiral auxiliary-promoted Diels-Alder [4+2]-cycloaddition reaction.

1.7.2 Cyclometalated Complexes as Resolution Agents

By nature, most cyclometalated complexes are Lewis acids. As such, one of the earliest uses of chiral metallacycles involved the optical resolution of racemic compounds. Two main methods exist to separate enantiomers from a given racemic mixture: (a) a physical separation of the resultant diastereomers, formed *via* the coordination of the racemate to the enantiopure cyclometalated complex, prior to release of the enantiomers upon chemical degradation, and (b) a chiral recognition of one form of the enantiomer to the metallacycle due to higher affinity to the host (a process akin to kinetic resolution).

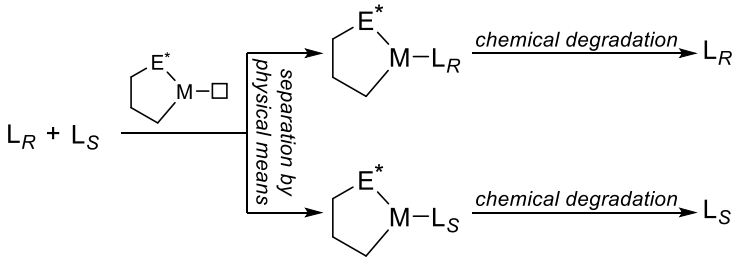

Scheme 1.68. Resolution by physical separation of diastereomers.

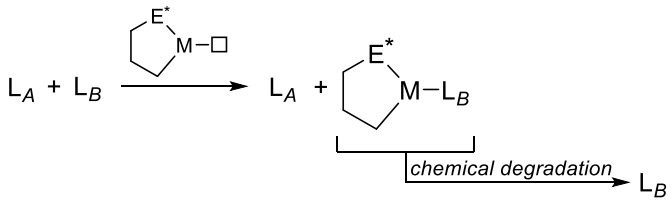

Scheme 1.69. Resolution by chiral recognition.

The optical resolution of *o*-phenylenebis(methylphenylphosphine) was achieved *via* the use of cyclopalladated (*R*)-*N*,*N*-dimethyl-1-phenylethylamine complex as the resolving agent.[111] The synthesized racemic 1,2-diphosphine was coordinated to the enantiopure palladacycle affording two internal disastereomers. Treatment of the reaction mixture with ammonium hexafluorophosphate selectively precipitated one of the adducts. Further recrystallization of the two pots of enantioenriched diastereomers yielded both isomers with similar opposing specific optical rotation. Finally, the liberation of the phosphines was achieved *via* a two-step procedure to provide the enantiomerically pure 1,2-diphosphines in excellent overall yield.

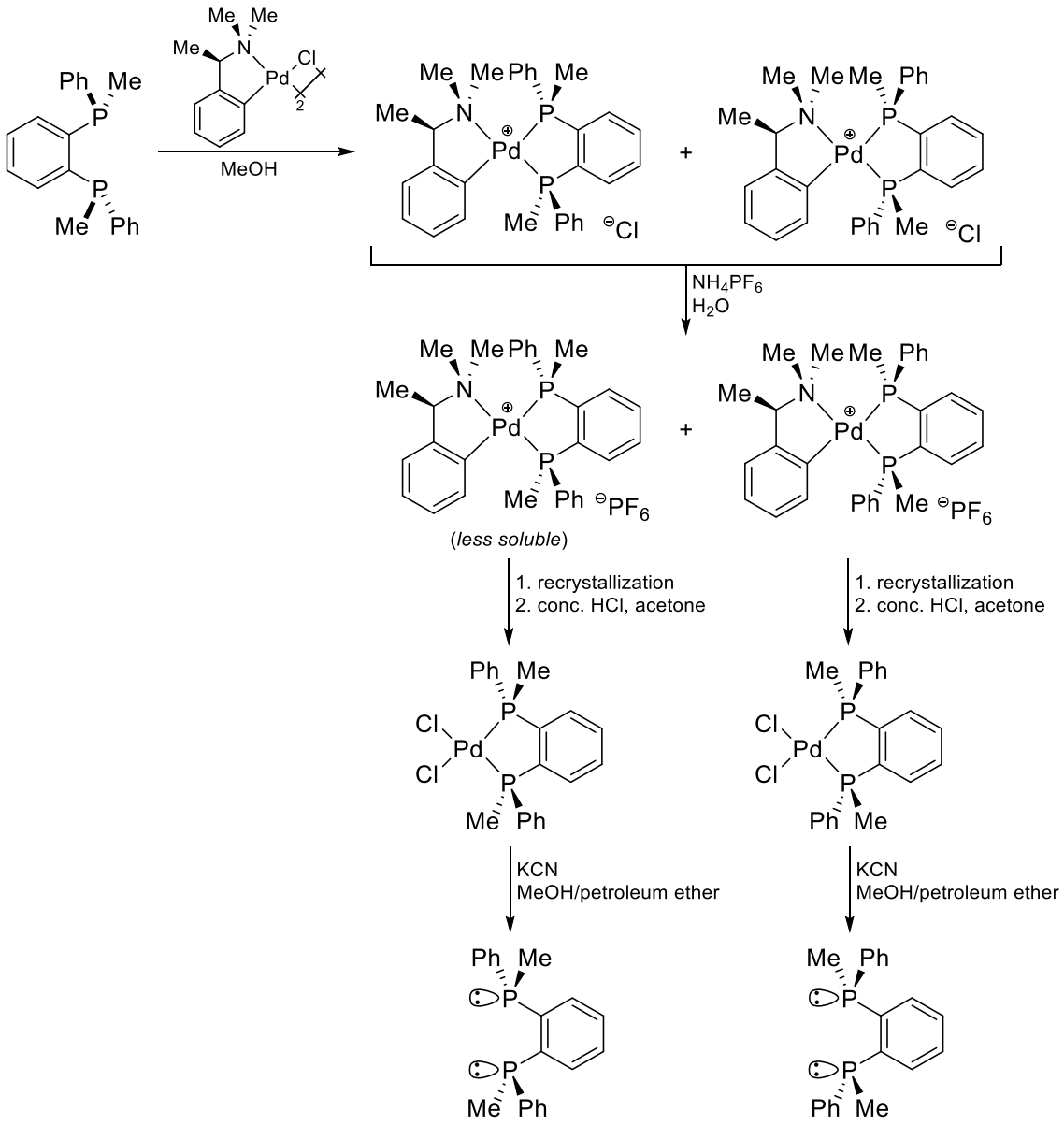

Scheme 1.70. Resolution of racemic *o*-phenylenebis(methylphenylphosphine) by cyclopalladated (*R*)-*N*,*N*-dimethyl-1-phenylethylamine complex.

The chiral recognition of racemic 2-(alkylsulfinyl)phenol in a chiral-at-metal cycloiridated complex was published recently.[112] In the process, only the (*S*)-enantiomer of sulfoxide coordinates to the enantiopure host *δ*-[Ir({κ^2-*C*,*N*}-ppy)$_2$(NCMe)$_2$] forming a stable adduct under dynamic thermodynamic equilibrium. Separation of the complex from the uncoordinated (*R*)-isomer was achieved through precipitation and simple filtration. Further purification by recrystallization of the former, and column chromatography in the case of the latter, would provide the pure enantiomeric compounds. To liberate the coordinated enantiopure sulfoxide from the iridacycle, the complex was treated with ammonium hexafluorophosphate, followed by trifluoroacetic acid, in acetonitrile. It should be noted that the chiral-at-metal receptor could be reused without any degradation in terms of reactivity or stereoselectivity.

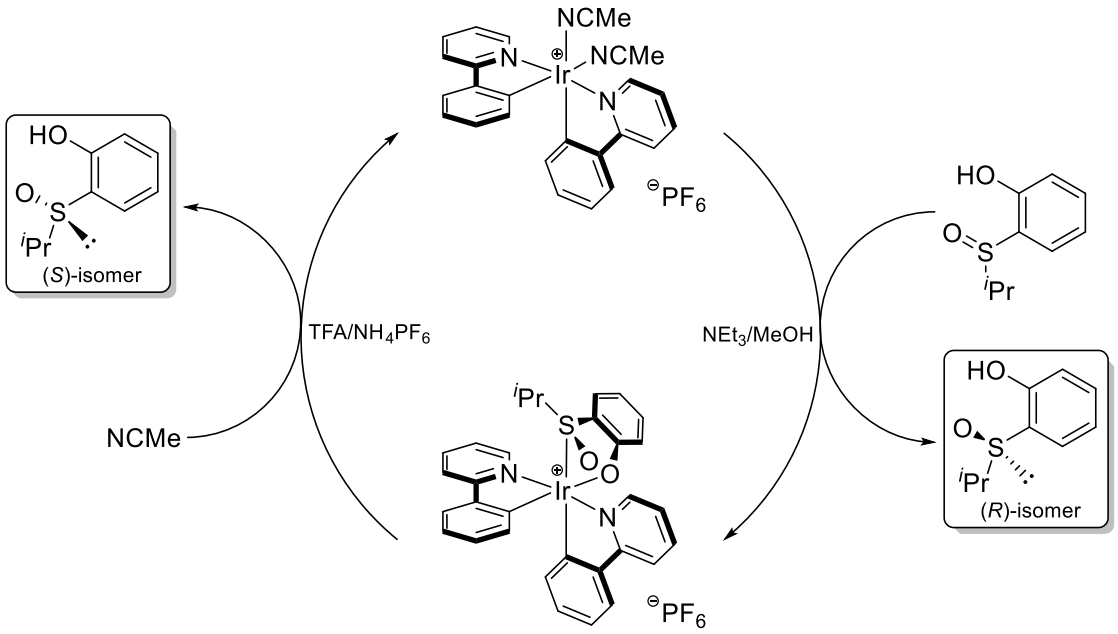

Scheme 1.71. Resolution of racemic 2-(alkylsulfinyl)phenol by cycloiridated complex *δ*-[Ir({κ^2-*C*,*N*}-ppy)$_2$(NCMe)$_2$].

1.7.3 Cyclometalated Complexes as Reactive Intermediates: The C–H Bond Functionalization Reaction

One of most significant contribution of cyclometalation to applications is the concept of ligand-directed C–H bond functionalization. The site-selective functionalization of unreactive carbon centers has provided an attractive strategy to generate compounds with new functionalities and/or with stereoselectivity (if the metallacycle consist of a chiral element within the molecule). Building on the idea that cyclometalated complexes could couple to building blocks stoichiometrically, the cycle could be closed through either decoordination of the more labile product or reductive elimination of the anionic ligands from the coordination sphere. Nonetheless, the complex must be able to regenerate itself for the process to be deemed catalytic.

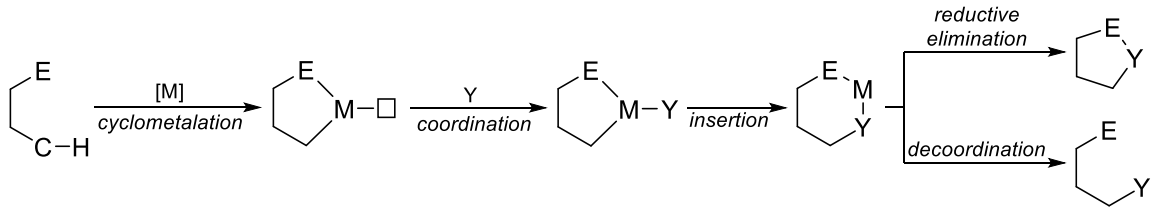

Scheme 1.72. General schematic to catalytic C–H bond functionalization reaction.

Extensive research into the topic over the past decades have led to the optimization, as well as the development, of numerous protocols on C–H bond functionalization.[30, 113] Since the intention of the thesis was to provide an overview of the topic, we will cover only recent progress on the area. Nonetheless, the technique has become an indispensable tool to activate C–H bonds and can be mediated by numerous transition metal elements including, but not limited to, palladium,[114] ruthenium,[115] rhodium,[116] cobalt,[117] iron[118] and copper[119].

An interesting development involved the β-C_{sp3}–H iodination of ketones as a proof-of-concept catalytic reaction to direct C–H bond functionalization to the said bond.[120] Whilst the procedure required the transformation of the carbonyl moiety to its transient oxime-based directing group, the installation of the commercially-available aminooxyacetic acid auxiliary to the ketone functionality was simple and did not necessitate addition purification. The C–H bond activation soon followed to provide a

metallacyclic intermediate (supported by the isolation of a trapped palladacycle when the reaction was performed stoichiometrically) which quickly iodized the activated sp^3-carbon to afford the *β*-iodoketone product. Nonetheless, it should be noted that, in some cases, diiodination was observed in some substrates. It is also worth highlighting that the reaction will not proceed efficiently if *O*-methyl oxime, instead of *imino*-carboxyl, was utilized as the directing group.

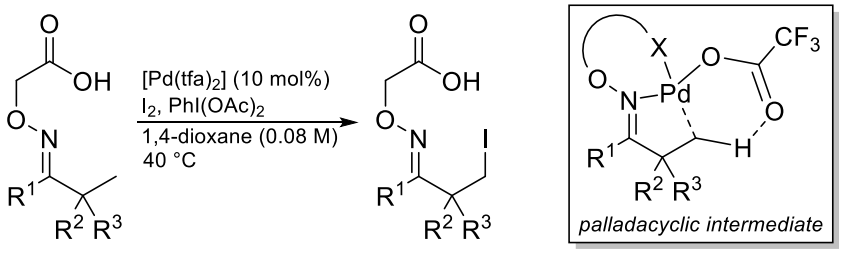

Scheme 1.73. *β*-C_{sp3}–H iodination *via* palladium(II)-catalyzed C–H bond activation reaction.

Another impressive work involved the tuning of the ancillary Cp ligand to alter the reaction pathway of a catalyzed reaction. In the study, *N*-pivaloyloxybenzamide was envisioned to cyclized with derivatives of $[RhCp^XCl_2]_2$ to provide a rhodacycle, which subsequently inserted a conjugated enynone moiety into the cyclorhodated complex to provide multi-ring heterocyclic systems.[121] It was found that an electron-deficient Cp^X ligand would initiate a 5-*exo*-*dig* cyclization prior to insertion to give a carbene intermediate. The carbene then inserts into the rhodacycle to give a six-membered species, which consequently afforded the bicyclic quaternary carbon-centered heterocycle upon reductive elimination. On the other hand, the electron-donating Cp^X ligand would induce insertion of the alkyne directly to the *ortho*-rhodated complex to provide a seven-membered cyclometalated complex. Rearrangement quickly proceeded to offer the tricyclic heterocycle. It should be noted that the protocol was also sensitive to steric effects, although its influence was less prevalent, when compared against electronic effects, based on theoretical calculations.

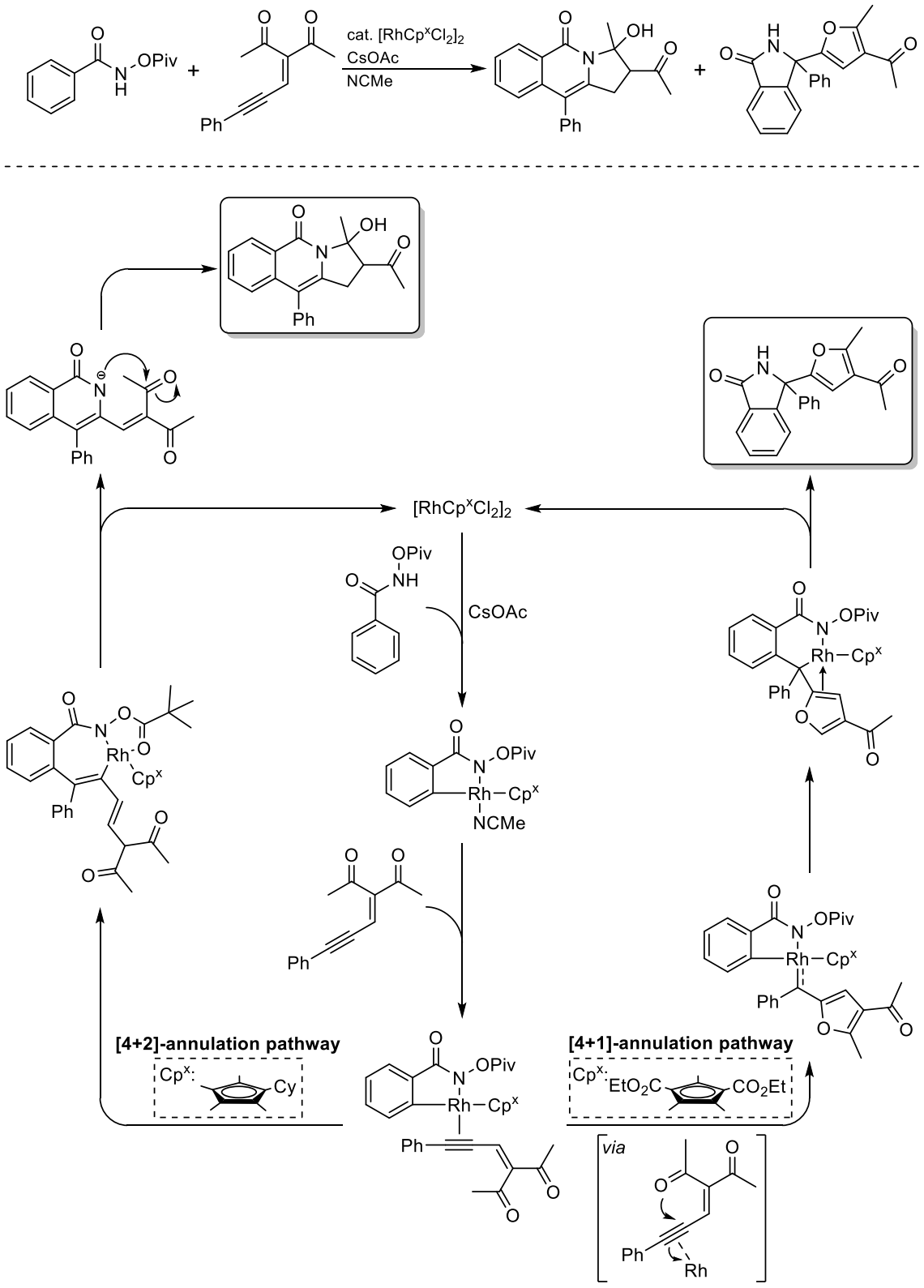

Scheme 1.74. Proposed mechanism to [4+1]/[4+2] annulation mediated by rhodium Cp-based catalyst.

Lastly, we describe the ligand-mediated *meta*-C–H bond functionalization of benzylamines. In the earlier cases, functionalization of the substrates all occurred at the *ortho*-position of the aromatic ring. While the reactions were regioselective, a limitation of the C–H bond functionalization reactions was its difficulty to activate bonds beyond the proximity of the coordinated metal. An elegant solution to this was to leverage on the *ortho*-metalation and translate the activation to the *meta*-site *via* a transient mediator.[122] Here, a benzylamine derivative could be functionalized at the *meta*-position *via* a palladium-catalyzed procedure involving 2-carbomethoxynorbornene as the transient mediator.[123]

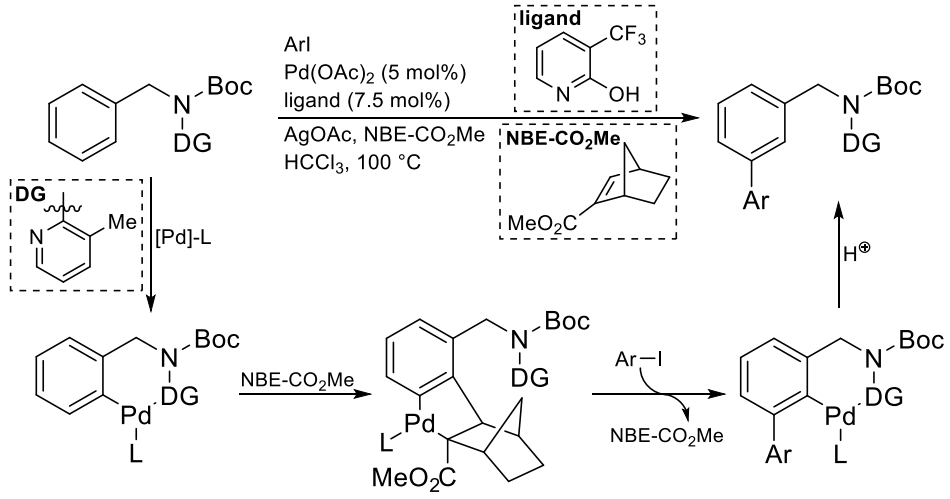

Scheme 1.75. *meta*-C–H bond functionalization of benzylamine derivatives.

In the above example, the benzylamine derivative was *ortho*-metalated providing a six-membered palladacycle intermediate. A molecule of norbornene derivative then coordinates onto palladium and inserts into the aromatic ring. Subsequently, the intermediate activates its *ortho*-C–H bond, directed by the carbanion donor, resulting in a *meta*-metalated species. The *meta*-carbon was then functionalized and returned to its *ortho*-palladated form, releasing the norbornene moiety. Protonolysis of the complex then afforded the *meta*-functionalized product.

1.7.4 Cyclometalated Complexes as Catalysts

In many ways, cyclometalated complexes are versatile. Even as catalysts, numerous modes of activations exist to push reactions towards its desired pathway. Owning to its tunable nature, the compounds can vary, with regards to its electronics and sterics, to participate in catalytic oxidative-reductive pathways or simply through activation of substrates as Lewis acids. Furthermore, ligands within these complexes can sometimes even act as sites for catalysis without the need for the substrates to interact with the metal center.

The use of metallacycles as catalysts was reported as early as the 1980s.[20b] While it was not as widespread in the past, its use in catalysis in the recent decades has since expanded extensively to include numerous applications. As such, a comprehensive summary into all its catalytic applications is difficult. We will, however, describe some of the more important, as well as recent, works in the field.

1.7.4.1 Cross-Coupling Reactions

Whilst the first catalytic application was reported much earlier, metallacycles as catalysts did not really take off until the use of a tris-*o*-tolylphosphine-derived palladacycle for the carbon-carbon bond formation reaction. Developed by Herrmann in 1995, the phosphapalladacycle was found to be extremely robust for the coupling of aryl halides and styrene derivatives.[5] The same complex can also participate as efficient catalysts for other cross-coupling protocols.[124]

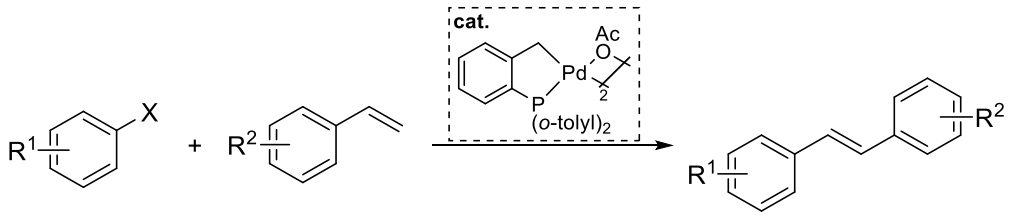

Scheme 1.76. Catalytic Heck-type cross coupling mediated by Herrmann catalyst.

Disappointingly, further investigations revealed the actual role of the palladacycle to be generators of lowly-ligated colloidal palladium particles. An illustration of the effect can be described from the heterogenous catalytic experiments performed by Nowotny in which the immobilized cyclopalladated complex were shown to be inactive upon further use of the catalyst after its initial run.[125] In other cases, palladium colloids were detected from transmission electron microscopy.[126] Nonetheless, it should be noted that the slow release of the nanoparticles by the palladacycles allowed the reaction to progress efficiently without the need for any other external ligands or stabilizers.

1.7.4.2 Hydrophosphination Reactions

Suffering from reduced efficiency and selectivities, acid- and base-catalyzed hydrophosphination reactions often leads to uncontrollable reactions or undesirable products.[127] The limitations of these traditional methods pressed for the development of novel approaches for selective catalytic hydrophosphination procedures.

Access to stereo- and regio-specific Markovnikov addition of secondary phosphines to activated olefins have been perfected by the research groups of Duan and Leung. In both cases, cyclopalladated complexes were shown to be efficient catalysts for the catalytic asymmetric hydrophosphination of chalcone and its derivatives.[128]

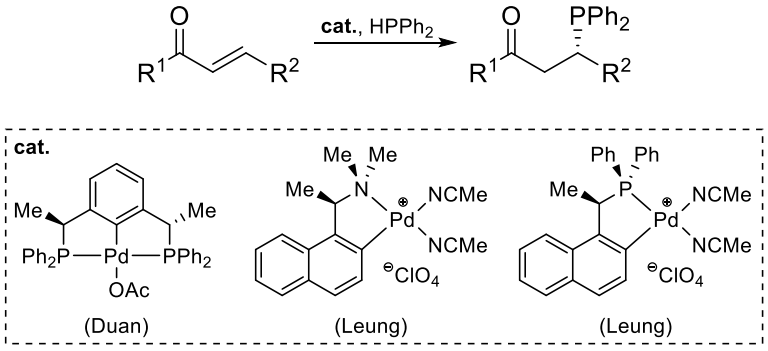

Scheme 1.77. Catalytic asymmetric hydrophosphination of chalcone and its derivatives.

The expansion of scope to other olefin-containing functionalities including, but not limited to, imines,[129] aldehydes,[130] malonates,[131] α-ketoesters,[132] sulfonic esters,[133] *N*-enoyl phthalimides[134] and alkenylisoxazoles[135] were also performed by the two groups. Whilst the protocols utilized palladacycles as catalysts, the mechanistic aspects of the reactions were different due to the availability of vacant sites within the complexes. In the case of the cyclopalladated pincer complex, the sole vacant site adds the phosphide moiety to the activated substrate through an external nucleophilic attack. On the other hand, with the privilege of having two labile ligands within its coordination sphere, the bisacetonitrile complex inserts the phosphide *via* an intramolecular nucleophilic attack onto the substrate.

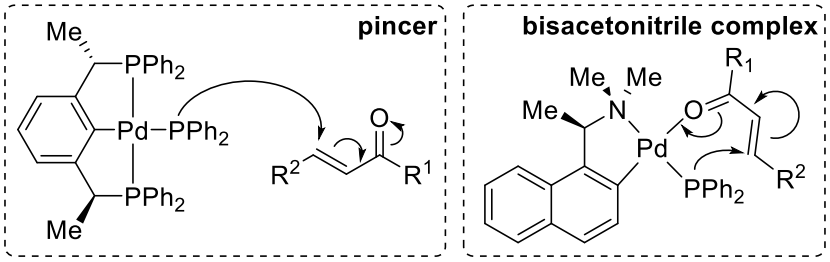

Figure 1.17. Mechanistic aspects to the addition of diphenylphosphine to chalcone derivatives by chiral cyclopalladated pincer and bidentate *C,N* complexes.

More interestingly, when optically-active modified pincer complex and *C**,*P*-bisacetonitrile complexes were compared in the catalytic asymmetric hydrophosphination of $\alpha,\beta,\gamma,\delta$-alkylidenemalonate ester, the two catalysts portrayed different regio-selectivities affording the adducts with the phosphine moiety at different positions.[136] Such observation was attributed to steric effects posed by the bulkier pincer catalyst during its attack at the malonate species.

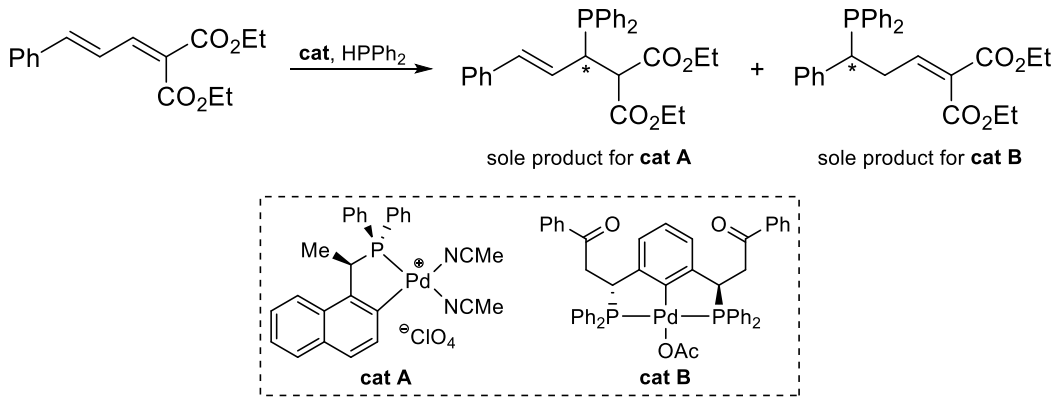

Scheme 1.78. Catalytic asymmetric hydrophosphination of *α*,*β*,*γ*,*δ*-alkylidenemalonate ester.

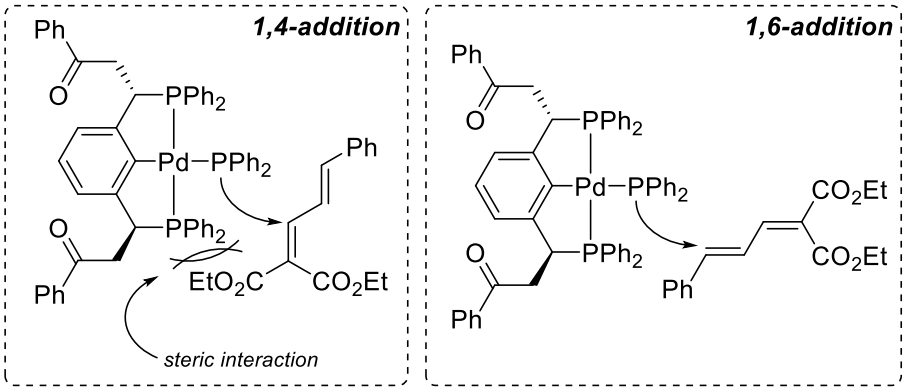

Figure 1.18. Steric effects associated with the pincer complex in the addition procedure.

1.7.4.3 Hydrogen Transfer Reactions

The catalytic transfer hydrogenation reaction mediated by half sandwich cyclometalated species is an interesting example in which the process does not directly involve the metal center. Depending on the type of donor coordinated to the metal, the catalytic cycle can vary significantly.

In the case of *imino*-type iridacycles, theoretical calculations[137] revealed that the catalyst precursor, in the presence of formic acid/triethylamine azeotrope, would provide a *formido* complex which readily eliminates carbon dioxide to give its *hydrido* derivative. The compound then interacts with a protonated iminium species, reducing the latter upon exchange with a molecule of deprotonated formic acid, regenerating the catalyst at the same time.

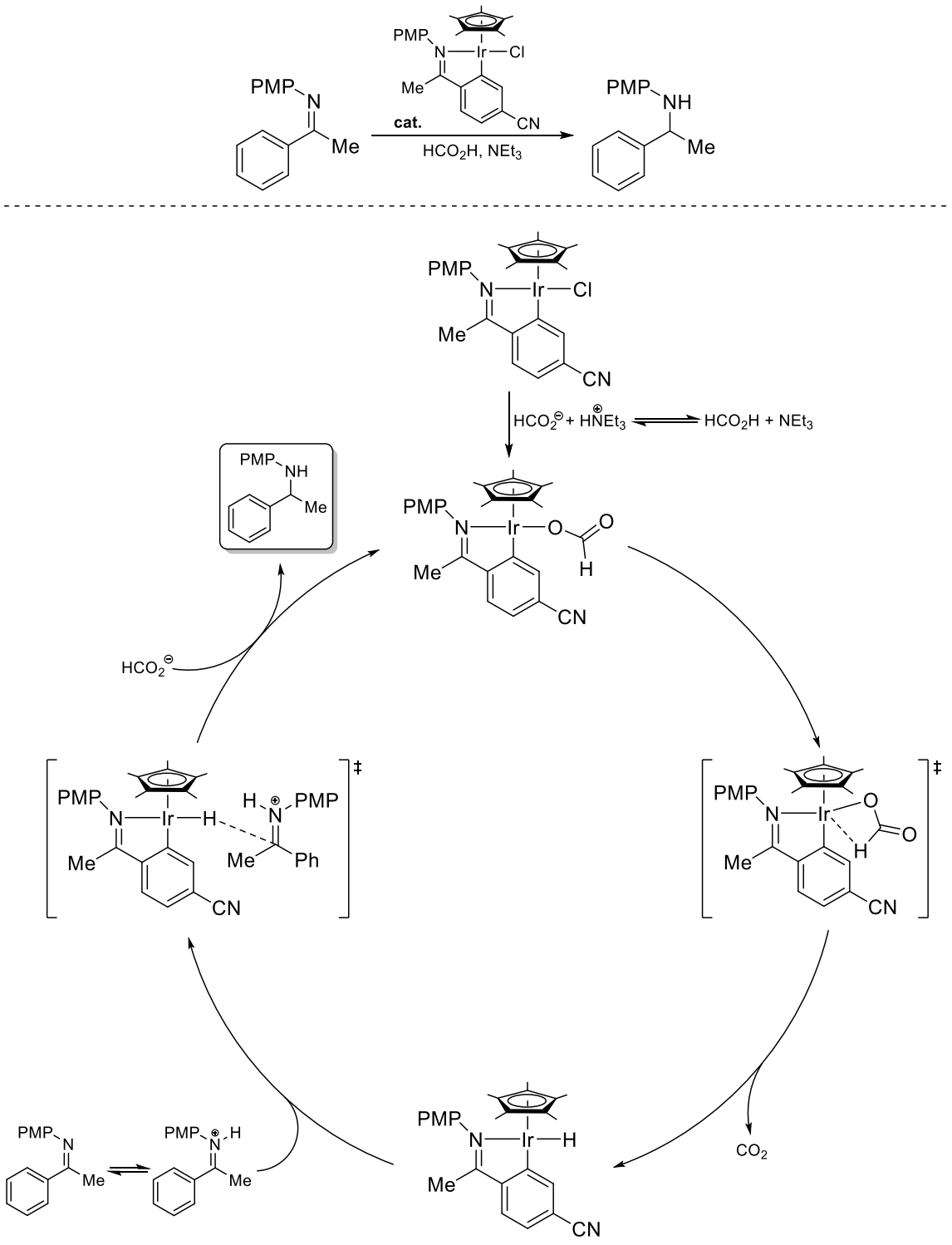

Scheme 1.79. Catalytic cycle for the hydrogen transfer reaction by cycloiridated *imino*-based complex.

On the other hand, an *amino*-based iridacycle would catalyzed the hydrogen transfer process through a cyclometalated *amido* intermediate (*see next page for catalytic cycle*).[104] The latter active species can be obtained through a deprotonation-abstraction process initiated by the base. The *amido* functionality was then protonated by the alcoholic solvent prior to coordination of the charged alkoxide species to the iridium(III) center. The complex subsequently undergoes *β*-hydride elimination affording an *ortho*-iridated *hydrido*-derived complex. The substrate finally enters the catalytic cycle and was reduced *via* a six-membered transition state to provide the hydrogenated product. It should be noted that the protocol could be applied to optically-active *pseudo*-tetrahedral metallacycles to afford its corresponding enantioenriched compounds.[88c, 103-104, 138]

The process can also be exploited for the alkylation of amines through a stepwise oxidation-reductive amination-reduction procedure. In an example, benzyl alcohol was utilized to react with various derivatives of aniline to provide a range of benzylated amines.[139] The scope of the reaction was then expanded to include other alkyl alcohols or symmetrical secondary amines as substrates for the alkylation of anilines.[139]

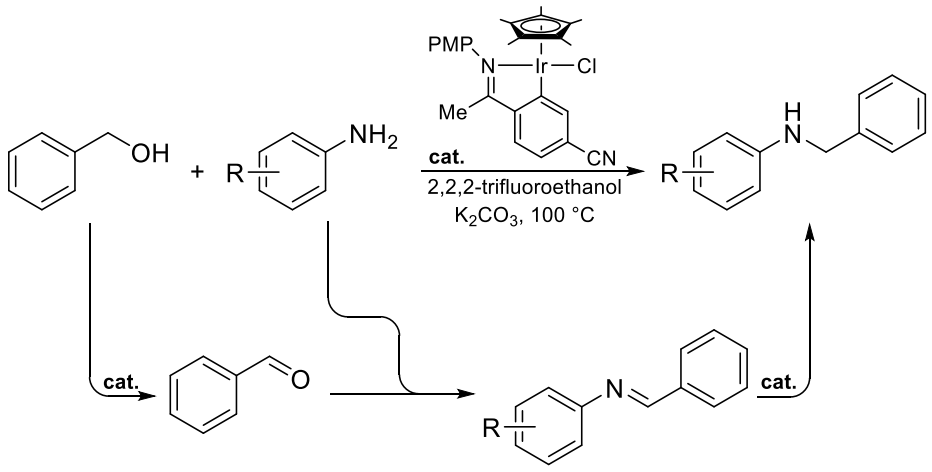

Scheme 1.80. Alkylation of amines by cycloiridated complexes through hydrogen transfer pathway.

Lastly, whilst the discussion of catalytic hydrogen transfer reactions within the section concentrates on *pseudo*-tetrahedral cycloiridated complexes, it should be emphasized that the reaction could be applied to metallacycles of other transition metal elements.

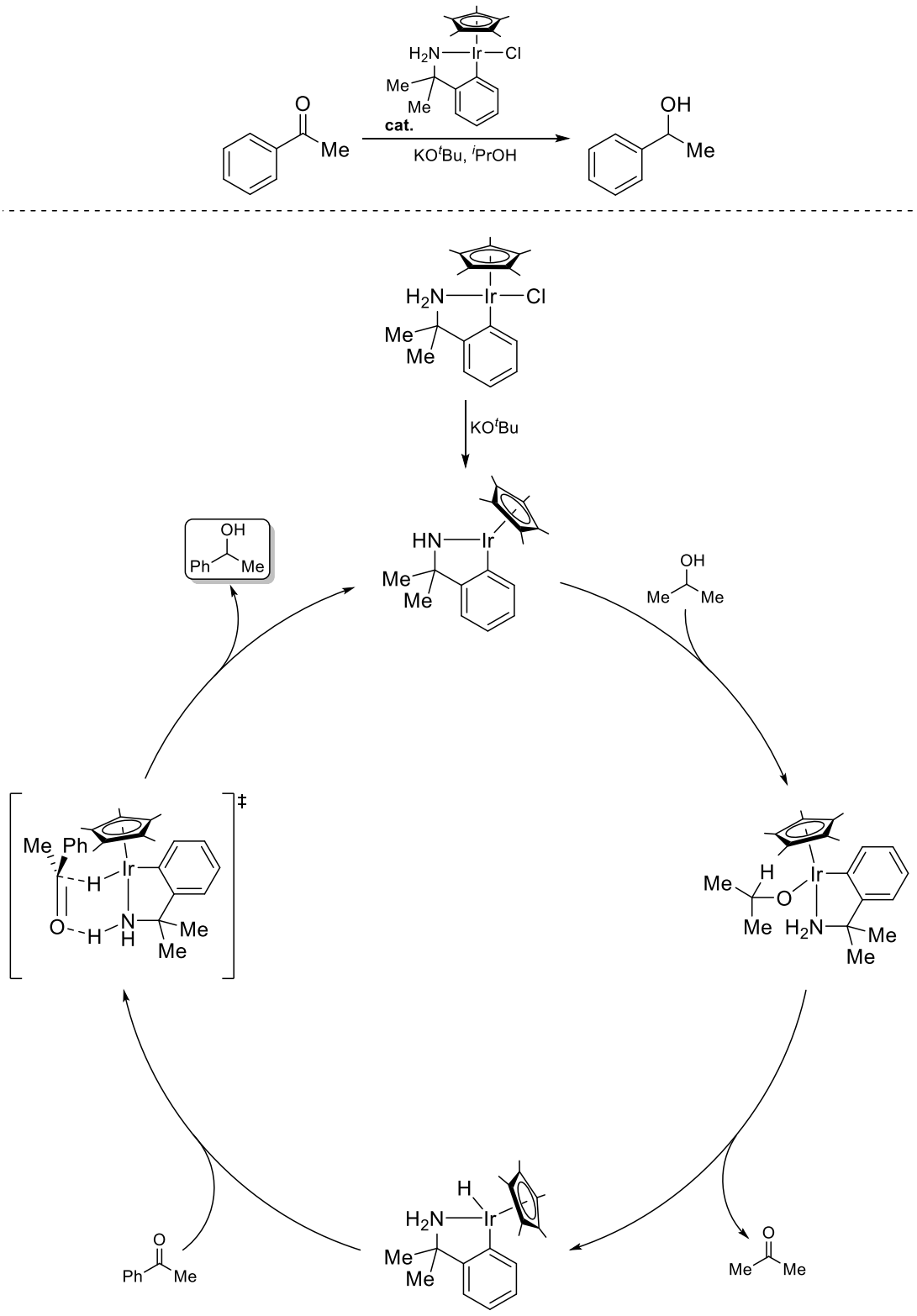

Scheme 1.81. Catalytic cycle for the hydrogen transfer reaction by cycloiridated *amino*-based complex.

1.8 Our Conquest into Cyclometalation Chemistry

With an interest in asymmetric synthesis and catalysis, our group has been utilizing chiral cyclometalated complexes as auxiliaries and catalysts for the generation of optically-active compounds.[110, 140] Particularly, the bidentate cyclopalladated *N*,*N*-dimethyl-1-naphthylethylamine complexes has been efficient in numerous asymmetric applications performed in our group (*refer to* sections 1.7.1.3 *and* 1.7.4.2 *for examples*).[110, 140a, 140b]

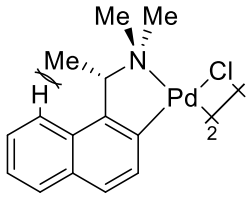

Figure 1.19. Cyclopalladated *N*,*N*-dimethyl-1-naphthylethylamine complex.

An important feature within the palladacycle which grants selectivity in its applications was the presence of stereogenic lock within the molecule. The lock was effected from an intramolecular interaction between two groups, namely the methyl substituent at the stereogenic carbon center and its neighboring proton on the naphthalene ring, which kept the five-membered puckered ring system from undergoing interchanging conformational ring flip.[141] The consequence was a complex with some form of chiral helicity about its ligand framework which could dramatically amplify the stereoinduction effects to the substrates in applications.

Based on this concept, we set off in a journey to expand our collection of metallacycles. Encompassing the conformational locking mechanism into a new cyclopalladated system, we constructed a novel molecule with 1-(9-phenanthryl)-ethylamine motif.[142] The idea was to enhance stereoselectivity through extended projection of the chiral ligand framework *via* an additional spacer group near the coordination sphere to influence greater stereochemical induction to the substrate. As a proof of concept, we put the optically-active auxiliary into use in the asymmetric *endo*-[4+2]-cycloaddition reaction.[142] The experiment was met with significant improvements to the selectivity of the protocol as compared to the 1-naphthylethylamine-based cyclopalladated complex.

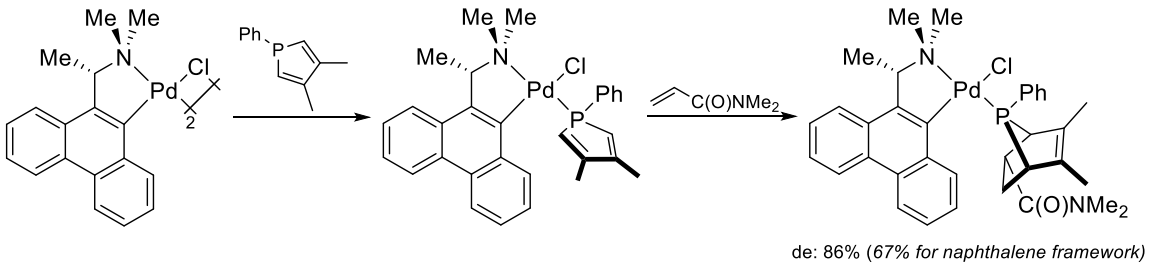

Scheme 1.82. Asymmetric *endo*-[4+2]-cycloaddition reaction mediated by 9-phenanthrene-based palladacycle.

With the earlier success, we proceeded to tweak the ligand motif gradually to understand the role of each substituent within the cyclometalating ligand.[143] Experiments into the extent of conformational lock were also reviewed in these studies. Generally, in most of these cases, enhancement in stereoselectivity was observed, although bulkier projecting spacer groups were shown to slow the asymmetric Diels-Alder [4+2]-cycloaddition procedure.[143a]

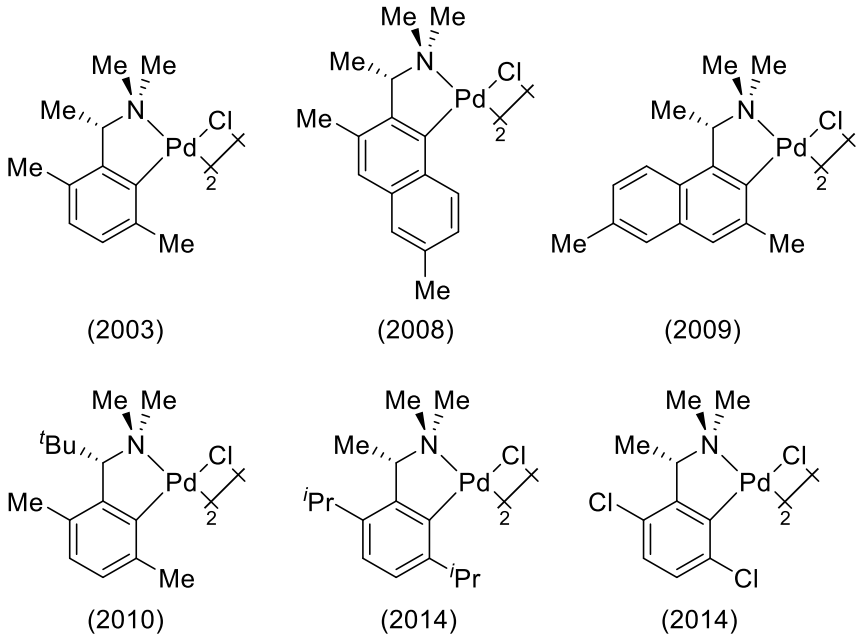

Figure 1.20. Cyclopalladated *C**,*N*-palladacycles developed by our group.

Simultaneously, we researched upon modification of the donor group to its phosphine and arsine derivative.[38, 144] Whilst the arsine-based cyclopalladated complex has limited applications at the time of writing, the activity of the phosphorus-based palladacycle in asymmetric applications were robust and efficient.[140a]

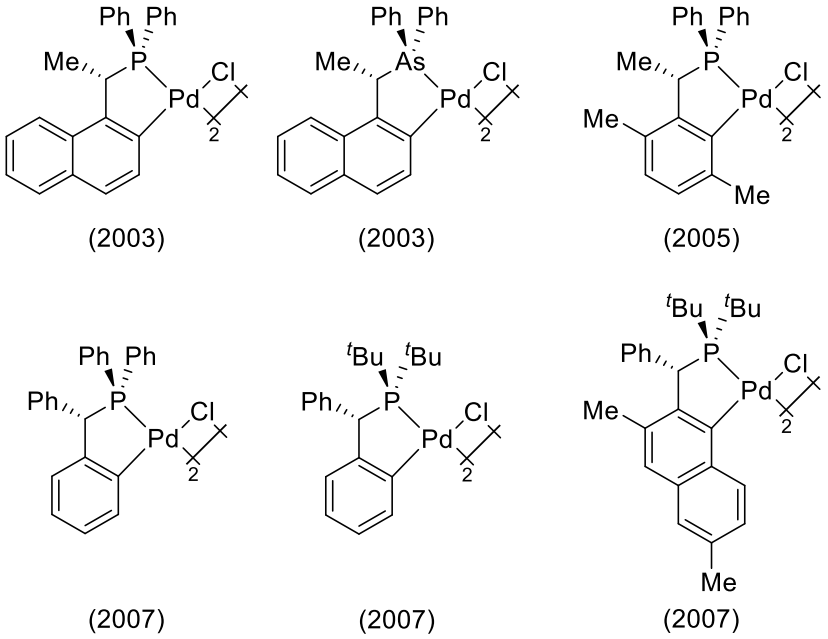

Figure 1.21. Cyclopalladated *C**,*P*-palladacycles developed by our group.

A practical disadvantage in the generation of our *C**,*N*- and *C**,*P*-cyclopalladated complexes was the need for optical resolution at some stage into its synthesis (*see* Scheme 1.83; *exemplified by the synthesis of the 1-ethylnaphthylphosphine palladacycle*).[38, 142-145] As such, access to optically-pure cyclometalating agents through asymmetric catalysis would present benefits to the formation of these chiral metallacycles in two ways: (a) the ability to produce significant quantities of chiral motifs with small amounts of catalyst, and (b) the reduced tediousness to obtain the chiral cyclometalating ligand through optical resolution (which, consequently, reduces cost and waste, as well as saving time for the chemist). Through the catalytic asymmetric hydrophosphination protocol we have developed, we were able to afford *C**-chiral tertiary phosphine ligands which can be utilized as cyclometalating ligands for the synthesis of new chiral cyclopalladated complexes.[146]

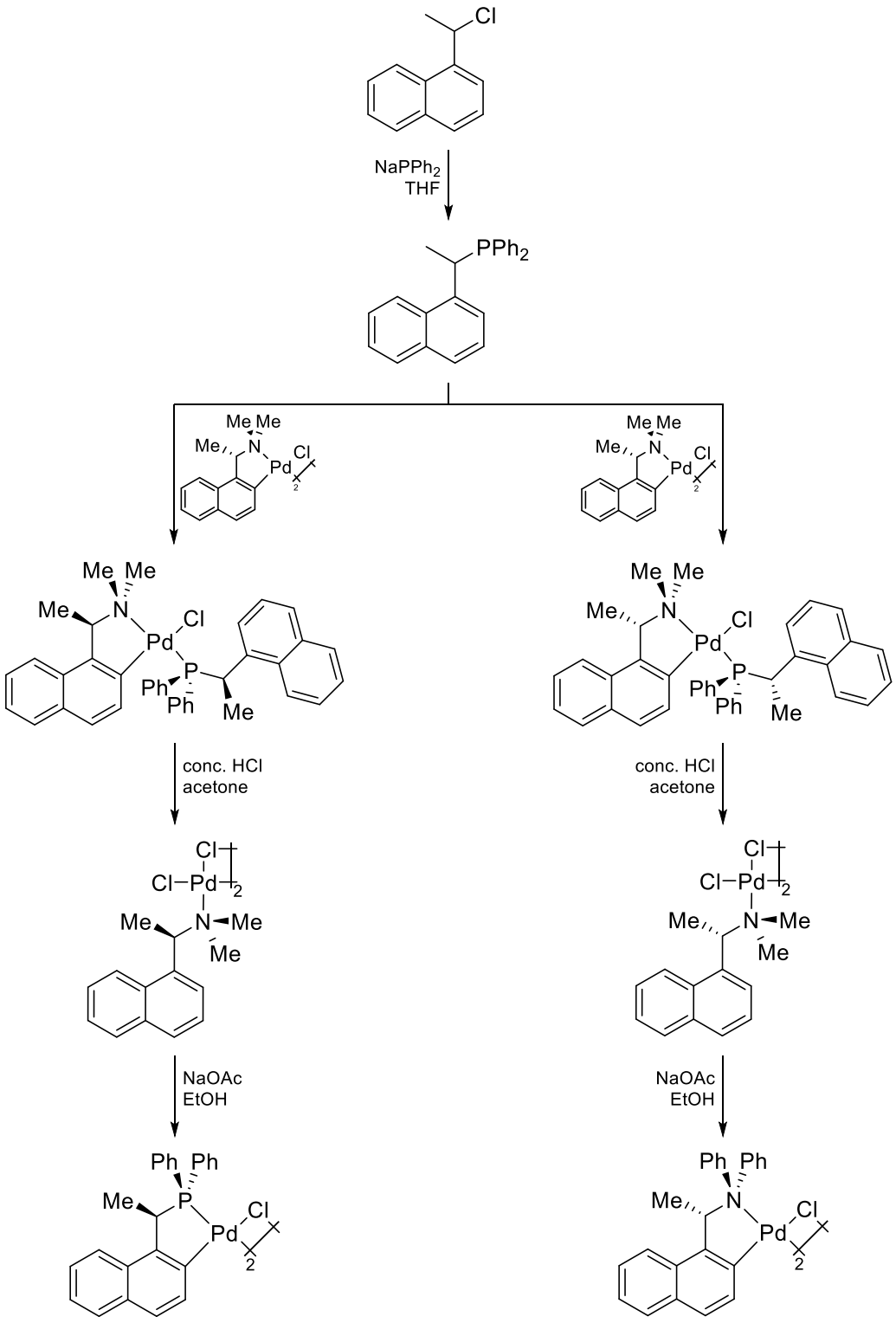

Scheme 1.83. Synthesis of chiral cyclopalladated 1-ethylnaphthylphosphine complexes from 1-(1-chloroethyl)naphthalene.

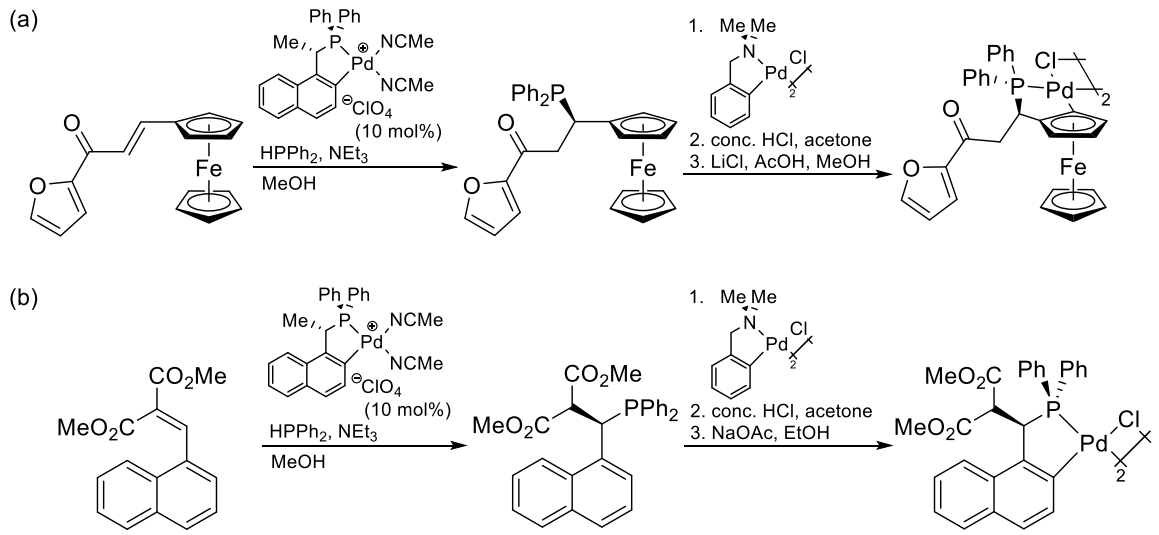

Scheme 1.84. Synthesis of chiral cyclopalladated complexes ((a) ferrocenyl-based palladacycle (2014) and (b) naphthalene-based palladacycle (2017)) from cyclometalating ligands obtained *via* catalytic asymmetric hydrophosphination reaction.

We have also begun the expansion of our library of metallacycles to chiral terdentate pincer complexes. Through catalytic asymmetric hydrophosphination, we were able to generate its chiral cyclometalating ligand, which upon further cyclometalation would yield their corresponding optically-active *P*,*C*,*P*[136, 147] *P*,*C*,*N*[147] and *S*,*C*,*N*[148] pincer-type metallacycles. It is also worth mentioning that these pincer compounds are efficient as catalysts in asymmetric applications.[149]

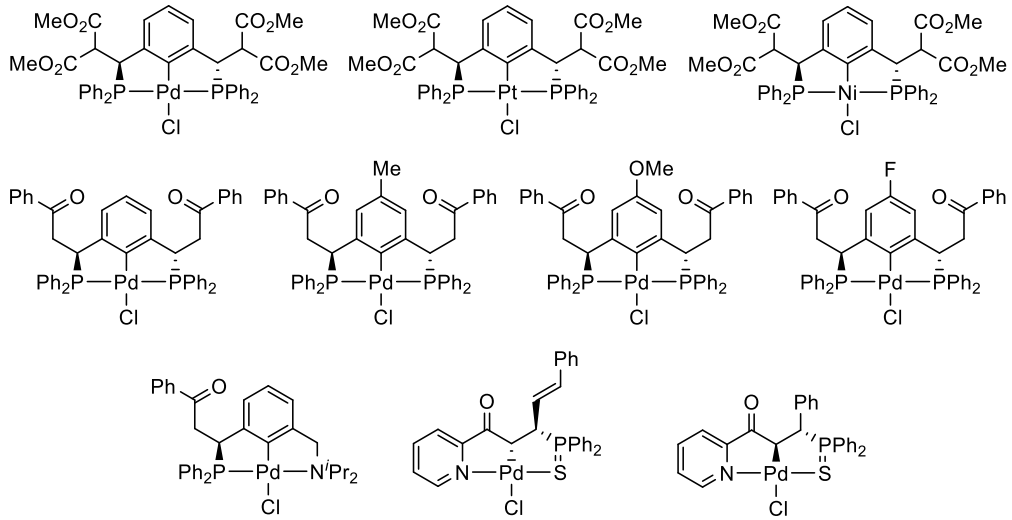

Figure 1.22. Chiral pincer complexes developed by our group.

1.9 Outlook and Research Objectives

The chemistry of cyclometalation is fascinating. Despite being one of the most developed areas in organometallic chemistry with a history of more than half a century, the field remained popular and continues to be updated with new concepts and applications with each passing day.

Over the past decade, we have been building knowledge on the electronic and structural aspects of cyclopalladated complexes.[38, 141c, 142-146, 150] Together with its spectroscopic and crystallographic data, as well as assistance from consequences in applications such as asymmetric Diels-Alder [4+2]-cycloaddition reactions or catalytic asymmetric hydrophosphination protocols,[140a] we were able finetune these chiral palladacyclic compounds to suit our needs.

With much work completed in the field of cyclopalladation, we felt the urge to expand and understand an area outside palladium. Provided that the chemistry of transition metal elements is the chemistry of the *d* electrons, we believed that the expansion would be beneficial to the group in the long run. Returning to the primitive cyclometalating 1-naphthylethylamine motif in which we have vast knowledge upon, we hope to use the framework as a standard as we set off for a new journey.

The chemistry of cycloiridation is a developing field.[98a, 151] Together with its newly-found enhanced activities in applications, we aimed to be able to generate novel chiral iridacyclic complexes for asymmetric applications. Furthermore, through minor modifications to the carbon framework of the 1-naphthylethylamine, we hope to build knowledge on the chemistry of these complexes with regards to their electronic and steric effects.

REFERENCES

1. Kleiman, J. P.; Dubeck, M. *J. Am. Chem. Soc.* **1963**, *85*, 1544-1545.
2. (a) Semion, V. A.; Barinov, I. V.; Ustynyuk, Y. A.; Struchkov, Y. T. *J. Struct. Chem.* **1972**, *13*, 512-513; (b) Bruce, M. I.; Iqbal, M. Z.; Stone, F. G. A. *J. Chem. Soc. A* **1970**, 3204-3209.
3. Cope, A. C.; Siekman, R. W. *J. Am. Chem. Soc.* **1965**, *87*, 3272-3273.
4. Cope, A. C.; Friedrich, E. C. *J. Am. Chem. Soc.* **1968**, *90*, 909-913.
5. Herrmann, W. A.; Brossmer, C.; Öfele, K.; Reisinger, C.-P.; Priermeier, T.; Beller, M.; Fischer, H. *Angew. Chem. Int. Ed. Engl.* **1995**, *34*, 1844-1848.
6. (a) Gensch, T.; Hopkinson, M. N.; Glorius, F.; Wencel-Delord, J. *Chem. Soc. Rev.* **2016**, *45*, 2900-2936; (b) Dong, Z.; Ren, Z.; Thompson, S. J.; Xu, Y.; Dong, G. *Chem. Rev.* **2017**, *117*, 9333-9403; (c) Hummel, J. R.; Boerth, J. A.; Ellman, J. A. *Chem. Rev.* **2017**, *117*, 9163-9227.
7. (a) Gunanathan, C.; Milstein, D. *Chem. Rev.* **2014**, *114*, 12024-12087; (b) Michon, C.; MacIntyre, K.; Corre, Y.; Agbossou-Niedercorn, F. *ChemCatChem* **2016**, *8*, 1755-1762; (c) Adhikary, A.; Guan, H. *ACS Catal.* **2015**, *5*, 6858-6873.
8. (a) Ma, D.-L.; Lin, S.; Wang, W.; Yang, C.; Leung, C.-H. *Chem. Sci.* **2017**, *8*, 878-889; (b) Lowry, M. S.; Bernhard, S. *Chem. Eur. J.* **2006**, *12*, 7970-7977; (c) Huo, S.; Carroll, J.; Vezzu, D. A. K. *Asian J. Org. Chem.* **2015**, *4*, 1210-1245; (d) Fleetham, T.; Li, G.; Li, J. *Adv. Mater.* **2017**, *29*, 1601861-1601861.
9. (a) Liu, Z.; Sadler, P. J. *Acc. Chem. Res.* **2014**, *47*, 1174-1185; (b) Sophie, J.; Fritz, E. K.; Angela, C. *Curr. Med. Chem.* **2017**, *24*, 1-25.
10. (a) Jung, M. E.; Piizzi, G. *Chem. Rev.* **2005**, *105*, 1735-1766; (b) Beesley, R. M.; Ingold, C. K.; Thorpe, J. F. *J. Chem. Soc., Trans.* **1915**, *107*, 1080-1106.
11. Albrecht, M. *Chem. Rev.* **2010**, *110*, 576-623.
12. Ryabov, A. D. *Chem. Rev.* **1990**, *90*, 403-424.
13. Bennett, R. L.; Bruce, M. I.; Stone, F. G. A. *J. Organomet. Chem.* **1972**, *38*, 325-334.
14. (a) Van Beek, J. A. M.; Van Koten, G.; Ramp, M. J.; Coenjaarts, N. C.; Grove, D. M.; Goubitz, K.; Zoutberg, M. C.; Stam, C. H.; Smeets, W. J. J.; Spek, A. L. *Inorg. Chem.* **1991**, *30*, 3059-3068; (b) Longoni, G.; Fantucci, P.; Chini, P.; Canziani, F. *J. Organomet. Chem.* **1972**, *39*, 413-425.
15. Shaw, B. L. *J. Organomet. Chem.* **1980**, *200*, 307-318.
16. Pearson, R. G. *J. Chem. Educ.* **1987**, *64*, 561-567.
17. Albert, J.; Granell, J.; Sales, J.; Solans, X.; Font-Altaba, M. *Organometallics* **1986**, *5*, 2567-2568.
18. Jones, W. D. *Inorg. Chem.* **2005**, *44*, 4475-4484.
19. Dunina, V. V.; Zalevskaya, O. A.; Potapov, V. M. *Russ. Chem. Rev.* **1988**, *57*, 250-269.
20. (a) Dunina, V. V. *Curr. Org. Chem.* **2011**, *15*, 3415-3440; (b) Dupont, J.; Consorti, C. S.; Spencer, J. *Chem. Rev.* **2005**, *105*, 2527-2572; (c) Bruce, M. I. *Angew. Chem. Int. Ed. Engl.* **1977**, *16*, 73-86; (d) Dehand, J.; Pfeffer, M. *Coord. Chem. Rev.* **1976**, *18*, 327-352.
21. Deeming, A. J.; Rothwell, I. P. *J. Organomet. Chem.* **1981**, *205*, 117-131.
22. Gill, D. F.; Mann, B. E.; Shaw, B. L. *J. Chem. Soc., Dalton Trans.* **1973**, 270-278.
23. Omae, I., Reasons Why Organometallic Intramolecular-Coordination Five-Membered Ring Compounds are Extremely Easily Synthesized through Cyclometalation Reactions. In *Cyclometalation Reactions: Five-Membered Ring Products as Universal Reagents*, Springer: 2014; pp 55-86.
24. Dunina, V. V.; Kuz'mina, L. G.; Kazakova, M. Y.; Gorunova, O. N.; Grishin, Y. K.; Kazakova, E. I. *Eur. J. Inorg. Chem.* **1999**, 1029-1039.
25. Morales-Morales, D., Introduction. In *Palladacycles*, Wiley-VCH Verlag GmbH & Co. KGaA: 2008; pp 1-12.
26. Moynahan, E. B.; Popp, F. D.; Werneke, M. F. *J. Organomet. Chem.* **1969**, *19*, 229-232.
27. Rosenblum, M.; Santer, J. O.; Howells, W. G. *J. Am. Chem. Soc.* **1963**, *85*, 1450-1458.
28. Gaunt, J. C.; Shaw, B. L. *J. Organomet. Chem.* **1975**, *102*, 511-516.
29. Sokolov, V. I.; Troitskaya, L. L.; Reutov, O. A. *J. Organomet. Chem.* **1979**, *182*, 537-546.
30. Ackermann, L. *Chem. Rev.* **2011**, *111*, 1315-1345.
31. (a) Davies, D. L.; Donald, S. M. A.; Macgregor, S. A. *J. Am. Chem. Soc.* **2005**, *127*, 13754-13755; (b) Davies, D. L.; Donald, S. M. A.; Al-Duaij, O.; Macgregor, S. A.; Pölleth, M. *J. Am. Chem. Soc.* **2006**, *128*, 4210-4211.

32. Rabaa, H.; Saillard, J. Y.; Hoffmann, R. *J. Am. Chem. Soc.* **1986**, *108*, 4327-4333.
33. Sajjad, M. A.; Christensen, K. E.; Rees, N. H.; Schwerdtfeger, P.; Harrison, J. A.; Nielson, A. J. *Chem. Commun.* **2017**, *53*, 4187-4190.
34. Perutz, R. N.; Sabo-Etienne, S. *Angew. Chem. Int. Ed.* **2007**, *46*, 2578-2592.
35. Crabtree, R. H., Metal Alkyls, Aryls, and Hydrides and Related σ-Bonded Ligands. In *The Organometallic Chemistry of the Transition Metals*, John Wiley & Sons, Inc.: 2005; pp 53-85.
36. Urriolabeitia, E. P., Oxidative Addition and Transmetallation. In *Palladacycles*, Wiley-VCH Verlag GmbH & Co. KGaA: 2008; pp 35-67.
37. Ryabov, A. D. *Inorg. Chem.* **1987**, *26*, 1252-1260.
38. Ng, J. K.-P.; Tan, G.-K.; Vittal, J. J.; Leung, P.-H. *Inorg. Chem.* **2003**, *42*, 7674-7682.
39. Yao, Q.; Kinney, E. P.; Zheng, C. *Org. Lett.* **2004**, *6*, 2997-2999.
40. Ryabov, A. D.; Yatsimirskii, A. K. *Inorg. Chem.* **1984**, *23*, 789-790.
41. Albrecht, M.; Dani, P.; Lutz, M.; Spek, A. L.; van Koten, G. *J. Am. Chem. Soc.* **2000**, *122*, 11822-11833.
42. Baba, S.; Kawaguchi, S. *Inorg. Nucl. Chem. Lett.* **1975**, *11*, 415-420.
43. Avshu, A.; O'Sullivan, R. D.; Parkins, A. W.; Alcock, N. W.; Countryman, R. M. *J. Chem. Soc., Dalton Trans.* **1983**, 1619-1624.
44. Fuchita, Y.; Tsuchiya, H. *Polyhedron* **1993**, *12*, 2079-2080.
45. Vicente, J.; Saura-Llamas, I. *Comments Inorg. Chem.* **2007**, *28*, 39-72.
46. Valeria, V. D.; Olga, N. G. *Russ. Chem. Rev.* **2004**, *73*, 309-350.
47. (a) Romeo, R.; Arena, G.; Monsu Scolaro, L. *Inorg. Chem.* **1992**, *31*, 4879-4884; (b) Pacchioni, G.; Bagus, P. S. *Inorg. Chem.* **1992**, *31*, 4391-4398; (c) Rahman, M. M.; Liu, H. Y.; Eriks, K.; Prock, A.; Giering, W. P. *Organometallics* **1989**, *8*, 1-7.
48. Cheney, A. J.; Shaw, B. L. *J. Chem. Soc., Dalton Trans.* **1972**, 860-865.
49. Shaw, B. L.; Truelock, M. M. *J. Organomet. Chem.* **1975**, *102*, 517-525.
50. Valeria, V. D.; Olga, N. G. *Russ. Chem. Rev.* **2005**, *74*, 871-913.
51. Otsuka, S.; Nakamura, A.; Kano, T.; Tani, K. *J. Am. Chem. Soc.* **1971**, *93*, 4301-4303.
52. Allen, D. G.; McLaughlin, G. M.; Robertson, G. B.; Steffen, W. L.; Salem, G.; Wild, S. B. *Inorg. Chem.* **1982**, *21*, 1007-1014.
53. Fuchita, Y.; Yoshinaga, K.; Ikeda, Y.; Kinoshita-Kawashima, J. *J. Chem. Soc., Dalton Trans.* **1997**, 2495-2500.
54. Dickmu, G. C.; Smoliakova, I. P. *J. Organomet. Chem.* **2014**, *772-773*, 42-48.
55. Günay, M. E.; Richards, C. J. *Organometallics* **2009**, *28*, 5833-5836.
56. Cheng, G.-J.; Yang, Y.-F.; Liu, P.; Chen, P.; Sun, T.-Y.; Li, G.; Zhang, X.; Houk, K. N.; Yu, J.-Q.; Wu, Y.-D. *J. Am. Chem. Soc.* **2014**, *136*, 894-897.
57. Dunina, V. V.; Gorunova, O. g. N.; Kuz'mina, L. G.; Livantsov, M. V.; Grishin, Y. K. *Tetrahedron: Asymmetry* **1999**, *10*, 3951-3961.
58. Ren, Z.; Mo, F.; Dong, G. *J. Am. Chem. Soc.* **2012**, *134*, 16991-16994.
59. Ren, Z.; Dong, G. *Organometallics* **2016**, *35*, 1057-1059.
60. Iwai, T.; Tanaka, R.; Sawamura, M. *Organometallics* **2016**, *35*, 3959-3969.
61. Strohmann, C.; Abele, B. C.; Lehmen, K.; Villafañe, F.; Sierra, L.; Martín-Barrios, S.; Schildbach, D. *J. Organomet. Chem.* **2002**, *661*, 149-158.
62. Koller, S. G.; Martín-Romo, R.; Melero, J. S.; Colquhoun, V. P.; Schildbach, D.; Strohmann, C.; Villafañe, F. *Organometallics* **2014**, *33*, 7329-7332.
63. Calmuschi-Cula, B.; Englert, U. *Organometallics* **2008**, *27*, 3124-3130.
64. Puddephatt, R. J. *Coord. Chem. Rev.* **2001**, *219-221*, 157-185.
65. Crespo, M.; Martinez, M.; Sales, J.; Solans, X.; Font-Bardia, M. *Organometallics* **1992**, *11*, 1288-1295.
66. Bernhardt, P. V.; Gallego, C.; Martinez, M. *Organometallics* **2000**, *19*, 4862-4869.
67. Martín, R.; Crespo, M.; Font-Bardia, M.; Calvet, T. *Organometallics* **2009**, *28*, 587-597.
68. Zucca, A.; Maidich, L.; Carta, V.; Petretto, G. L.; Stoccoro, S.; Agostina Cinellu, M.; Pilo, M. I.; Clarkson, G. J. *Eur. J. Inorg. Chem.* **2014**, 2278-2287.
69. Capape, A.; Crespo, M.; Granell, J.; Font-Bardia, M.; Solans, X. *Dalton Trans.* **2007**, 2030-2039.
70. Skapski, A. C.; Sutcliffe, V. F.; Young, G. B. *J. Chem. Soc., Chem. Commun.* **1985**, 609-611.
71. Butschke, B.; Schwarz, H. *Chem. Sci.* **2012**, *3*, 308-326.

72. Minghetti, G.; Doppiu, A.; Zucca, A.; Stoccoro, S.; Cinellu, M. A.; Manassero, M.; Sansoni, M. *Chem. Heterocycl. Comp.* **1999**, *35*, 992-1000.
73. Stoccoro, S.; Chelucci, G.; Cinellu, M. A.; Zucca, A.; Minghetti, G. *J. Organomet. Chem.* **1993**, *450*, C15-C16.
74. Zucca, A.; Cordeschi, D.; Stoccoro, S.; Cinellu, M. A.; Minghetti, G.; Chelucci, G.; Manassero, M. *Organometallics* **2011**, *30*, 3064-3074.
75. Maidich, L.; Dettori, G.; Stoccoro, S.; Cinellu, M. A.; Rourke, J. P.; Zucca, A. *Organometallics* **2015**, *34*, 817-828.
76. Djukic, J.-P.; Sortais, J.-B.; Barloy, L.; Pfeffer, M. *Eur. J. Inorg. Chem.* **2009**, 817-853.
77. Parshall, G. W.; Knoth, W. H.; Schunn, R. A. *J. Am. Chem. Soc.* **1969**, *91*, 4990-4995.
78. James, B. R.; Markham, L. D.; Wang, D. K. W. *J. Chem. Soc., Chem. Commun.* **1974**, 439-440.
79. Stolzenberg, A. M.; Muetterties, E. L. *Organometallics* **1985**, *4*, 1739-1742.
80. Bruce, M. I.; Iqbal, M. Z.; Stone, F. G. A. *J. Chem. Soc. D* **1970**, 1325-1327.
81. Bruce, M. I.; Iqbal, M. Z.; Stone, F. G. A. *J. Chem. Soc. A* **1971**, 2820-2828.
82. Katsuma, H.; Yayoi, O.; Yoko, O. *Bull. Chem. Soc. Jpn.* **1979**, *52*, 1372-1376.
83. Hijazi, A.; Djukic, J.-P.; Pfeffer, M.; Ricard, L.; Kyritsakas-Gruber, N.; Raya, J.; Bertani, P.; de Cian, A. *Inorg. Chem.* **2006**, *45*, 4589-4591.
84. Jia, W.-G.; Zhang, T.; Xie, D.; Xu, Q.-T.; Ling, S.; Zhang, Q. *Dalton Trans.* **2016**, *45*, 14230-14237.
85. Bruce, M. I.; Gardner, R. C. F.; Stone, F. G. A. *J. Organomet. Chem.* **1972**, *40*, C39-C41.
86. Joslin, F. L.; Mague, J. T.; Roundhill, D. M. *Organometallics* **1991**, *10*, 521-524.
87. Abbenhuis, H. C. L.; Pfeffer, M.; Sutter, J. P.; de Cian, A.; Fischer, J.; Ji, H. L.; Nelson, J. H. *Organometallics* **1993**, *12*, 4464-4472.
88. (a) Sortais, J.-B.; Pannetier, N.; Holuigue, A.; Barloy, L.; Sirlin, C.; Pfeffer, M.; Kyritsakas, N. *Organometallics* **2007**, *26*, 1856-1867; (b) Jerphagnon, T.; Gayet, A. J. A.; Berthiol, F.; Ritleng, V.; Mršić, N.; Meetsma, A.; Pfeffer, M.; Minnaard, A. J.; Feringa, B. L.; de Vries, J. G. *Chem. Eur. J.* **2009**, *15*, 12780-12790; (c) Pannetier, N.; Sortais, J.-B.; Issenhuth, J.-T.; Barloy, L.; Sirlin, C.; Holuigue, A.; Lefort, L.; Panella, L.; de Vries, J. G.; Pfeffer, M. *Adv. Synth. Catal.* **2011**, *353*, 2844-2852.
89. Trnka, T. M.; Morgan, J. P.; Sanford, M. S.; Wilhelm, T. E.; Scholl, M.; Choi, T.-L.; Ding, S.; Day, M. W.; Grubbs, R. H. *J. Am. Chem. Soc.* **2003**, *125*, 2546-2558.
90. Abdur-Rashid, K.; Fedorkiw, T.; Lough, A. J.; Morris, R. H. *Organometallics* **2004**, *23*, 86-94.
91. Toner, A.; Matthes, J.; Gründemann, S.; Limbach, H.-H.; Chaudret, B.; Clot, E.; Sabo-Etienne, S. *Proc. Natl. Acad. Sci. U.S.A* **2007**, *104*, 6945-6950.
92. Wang, C.; Xiao, J. *Chem. Commun.* **2017**, *53*, 3399-3411.
93. Bennett, M. A.; Milner, D. L. *Chem. Commun. (London)* **1967**, 581-582.
94. Bennett, M. A.; Milner, D. L. *J. Am. Chem. Soc.* **1969**, *91*, 6983-6994.
95. Duff, J. M.; Shaw, B. L. *J. Chem. Soc., Dalton Trans.* **1972**, 2219-2225.
96. (a) Einstein, F. W. B.; Gilchrist, A. B.; Rayner-Canham, G. W.; Sutton, D. *J. Am. Chem. Soc.* **1972**, *94*, 645-647; (b) Einstein, F. W. B.; Sutton, D. *J. Chem. Soc., Dalton Trans.* **1973**, 434-438.
97. Nonoyama, M. *J. Organomet. Chem.* **1975**, *86*, 263-267.
98. (a) Wei, W.; Lima, S. A. M.; Djurovich, P. I.; Bossi, A.; Whited, M. T.; Thompson, M. E. *Polyhedron* **2018**, *140*, 138-145; (b) Matteucci, E.; Baschieri, A.; Mazzanti, A.; Sambri, L.; Ávila, J.; Pertegás, A.; Bolink, H. J.; Monti, F.; Leoni, E.; Armaroli, N. *Inorg. Chem.* **2017**, *56*, 10584-10595; (c) Yang, C.; Mehmood, F.; Lam, T. L.; Chan, S. L.-F.; Wu, Y.; Yeung, C.-S.; Guan, X.; Li, K.; Chung, C. Y.-S.; Zhou, C.-Y.; Zou, T.; Che, C.-M. *Chem. Sci.* **2016**, *7*, 3123-3136; (d) Han, Y.; Cao, H.-T.; Sun, H.-Z.; Shan, G.-G.; Wu, Y.; Su, Z.-M.; Liao, Y. *J. Mater. Chem. C* **2015**, *3*, 2341-2349.
99. Han, Y.-F.; Jin, G.-X. *Chem. Soc. Rev.* **2014**, *43*, 2799-2823.
100. Bauera, W.; Prema, M.; Polbornb, K.; Sünkela, K.; Steglichb, W.; Beck, W. *Eur. J. Inorg. Chem.* **1998**, 485-493.
101. Davies, D. L.; Al-Duaij, O.; Fawcett, J.; Giardiello, M.; Hilton, S. T.; Russell, D. R. *Dalton Trans.* **2003**, 4132-4138.
102. Barloy, L.; Issenhuth, J.-T.; Weaver, M. G.; Pannetier, N.; Sirlin, C.; Pfeffer, M. *Organometallics* **2011**, *30*, 1168-1174.

103. Féghali, E.; Barloy, L.; Issenhuth, J.-T.; Karmazin-Brelot, L.; Bailly, C.; Pfeffer, M. *Organometallics* **2013**, *32*, 6186-6194.
104. Arita, S.; Koike, T.; Kayaki, Y.; Ikariya, T. *Organometallics* **2008**, *27*, 2795-2802.
105. Broeckx, L. E. E.; Lutz, M.; Vogt, D.; Muller, C. *Chem. Commun.* **2011**, *47*, 2003-2005.
106. Mathey, F., General Topics. In *Transition Metal Organometallic Chemistry*, Mathey, F., Ed. Springer Singapore: Singapore, 2013; pp 1-25.
107. Holton, R. A.; Sibi, M. P.; Murphy, W. S. *J. Am. Chem. Soc.* **1988**, *110*, 314-316.
108. Dangel, B. D.; Godula, K.; Youn, S. W.; Sezen, B.; Sames, D. *J. Am. Chem. Soc.* **2002**, *124*, 11856-11857.
109. Leung, P.-H.; He, G.; Lang, H.; Liu, A.; Loh, S.-K.; Selvaratnam, S.; Mok, K. F.; White, A. J. P.; Williams, D. J. *Tetrahedron* **2000**, *56*, 7-15.
110. Leung, P.-H. *Acc. Chem. Res.* **2004**, *37*, 169-177.
111. Roberts, N. K.; Wild, S. B. *J. Am. Chem. Soc.* **1979**, *101*, 6254-6260.
112. Yao, S.-Y.; Chen, X.-Y.; Ou, Y.-L.; Ye, B.-H. *Inorg. Chem.* **2017**, *56*, 878-885.
113. (a) Roudesly, F.; Oble, J.; Poli, G. *J. Mol. Catal. A: Chem.* **2017**, *426*, 275-296; (b) Xue, X.-S.; Ji, P.; Zhou, B.; Cheng, J.-P. *Chem. Rev.* **2017**, *117*, 8622-8648; (c) Davies, D. L.; Macgregor, S. A.; McMullin, C. L. *Chem. Rev.* **2017**, *117*, 8649-8709; (d) Gulías, M.; Mascareñas, J. L. *Angew. Chem. Int. Ed.* **2016**, *55*, 11000-11019.
114. He, J.; Wasa, M.; Chan, K. S. L.; Shao, Q.; Yu, J.-Q. *Chem. Rev.* **2017**, *117*, 8754-8786.
115. Ackermann, L. *Org. Process Res. Dev.* **2015**, *19*, 260-269.
116. (a) Zhang, B.; Wang, H.-W.; Kang, Y.-S.; Zhang, P.; Xu, H.-J.; Lu, Y.; Sun, W.-Y. *Org. Lett.* **2017**, *19*, 5940-5943; (b) Xia, J.; Kong, L.; Zhou, X.; Zheng, G.; Li, X. *Org. Lett.* **2017**, *19*, 5972-5975; (c) Yang, J.-F.; Wang, R.-H.; Wang, Y.-X.; Yao, W.-W.; Liu, Q.-S.; Ye, M. *Angew. Chem. Int. Ed.* **2016**, *55*, 14116-14120; (d) Thenarukandiyil, R.; Thrikkykkal, H.; Choudhury, J. *Organometallics* **2016**, *35*, 3007-3013; (e) Hu, X.-H.; Yang, X.-F.; Loh, T.-P. *ACS Catal.* **2016**, *6*, 5930-5934.
117. (a) Kommagalla, Y.; Chatani, N. *Coord. Chem. Rev.* **2017**, *350*, 117-135; (b) Yoshino, T.; Matsunaga, S. *Adv. Synth. Catal.* **2017**, *359*, 1245-1262; (c) Gao, K.; Yoshikai, N. *Acc. Chem. Res.* **2014**, *47*, 1208-1219.
118. Shang, R.; Ilies, L.; Nakamura, E. *Chem. Rev.* **2017**, *117*, 9086-9139.
119. Guo, X.-X.; Gu, D.-W.; Wu, Z.; Zhang, W. *Chem. Rev.* **2015**, *115*, 1622-1651.
120. Zhu, R.-Y.; Liu, L.-Y.; Yu, J.-Q. *J. Am. Chem. Soc.* **2017**, *139*, 12394-12397.
121. Hong, S. Y.; Jeong, J.; Chang, S. *Angew. Chem. Int. Ed.* **2017**, *56*, 2408-2412.
122. Wang, X.-C.; Gong, W.; Fang, L.-Z.; Zhu, R.-Y.; Li, S.; Engle, K. M.; Yu, J.-Q. *Nature* **2015**, *519*, 334-338.
123. Wang, P.; Farmer, M. E.; Yu, J.-Q. *Angew. Chem. Int. Ed.* **2017**, *56*, 5125-5129.
124. (a) Beller, M.; Fischer, H.; Herrmann, W. A.; Öfele, K.; Brossmer, C. *Angew. Chem. Int. Ed. Engl.* **1995**, *34*, 1848-1849; (b) Herrmann, W. A.; Reisinger, C.-P.; Öfele, K.; Broβmer, C.; Beller, M.; Fischer, H. *J. Mol. Catal. A: Chem.* **1996**, *108*, 51-56; (c) Louie, J.; Hartwig, J. F. *Angew. Chem. Int. Ed. Engl.* **1996**, *35*, 2359-2361.
125. Nowotny, M.; Hanefeld, U.; Koningsveld, H. v.; Maschmeyer, T. *Chem. Commun.* **2000**, 1877-1878.
126. (a) Rocaboy, C.; Gladysz, J. A. *New J. Chem.* **2003**, *27*, 39-49; (b) Rocaboy, C.; Gladysz, J. A. *Org. Lett.* **2002**, *4*, 1993-1996.
127. Koshti, V.; Gaikwad, S.; Chikkali, S. H. *Coord. Chem. Rev.* **2014**, *265*, 52-73.
128. (a) Huang, Y.; Pullarkat, S. A.; Li, Y.; Leung, P.-H. *Inorg. Chem.* **2012**, *51*, 2533-2540; (b) Huang, Y.; Pullarkat, S. A.; Li, Y.; Leung, P.-H. *Chem. Commun.* **2010**, *46*, 6950-6952; (c) Feng, J.-J.; Chen, X.-F.; Shi, M.; Duan, W.-L. *J. Am. Chem. Soc.* **2010**, *132*, 5562-5563.
129. Huang, Y.; Chew, R. J.; Pullarkat, S. A.; Li, Y.; Leung, P.-H. *J. Org. Chem.* **2012**, *77*, 6849-6854.
130. Chen, Y.-R.; Duan, W.-L. *Org. Lett.* **2011**, *13*, 5824-5826.
131. Xu, C.; Jun Hao Kennard, G.; Hennersdorf, F.; Li, Y.; Pullarkat, S. A.; Leung, P.-H. *Organometallics* **2012**, *31*, 3022-3026.
132. Chew, R. J.; Teo, K. Y.; Huang, Y.; Li, B.-B.; Li, Y.; Pullarkat, S. A.; Leung, P.-H. *Chem. Commun.* **2014**, *50*, 8768-8770.
133. Lu, J.; Ye, J.; Duan, W.-L. *Org. Lett.* **2013**, *15*, 5016-5019.
134. Chew, R. J.; Lu, Y.; Jia, Y.-X.; Li, B.-B.; Wong, E. H. Y.; Goh, R.; Li, Y.; Huang, Y.; Pullarkat, S. A.; Leung, P.-H. *Chem. Eur. J.* **2014**, *20*, 14514-14517.

135. Chew, R. J.; Huang, Y.; Li, Y.; Pullarkat, S. A.; Leung, P.-H. *Adv. Synth. Catal.* **2013**, *355*, 1403-1408.
136. Yang, X.-Y.; Gan, J. H.; Li, Y.; Pullarkat, S. A.; Leung, P.-H. *Dalton Trans.* **2015**, *44*, 1258-1263.
137. Chen, H.-Y. T.; Wang, C.; Wu, X.; Jiang, X.; Catlow, C. R. A.; Xiao, J. *Chem. Eur. J.* **2015**, *21*, 16564-16577.
138. Sato, Y.; Kayaki, Y.; Ikariya, T. *Chem. Asian. J.* **2016**, *11*, 2924-2931.
139. Zou, Q.; Wang, C.; Smith, J.; Xue, D.; Xiao, J. *Chem. Eur. J.* **2015**, *21*, 9656-9661.
140. (a) Chew, R. J.; Leung, P.-H. *Chem. Rec.* **2016**, *16*, 141-158; (b) Leung, P.-H.; Ng, K.-H.; Li, Y.; J. P. White, A.; J. Williams, D. *Chem. Commun.* **1999**, 2435-2436; (c) Gan, K.; Ng, J. S.; Sadeer, A.; Pullarkat, S. A. *Synlett* **2016**, *27*, 254-258; (d) Gan, K.; Sadeer, A.; Ng, J. S.; Lu, Y.; Pullarkat, S. A. *Org. Chem. Front.* **2015**, *2*, 1059-1065; (e) Wong, J.; Gan, K.; Chen, H. J.; Pullarkat, S. A. *Adv. Synth. Catal.* **2014**, *356*, 3391-3400.
141. (a) Alcock, N. W.; Brown, J. M.; Hulmes, D. I. *Tetrahedron: Asymmetry* **1993**, *4*, 743-756; (b) Alcock, N. W.; Hulmes, D. I.; Brown, J. M. *J. Chem. Soc., Chem. Commun.* **1995**, 395-397; (c) Ng, J. K. P.; Chen, S.; Tan, G. K.; Leung, P.-H. *Tetrahedron: Asymmetry* **2007**, *18*, 1163-1169.
142. Li, Y.; Ng, K.-H.; Selvaratnam, S.; Tan, G.-K.; Vittal, J. J.; Leung, P.-H. *Organometallics* **2003**, *22*, 834-842.
143. (a) Yap, J. S. L.; Chen, H. J.; Li, Y.; Pullarkat, S. A.; Leung, P.-H. *Organometallics* **2014**, *33*, 930-940; (b) Yap, J. S. L.; Li, B. B.; Wong, J.; Li, Y.; Pullarkat, S. A.; Leung, P.-H. *Dalton Trans.* **2014**, *43*, 5777-5784; (c) Ding, Y.; Zhang, Y.; Li, Y.; Pullarkat, S. A.; Andrews, P.; Leung, P.-H. *Eur. J. Inorg. Chem.* **2010**, 4427-4437; (d) Ding, Y.; Li, Y.; Pullarkat, S. A.; Leng Yap, S.; Leung, P.-H. *Eur. J. Inorg. Chem.* **2009**, 267-276; (e) Ding, Y.; Li, Y.; Zhang, Y.; Pullarkat, S. A.; Leung, P.-H. *Eur. J. Inorg. Chem.* **2008**, 1880-1891; (f) Li, Y.; Selvaratnam, S.; Vittal, J. J.; Leung, P.-H. *Inorg. Chem.* **2003**, *42*, 3229-3236.
144. (a) Ding, Y.; Chiang, M.; Pullarkat, S. A.; Li, Y.; Leung, P.-H. *Organometallics* **2009**, *28*, 4358-4370; (b) Ng, J. K.-P.; Chen, S.; Tan, G.-K.; Leung, P.-H. *Eur. J. Inorg. Chem.* **2007**, 3124-3134; (c) Ng, J. K.-P.; Li, Y.; Tan, G.-K.; Koh, L.-L.; Vittal, J. J.; Leung, P.-H. *Inorg. Chem.* **2005**, *44*, 9874-9886.
145. Ng, J. K.-P.; Chen, S.; Li, Y.; Tan, G.-K.; Koh, L.-L.; Leung, P.-H. *Inorg. Chem.* **2007**, *46*, 5100-5109.
146. (a) Li, X.-R.; Yang, X.-Y.; Li, Y.; Pullarkat, S. A.; Leung, P.-H. *Dalton Trans.* **2017**, *46*, 1311-1316; (b) Gan, K.; Sadeer, A.; Xu, C.; Li, Y.; Pullarkat, S. A. *Organometallics* **2014**, *33*, 5074-5076.
147. Yang, X.-Y.; Tay, W. S.; Li, Y.; Pullarkat, S. A.; Leung, P.-H. *Organometallics* **2015**, *34*, 1582-1588.
148. (a) Yang, X.-Y.; Tay, W. S.; Li, Y.; Pullarkat, S. A.; Leung, P.-H. *Chem. Commun.* **2016**, *52*, 4211-4214; (b) Tay, W. S.; Yang, X.-Y.; Li, Y.; Pullarkat, S. A.; Leung, P.-H. *RSC Adv.* **2016**, *6*, 75951-75959.
149. (a) Tay, W. S.; Yang, X.-Y.; Li, Y.; Pullarkat, S. A.; Leung, P.-H. *Chem. Commun.* **2017**, *53*, 6307-6310; (b) Yang, X.-Y.; Tay, W. S.; Li, Y.; Pullarkat, S. A.; Leung, P.-H. *Organometallics* **2015**, *34*, 5196-5201; (c) Li, X.-R.; Chew, R. J.; Li, Y.; Leung, P.-H. *Aust. J. Chem.* **2016**, *69*, 499-504.
150. Jia, Y.-X.; Li, B.-B.; Li, Y.; Pullarkat, S. A.; Xu, K.; Hirao, H.; Leung, P.-H. *Organometallics* **2014**, *33*, 6053-6058.
151. (a) Arthurs, R. A.; Horton, P. N.; Coles, S. J.; Richards, C. J. *Eur. J. Inorg. Chem.* **2017**, 229-232; (b) Navarro, M.; Smith, C. A.; Albrecht, M. *Inorg. Chem.* **2017**, *56*, 11688-11701; (c) Zhou, T.; Li, L.; Li, B.; Song, H.; Wang, B. *Organometallics* **2018**, *37*, 476-481; (d) Sun, R.; Zhang, S.; Chu, X.; Zhu, B. *Organometallics* **2017**, *36*, 1133-1141.

CHAPTER 2

Challenges to Cyclometalation
Steric Effects Leading to Competing Pathways and New Cyclometalated Iridium(III) Complexes

ABSTRACT

The iridation of (*R*)-*N*,*N*-dimethyl-1-(1-naphthyl)ethylamine in the presence of base afforded an assortment of products ranging from organic molecules to coordinated systems and cyclometalated complexes. The transformation affirmed the postulation by which steric effects within coordination sphere of the metal center would drive the reaction to undergo a *β*-hydride elimination-like decomposition, competing alongside *ortho*-metalation, thus leading to reactive metallacyclic or iminium intermediates. The same procedure also generated an unprecedented carbocyclic η^1,η^2-cycloiridated species that could not be attained from the direct cyclometalation of its organic counterpart.

Keywords: *N*-Dealkylation / C–N Bond Cleavage / Cycloiridation / Cyclometalated Complexes / Coordination Complexes

1 INTRODUCTION

1.1 The Venture into Cycloiridation Chemistry

First utilized by Wild to generate an optically-active cyclopalladated complex for improved optical resolution procedure,[1] *N*,*N*-dimethyl-1-naphthylethylamine (**L1**) and its derivatives have since been deployed as ligands for the synthesis of a myriad of palladacycles within our group.[2]

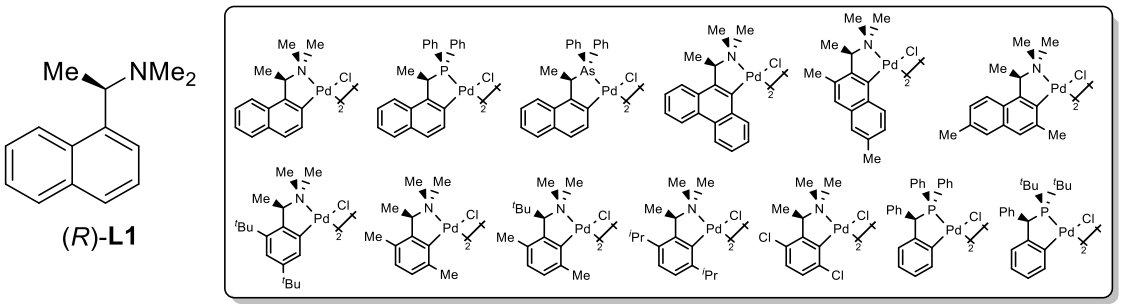

Figure 2.1. The *N*,*N*-dimethyl-1-naphthylethylamine ligand and its cyclopalladated derivatives.

The effectiveness of these palladacycles in applications, be it as a catalyst or chiral auxiliary, stems from the conformational rigidity within the five-membered puckered ring system in the complex.[3] As the structural aspects of the metallacycles would be the highlight for subsequent chapters, we will not delve deeper into the structural analysis of these compounds.

Our interest in cyclometalation has led us into the development of numerous ligand motifs for structural investigation in the bidentate *C,N*-,[2a-h] *C,P*-[2i-m] and *C,As*-[2m] systems as shown earlier in Figure 2.1. Moreover, we have recently investigated various types of nickel-, palladium- and platinum-based terdentate pincer complexes of *P,C,P*-,[4] *P,C,N*-[4a] and *S,C,N*-[5]nature. With much knowledge into cyclopalladation and, possibly, cycloplatination, we hope to expand our library of chiral metallacycles to other transition metal elements.

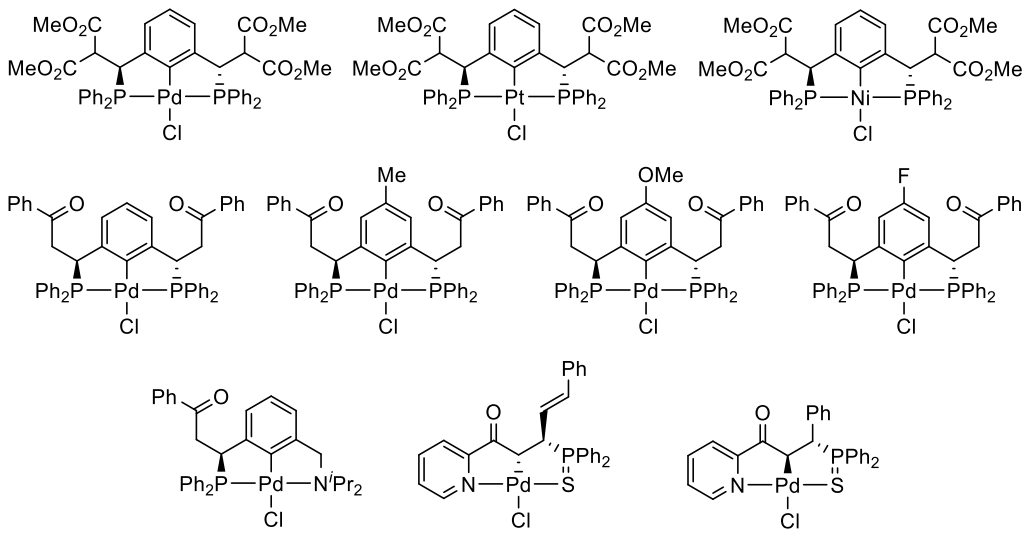

Figure 2.2. Chiral pincer complexes developed by our group.

The emergence and recent developments of cycloiridation chemistry have been extensively discussed earlier in the introductory chapter. We were particularly interested in the half sandwich iridacycles due to its unique geometry and similarities in terms of its mode of activation. The structure of these complexes is of type ML_3X_3 which should exhibit an octahedral structure. However, the bulky L_2X 1,2,3,4,5-pentamethylcyclopentadienyl (Cp*) ligand occupies three *facial* positions within the octahedral complex leaving only the remaining three *facial* coordination sites for the other

ligands. In this configuration, the Cp*-iridium complex resembles a carbon moiety and its geometry can be termed as *pseudo*-tetrahedral. It is important to note that the compound is not truly tetrahedral in nature since bond angles between the ligands within the complex is closer to 90° (ideal bond angle in octahedral compounds) than 109.5° (ideal bond angle in tetrahedral carbon). Nonetheless, the complex can exhibit some characteristics of tetrahedral compounds, particularly central chirality when coordinated to three distinct ligands.

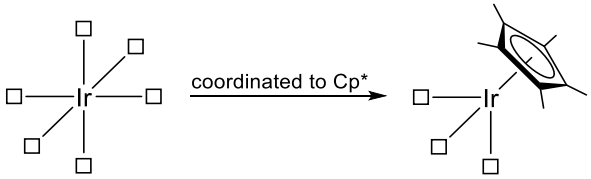

Scheme 2.1. Coordination mode of Cp* ligand to iridium.

Among the multitude of ligands that were available to us, (*R*)-*N*,*N*-dimethyl-1-naphthylethylamine (*R*)-**L1** was chosen to be the cyclometalating ligand for the cycloiridation procedure. Several reasons justified the selection: (a) the use of a ligand motif in which its electronic and steric factors within a specific cyclometalated system have been fully explored and understood, (b) the presence of a tertiary amine donor moiety to enhance the cyclization process, (c) the ease of synthesis of the ligand, and (d) the commercial-availability of the enantiopure starting material for the synthesis of the ligand.

1.2 Preliminary Studies and its Objectives

Attempts into cycloiridation of (*R*)-**L1** with $[IrCp^*Cl_2]_2$ under reaction conditions determined by Davies[6] returned no conversion of the amine. The reaction mixture was then heated to reflux in hopes to push the reaction forward to initialize the cycloiridation procedure. Gratifyingly, transformation took place under elevated temperatures. However, upon isolation of the products, the protocol afforded byproducts instead of the expected cyclometalated complex.

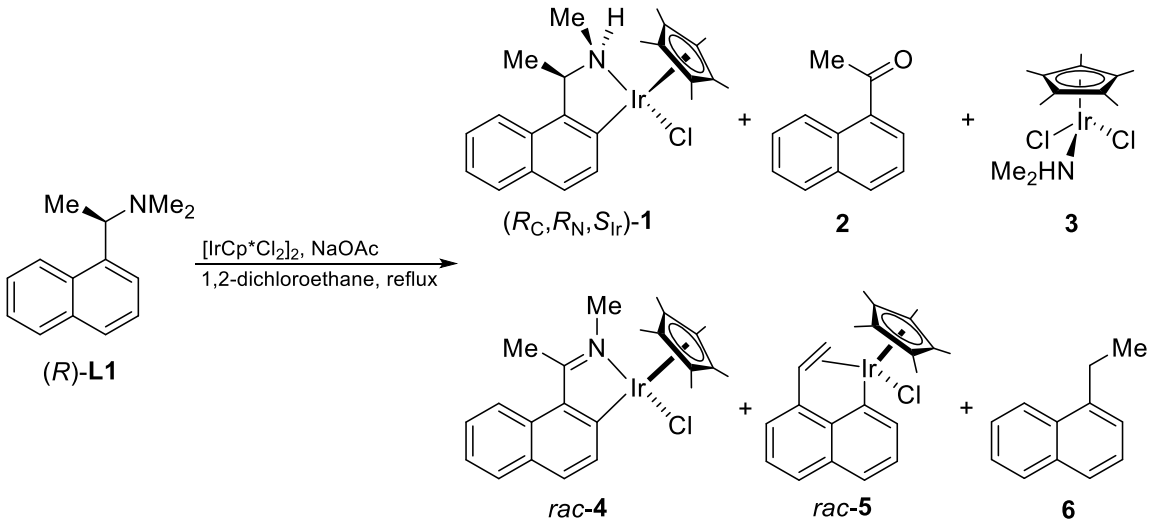

Scheme 2.2. Attempted cycloiridation of (*R*)-*N*,*N*-dimethyl-1-naphthylethylamine (*R*)-**L1**.

The compounds obtained from the reaction were interesting and unexpected. The closest resemblance to the desired metallacycle was iridacycle (R_C,R_N,S_{Ir})-**1**, although it lacked a *N*-methyl substituent to mirror the former complex. Possible oxidation of the ligand was also speculated since 1-acetonaphthone **2** and imine-based cycloiridated complex *rac*-**4** were isolated. The remaining three products generally contained fragments of the ligand within their molecular structure.

Although it was simple to identify the ligand fragments within the products, an immediate explanation into the formation of the byproducts were difficult, especially since many bonds were cleaved in the process. We were also taken aback by the failure of the cycloiridation procedure since the iridium(III) metal center is more electrophilic than its palladium(II) counterpart. As such, we questioned the differences between the two processes. In addition, we are fascinated with the unusual formation of the products. By probing into the reaction mechanisms of the protocol, we seek to understand, as well as to appreciate, the chemistry behind the attempted iridation procedure. Furthermore, with more research delving into applications of cycloiridated complexes and iridium-mediated C–H bond functionalization reactions, we hope that the work could provide insights to the field.

2 RESULTS AND DISCUSSION

2.1 The Attempted Cycloiridation Reaction

As discussed earlier, the iridation of (*R*)-**L1** with $[IrCp^*Cl_2]_2$ and NaOAc in refluxing 1,2-dichloroethane yielded a variety of byproducts ranging from cycloiridated systems and coordinated amines to organic molecules.

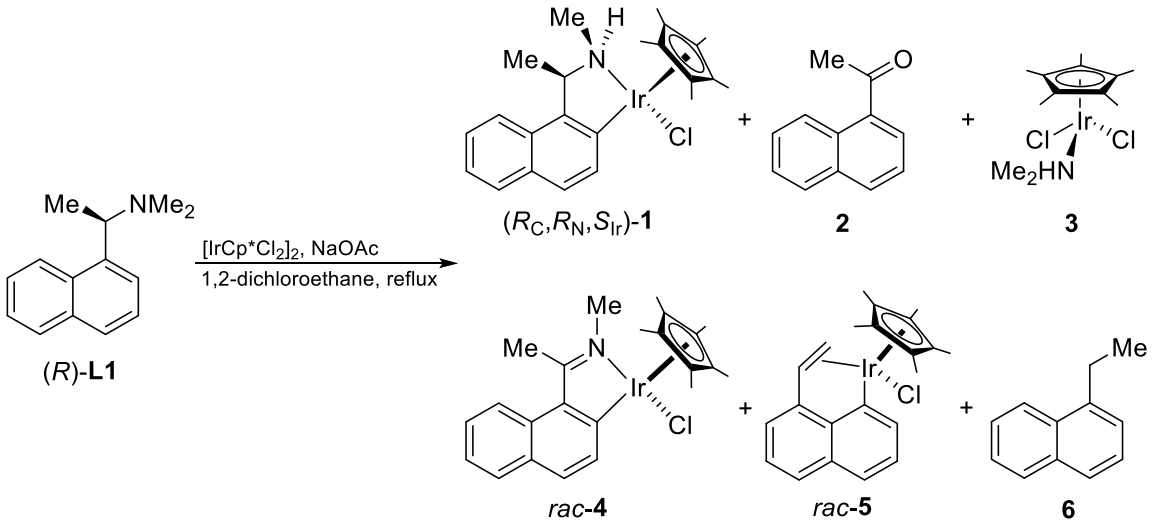

Scheme 2.3. The iridation reaction of (*R*)-*N*,*N*-dimethyl-1-naphthylethylamine (*R*)-**L1**.

Six products – optically-active *N*-demethylated iridacycle (R_C,R_N,S_{Ir})-**1**, 1-acetonaphthone **2**, coordinated dimethylamine iridium(III) complex **3**, racemic *ortho*-iridated imine complex *rac*-**4**, racemic η^1,η^2-cycloiridated complex *rac*-**5** and 1-ethylnaphthalene **6** – were isolated in variable amounts from the crude reaction mixture *via* column chromatography. The products varied significantly in polarity and could be collected as fractions in order of **6** (*n*-hexane), **2** (*n*-hexane/CH_2Cl_2 mixture (2:1)), *rac*-**5** (CH_2Cl_2), (R_C,R_N,S_{Ir})-**1** (CH_2Cl_2/EtOAc mixture (100:1)), *rac*-**4** (CH_2Cl_2/EtOAc mixture (10:1)) and **3** (CH_2Cl_2/EtOAc mixture (1:1)). Each of these compounds will be individually discussed in later sections.

It should be noted that the products do not account for all tertiary amine ligand (*R*)-**L1** present in the reaction mixture. In most cases, isolation of the unreacted amine has been difficult unless the reaction time was short, typically below 48 h. Coordinated (*R*)-**L1** species has also not been isolated or observed in the reaction. Residual $[IrCp^*Cl_2]_2$, on the other hand, could be almost quantifiably recovered most of the time. On the whole, we believed that the metalation procedure afforded other byproducts. However, despite numerous attempts at isolation, we were only able to consistently attain and elucidate these six compounds.

Yields of the products, in general, differed according to reaction times. Although they might provide insights into the reaction mechanism, the low isolated yields for majority of the products made drawing a definitive conclusion difficult. Nonetheless, we were able to piece some information from the data.

Table 2.1. Reaction yields of products in the attempted cycloiridation of (*R*)-*N*,*N*-dimethyl-1-naphthylethylamine (*R*)-**L1**.[a]

		percentage yield[b] *(%)*					
entry	time (d)	(R_C,R_N,S_{Ir})-**1**	**2**	**3**	*rac*-**4**	*rac*-**5**	**6**
1	1	2	32	16	1	<1	-
2	2	4	48	22	2	2	<1
3	5	2	53	15	4	2	1
4	10	1	59	12	4	1	<1
5[c]	30	<1	61	8	3	-	<1

[a]Reactions were carried out with (*R*)-**L1** (0.25 mmol), $[IrCp^*Cl_2]_2$ (0.125 mmol) and NaOAc (0.28 mmol) in refluxing 1,2-dicholoroethane (5 mL) for the stated duration. [b]Average isolated yield (over two runs). [c]Reaction was only performed once.

An bell-shaped trend was observed for iridacycle (R_C,R_N,S_{Ir})-**1** and coordinated dimethylamine complex **3**, indicating that the complexes could act as intermediates for the other products within the same reaction. A similar trend can also be said for cycloiridated complexes *rac*-**4** and *rac*-**5**, as well as 1-ethylnaphthalene **6**. However, due to their low yields (and, thus, higher margin of error with regards to isolation), it was not advisable to comment on these compounds. On the other hand, 1-acetonaphthone **2** portrayed a continuous upward trend with regards to yield, although its formation begun to plateau after two days into the reaction. Nevertheless, the results reflected the inertness of the organic molecule under the reaction conditions and, possibly, its identity as an end product within the cyclometalation procedure.

Lastly, we performed the same reaction with *rac*-*N*,*N*-dimethyl-1-naphthylethyl-*α*-*d*-amine *rac*-**L1'** to gain further insights into the formation of the products.

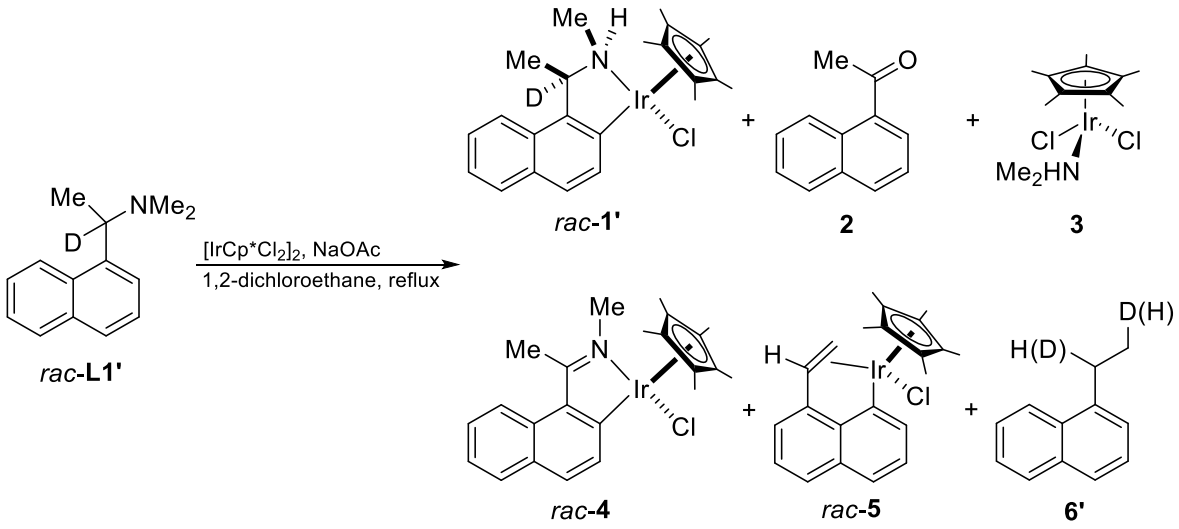

Scheme 2.4. The iridation reaction of *rac*-*N*,*N*-dimethyl-1-naphthylethyl-*α*-*d*-amine *rac*-**L1'**.

To obtain sufficient products for isolation and characterization, the two-day process was selected for the protocol. With regards to chemical yield, the reaction provided similar amounts of each product to its non-deuterated counterparts. Of all the compounds obtained, presence of deuterium was observed in *N*-demethylated iridacycle *rac*-**1'** and 1-ethylnaphthalene **6'**. To our surprise, olefin-type cycloiridated complex *rac*-**5** showed absence of deuterium on the alkene functionality despite the free amine *rac*-**L1'** having a deuterium at the *α*-carbon prior to the metalation procedure. Whenever relevant, we will discuss the formation of the individual deuterated products in later sections.

Synthesis of Cyclometalating Ligands

(*R*)-*N*,*N*-dimethyl-1-naphthylethylamine (*R*)-L1

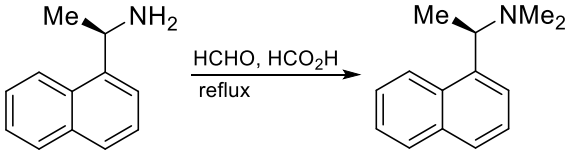

The methylated tertiary amine can be obtained from its corresponding primary amine *via* the Eschweiler-Clarke reaction. Utilizing excess formic acid and formaldehyde, the amine moiety was continuously methylated through reductive amination until the formation of the desired tertiary amine. The product can be obtained in quantitative yield and retains the stereochemistry of the substrate.

rac-*N*,*N*-dimethyl-1-naphthylethyl-α-*d*-amine *rac*-L1'

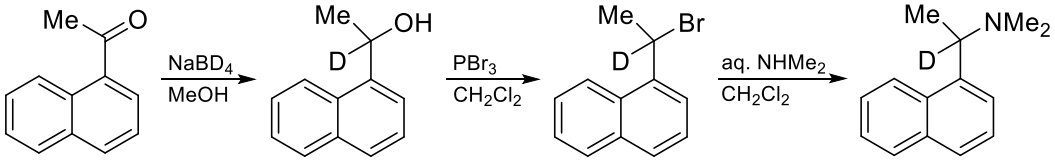

rac-**L1'**

The synthesis begin from the reduction of 1-acetonaphthone with $NaBD_4$ as the reducing agent. Treatment of borate intermediate with aqueous NaOH solution then provided the corresponding alcohol in quantitative yields. Phosphorus tribromide was subsequently employed to halogenate the alcohol functionality through nucleophilic substitution. Finally, the organobromide undergoes another nucleophilic substitution, this time with aqueous dimethylamine, to afford the desired racemic ligand *rac*-**L1'** in 93% yield.

2.1.1 (R_C,R_N,S_{Ir})-(1,2,3,4,5-Pentamethylcyclopentadienyl){(κ^2-*C*,*N*)-1-[1-(*N*-methyl-amino)ethyl]naphthyl}iridium(III) Chloride, (R_C,R_N,S_{Ir})-1

Isolated as an orange solid, cycloiridated complex **1** was characterized preliminarily *via* NMR spectroscopy and single crystal x-ray crystallography.

Spectroscopically, the successful cyclometalation was determined from the absence of an aromatic proton from the ^{1}H NMR spectrum. In addition, the spectrum also revealed an unexpected loss of a *N*-methyl substituent with only one methyl group at the nitrogen center based on relative integral ratios at 3.02 ppm. Supporting the observation was the single characteristic *N*-methyl carbon resonance signal at 66.89 ppm in the ^{13}C NMR spectrum (the two *N*-methyl groups are magnetically-inequivalent upon cyclometalation).

As described earlier in the introductory section, the loss of this methyl group was surprising. C–N bonds generally has high bond dissociation energy[7] and its cleavages are uncommon[8] in literature. It is also worth mentioning that the complex has additional stereogenic centers at nitrogen and iridium. Since the stereogenicity at carbon was determined by ligand (*R*)-**L1**, the reaction could afford four possible diastereomers. Returning to the ^{1}H NMR spectrum, we noticed that only one Cp* resonance signal at 1.67 ppm was observable. Likewise, the ^{13}C NMR reflected similar consensus with the methyl substituents on the cyclopentadienyl ring depicting a single signal at 9.36 ppm. A certain selectivity was, thus, hinted for the C–N bond cleavage process within the cycloiridation procedure.

To confirm the cleavage of the C–N bond and determine the stereochemistry at the stereogenic centers within the complex, crystals of cycloiridated complex **1**, in the form of orthorhombic orange blocks, were obtained through recrystallization from a solvent mixture of *n*-hexane and dichloromethane.

The molecular structure of the complex confirmed the loss of the *N*-methyl substituent within the ligand framework. Geometrically, the compound conformed to an expected *pseudo*-tetrahedral structure at the iridium center. The absolute configurations at carbon, nitrogen and iridium were also determined to be *R*, *R* and *S*, respectively, according to Cahn-Ingold-Prelog sequence rules.[9]

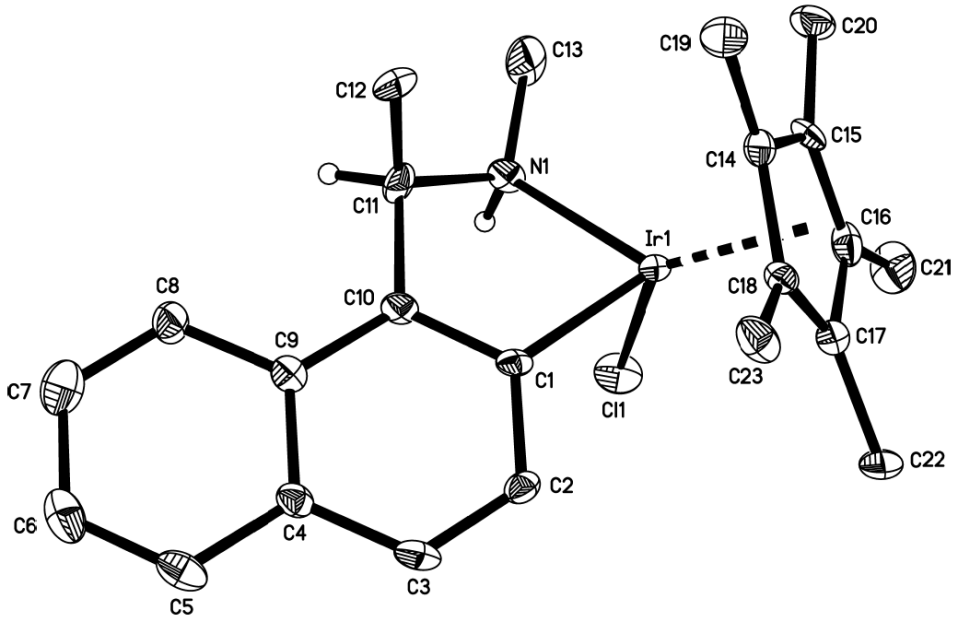

Figure 2.3. Molecular structure of cycloiridated complex (R_C,R_N,S_{Ir})-**1** with thermal ellipsoids shown at 50% probability. Hydrogen atoms except H(C11) and H(N1) are omitted for clarity. Selected bond lengths and angles: N−Ir (2.134(5) Å), C_1−Ir (2.035(7) Å), Cl−Ir (2.4338(18) Å), N−Ir−C_1 (76.8(2)°), N−Ir−Cl (81.94(17)°), C_1−Ir−Cl (86.19(19)°).

With the structure of the complex now at hand, we performed a fragmentation analysis to breakdown the formation of the complex in the iridation procedure. Here, we see that the complex retained much of the ligand motif other than a moiety of the *N*-methyl substituent. The carbon stereogenic center was also left unscathed indicating that the *N*-demethylation procedure did not involve the chiral carbon center. This was further supported by the deuterium studies involving the iridation of deuterated ligand *rac*-**L1'**.

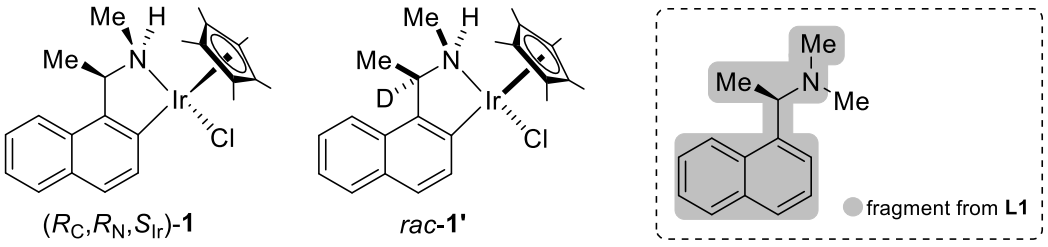

Figure 2.4. Fragmentation analysis for (R_C,R_N,S_{Ir})-**1** and *rac*-**1'**.

We have reported two similar instances of *N*-demethylation in 2014.[2a, 2b] In these investigations, the process was observed when attempts were made to cyclopalladate two sterically hindered tertiary amine ligands. Whilst ligand (*R*)-**L1** is sterically less hindered in the cyclopalladated systems, we supposed that the steric crowd about the coordination sphere of iridium was significant to initiate such a process. We will discuss these effects in Section 2.2.

Recap on Past Work...

The *N*-Demethylation of Tertiary Amines

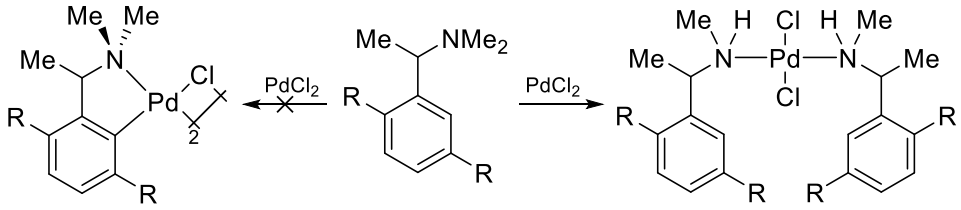

Novel *N*,*N*-dimethyl-1-arylethylamines were found to undergo chemoselective *N*-demethylation reaction when reacted with palladium(II) salts under mild conditions. A *β*-hydride elimination pathway was postulated and suggested to be driven by steric crowding about the metal center, greatly influenced by the bulky projecting group (substituent at *meta* position) on the aromatic ring.

Mechanistically, we proposed a modified reaction mechanism to the *N*-demethylation process. It was suggested that an agostic interaction between the metal and the C–H bond of the *N*-methyl substituent would either cycloiridate or oxidize the coordinated tertiary amine complex to its three-membered iridacycle or iminium species respectively. The reactive intermediates then readily undergo hydrolysis to provide an *α*-aminoalcohol species, which instantaneously eliminate a molecule of formaldehyde to give its chiral secondary amine derivative (*R*)-**L2**. The latter can then undergo direct cycloiridation with $[IrCp^*Cl_2]_2$, in the presence of NaOAc, to provide cycloiridated complex (R_C,R_N,S_{Ir})-**1**.

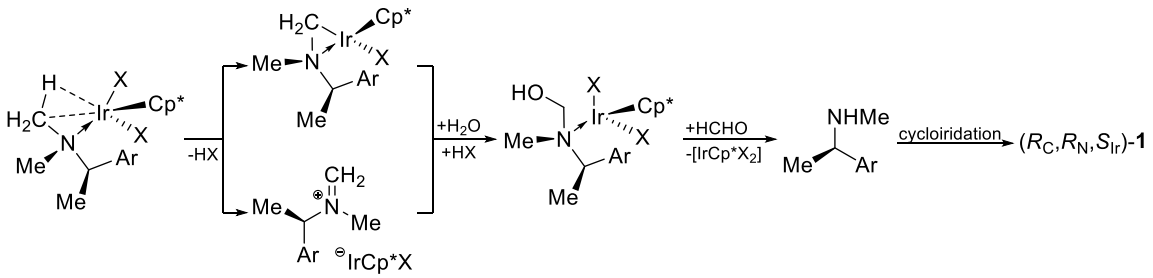

Scheme 2.5. Proposed *N*-demethylation mechanism to (R_C,R_N,S_{Ir})-**1** (X = Cl, OAc).

It should be noted that the direct cycloiridation of (*R*)-**L2** has been performed and solely produced (R_C,R_N,S_{Ir})-**1** as the only isomer (hence, the reason why only one isomer was isolated for the *N*-demethylation of (*R*)-**L1**). The experiment also presented a plausible pathway for the formation of (R_C,R_N,S_{Ir})-**1** in the *N*-demethylation reaction. More details on the direct cycloiridation procedure will be covered in Chapter 3.

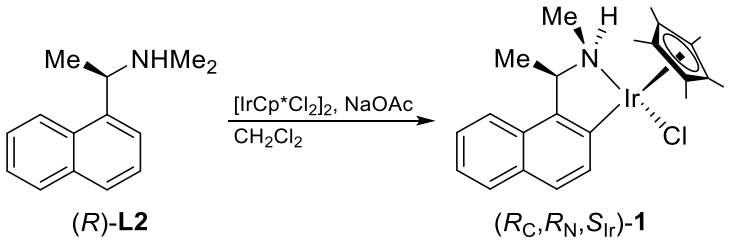

Scheme 2.6. Direct cycloiridation of (*R*)-**L2** to afford (R_C,R_N,S_{Ir})-**1**.

Lastly, the proposed mechanism suggested the presence of residual water hydrolyzing the three-membered iridacycle or iminium intermediate. We proceeded to attempt the reaction under anhydrous conditions in hopes of obtaining either reactive intermediates. Disappointingly, despite numerous trials, we were unable to isolate these compounds or determined their existence spectroscopically.

2.1.2 1-Acetonaphthone, 2

1-Acetonaphthone **2** presented the highest yielding product in the iridation reaction. Its formation generally retained much of the ligand scaffold other than the amine moiety.

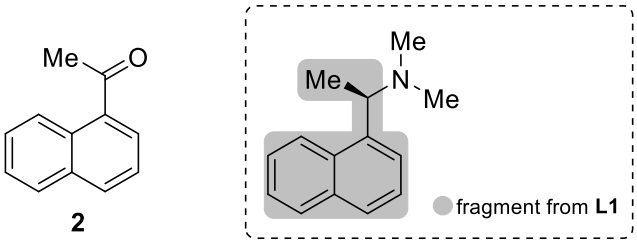

Figure 2.5. Fragmentation analysis for **2**.

Recalling the earlier proposed mechanism, it seemed that the product can be attained if the agostic interaction occurred at the C–H bond on carbon stereogenic center of the ligand motif. Like the *N*-demethylation procedure, a three-membered iridacycle or iminium intermediate was assumed after the activation process. Subsequently, the reactive species can be hydrolyzed to afford an α-aminoalcohol species, which rapidly released a molecule of coordinated dimethylamine iridium(III) complex **3** to provide the carbonyl compound.

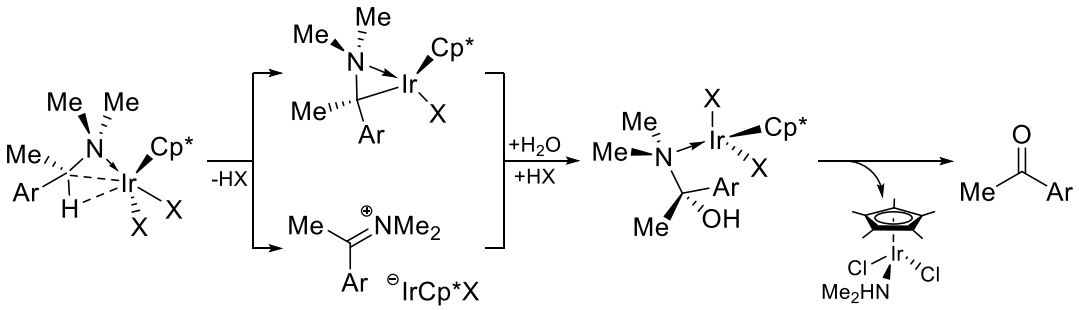

Scheme 2.7. Proposed mechanism to access 1-acetonaphthone **2** (X = Cl, OAc).

The higher yield of the product was hypothesized to be attributable to the acidic nature of the benzylic proton on the ligand. As such, it seemed to be easier to activate the said C–H bond than that on the *N*-methyl substituent.

It is also worth mentioning that the product contained a carbonyl moiety despite the absence of oxygen-containing reagents other than NaOAc. Since it was suggested that the source of oxygen atom originated from residual water in the reaction mixture, we attempted the reaction under dry conditions. However, as stated earlier, we were unable to isolate any intermediates or determined their existence spectroscopically despite the high yield of the organic product.

2.1.3 Dichloro(dimethylamino)-1,2,3,4,5-pentamethylcyclopentadienyl Iridium(III), 3

Coordinated amine complex **3** presented the second highest yielding product in the metalation protocol, although its yield began to plummet after two days. When left to stand in solution at room temperature, it was observed that the dimethylamine ligand would dissociate and return the metal back to its stable $[IrCp^*Cl_2]_2$ form. The transformation was also observed when chromatographed on silica gel.

The simple unwhelming structure suggested that the formation of the complex to be a mere coordination of dimethylamine to $[IrCp^*Cl_2]_2$. In addition, as described earlier, the compound provided a direct evidence to the cleavage of C–N bond in the iridation procedure.

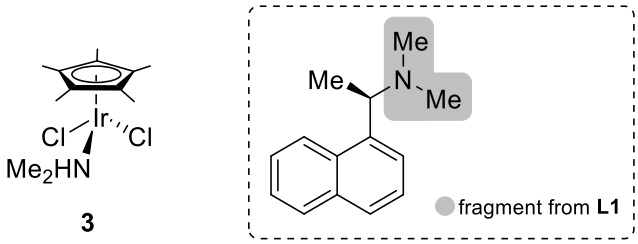

Figure 2.6. Fragmentation analysis for **3**.

2.1.4 *rac*-(1,2,3,4,5-Pentamethylcyclopentadienyl){(κ^2-*C*,*N*)-1-[1-(*N*-methylimino) ethyl]naphthyl}iridium(III) Chloride, *rac*-4

Cycloiridated imine complex *rac*-**4** was isolated as a dark red powder and characterized by NMR spectroscopy and single crystal x-ray crystallography.

Like iridacycle (R_C,R_N,S_{Ir})-**1**, the compound was determined to be successfully cyclometalated from the absence of a proton at the aromatic ring. The complex also reflected a loss of a methyl substituent at the nitrogen center based on relative integral ratios. The oxidation of the amine moiety was determined from the absence of the characteristic *C*-chiral proton signal and the downfield shift in resonance signal of the *C*-methyl protons to 2.98 ppm (the initial doublet resonance signal has also transformed to a singlet, indicative of no $^3J_{CH}$).

We proceeded to recrystallize the complex from a solvent mixture of *n*-hexane and dichloromethane and confirmed its molecular structure based on single crystal x-ray crystallography as shown in Figure 2.7.

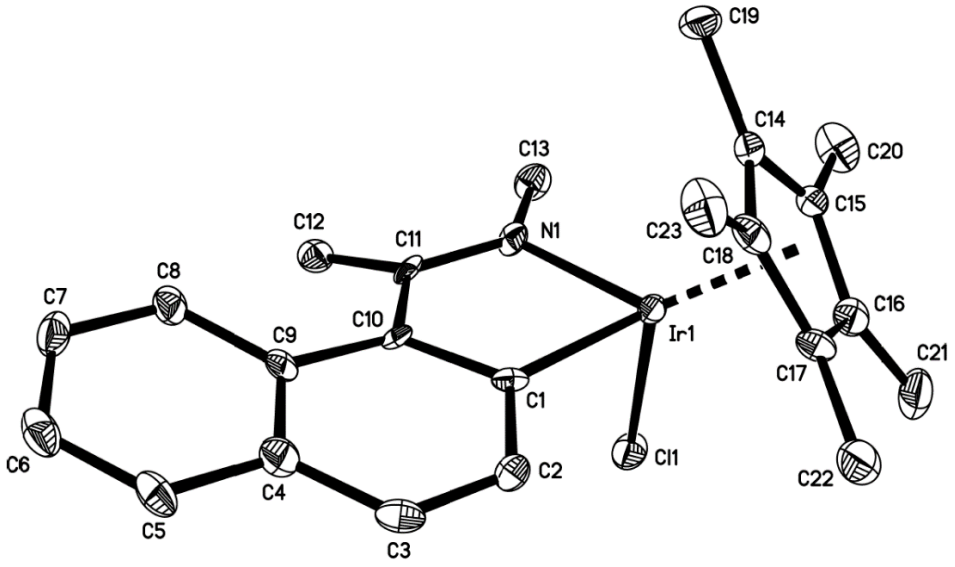

Figure 2.7. Molecular structure of cycloiridated complex *rac*-**4** with thermal ellipsoids shown at 50% probability. Hydrogen atoms are omitted for clarity. Selected bond lengths and angles: N−Ir (2.070(7) Å), C_1−Ir (2.028(8)Å), Cl−Ir (2.405(2) Å), N−Ir−C_1 (77.7(3)°), N−Ir−Cl (82.8(2)°), C_1−Ir−Cl (90.5(2)°).

Whilst oxidation of an amine moiety is not uncommon, the oxidation of tertiary amine is rare since it would lead to quaternarization of the nitrogen center. Although it was not improbable for the iridium metal to coordinate to the π-cloud of the C=N bond, it was unlikely that the donor moiety would be able to direct the metal center to the activation site. Moreover, the quaternary nitrogen center would have to lose a methyl substituent at this stage to attain the cycloiridated product.

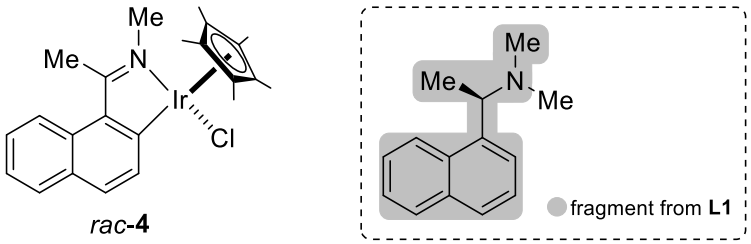

Figure 2.8. Fragmentation analysis for *rac*-**4**.

It seemed more likely that the C–N bond cleavage process occurred prior to cyclization of the imine moiety to the iridium(III) center. With such a postulation, the prior intermediate must, therefore, be iridacycle (R_C,R_N,S_{Ir})-**1**. To support the hypothesis, we took complex (R_C,R_N,S_{Ir})-**1** and heated it in hot 1,2-dichloromethane. In the absence of NaOAc, the complex was extremely stable with no trace of decomposition even after five days of heating. However, upon refluxing the mixture in the presence of NaOAc, small amounts of cycloiridated imine complex *rac*-**4** could be isolated. The result would also support the decrease in yield of (R_C,R_N,S_{Ir})-**1** for extended periods in the iridation procedure.

Lastly, it is worth mentioning that the resulting cycloiridated imine complex **4** was racemic. This was despite the dehydrogenation protocol not involving the metal center. Such would portray the labile nature of the imine moiety within the complex.

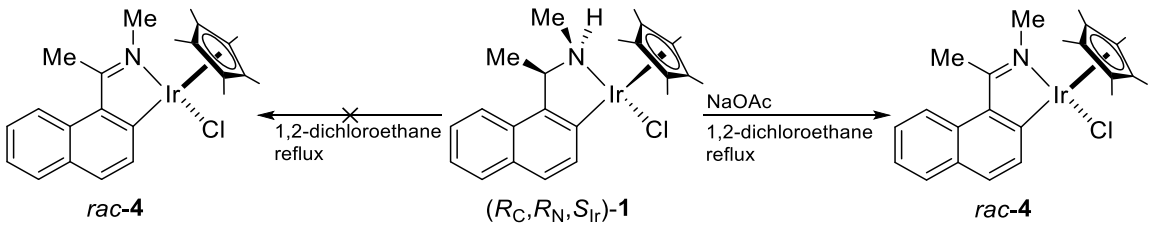

Scheme 2.8. Control experiment on the dehydrogenation process of (R_C,R_N,S_{Ir})-**1**.

2.1.5 *rac*-(1,2,3,4,5-Pentamethylcyclopentadienyl){(κ^2-*C*,[η^2-ethylene])-1-naphthylethene}iridium(III) Chloride, *rac*-5

Perhaps the most interesting cyclometalated complex from the reaction mixture was iridacycle *rac*-**5**. The olefin-type cycloiridated complex was obtained as bright orange powder upon isolation and can be recrystallized from a solvent mixture of *n*-hexane and dichloromethane to afford yellow block-like crystals.

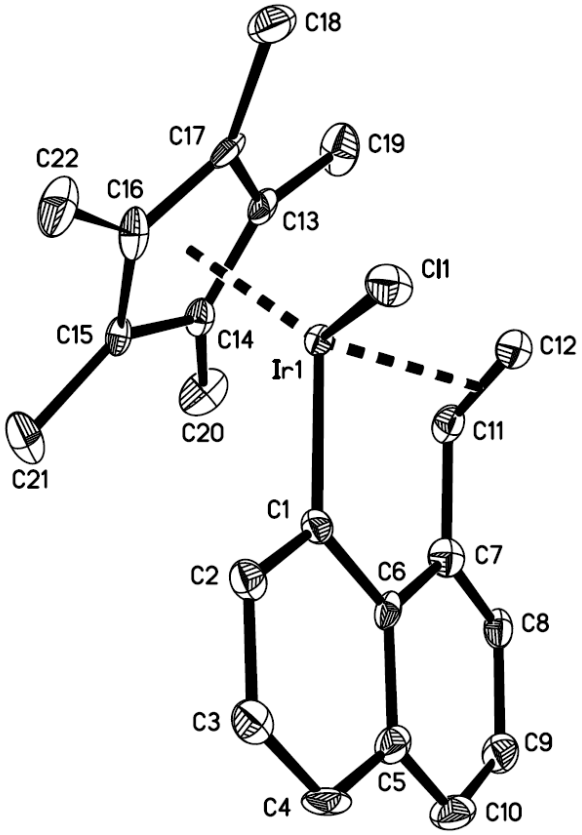

Figure 2.9. Molecular structure of cycloiridated complex *rac*-**5** with thermal ellipsoids shown at 50% probability. Hydrogen atoms are omitted for clarity. Selected bond lengths and angles: Ir−C_1 (2.050(6) Å), Ir−C_{11} (2.171(7) Å), Ir−C_{12} (2.131(7) Å), Ir−Cl (2.405(2) Å), C_{11}–C_{12} (1.407(10) Å), C_1−Ir−Cl (83.6(2)°), C_{11}–Ir–C_{12} (38.2(3)°), C_7–C_{11}–C_{12} (122.1(6)°).

Crystallographically, the complex depicted a *pseudo*-tetrahedral cycloiridated complex in which the iridium center was chelated by an anionic carbanion on the aromatic ring and the π-bond about the olefin moiety. Although coordination onto π-electrons of a bond is not uncommon in organometallic chemistry,[10] such chelation are extremely rare in

cyclometalated entities.[11] The C=C olefinic bond length (141 pm) within the complex was found to be slightly longer than that to a free alkene (134 pm).[12] A comparison against a structurally analogous iridium(III) cyclopentadienyl complex also revealed similar bond lengths between iridium and both carbon moieties of the olefin functionality.[11] Along the plane of the naphthalene system, the alkene moiety was found to lie out of the plane by 63.8°, tilting 30.4° off along the Ir–Cl axis.

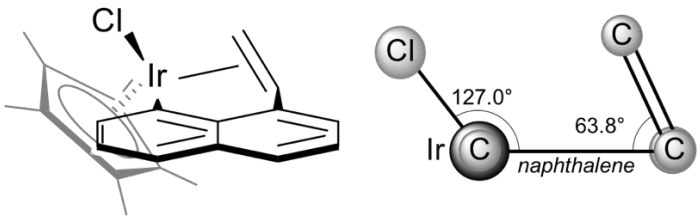

Figure 2.10. Three-dimensional representation of *rac*-**5** about the plane of the naphthalene ring.

It is also worth noting that the 1-vinylnapthalene ligand was cyclized at position-8 of the naphthalene ring instead of the *ortho* position. We believed that the observation was attributable to the larger $C_{Ar}–C_{\alpha}–E_{\pi\text{-bond}}$ bond angle (~120° instead of 109.5°) making it less likely to interact with the *ortho* proton either due to incorrect spatial orientation or increased proximity.

Spectroscopically, the NMR spectra were generally in line with the molecular structure of the complex. The ^{13}C NMR spectrum reflected the coordinated olefin moiety with its distinctive upfield chemical shifts of 56.16 ppm (ArCH=*C*H$_2$) and 80.82 ppm (Ar*C*H=CH$_2$). Coupling between the olefinic protons ($^3J_{HH}$) in the ^{1}H NMR were within expected values averaging 8.8 Hz and 11.3 Hz for *cis* and *trans* H–H coupling respectively.

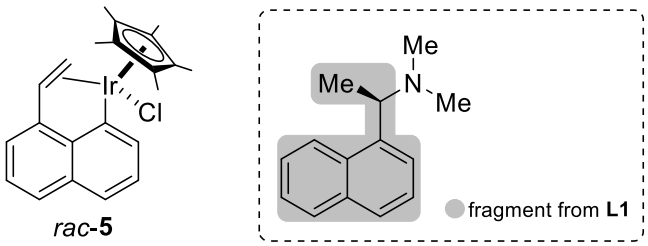

Figure 2.11. Fragmentation analysis for *rac*-**5**.

Like the other products in the metalation procedure, iridacycle *rac*-**5** resembled part of the ligand (*R*)-**L1** when broken down, specifically the hydrocarbon backbone of the ligand. Due to its unique point of activation at carbon-8 of the naphthalene ring, it was believed that the formation of the compound did not involve cycloiridated complexes (R_C,R_N,S_{Ir})-**1** and *rac*-**4**. Hence, we postulated that the product must have formed from the direct cycloiridation of 1-vinylnaphthalene or from a complexed intermediate.

We proceeded to cyclometalate 1-vinylnaphthalene with $[IrCp^*Cl_2]_2$ in the presence of NaOAc in refluxing 1,2-dichloroethane. Whilst the reaction did yield the desired iridacycle, the protocol was extremely inefficient with less than 1% *rac*-**5** isolated from the reaction mixture over three days (remaining 1-vinylnaphthalene could be quantitatively recovered). As such, we believed that the η^1,η^2-cycloiridated complex from the attempted cycloiridation reaction was not attained *via* this pathway.

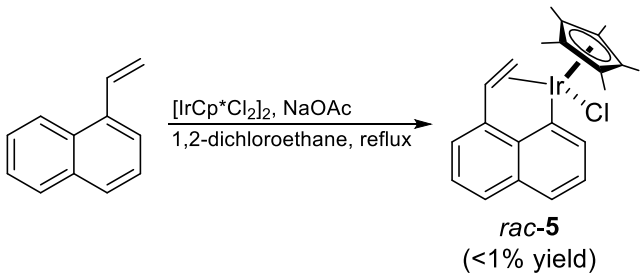

Scheme 2.9. Cycloiridation of 1-vinylnaphthalene with $[IrCp^*Cl_2]_2$.

Lastly, we consider the formation of the coordinated olefin compound *via* a complexed intermediate. Since the directing efficacy of the alkene moiety is poor, we hypothesized that the cycloiridated intermediate must be directed by the amine functionality. A six-membered metallacycle was proposed to be the intermediate. A dehydroamination process would then take place, releasing a molecule of dimethylamine, to provide olefin-type cycloiridated complex *rac*-**5**. It should also be recalled that the iridation of deuterated ligand *rac*-**L1'** afforded the same metallacycle with no deuterium within its molecular structure. As such, the dehydroamination procedure must involve the proton at the carbon stereogenic center in a *β*-hydride elimination-like mechanistic pathway or a proton migration to the coordinated amine moiety.

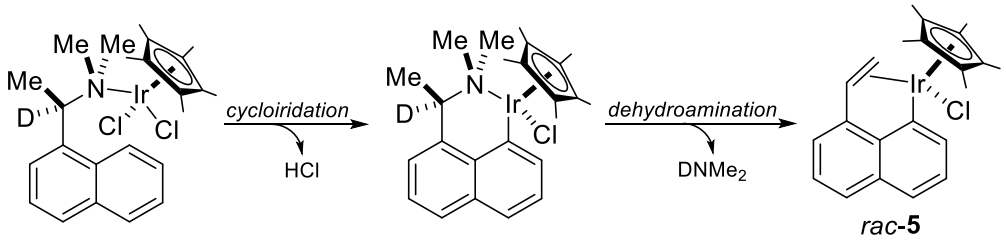

Scheme 2.10. Proposed mechanism to *rac*-**5** *via* complexed intermediate.

Whilst the proposed mechanism was plausible, proof of formation of the cycloiridated intermediate within the reaction was not attained. In addition, attempts to obtain the cycloiridated species by other means were also unsuccessful. Lastly, it should be noted that the formation of the six-membered iridacycle intermediate is less favorable than its five-membered counterpart.[13]

2.1.6 1-Ethylnaphthlene, 6

Finally, we take a look at the last product of the iridation reaction – 1-ethylnaphthalene **6**. Analyzing its structure, the compound was believed to be formed from the hydrocarbon component of the ligand (*R*)-**L1**. However, what made the product interesting was its lack of functional groups within the molecule.

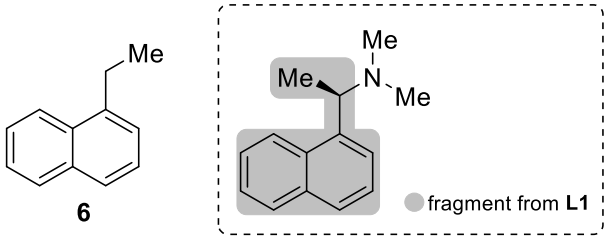

Figure 2.12. Fragmentation analysis for **6**.

Reviewing the possible origins of the product suggested that the compound came from olefin-type cycloiridated complex *rac*-**5**. The complex was believed to undergo hydrogenation (with its source of hydrogen possibly originating from the dehydrogenation of (R_C,R_N,S_{Ir})-**1** to *rac*-**4**) to provide a monodentate *C*-coordinated iridium(III) complex. The latter would then be protonated through protonolysis to afford the hydrocarbon.

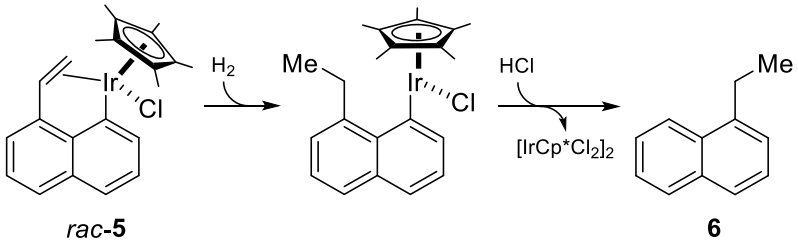

Scheme 2.11. Proposed mechanism to the formation of 1-ethylnaphthalene **6**.

To gain a further understanding on the reaction, we referred to its deuterium studies involving deuterated amine ligand *rac*-**L1'**. In an ideal situation, the reaction should afford two variants of hydrocarbon **6'** with one form having deuterium on the α-carbon while another is deuterated at the β-carbon.

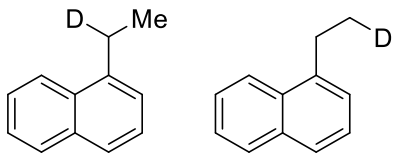

6'

Figure 2.13. Possible variants of deuterated 1-ethylnaphthalene **6'**.

Spectroscopically, the results were intriguing. While we did observed the presence of deuterium on both α- and β-carbon of the organic molecule, deuterium levels were relatively low at 18.8% and 4.6% respectively (compared to 92.5% at the α-carbon of ligand *rac*-**L1'** prior to the reaction). This represented an alternate source of hydrogen from the reaction mixture that was unknown to us. Alternatively, the η^1,η^2-iridacycle could undergo a separate distinct mechanism that adds the hydrogen atoms to the organic framework within the complex to produce the desire compound.

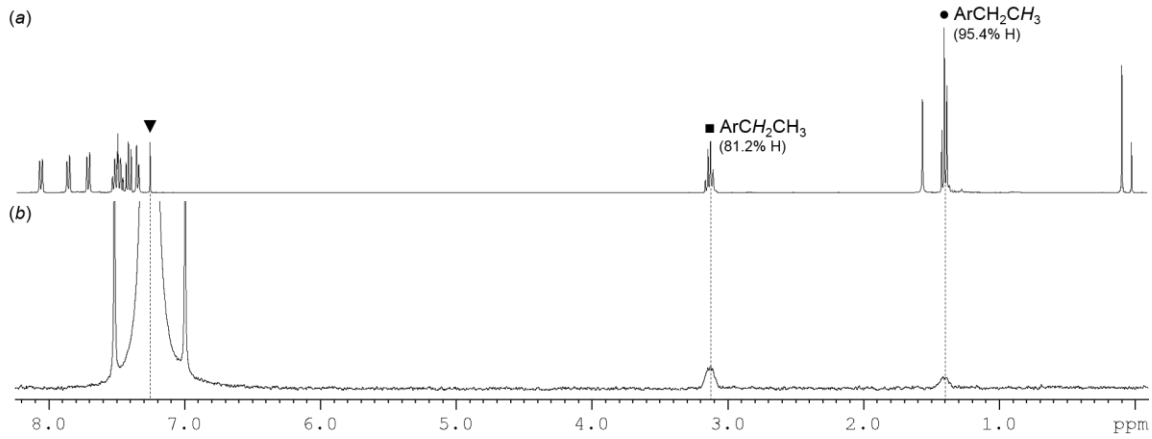

Figure 2.14. NMR spectra ((*a*) ^{1}H NMR and (*b*) ^{2}H NMR) of 1-ethylnaphthalene **6'**. Compounds are dissolved in $CDCl_3$ and their spectra were acquired at 400 MHz (● at 1.40 ppm ($ArCH_2CH_3$), ■ at 3.13 ppm ($ArCH_2CH_3$) and ▼ at 7.26 ppm (residual solvent of $CDCl_3$ [in ^{1}H NMR]; $CDCl_3$ [in ^{2}H NMR])).

2.2 Steric Hindrance as a Cause to Failed Cyclometalation

As described in section 2.1.1, it was postulated that the failure to obtain the desired cyclometalated product (and the formation of the byproducts in our attempt) was attributable to steric crowd about the coordination sphere of iridium based on our past work. As such, we investigate the effects of steric hindrance on cycloiridation with $[IrCp^*Cl_2]_2$ in this section.

Geometrically, palladacycles have greater spatial capacity about the coordination sphere at palladium. Whilst the cyclometalating ligands were bounded within the same approximate 90° bite angle of the bidentate ligand in the Cp*-based iridacycles, its degree of freedom was restricted by the presence of other ligands within the coordination sphere of iridium. As such, we hypothesized that the iridium(III) Cp*-based complexes have less tolerance towards steric hindrance as compared to its palladium square-planar counterpart during the cyclometalation process (a possible reason why ligand **L1** could cyclize in palladium, but not in iridium).

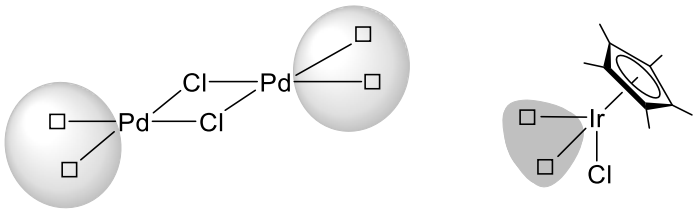

Figure 2.15. Coordination modes for cyclometalating ligands on palladium and iridium.

With the observation that an additional *N*-methyl substituent could affect the cycloiridation procedure, we designed a series of experiments involving two cyclometalating ligands to determine the extent at which cycloiridation fails to proceed.

2.2.1 Cycloiridation of *N*,*N*-Dimethyl-1-naphthylmethylamine L3

The first experiment involved cyclometalating ligand *N*,*N*-dimethyl-1-naphthylmethylamine **L3**. The cycloiridation process proceeded smoothly, albeit sluggishly, affording the desired cycloiridated complex *rac*-**7** after 24 h in 73% yield. It is also worth mentioning that the *ortho*-iridation protocol can proceed at room temperature, with no indication of the byproducts observed in the iridation of ligand (*R*)-**L1**.

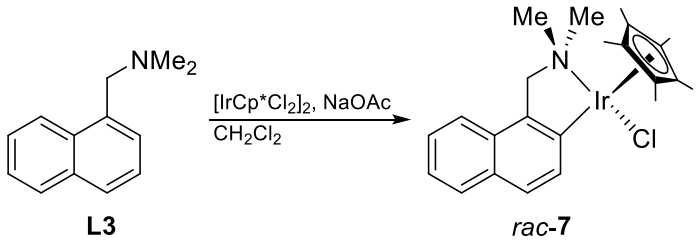

Scheme 2.12. Cycloiridation of *N*,*N*-dimethyl-1-naphthylmethylamine **L3**.

Characteristically, the successful cyclometalation was determined from the absence of one proton from the aromatic system. The complex also reflected distinctive resonance signals for each of its *N*-methyl substituents (at 2.96 ppm and 3.11 ppm) and its acidic *α*-protons (at 3.99 ppm and 4.48 ppm), representative of a cyclometalated complex (due to restricted rotation within the five-membered organometallic ring).

Synthesis of Cyclometalating Ligands

1-Naphthylmethylamine L3

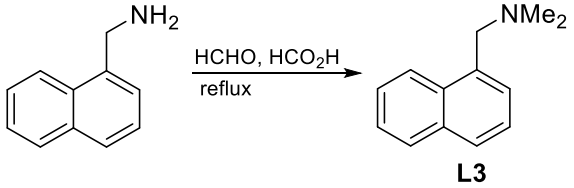

Similar to its chiral derivative **L1**, the methylated tertiary amine ligand **L3** can be synthesized from its corresponding primary amine *via* the Eschweiler-Clarke reaction. The product was obtained from refluxing the amine in excess formic acid and formaldehyde for at least 16 h. The product can be isolated in near quantitative yield *via* column chromatography on silica gel with triethylamine and dichloromethane (1:50) as eluent.

The cycloiridated complex was subsequently recrystallized as red monoclinic crystals, in the form of blocks, from a solvent mixture of *n*-hexane and dichloromethane for confirmation of molecular structure by single crystal x-ray crystallography. Structural analysis of the complex will be covered in Chapter 4 of the thesis.

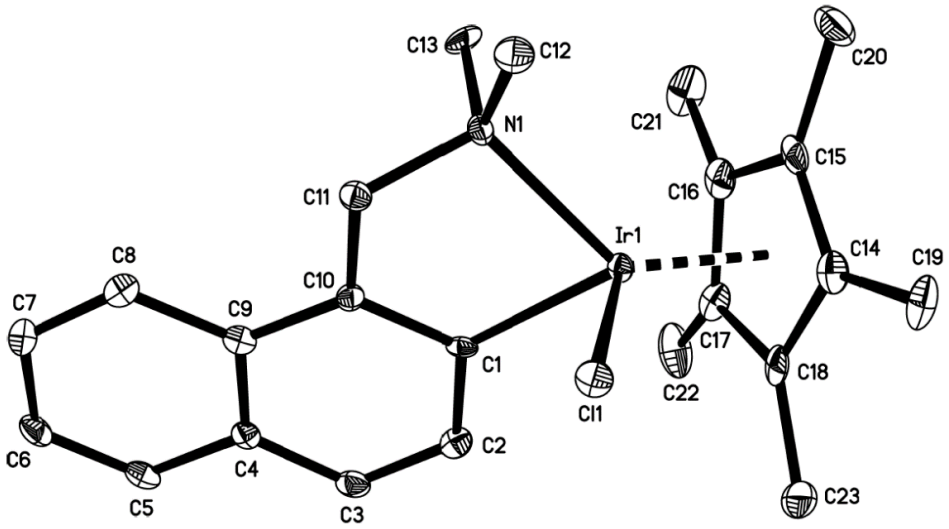

Figure 2.16. Molecular structure of cycloiridated complex *rac*-**7** with thermal ellipsoids shown at 50% probability. Hydrogen atoms are omitted for clarity. Selected bond lengths and angles: N−Ir (2.192(5) Å), C_1−Ir (2.043(6) Å), Cl−Ir (2.438(2) Å), N−Ir−C_1 (78.5(2)°), N−Ir−Cl (85.9(1)°), C_1−Ir−Cl (87.8(2)°).

Together with the direct cycloiridation of chiral secondary amine (*R*)-**L2**, it seemed that an additional methyl substituent within the framework could potentially impact cycloiridation as a whole. Comparing both cases, we speculated that the methyl groups brought the iridium center closer to the aromatic C–H bond for activation *via* the Thorpe-Ingold effect[14] to initiate the cyclometalation procedure. However, enhancing it further with an additional alkyl moiety pushed the metal through its limits such that it had to relieve itself possibly through *N*-demethylation to release the stress of steric crowding within the coordination sphere of the metal. It should also be noted that such a case was only present in the iridium(III) Cp*-based complexes (and not in the palladacycles) due to the existence of the bulky Cp* moiety which constricted the coordinative space within the iridium(III) complex.

2.2.2 Iridation of (*R*)-*N*,*N*-Dimethyl-1-phenylethylamine (*R*)-L4

A distinctive feature of ligand (*R*)-*N*,*N*-dimethyl-1-naphthylethylamine (*R*)-**L1** was its configuration lock upon cyclometalation.[3] The lock, which fixates the five-membered puckered ring within the complex to a certain configuration (*to be discussed in greater detail in* Chapter 3 *of the thesis*), may impose steric requirements to the complex such that cycloiridation may not proceed efficiently.

Since iridacycle *rac*-**7** does not have such locking mechanism within its structure, we cannot conclusively determine if it was the configurational lock or the additional methyl substituent that resulted in the failed direct cycloiridation of ligand (*R*)-**L1**. As such, we synthesized its phenyl derivative (*R*)-**L4** and utilized it for the iridation procedure.

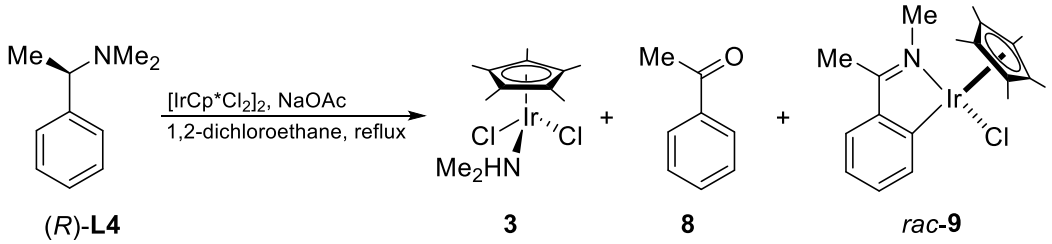

Scheme 2.13. The iridation reaction of (*R*)-*N*,*N*-dimethyl-1-phenylethylamine (*R*)-**L4**.

Synthesis of Cyclometalating Ligands

(*R*)-1-Phenylethylamine L4

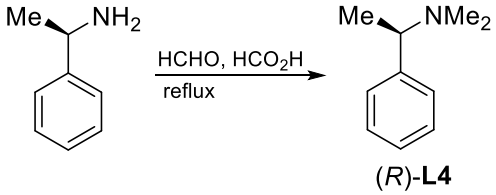

(*R*)-1-Phenylethylamine (*R*)-**L4** was synthesized from its corresponding primary amine *via* the Eschweiler-Clarke reaction. The primary amine was refluxed in excess formic acid and formaldehyde for 16 h affording the tertiary amine after workup in near quantitative yields. The process also retained its stereochemistry after the reaction.

Gratifyingly, the experiment was found to proceed *via* the competing pathway affording coordinated dimethylamine iridium(III) complex **3**, acetophenone **8** and cycloiridated imine complex *rac*-**9**. The reaction shed light onto two areas: (a) the stereogenic locking mechanism was not the cause for the failure to direct cyclometalation, and (b) the additional methyl substituent at either the nitrogen atom or α-carbon implicated the iridation procedure, resulting in the formation of the byproducts.

It was, however, surprising that we could not isolate iridacycle (R_C,R_N,S_{Ir})-**10** from the reaction mixture. Nonetheless, we were able to collect fractions of *rac*-**9** from the chromatographed mixture which were representative of the oxidized variants of iridacycle (R_C,R_N,S_{Ir})-**10**. Together with coordinated dimethylamine complex **3** and acetophenone **8**, the reaction completed the picture of the *N*-dealkylation process.

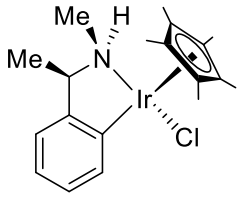

(R_C,R_N,S_{Ir})-**10**

Figure 2.17. Molecular structure of cycloiridated complex (R_C,R_N,S_{Ir})-**10**.

3 SUMMARY AND CONCLUSION

In the chapter, we observed an interesting phenomenon in which an unsuccessful cycloiridation procedure would lead to byproducts stemming from *N*-demethylation protocols, and subsequent smaller byprocesses after the formation of the dealkylated products. The competing pathway was found to be driven by steric hindrance about the coordination sphere of the metal center, enhanced by implications from the Thorpe-Ingold effect.

In an earlier work,[2a] we had concluded that such procedures were due to steric obstructions by projecting groups on the ligand motif which prevented the activation of C–H bond by the metal center. Our current work highlighted the need to account for other ligands, in addition to the involved cyclometalating ligand, about the metal center when considering cyclometalation or its related reactions.

With much research going into the formation of cyclometalated complexes and its more popular metal-mediated C–H bond functionalization reactions (which involved metallacycles as reactive intermediates), we hope that the work could serve as a reference to byproducts and/or new modes of activation for novel access to synthetically-useful chemicals.

REFERENCES

1. Allen, D. G.; McLaughlin, G. M.; Robertson, G. B.; Steffen, W. L.; Salem, G.; Wild, S. B. *Inorg. Chem.* **1982**, *21*, 1007-1014.
2. (a) Yap, J. S. L.; Ding, Y.; Yang, X.-Y.; Wong, J.; Li, Y.; Pullarkat, S. A.; Leung, P.-H. *Eur. J. Inorg. Chem.* **2014**, 5046-5052; (b) Yap, J. S. L.; Chen, H. J.; Li, Y.; Pullarkat, S. A.; Leung, P.-H. *Organometallics* **2014**, *33*, 930-940; (c) Yap, J. S. L.; Li, B. B.; Wong, J.; Li, Y.; Pullarkat, S. A.; Leung, P.-H. *Dalton Trans.* **2014**, *43*, 5777-5784; (d) Ding, Y.; Zhang, Y.; Li, Y.; Pullarkat, S. A.; Andrews, P.; Leung, P.-H. *Eur. J. Inorg. Chem.* **2010**, 4427-4437; (e) Ding, Y.; Li, Y.; Pullarkat, S. A.; Leng Yap, S.; Leung, P.-H. *Eur. J. Inorg. Chem.* **2009**, 267-276; (f) Ding, Y.; Li, Y.; Zhang, Y.; Pullarkat, S. A.; Leung, P.-H. *Eur. J. Inorg. Chem.* **2008**, 1880-1891; (g) Li, Y.; Ng, K.-H.; Selvaratnam, S.; Tan, G.-K.; Vittal, J. J.; Leung, P.-H. *Organometallics* **2003**, *22*, 834-842; (h) Li, Y.; Selvaratnam, S.; Vittal, J. J.; Leung, P.-H. *Inorg. Chem.* **2003**, *42*, 3229-3236; (i) Ding, Y.; Chiang, M.; Pullarkat, S. A.; Li, Y.; Leung, P.-H. *Organometallics* **2009**, *28*, 4358-4370; (j) Ng, J. K.-P.; Chen, S.; Tan, G.-K.; Leung, P.-H. *Eur. J. Inorg. Chem.* **2007**, 3124-3134; (k) Ng, J. K.-P.; Chen, S.; Li, Y.; Tan, G.-K.; Koh, L.-L.; Leung, P.-H. *Inorg. Chem.* **2007**, *46*, 5100-5109; (l) Ng, J. K.-P.; Li, Y.; Tan, G.-K.; Koh, L.-L.; Vittal, J. J.; Leung, P.-H. *Inorg. Chem.* **2005**, *44*, 9874-9886; (m) Ng, J. K.-P.; Tan, G.-K.; Vittal, J. J.; Leung, P.-H. *Inorg. Chem.* **2003**, *42*, 7674-7682.
3. (a) Alcock, N. W.; Hulmes, D. I.; Brown, J. M. *J. Chem. Soc., Chem. Commun.* **1995**, 395-397; (b) Valk, J.-M.; Claridge, T. D. W.; Brown, J. M.; Hibbs, D.; Hursthouse, M. B. *Tetrahedron: Asymmetry* **1995**, *6*, 2597-2610; (c) Alcock, N. W.; Brown, J. M.; Hulmes, D. I. *Tetrahedron: Asymmetry* **1993**, *4*, 743-756.
4. (a) Yang, X.-Y.; Tay, W. S.; Li, Y.; Pullarkat, S. A.; Leung, P.-H. *Organometallics* **2015**, *34*, 1582-1588; (b) Yang, X.-Y.; Tay, W. S.; Li, Y.; Pullarkat, S. A.; Leung, P.-H. *Organometallics* **2015**, *34*, 5196-5201; (c) Yang, X.-Y.; Gan, J. H.; Li, Y.; Pullarkat, S. A.; Leung, P.-H. *Dalton Trans.* **2015**, *44*, 1258-1263.
5. (a) Yang, X.-Y.; Tay, W. S.; Li, Y.; Pullarkat, S. A.; Leung, P.-H. *Chem. Commun.* **2016**, *52*, 4211-4214; (b) Tay, W. S.; Yang, X.-Y.; Li, Y.; Pullarkat, S. A.; Leung, P.-H. *RSC Adv.* **2016**, *6*, 75951-75959.
6. Davies, D. L.; Al-Duaij, O.; Fawcett, J.; Giardiello, M.; Hilton, S. T.; Russell, D. R. *Dalton Trans.* **2003**, 4132-4138.
7. Blanksby, S. J.; Ellison, G. B. *Acc. Chem. Res.* **2003**, *36*, 255-263.
8. Ouyang, K.; Hao, W.; Zhang, W.-X.; Xi, Z. *Chem. Rev.* **2015**, *115*, 12045-12090.
9. Sloan, T. E., Stereochemical Nomenclature and Notation in Inorganic Chemistry. In *Topics in Stereochemistry*, John Wiley & Sons, Inc.: 2007; pp 1-36.
10. Crabtree, R. H., Complexes of π-Bound Ligands. In *The Organometallic Chemistry of the Transition Metals*, John Wiley & Sons, Inc.: 2005; pp 125-158.
11. Wakefield, J. B.; Stryker, J. M. *Organometallics* **1990**, *9*, 2428-2430.
12. Bond, G. C. *Platinum Met. Rev.* **2000**, *44*, 146-154.
13. Omae, I., Reasons Why Organometallic Intramolecular-Coordination Five-Membered Ring Compounds are Extremely Easily Synthesized through Cyclometalation Reactions. In *Cyclometalation Reactions: Five-Membered Ring Products as Universal Reagents*, Springer: 2014; pp 55-86.
14. (a) Beesley, R. M.; Ingold, C. K.; Thorpe, J. F. *J. Chem. Soc., Trans.* **1915**, *107*, 1080-1106; (b) Jung, M. E.; Piizzi, G. *Chem. Rev.* **2005**, *105*, 1735-1766.

CHAPTER 3

Stereogenic Lock in Cycloiridated Complexes
A Consideration for Chiral Catalyst and Auxiliary Design

ABSTRACT

A series of optically-active *pseudo*-tetrahedral five-membered cyclometalated 1-naphthylethylamine iridium(III) complexes were prepared and characterized to analyze the efficacy of the stereogenic conformational lock in both solid and solution phases. The synthesis of the iridacycles was diastereoselective, and the compounds were found to be conformationally rigid. In comparison to its phenyl derivative, the structural lock prevented oxidation of the amine moiety within the five-membered organometallic ring during its synthesis. With up to three stereogenic centers in one of the naphthalene complexes, the stereochemistry of the metallacycle remained stable to both thermal and chemical changes. In terms of catalytic performance, the complexes displayed excellent activity for the asymmetric hydrogen transfer reaction, albeit with modest enantioselectivities.

Keywords: Cycloiridated Complexes / Coordination Complexes / Stereogenic Lock / Conformational Lock / Catalyst and Auxiliary Design

1 INTRODUCTION

1.1 Stereogenic Lock

Quintessential to our work, stereogenic lock within a cyclometalated system plays a vital role in the outcome of our research. In most cases, a form of this conformational lock conveys stereogenic information to the prochiral substrate such that attack by the electronically-rich species is selectively controlled by the ligand motif to enhance enantioselectivity in reactions.

Whilst the system has worked its way silently in applications,[1] the idea was only conceptualized in 1993 by Alcock when crystallographic studies of these complexes were performed.[2] In the work, a comparison was made between cyclopalladated complexes of *N*,*N*-dimethyl-1-phenylethylamine and *N*,*N*-dimethyl-1-naphthylethylamine.

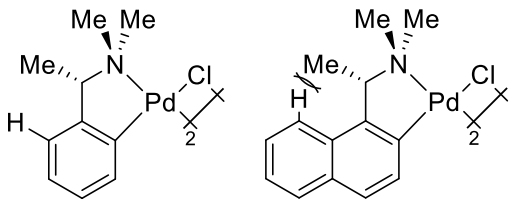

Figure 3.1. Chiral (*S*)-*N*,*N*-dimethyl-1-phenylethylamine and (*S*)-*N*,*N*-dimethyl-1-naphthylethylamine palladacycles.

It was found that an intramolecular interaction existed between the methyl substituent at the stereogenic carbon center and the neighboring proton at position-8 of the aromatic ring in the complexes of (*S*)-*N*,*N*-dimethyl-1-naphthylethylamine. Such spatial interaction locked the five-membered organometallic ring in a fixed λ configuration (and the δ configuration for the *R* isomer) preventing the cyclic system from undergoing a continuous C_2/C_s-interchanging conformational ring flip. The phenyl derivative, on the other hand, did not have the privilege of such steric interaction within its structure, providing complexes of both δ and λ conformations upon recrystallization. These interactions were also found to exist in the naphthalene complex (and not in its phenyl counterparts) at solution phase as proven by spectroscopic studies.[3]

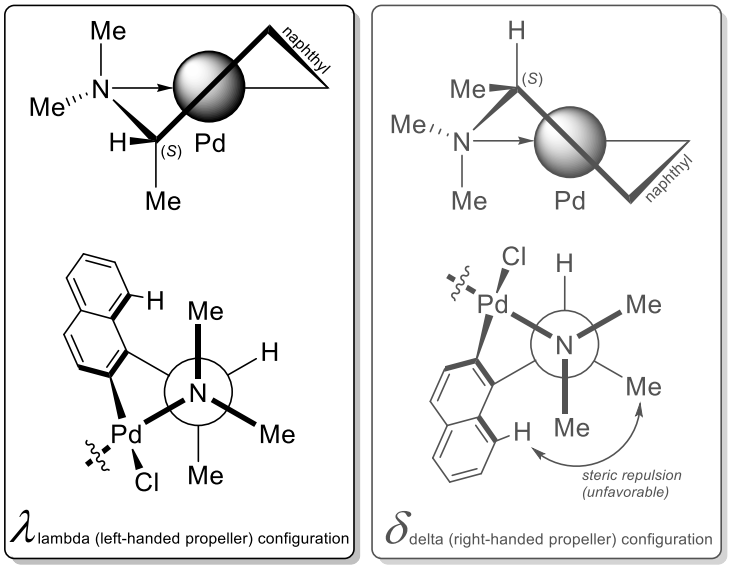

Figure 3.2. Possible conformations of cyclopalladated complex (*S*)-*N*,*N*-dimethyl-1-naphthylethylamine.

Conceptual Snippets

The C_2/C_s-Interchanging Ring Flip

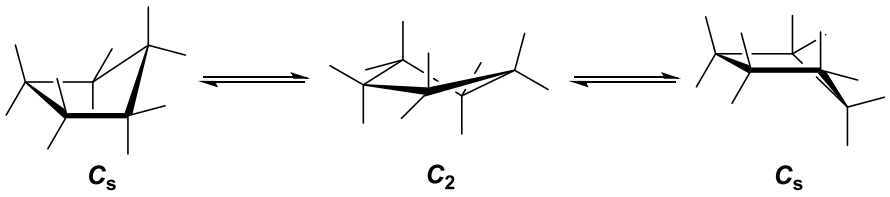

In five-membered cyclic ring systems, the puckered ring can interconvert between two low-energy conformations – the *envelope* (with C_s plane of symmetry) and *half-chair* (with C_2 axis of symmetry). While the envelop conformation has the lowest energy between the two forms, the energy barrier to the half-chair state is generally low such that interconversion can easily occur at room temperature.

The retention of configuration in the naphthalene system was, therefore, found to be superior since the lack of interchangeability permits the stereogenic information to be transferred more efficiently to the substrates from the cyclopalladated framework *via* the metal center. The effect of this critical feature in the design of these palladacyclic analogues has been evident in numerous asymmetric applications performed by our group.[4]

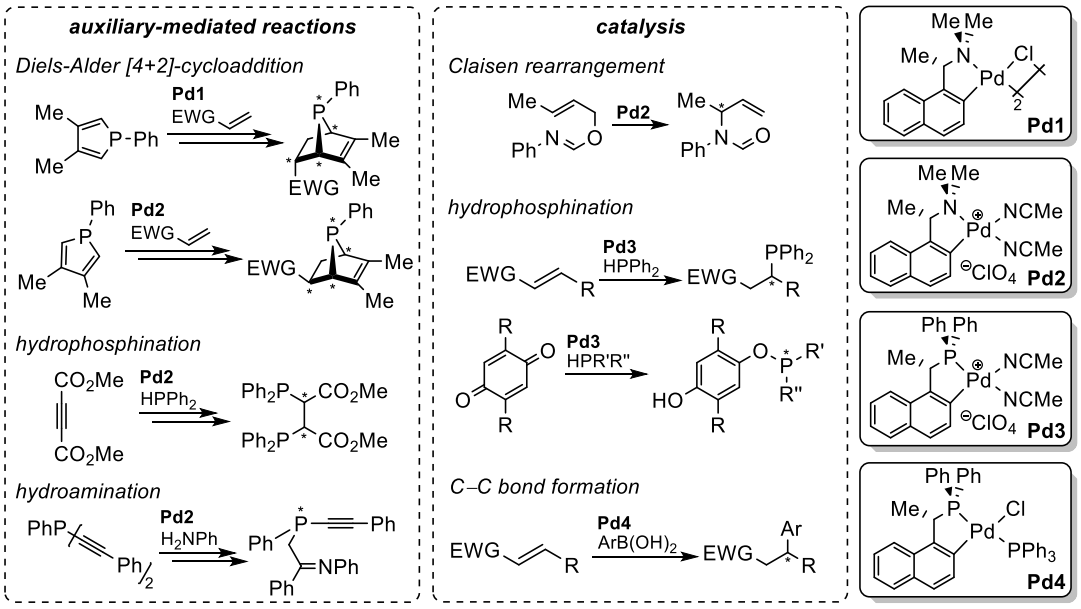

Figure 3.3. Selected stereogenically-locked palladacycle-mediated asymmetric applications performed by our group.

1.2 Research Objectives

We have been interested in developing new chiral cyclometalated systems for asymmetric applications. Over the past decade, our endeavor into the field has generated numerous novel metallacycles and these compounds have been extremely successful in asymmetric catalysis and syntheses.[5] Of specific mention is the bidentate stereogenically-locked species in which we have performed various structural studies to determine their extent of conformational lock.[5g-s] With significant knowledge on the effects of these conformationally-rigid ligand motifs in cyclopalladation chemistry and its consequences in asymmetric applications, we now seek to understand and, possibly, extend the concept of stereogenic lock to metallacycles of other transition metal elements.

Earlier in Chapter 2, we have revealed our intentions to expand our study of cyclometalated systems to half sandwich iridium(III) Cp*-based compounds. Whilst the iridation of tertiary amine (*R*)-*N*,*N*-dimethyl-1-naphthylethylamine (*R*)-**L1** did not yield the complex of interest, the protocol did provide an *ortho*-iridated secondary amine species that closely resembled the desired complex. As such, we believed that the compound could serve as a good starting point for the extension of our study into the chemistry of cycloiridation, specifically on the extent of conformational lock in these complexes.

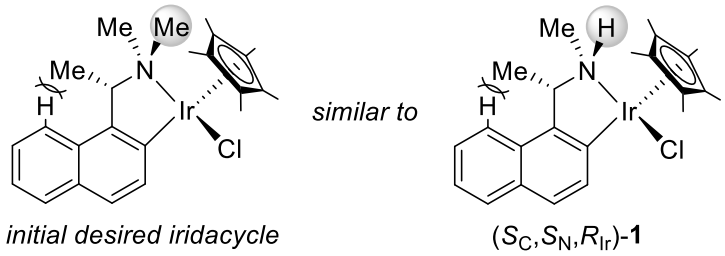

Figure 3.4. Similarities between the initial desired iridacycle and (S_C,S_N,R_{Ir})-**1**.

Lastly, whilst we highlighted the concept of stereogenic lock to cyclometalated complexes in the thesis, we believe that the idea could be implanted to the design of multidentate ligands systems and five-membered cyclic organocatalysts with analogous frameworks to enhance enantioselectivities in applications.

2 RESULTS AND DISCUSSION

2.1 The Direct Cycloiridation of (*S*)-L2

Recalling the failure to directly cycloiridate tertiary amine ligand (*S*)-**L1** (and the small consolation in attaining minute amounts of *N*-demethylated iridacycle (S_C,S_N,R_{Ir})-**1**) due to the immense steric crowd about the coordination sphere of iridium, we turned to its secondary amine derivative (*S*)-**L2** for direct cyclometalation with $[IrCp^*Cl_2]_2$ in the presence of NaOAc. Gratifyingly, unlike the former reaction, the latter protocol proceeded efficiently, affording the two cyclic organometallic complexes (S_C,S_N,R_{Ir})-**1** and (S_C,R_{Ir})-**11** in yields of 97% and 2% respectively.

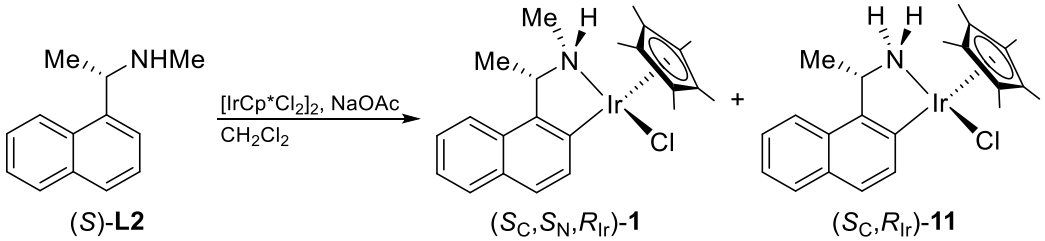

Scheme 3.1. Cycloiridation of optically-active secondary amine (*S*)-**L2**.

Synthesis of Cyclometalating Ligands

(*S*)-*N*-methyl-1-naphthylethylamine (*S*)-L2

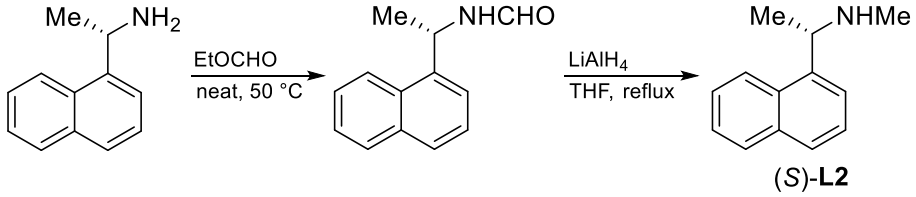

The chiral secondary amine (*S*)-**L2** can be obtained from its corresponding primary amine *via* a two-step one-pot procedure. The primary amine was first reacted with ethyl formate at 50 °C under neat conditions to provide a formamide derivative. The compound was then dissolved and reduced with lithium aluminum hydride to afford the desired secondary amine in 54% yield after purification by vacuum distillation.

The reaction presented two notable findings: (a) the existence of only one stereoisomer for each of the primary and secondary *amino* complexes, and (b) the formation of *N*-demethylated complex (S_C,R_{Ir})-**11** where a C−N bond was cleaved during the transformation. Two arguments exist to rationalize the formation of iridacycle (S_C,R_{Ir})-**11**: (a) the reaction could originate from the *ortho*-iridation of residual primary amine present in (*S*)-**L2** during its synthesis, and (b) a possible *N*-demethylation procedure as described in Chapter 2 of the thesis.

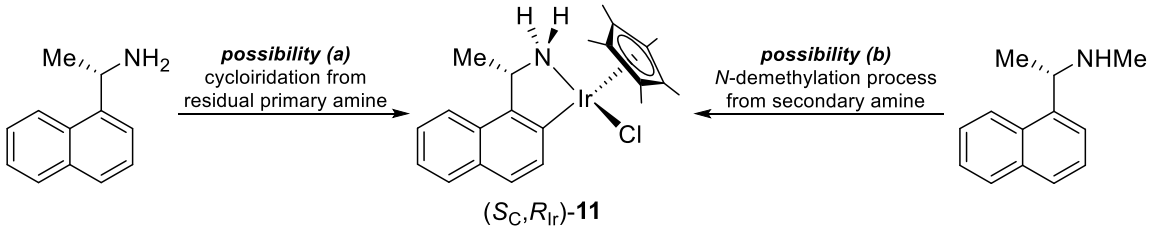

Scheme 3.2. Possible pathways to cycloiridated complex (S_C,R_{Ir})-**11**.

To eliminate the possibility of the former, its racemic variant *rac*-**L2**, prepared *via* a protocol that did not involve the primary amine derivative, was utilized for cycloiridation. As expected, the reaction once again yielded both complexes, confirming the *N*-demethylation of the secondary amine prior to cyclometalation to provide iridacycle (S_C,R_{Ir})-**11**.

Synthesis of Cyclometalating Ligands

***rac*-*N*-methyl-1-naphthylethylamine *rac*-L2**

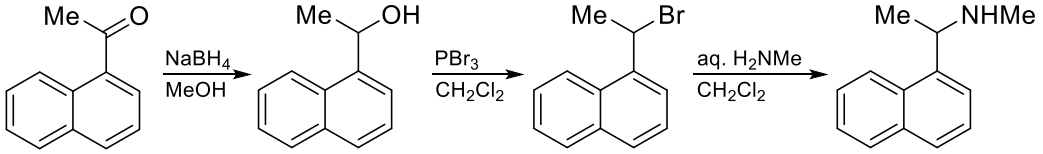

rac-**L2**

The synthesis begin from the reduction of 1-acetonapthone with $NaBH_4$ to provide the corresponding alcohol in quantitative yields. The product was then treated with PBr_3 to obtain an organobromide species, which can further undergo nucleophilic substitution with excess aqueous methylamine solution to afford the desired secondary amine in 85% yield after purification by column chromatography.

2.1.1 (S_C,S_N,R_{Ir})-(1,2,3,4,5-Pentamethylcyclopentadienyl){(κ^2-*C*,*N*)-1-[1-(*N*-methylamino)ethyl]naphthyl}iridium(III) Chloride, (S_C,S_N,R_{Ir})-1

As mentioned earlier, the direct cycloiridation procedure was selective and yielded only one stereoisomer of complex **1**, in the form of (S_C,S_N,R_{Ir})-**1**, despite it containing three chiral centers at carbon, nitrogen and iridium. The compound was found to be stable in both air and moisture, and its stereochemistries remained consistent over a wide range of temperatures. Details into the physical and chemical stability of the stereogenic centers within the complex will be conversed in later sections.

Since the structure of iridacycle (S_C,S_N,R_{Ir})-**1** has been determined earlier (*see* Chapter 2, Section 2.1.1), we will proceed with the discussion of stereogenic lock within the complex.

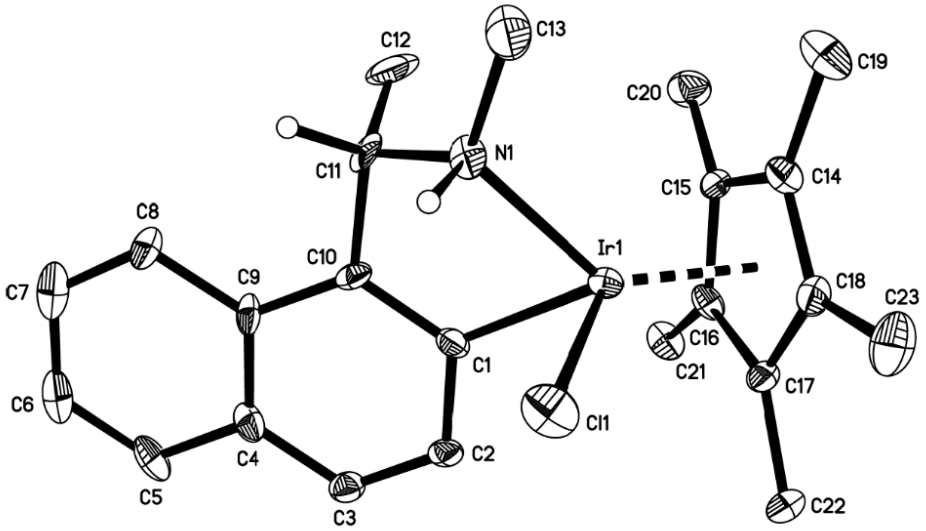

Figure 3.5. Molecular structure of cycloiridated complex (S_C,S_N,R_{Ir})-**1** with thermal ellipsoids shown at 50% probability. Hydrogen atoms except H(C11) and H(N1) are omitted for clarity. Selected bond lengths and angles: N−Ir (2.151(8) Å), C_1−Ir (2.040(9) Å), Cl−Ir (2.425(3) Å), N−Ir−C_1 (76.7(3)°), N−Ir−Cl (82.5(2)°), C_1−Ir−Cl (86.6(3)°).

Crystallographically, the *pseudo*-tetrahedral cycloiridated complex featured its five-membered organometallic ring system adopting a static λ configuration with the stereogenic *C*-methyl substituent locked in place at the axial position. It should be noted that, at this certain conformation, the axial methyl group would experience a significant amount of steric repulsion from the massive Cp* ring due to 1,3-diaxial η^5-Cp*-methyl

interactions. Nonetheless, the stereogenic lock evidently remained robust and kept the ring from interconversion in the solid state as shown in the crystal structure.

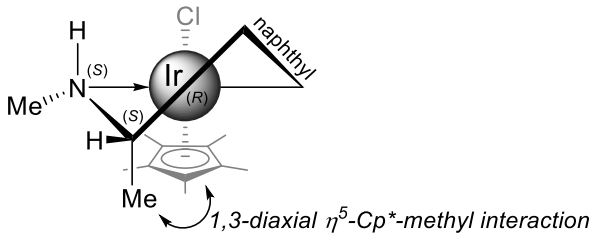

Figure 3.6. Preferred λ conformation of cycloiridated complex (S_C,S_N,R_{Ir})-**1**.

The determination of the stereogenic lock in solution phase was performed by means of 2D ^{1}H–^{1}H NOESY NMR spectroscopy.

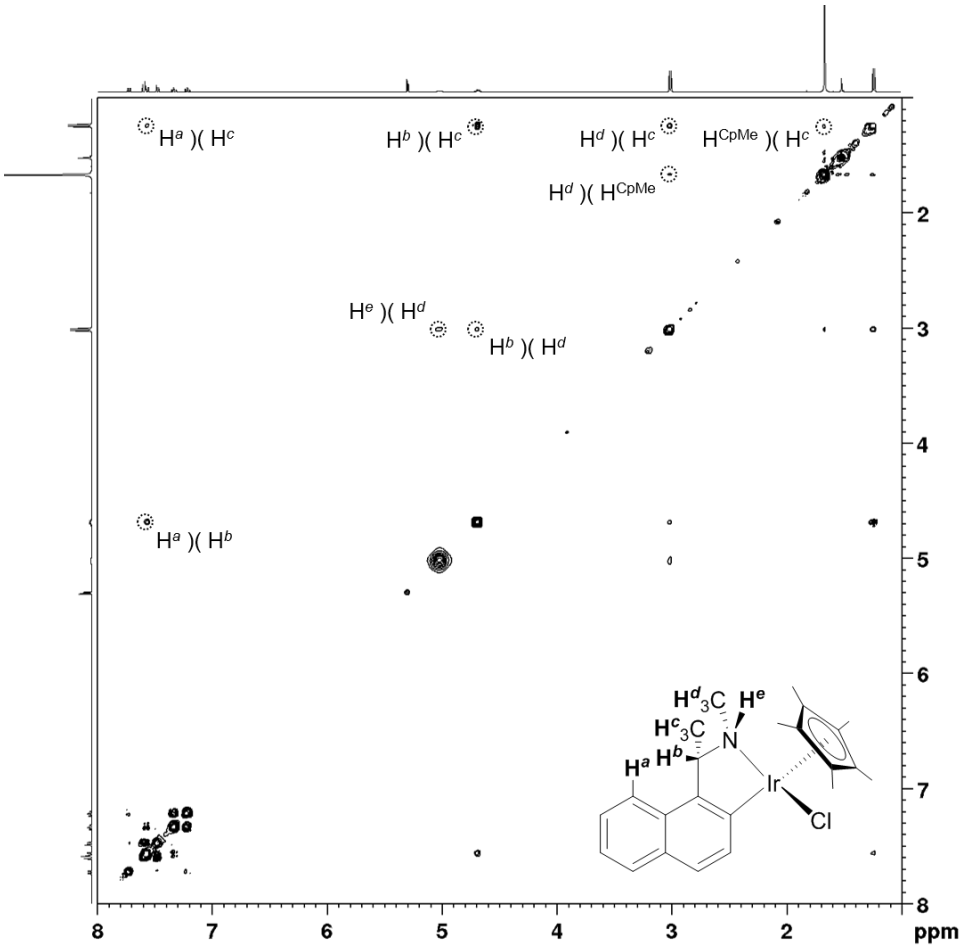

Figure 3.7. 2D ^{1}H-^{1}H NOESY NMR spectrum of cycloiridated complex (S_C,S_N,R_{Ir})-**1**.

Cross peaks relating to H^a–H^c interactions revealed that the five-membered puckered ring has adopted a single configuration, affirming that a structural lock exists between the methyl substituent at the carbon stereogenic center and its neighboring naphthalene proton. In addition, the spectrum exhibited spatial interactions between the *C*-chiral methyl substituent, as well as the *N*-chiral methyl group, with the large cyclopentadienyl methyl moiety, as shown by cross peaks H^c–H^{CpMe} and H^d–H^{CpMe} respectively. Furthermore, the lack of NOE interactions of H^b and H^e with the bulky Cp* ring system detailed the absence of interchanging conformational ring flip within the molecule.

2.1.2 (S_C,R_{Ir})-(1,2,3,4,5-Pentamethylcyclopentadienyl){(κ^2-*C*,*N*)-1-[1-aminoethyl]-naphthyl}iridium(III) Chloride, (S_C,R_{Ir})-11

The orange primary amine-based *ortho*-iridated complex **11** could be isolated as a byproduct from the reaction, although the fraction was only evident to us upon chromatography at 1 mmol scale. Despite its low yield (2%) in the reaction, it should be noted that the iridacycle can be generated in higher amounts (90%) through direct cycloiridation from its commercially-available primary amine ligand (*S*)-**L5** under identical experimental conditions.

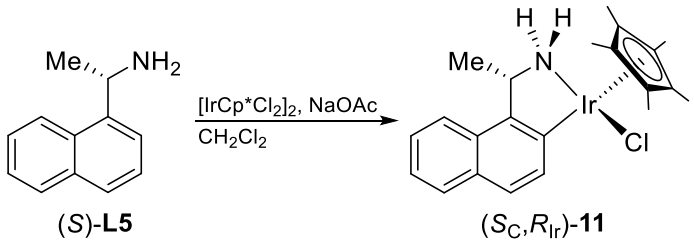

(*S*)-**L5** (S_C,R_{Ir})-**11**

Scheme 3.3. Cycloiridation of optically-active primary amine (*S*)-**L5**.

Like the secondary amine analogue, iridacycle **11** was found to afford only one diastereomer based on the Cp* singlet at 1.74 ppm within the ^{1}H NMR spectrum. The same spectrum also revealed a set of broad nonequivalent NH_2 signals at 3.70 and 4.78 ppm, typical of chelating complexes.

Single-crystal x-ray crystallographic studies determined that the recrystallized *ortho*-metalated complex conformed to a *pseudo*-tetrahedral structure with chirality at carbon and iridium to be *S* and *R*, respectively, according to Cahn−Ingold−Prelog sequence rules.[6] The molecule also presented an expected static λ conformation about the puckered ring system in its solid state with its stereogenic *C*-methyl substituent locked in place at the axial position.

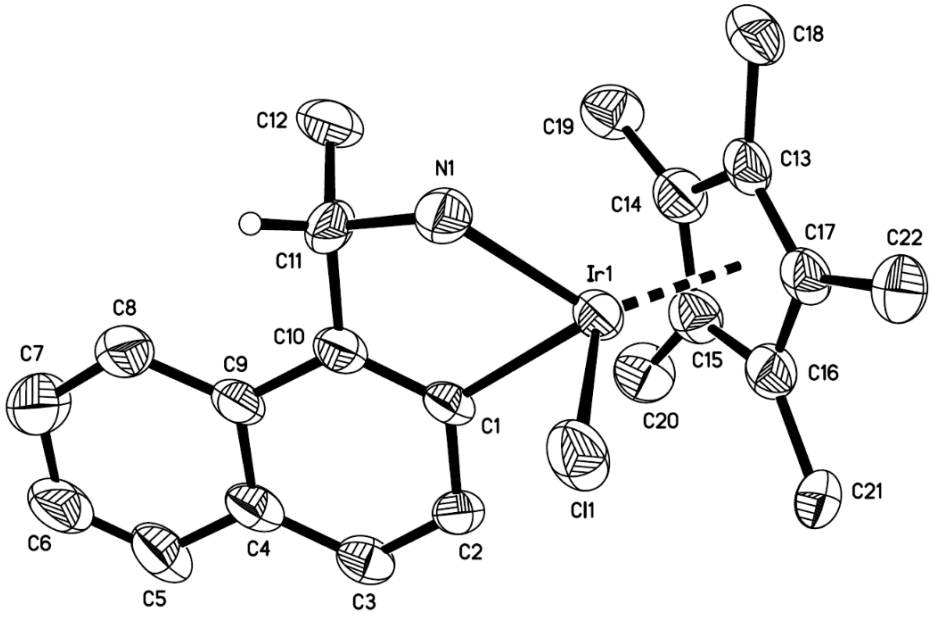

Figure 3.8. Molecular structure of cycloiridated complex (S_C,R_{Ir})-**11** with thermal ellipsoids shown at 50% probability. Hydrogen atoms except H(C11) are omitted for clarity. Selected bond lengths and angles: N−Ir (2.122(8) Å), C_1−Ir (2.060(9) Å), Cl−Ir (2.431(3) Å), N−Ir−C_1 (76.8(3)°), N−Ir−Cl (82.5°), C_1−Ir−Cl (86.8°).

We proceeded to determine of the existence of the stereogenic lock in solution phase by means of 2D $^{1}H-^{1}H$ NOESY NMR spectroscopy.

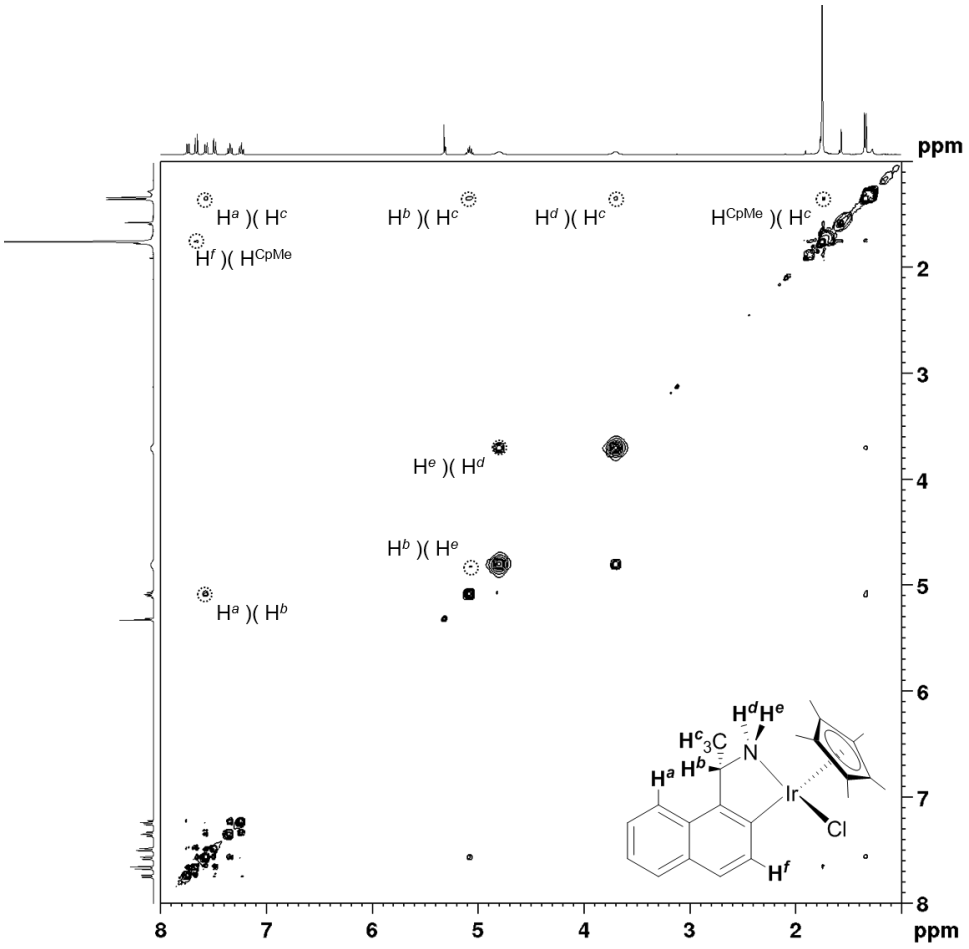

Figure 3.9. 2D ^{1}H-^{1}H NOESY NMR spectrum of cycloiridated complex (S_C,R_{Ir})-**11**.

Generally, (S_C,R_{Ir})-**11** presented similar key interactions in comparison to (S_C,S_N,R_{Ir})-**1**. More importantly, the continual presence of the stereogenic lock between the *C*-chiral methyl group and its adjacent aromatic proton remained, represented by cross peaks H^{a}–H^{c}. Central to a pool of protons surrounding it, the *C*-chiral methyl protons continued to interact spatially with its neighboring hydrogen atoms providing cross peaks H^{CpMe}–H^{c}, H^{b}–H^{c} and H^{d}–H^{c}. The lack of NOE interactions of H^{b} and H^{e} with the massive Cp* ring system further implied the absence of interchanging conformational ring flip within the molecule.

2.2 The Attempted Cycloiridation of 1-Phenylethylamine Derivatives

The apparent progression to the investigation of stereogenic lock in cycloiridated complexes is to include the phenyl derivatives in the study. As such, we proceeded to synthesize its secondary amine derivative (*R*)-**L6** and utilized it for cycloiridation.

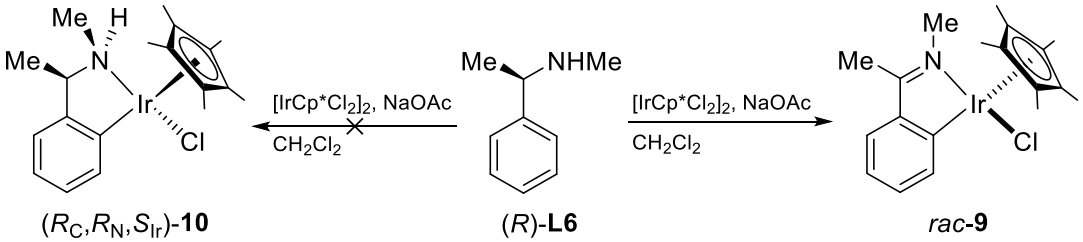

Scheme 3.4. The iridation of (*R*)-*N*-methyl-1-phenylethylamine (*R*)-**L6**.

Disappointingly, the procedure did not afford the desired cycloiridated complex (R_C,R_N,S_{Ir})-**10**. Instead, racemic *imino* iridacycle *rac*-**9** was isolated as the major product in 42% yield. It should be mentioned that an additional optically-active orange oil-like substance, in significant amounts, could also be obtained. However, further purification and characterization of the compound proved to be challenging.

Synthesis of Cyclometalating Ligands

(*R*)-*N*-methyl-1-phenylethylamine (*R*)-L6

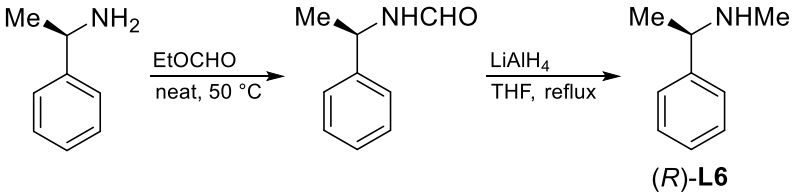

Like its naphthalene counterpart, the chiral phenyl-based secondary amine (*R*)-**L6** can be attained *via* the same two-step one-pot procedure. The primary amine was first heated with ethyl formate at 50 °C under neat conditions to provide a light brown cake-like formamide compound. The product was subsequently dissolved in THF and reduced with $LiAlH_4$ to afford the desired secondary amine in 49% yield after purification by vacuum distillation.

Recalling the iridation procedure of (*R*)-*N*,*N*-dimethyl-1-phenylethylamine (*R*)-**L4** in Chapter 2, the same *imino* iridacycle was isolated from the reaction. Of particular mention was the proposed intermediate of (*R*)-*N*-methyl-1-phenylethylamine (*R*)-**L6** that can be derived from the *N*-demethylation of tertiary amine (*R*)-**L4**. The formation of the *imino* product *rac*-**9** (and not the postulated iridacycle (R_C,R_N,S_{Ir})-**10**) in the iridation process can, thus, be rationalized from our current experiment involving the attempted cycloiridation of secondary amine ligand (*R*)-**L6**.

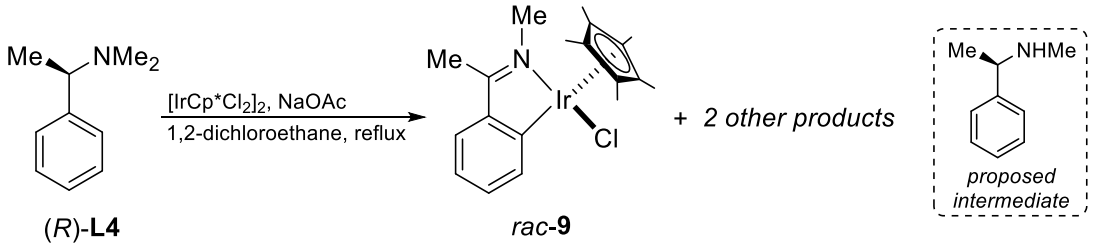

Scheme 3.5. The iridation reaction of (*R*)-*N*,*N*-dimethyl-1-phenylethylamine (*R*)-**L4**.

We proceeded to recrystallize cycloiridated complex *rac*-**9** from a solvent mixture of *n*-hexane and dichloromethane obtaining orange triclinic crystals, in form of plates, for confirmation of structure by single crystal x-ray crystallography.

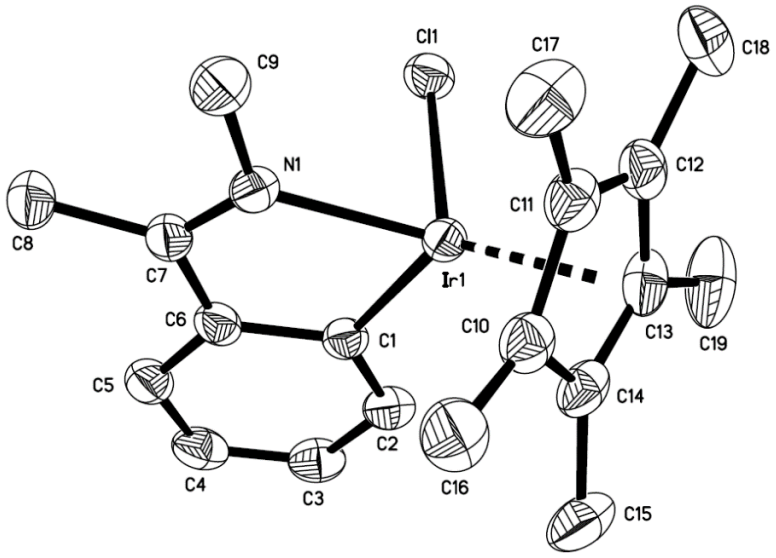

Figure 3.10. Molecular structure of cycloiridated complex *rac*-**9** with thermal ellipsoids shown at 50% probability. Hydrogen atoms are omitted for clarity. Selected bond lengths and angles: N−Ir (2.082(3) Å), C_1−Ir (2.030(3) Å), Cl−Ir (2.400(1) Å), N−Ir−C_1 (77.6(1)°), N−Ir−Cl (84.4(1)°), C_1−Ir−Cl (87.5(1)°).

The oxidation of the amine moiety during the process of cyclometalation was not unheard of and has been observed by Pfeffer and co-workers during their cycloiridation procedure.[7] The stepwise oxidation−cyclometalation process presents one of the methods for obtaining these *imino*-metallacycles. Stirling has reported the racemization of enantiopure amines by an iridium(III) Cp* dihalogen complex through an *imino* intermediate, although it tends to proceed much more slowly in *chloro* complexes than in its *iodo* counterparts.[8] The resultant imine could then undergo *ortho*-iridation to afford the cycloiridated imine species. Alternatively, a cyclometalation−oxidation protocol could take place. Feringa and de Vries have documented the self-oxidation of a cationic (κ^2-*C*,*N*)-*N*-methylbenzylamine cycloiridated system to its *imino* variant in solution.[9]

Snippets from Literature

A Cyclometalation with Dehydrogenation

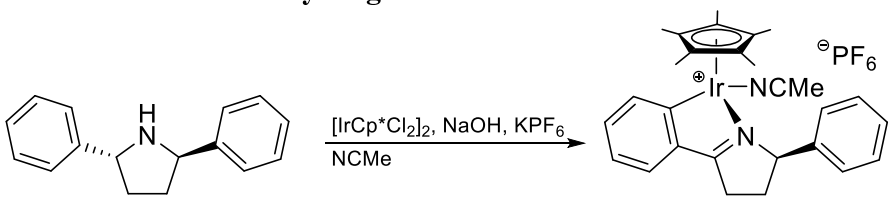

A pyrrolidine ligand was found to solely produce a cycloiridated pyrroline complex upon reaction with $[IrCp^*Cl_2]_2$ in the presence of NaOH and KPF_6 in acetonitrile. The mechanism to the oxidation was not known, although it was suspected that the iridium(III) precursor was involved in the process.

(Pfeffer, M. *et al. Organometallics* **2011**, *30*, 1168)

Racemization of Amines through Iminium Intermediates

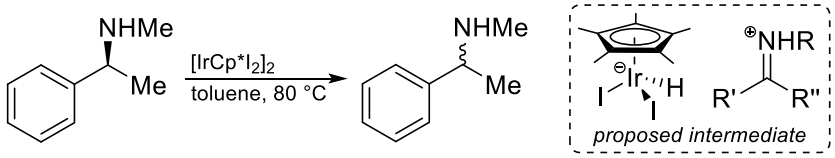

$[IrCp^*I_2]_2$ was found to be an efficient catalyst for the racemization of amines. Its *chloro* and *bromo* derivative can also catalyzed the reaction, although the procedure was observed to proceed at slower rates. Mechanistically, the racemization process was believed to involve an iminium intermediate.

(Stirling, M. J. *et al. Org. Biomol. Chem.* **2016**, *14*, 7092)

Snippets from Literature

Self-Oxidation of Cycloiridated Complexes

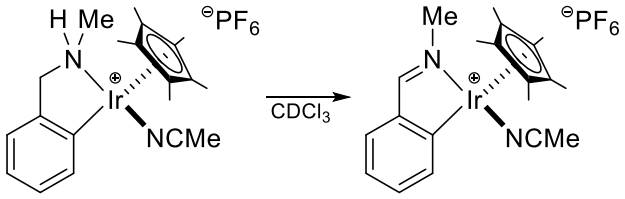

Whilst attempting to catalyze the racemization of chiral amines, it was noted that the cycloiridated *N*-methylbenzylamine catalyst has deactivated itself during the process. Further investigation through NMR studies led to the finding of self-oxidation in which the complex had transformed to its *imino* counterpart when the complex was left to stand in $CDCl_3$.

(Feringa, B. L. and de Vries, J. G. *et al. Chem. Eur. J.* **2009**, *15*, 12780)

In our last attempt to obtain a chiral phenyl-based cycloiridated complex for the determination of stereogenic lock, we tried to react commercially-available (*R*)-1-phenylethylamine ligand (*R*)-**L7** with $[IrCp^*Cl_2]_2$ in the presence of NaOAc.

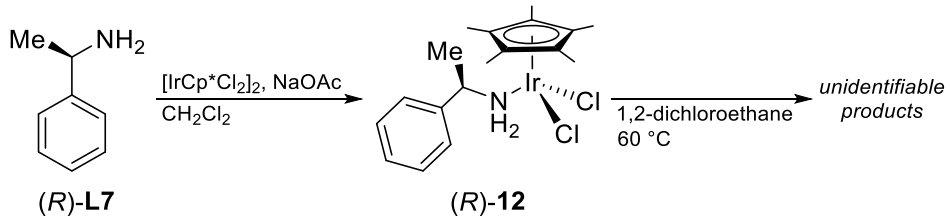

Scheme 3.6. The iridation reaction of (*R*)-1-phenylethylamine (*R*)-**L7**.

At room temperature, the protocol afforded only coordination product (*R*)-**12** in near quantitative yields. In hopes to push the reaction towards cyclometalation, we dissolved the complex in 1,2-dichloroethane and warmed the mixture to 60 °C. Disappointingly, the complex decomposed providing unidentifiable compounds.

It should be noted that Ikariya and Kayaki have recently synthesized various chiral cycloiridated benzylic *amino* complexes.[10] As such, we questioned the difference in reactivities between the amines of Ikariya and Kayaki with those of ours. It was known that the cyclopalladated equivalents of the former amines were conformationally rigid through stereogenic lock in both solid and solution phases.[11] Noting that our structurally locked iridacycles (S_C,S_N,R_{Ir})-**1** and (S_C,R_{Ir})-**11** can be isolated in their optically-active forms, we believed that the locking mechanism must have hindered the oxidative process. To provide the cycloiridated *imino* complex, the coordinated or cycloiridated amine would need to adopt a planar intermediary structure. However, due to the immense steric crowding about the metal center, the *C*-chiral methyl substituent-adjacent naphthalene proton interaction may have prevented the oxidation of the amine.

Snippets from Literature

Chiral Phenyl-Based Cycloiridated Complexes

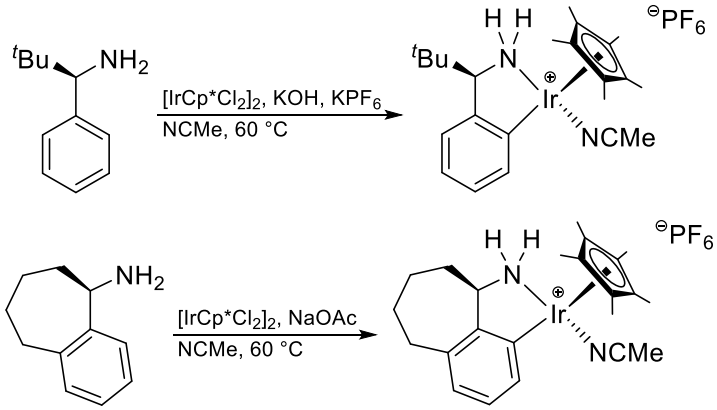

A series of optically-active *C*,*N*-cycloiridated complexes were synthesized, characterized and evaluated as catalyst for the asymmetric transfer hydrogenation reaction. The cyclometalation processes were successful and selective providing the chiral phenyl-based iridacycles in relatively high diastereomeric excess.

(Kayaki, Y. and Ikariya, T. *et al. Chem. Asian. J.* **2016**, *11*, 2924)

2.3 The Cycloiridation of *N*-Methyl-1-naphthylmethylamine

In order to verify the concept that the locking mechanism hindered the oxidative process, we looked into the cycloiridation of *N*-methyl-1-naphthylmethylamine **L8** (a naphthylalkylamine for which its cyclopalladated species was not known to be conformationally rigid).

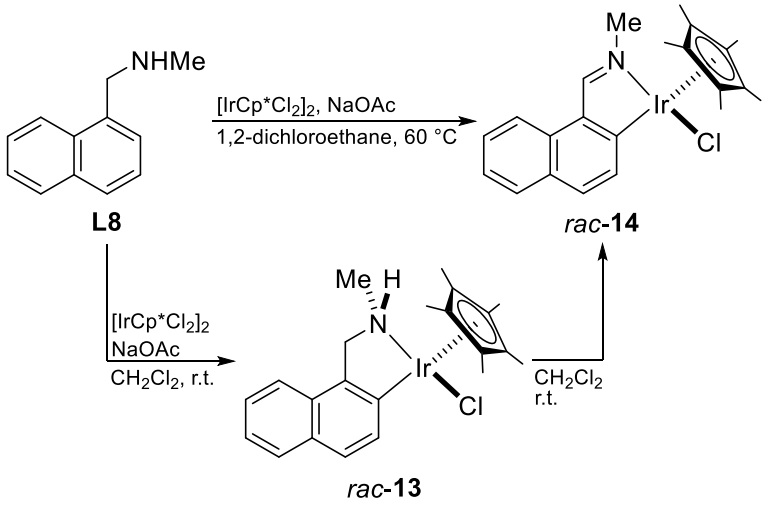

Scheme 3.7. The iridation reaction of *N*-methyl-1-naphthylmethylamine **L8**.

When the procedure was performed at room temperature, cycloiridated complex *rac*-**13** can be obtained in modest yield (31%) after three days of reaction. Upon leaving it to stand in an open environment in either solution or solid phase, the product oxidized relatively fast to provide the *aldimino* metallacycle *rac*-**14**. On the other hand, when kept in a closed environment, the oxidation procedure proceeded more sluggishly allowing the complex to be kept for longer periods (over one week at room temperature in solution). The results, thus, reflected the cyclometalation-oxidation mechanism of the oxidative process as discussed earlier in the last section. It has also revealed the critical role of the conformational lock in the coordinated system. With regards to the variance in conditions in which the complexed amine was found to oxidized, we speculated that the process either exist as an equilibrium with dihydrogen or was catalyzed by atmospheric oxygen. Lastly, it is worth mentioning that elevated temperatures pushed for a quicker oxidation; the *aldimino* iridacycle *rac*-**14** can be obtained in 61% yield after 16 h of reaction time at 60 °C.

Synthesis of Cyclometalating Ligands

***N*-methyl-1-naphthylmethylamine L8**

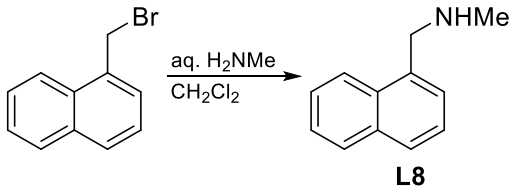

L8

Secondary amine **L8** can be obtained from its commercially-available organobromide species through simple nucleophilic substitution with twenty-fold excess of aqueous methylamine in dichloromethane. Purification of the crude product by column chromatography provided the desired product in 34% yield.

Red block-like crystals of cycloiridated complex *rac*-**13** were recrystallized from a solvent mixture of *n*-hexane and dichloromethane. Its molecular structure and relative stereochemistry was then confirmed by single-crystal x-ray crystallography.

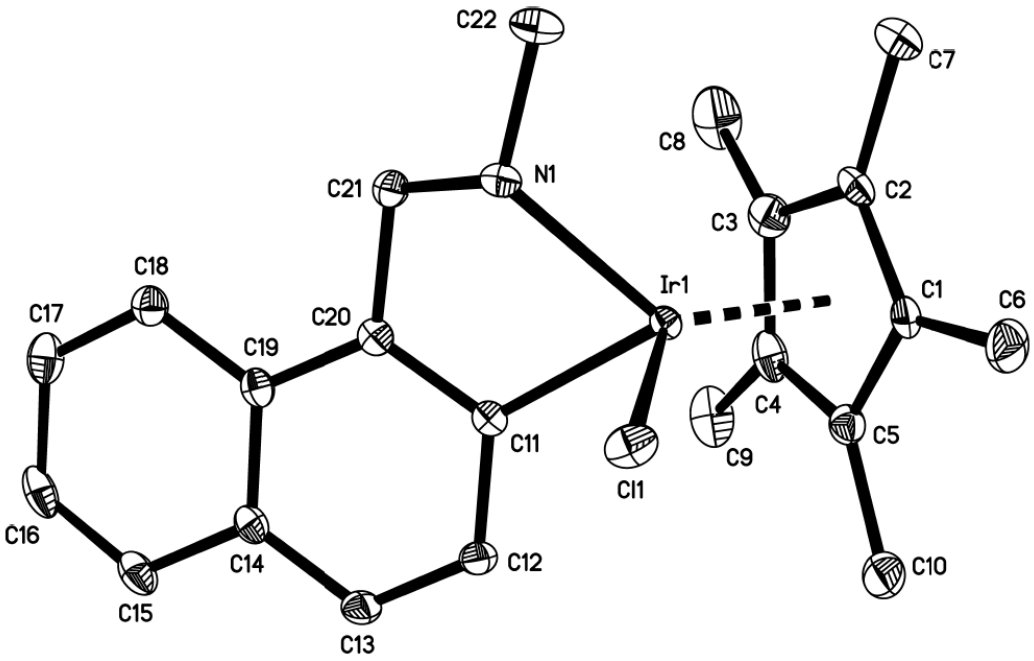

Figure 3.11. Molecular structure of cycloiridated complex *rac*-**13** with thermal ellipsoids shown at 50% probability. The structure presented in the figure has stereochemistry of *S* and *R* at nitrogen and iridium respectively. Hydrogen atoms are omitted for clarity. Selected bond lengths and angles: N−Ir (2.127(3) Å), C_{11}−Ir (2.046(4) Å), Cl−Ir (2.414(1) Å), N−Ir−C_{11} (76.8(1)°), N−Ir−Cl (84.8(1)°), C_{11}−Ir−Cl (87.1(1)°).

Similarly, the cycloiridated *aldimino* complex *rac*-**14** was subsequently recrystallized as orange needles from a solvent mixture of *n*-hexane and dichloromethane, and its molecular structure was confirmed by single-crystal x-ray crystallography.

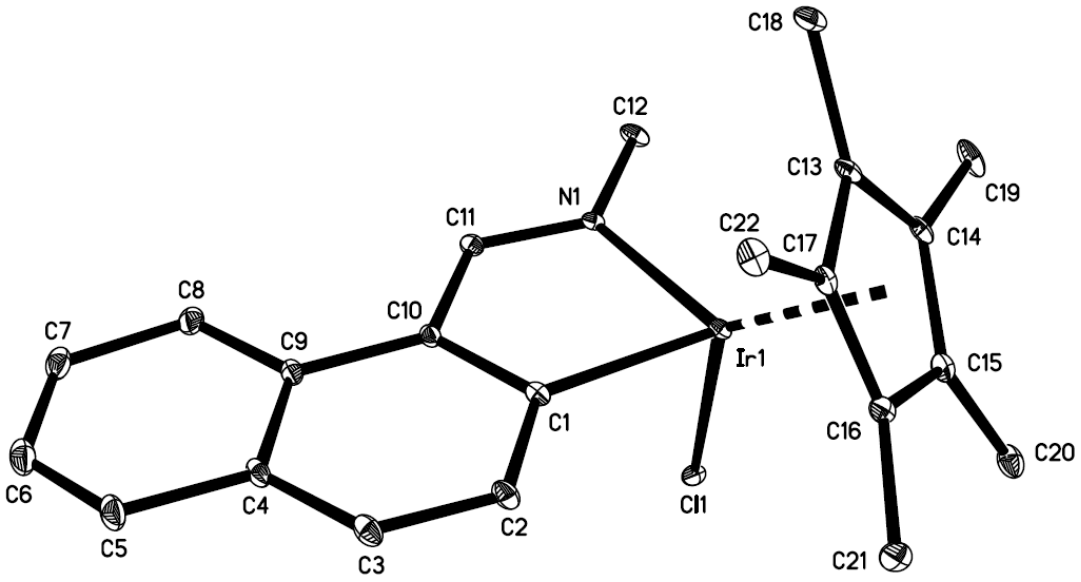

Figure 3.12. Molecular structure of cycloiridated complex *rac*-**14** with thermal ellipsoids shown at 50% probability. Hydrogen atoms are omitted for clarity. Selected bond lengths and angles: N−Ir (2.056(8) Å), C_1−Ir (2.025(10) Å), Cl−Ir (2.398(3) Å), N−Ir−C_1 (77.9(4)°), N−Ir−Cl (83.5(2)°), C_1−Ir−Cl (87.5(3)°).

2.4 Special Topic: Stereogenic Lock in Cycloruthenated 1-Arylethylamine Complexes

So far, we have demonstrated the possibility of incorporating a stereogenic lock system within cycloiridated complexes. Together with its palladacyclic counterparts,[11a] we would like to iterate our beliefs that these systems and its concepts can be extended to cyclometalated compounds of other transition metal elements.

During the peer-review process into the submission of the manuscript, a reviewer commented on existing cycloruthenated systems with analogous ligand motifs. As such, we researched into these compounds and analyzed them for the existence of conformational lock. It should be noted that discussion within this section were based on results in literature and no experiments were conducted on our side.

The cycloruthenation of 1-phenylethylamine and 1-naphthylethylamine were performed by Pfeffer and Barloy in 2007.[12] In their study, the aforementioned complexes were isolated and characterized by 2D ^{1}H-^{1}H ROESY NMR and single crystal x-ray crystallography. It should also be noted that their other diastereomers can be isolated, although less details about the compounds were provided in the article.

Spectroscopically, ruthenacycle **Ru1** was observed to have NOE interactions between the *P*-methyl substituent and the benzylic methyl group (a reflection of the δ conformer in the solution). On that basis, it was speculated that 1,3-diaxial phosphine-methyl interaction would push the complex for the λ configuration to reduce steric stress. Upon recrystallization of the compound, it was noted that the methyl substituent was found to be at the equatorial position within the puckered ring system. As such, these observations provided evident proof that an equilibrium exist between the two conformers.

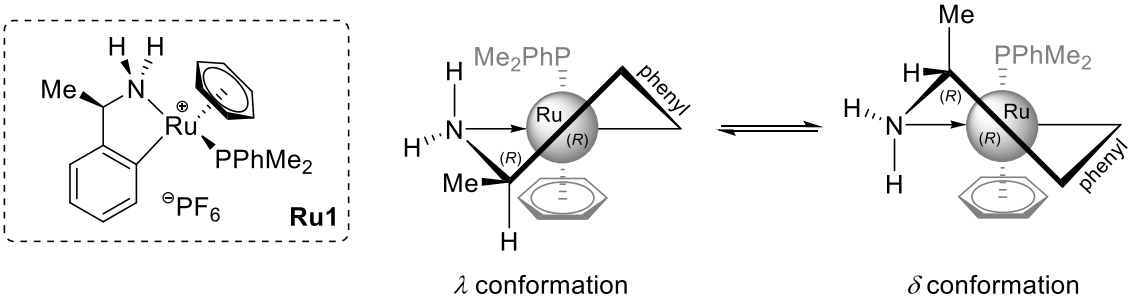

Scheme 3.8. Equilibrium between conformations of cycloruthenated complexes **Ru1**.

It is also worth mentioning that an earlier work by Nelson on a similar cycloruthenated complex suggested that the equilibrium between the conformers tended to lie towards the λ conformer to reduce residual strain within the chelate ring effected by the axial *C*-chiral methyl group.[13]

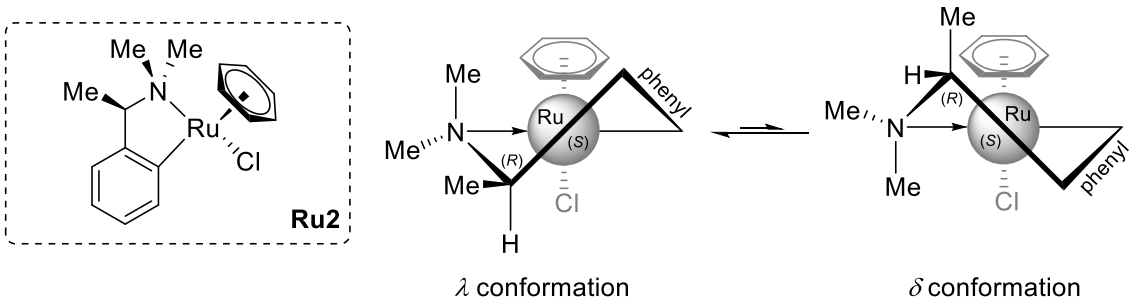

Scheme 3.9. Equilibrium between conformations of cycloruthenated complexes **Ru2**.

The naphthyl-based ruthenacycle **Ru3**,[12] on the other hand, depicted its molecular structure to have its stereogenic *C*-methyl moiety in the axial position, reflecting a possible δ configuration. 2D ^{1}H-^{1}H ROESY NMR studies further iterated the stable δ conformation through spatial interactions between the said methyl group and the η^{6}-benzene ligand. Although the existence of the other conformer cannot be fully ruled out, we strongly believe that the stereogenic lock had effected the fixation of the *C*-chiral methyl substituent at the axial position within the puckered ring system based on these observations.

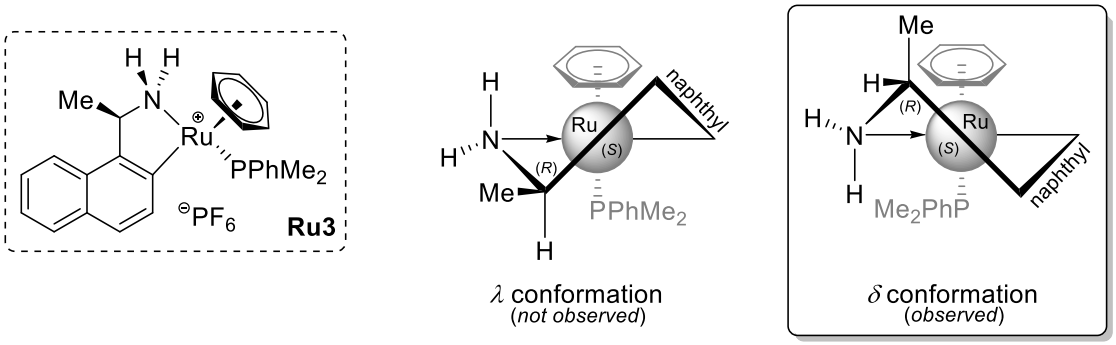

Figure 3.13. Possible conformations of cycloruthenated complexes **Ru3**.

2.5 Physical and Chemical Stability of Stereogenic Centers within Cycloiridated Complex (S_C,S_N,R_{Ir})-1

With certainty that the stereogenic lock was in place within cycloiridated complex (S_C,S_N,R_{Ir})-**1**, we proceeded to the next phase of investigation.

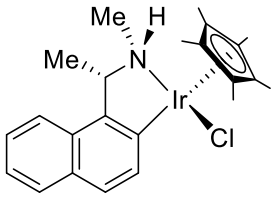

(S_C,S_N,R_{Ir})-**1**

Figure 3.14. Molecular structure of cycloiridated complex (S_C,S_N,R_{Ir})-**1**.

An interesting property of the iridacycle, compared to other optically-active Cp*-based cycloiridated complexes, was its ability to be generated diastereoselectively (recall that the direct cycloiridation procedure afforded solely one of four possible isomers). Provided that the stereochemistries of the stereogenic centers remained unaltered under physical or chemical stress, the complex could present potential uses as asymmetric catalysts and auxiliaries,[14] or even as therapeutic biological agents.[15] It is, thus, imperative that we explore the physical and chemical stability of these centers.

2.5.1 Physical Stability of Stereogenic Centers within Cycloiridated Complex (S_C,S_N,R_{Ir})-1

Unlike the fixed carbon central chirality within the iridacycle, inversion of stereochemistry at either nitrogen or iridium could be prevalent due to the labile nature of the donor ligand. To determine if such dynamic behavior exist within the complex, we proceeded with NMR studies on the iridacycle.

At room temperature, the stereochemistries within the compound were stable, as indicated from its ^{1}H NMR spectrum. However, it was not known if the iridacycle could isomerize when it was subjected to heat. The complex was dissolved in 1,2-dichloroethane (b.p. 83 °C) and placed under reflux conditions over a period of five days. The resulting red-brown solution was subsequently evaporated to dryness prior to analysis *via* ^{1}H NMR spectroscopy. When the methyl substituents on the Cp* ligand were used as a spectroscopic

handle for the determination of isomeric ratio, the resultant solution revealed only one Cp* resonance signal at 1.67 ppm, hinting no isomerization of the complex. To further investigate possible stereochemical inversions within the molecule during the heating process or dynamic behavior of the compound at room temperature (that was too fast at the timescale of the NMR), variable temperature (VT) NMR studies were performed in chloroform-*d* (b.p. 61 °C; m.p. −64 °C) at high and low temperatures.

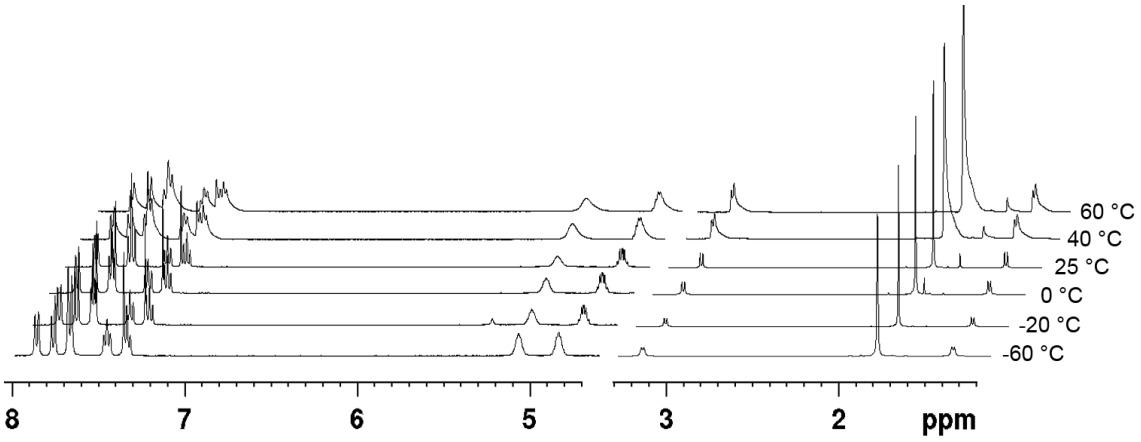

Figure 3.15. Variable temperature (VT) ^{1}H NMR studies on cycloiridated complex (S_C,S_N,R_{Ir})-**1** from −60 to 60 °C. The chemical shift range from 4.7 to 8.0 ppm has been magnified for clarity.

The VT NMR studies revealed no visible isomerization at both low and elevated temperatures. The spectroscopic handle remained as a singlet during both cooling and heating processes. Furthermore, the multiplities of the other resonance signals generally remained unchanged with only slight deviation in chemical shifts.

2.5.2 Chemical Stability of Stereogenic Center at Nitrogen within Cycloiridated Complex (S_C,S_N,R_{Ir})-1

Unlike the fixed stereogenic center at carbon, isomerization at the nitrogen center is probable within the complex due to nitrogen inversion upon decoordination. Furthermore, due to the acidic nature of the proton on the amine moiety, it could isomerize if a sufficiently strong base is present. As such, we aimed to determine if such isomerization would take place at the nitrogen atom when a deprotonation−protonation protocol was effected. Iridacycle (S_C,S_N,R_{Ir})-**1** was subjected to deprotonation with potassium *tert*-butoxide in dichloromethane-d_2 at room temperature under an inert atmosphere.

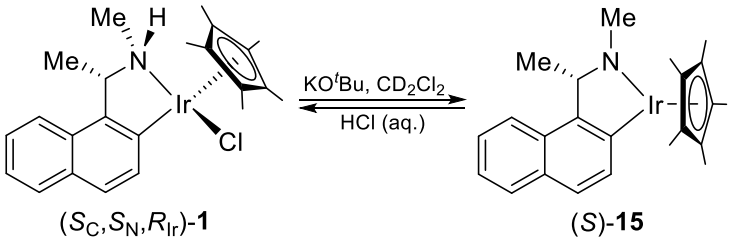

Scheme 3.10. Experiment on the stability of stereochemistry at nitrogen center.

Upon complete conversion to the *amido* intermediate (*S*)-**15**, the dark red mixture was hydrolyzed with aqueous hydrochloric acid to return iridacycle (S_C,S_N,R_{Ir})-**1**. Spectroscopic analysis revealed no isomerization of the hydrolyzed complex, offering a spectrum similar to that of pure (S_C,S_N,R_{Ir})-**1**. Analysis of the compound's optical activity using the D-line of sodium (589 nm) also returned a similar specific optical rotation of +106.8° (21 °C, *c* 0.1) (pure iridacycle (S_C,S_N,R_{Ir})-**1**: $[\alpha]_D$ (22 °C, *c* 0.5) = +102.1°), indicating that the complex remained structurally unaltered.

2.5.3 Chemical Stability of Stereogenic Center at Iridium within Cycloiridated Complex (S_C,S_N,R_{Ir})-1

In another experiment, the stability of the chiral center at iridium was explored. It was postulated that an exchange of ligand at the metal center must undergo a dissociative mechanism since the 18-electron species is coordinatively saturated. The replacement of a *chloride* ligand with a phosphine moiety would also provide a spectroscopic handle for the determination of isomerization by $^{31}P\{^{1}H\}$ NMR.

The ligated chloride in cycloiridated complex *rac*-**1** was first abstracted with silver(I) hexafluorophosphate in acetonitrile at room temperature. Triphenylphosphine was subsequently added to the pale-yellow mixture, with its crude $^{31}P\{^{1}H\}$ NMR spectrum revealing a singlet at 16.0 ppm, indicative of only one coordinated triphenylphosphine complex, and a PF_6^- septet resonance signal at −144.3 ppm.

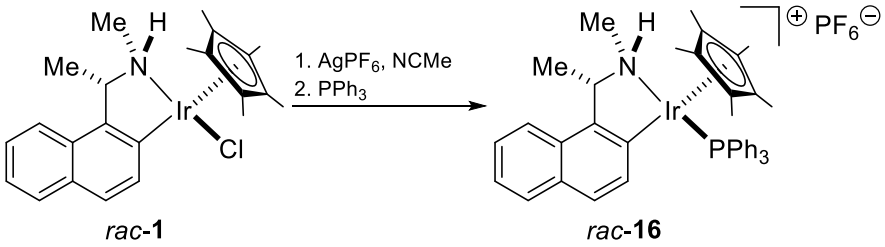

rac-**1** *rac*-**16**

Scheme 3.11. Experiment on the stability of stereochemistry at iridium center during ligand exchange.

The *phosphino* complex *rac*-**16** was subsequently recrystallized, and its molecular structure and relative stereochemistry were confirmed by single-crystal x-ray crystallography.

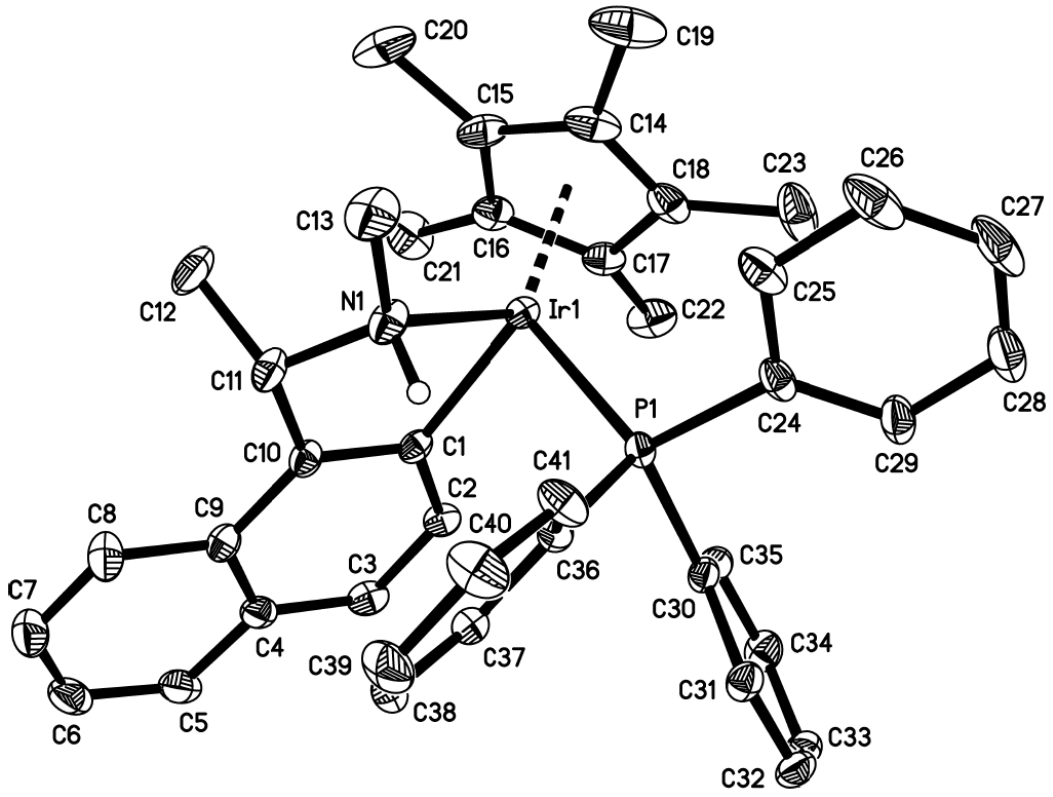

Figure 3.16. Molecular structure of cycloiridated complex *rac*-**16** with thermal ellipsoids shown at 50% probability. The structure presented in the figure has stereochemistry of *S*, *S* and *R* at carbon, nitrogen and iridium respectively. The hexafluorophosphate anion and hydrogen atoms except H(N1) are omitted for clarity. Selected bond lengths and angles: N−Ir (2.163(2) Å), C_1−Ir (2.067(2) Å), P−Ir (2.305(1) Å), N−Ir−C_1 (76.7(1)°), N−Ir−P (87.8(1)°), C_1−Ir−P (89.8(1)°).

2.6 Effects of Structure on Catalysis: Application in Asymmetric Hydrogen Transfer Reaction

With the knowledge that the stereogenic lock within the naphthalene-based cycloiridated complexes operates over a broad range of temperatures and reaction conditions, we proceeded to examine its effectiveness in the transmission of stereogenic information to the substrate in asymmetric applications. Considering that many piano-stool metallacycle-catalyzed reactions involved asymmetric hydrogen transfer reactions,[16] the model catalytic reduction was employed for the study.

The transfer hydrogenation protocol was carried out with acetophenone as the substrate and 2-propanol as the reducing agent. The optically-active cycloiridated precursors comprised of complexes (S_C,S_N,R_{Ir})-**1** and (S_C,R_{Ir})-**11**, which then can be readily deprotonated with potassium *tert*-butoxide to provide the active *amido* species. Whilst we were very much interested in comparing enantioselectivity of the protocol between catalysts with stereogenic lock and those without the locking mechanism, we were unable to gather the latter complexes due to complications discussed earlier in the chapter.

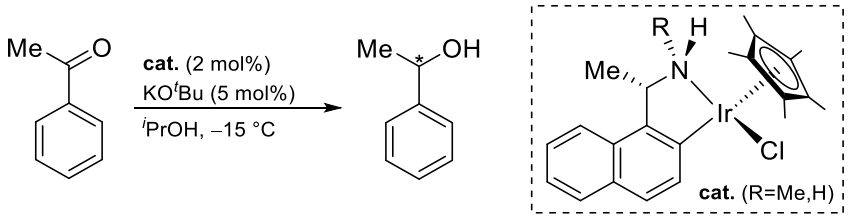

Scheme 3.12. The asymmetric hydrogen transfer reaction of acetophenone catalyzed by cycloiridated complexes (S_C,S_N,R_{Ir})-**1** and (S_C,R_{Ir})-**11**.

The initial run of the catalytic reaction was performed at −15 °C, and its activity profile was shown below.

Table 3.1. Conversion and enantiomeric excess profiles of the asymmetric hydrogen transfer reaction of acetophenone by chiral cycloiridated complexes at −15 °C.[a]

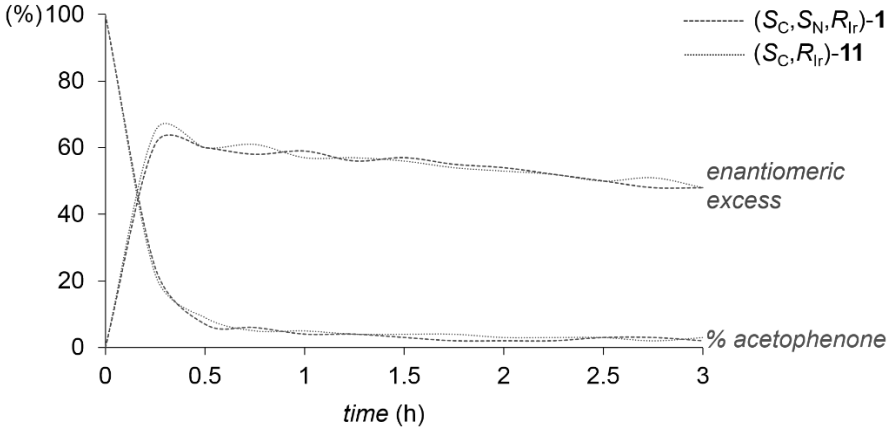

(S_C,S_N,R_{Ir})-**1**			(S_C,R_{Ir})-**11**		
time (min)	conversion[b] (%)	ee[b,c] (%)	time (min)	conversion[b] (%)	ee[b,c] (%)
0	0	n.a.[d]	0	0	n.a.[d]
15	76	(+) 61	15	78	(+) 65
30	93	(+) 60	30	91	(+) 60
45	94	(+) 58	45	95	(+) 61
60	96	(+) 59	60	95	(+) 57
75	96	(+) 56	75	96	(+) 57
90	97	(+) 57	90	96	(+) 56
105	98	(+) 55	105	96	(+) 54
120	98	(+) 54	120	97	(+) 53
135	98	(+) 52	135	97	(+) 52
150	97	(+) 50	150	97	(+) 50
165	97	(+) 48	165	98	(+) 51
180	98	(+) 48	180	97	(+) 48

[a]Reactions were carried out with acetophenone (0.5 mmol), 1,4-dimethoxybenzene (0.5 mmol), (S_C,S_N,R_{Ir})-**1** or (S_C,R_{Ir})-**11** (0.01 mmol), and KO^{t}Bu (0.05 mmol) in ^{i}PrOH at −15 °C for the stated duration. [b]Conversion and ee were determined by HPLC (Diacel Chiralpak IF column). [c]± notation (in parenthesis) was determined by optical activity studies. [d]Not applicable.

In terms of activity, both complexes performed outstandingly with the hydrogen transfer protocol approaching near completion (*ca.* 90% conversion) after 30 min in spite of the exponential decrease in reactivities with time after the initial burst at the beginning. Both compounds displayed similar reactivity with their conversion of acetophenone within 4% of each other at any point of time. With regard to its enantioselectivity, the catalysts only gave modest ee at best, with the primary *amino*-iridacycle achieving the highest measured ee after 15 min at 65%, although the reaction was only moderately complete

(78%). Expectedly, the enantioselectivity declined with time due to the continuous oxidation-reduction processes within the reaction vessel, reaching complete racemization overnight for both complexes.

We proceeded to vary the reaction conditions with complex (S_C,S_N,R_{Ir})-**1** as the catalyst.

Table 3.2. Asymmetric hydrogen transfer reaction of acetophenone by iridacycle (S_C,S_N,R_{Ir})-**1**.[a]

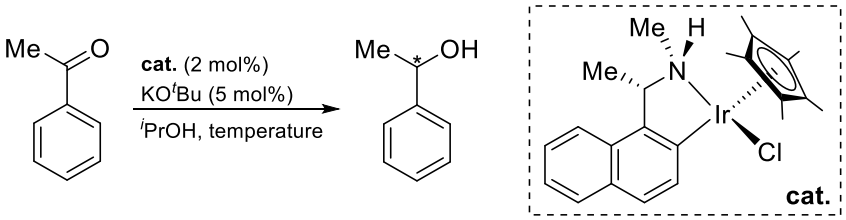

entry	temp (°C)	time (h)	conversn[b] (%)	ee[b,c] (%)
1	20	0.25	99	(+) 52
2[d]	20	96[e]	75	(+) 58
3	–15	1	96	(+) 59
4	–30	1.5	97	(+) 69

[a]Reactions were carried out with acetophenone (0.5 mmol), 1,4-dimethoxybenzene (0.5 mmol), (S_C,S_N,R_{Ir})-**1** (0.01 mmol), and KO^{t}Bu (0.05 mmol) in ^{i}PrOH at the desired temperature for the stated duration. [b]Conversion and ee were determined by HPLC (Diacel Chiralpak IF column). [c]± notation (in parenthesis) was determined by optical activity studies. [d]Reaction was conducted without KO^{t}Bu. [e]Reactions were halted after 96 h reaction time.

At room temperature, the transfer hydrogenation protocol progressed extremely efficiently, with the reaction approaching complete conversion within 15 min, albeit with a slight reduction in enantioselectivity. In the absence of base, the reaction was found to proceed, although its reactivity was greatly hindered, being incomplete even after 4 days of reaction time at room temperature. Nonetheless, the entry gave an ee (58%; entry 2) similar to that of the *amido* complex-mediated reaction at the same temperature (52%; entry 1). Finally, at lower temperature (−30 °C), the reaction remained efficient with a slight increase in enantioselectivity to 69%, in comparison to its counterpart at −15 °C (59%; entry 3).

3 SUMMARY AND CONCLUSION

In the chapter, we have synthesized and characterized a series of *pseudo*-tetrahedral cycloiridated 1-naphthylethylamine complexes. The compounds were subsequently studied for their structure and stereoselectivity in the catalytic asymmetric hydrogen transfer reaction. The investigation revealed the relevance of a stereogenic lock defined by the fixation of configuration within a small ring system through steric interaction within the molecular framework in both structural aspects, in terms of diastereoselectivity and stereostability, and enantioselectivity in asymmetric catalysis. Furthermore, we reviewed the practicality of structural lock to avoid side reactions within the complex which may render the enantiopure compound less beneficial for asymmetric applications.

Through this work, we aimed to establish the concepts of stereogenic lock which could be applied to the rational design of chiral catalysts and templates for asymmetric applications. We have also demonstrated the relevance of conformational rigidity in the outcome of asymmetric applications.

REFERENCES

1. (a) Allen, D. G.; McLaughlin, G. M.; Robertson, G. B.; Steffen, W. L.; Salem, G.; Wild, S. B. *Inorg. Chem.* **1982**, *21*, 1007-1014; (b) Wild, S. B. *Coord. Chem. Rev.* **1997**, *166*, 291-311; (c) Salem, G.; Wild, S. B. *Inorg. Chem.* **1983**, *22*, 4049-4054; (d) Leung, P. H.; McLaughlin, G. M.; Martin, J. W. L.; Wild, S. B. *Inorg. Chem.* **1986**, *25*, 3392-3395; (e) Martin, J. W. L.; Stephens, F. S.; Weerasuria, K. D. V.; Wild, S. B. *J. Am. Chem. Soc.* **1988**, *110*, 4346-4356; (f) Leung, P. H.; Willis, A. C.; Wild, S. B. *Inorg. Chem.* **1992**, *31*, 1406-1410.
2. Alcock, N. W.; Brown, J. M.; Hulmes, D. I. *Tetrahedron: Asymmetry* **1993**, *4*, 743-756.
3. Ng, J. K. P.; Chen, S.; Tan, G. K.; Leung, P.-H. *Tetrahedron: Asymmetry* **2007**, *18*, 1163-1169.
4. (a) Chew, R. J.; Leung, P.-H. *Chem. Rec.* **2016**, *16*, 141-158; (b) Wong, J.; Gan, K.; Chen, H. J.; Pullarkat, S. A. *Adv. Synth. Catal.* **2014**, *356*, 3391-3400; (c) Leung, P.-H. *Acc. Chem. Res.* **2004**, *37*, 169-177; (d) Leung, P.-H.; Ng, K.-H.; Li, Y.; J. P. White, A.; J. Williams, D. *Chem. Commun.* **1999**, 2435-2436.
5. (a) Tay, W. S.; Yang, X.-Y.; Li, Y.; Pullarkat, S. A.; Leung, P.-H. *Chem. Commun.* **2017**, *53*, 6307-6310; (b) Li, X.-R.; Yang, X.-Y.; Li, Y.; Pullarkat, S. A.; Leung, P.-H. *Dalton Trans.* **2017**, *46*, 1311-1316; (c) Yang, X.-Y.; Tay, W. S.; Li, Y.; Pullarkat, S. A.; Leung, P.-H. *Chem. Commun.* **2016**, *52*, 4211-4214; (d) Tay, W. S.; Yang, X.-Y.; Li, Y.; Pullarkat, S. A.; Leung, P.-H. *RSC Adv.* **2016**, *6*, 75951-75959; (e) Yang, X.-Y.; Tay, W. S.; Li, Y.; Pullarkat, S. A.; Leung, P.-H. *Organometallics* **2015**, *34*, 1582-1588; (f) Yang, X.-Y.; Tay, W. S.; Li, Y.; Pullarkat, S. A.; Leung, P.-H. *Organometallics* **2015**, *34*, 5196-5201; (g) Yap, J. S. L.; Li, B. B.; Wong, J.; Li, Y.; Pullarkat, S. A.; Leung, P.-H. *Dalton Trans.* **2014**, *43*, 5777-5784; (h) Yap, J. S. L.; Chen, H. J.; Li, Y.; Pullarkat, S. A.; Leung, P.-H. *Organometallics* **2014**, *33*, 930-940; (i) Gan, K.; Sadeer, A.; Xu, C.; Li, Y.; Pullarkat, S. A. *Organometallics* **2014**, *33*, 5074-5076; (j) Ding, Y.; Zhang, Y.; Li, Y.; Pullarkat, S. A.; Andrews, P.; Leung, P.-H. *Eur. J. Inorg. Chem.* **2010**, 4427-4437; (k) Ding, Y.; Li, Y.; Pullarkat, S. A.; Leng Yap, S.; Leung, P.-H. *Eur. J. Inorg. Chem.* **2009**, 267-276; (l) Ding, Y.; Chiang, M.; Pullarkat, S. A.; Li, Y.; Leung, P.-H. *Organometallics* **2009**, *28*, 4358-4370; (m) Ding, Y.; Li, Y.; Zhang, Y.; Pullarkat, S. A.; Leung, P.-H. *Eur. J. Inorg. Chem.* **2008**, 1880-1891; (n) Ng, J. K.-P.; Chen, S.; Tan, G.-K.; Leung, P.-H. *Eur. J. Inorg. Chem.* **2007**, 3124-3134; (o) Ng, J. K.-P.; Chen, S.; Li, Y.; Tan, G.-K.; Koh, L.-L.; Leung, P.-H. *Inorg. Chem.* **2007**, *46*, 5100-5109; (p) Ng, J. K.-P.; Li, Y.; Tan, G.-K.; Koh, L.-L.; Vittal, J. J.; Leung, P.-H. *Inorg. Chem.* **2005**, *44*, 9874-9886; (q) Ng, J. K.-P.; Tan, G.-K.; Vittal, J. J.; Leung, P.-H. *Inorg. Chem.* **2003**, *42*, 7674-7682; (r) Li, Y.; Selvaratnam, S.; Vittal, J. J.; Leung, P.-H. *Inorg. Chem.* **2003**, *42*, 3229-3236; (s) Li, Y.; Ng, K.-H.; Selvaratnam, S.; Tan, G.-K.; Vittal, J. J.; Leung, P.-H. *Organometallics* **2003**, *22*, 834-842.
6. Sloan, T. E., Stereochemical Nomenclature and Notation in Inorganic Chemistry. In *Topics in Stereochemistry*, John Wiley & Sons, Inc.: 2007; pp 1-36.
7. Barloy, L.; Issenhuth, J.-T.; Weaver, M. G.; Pannetier, N.; Sirlin, C.; Pfeffer, M. *Organometallics* **2011**, *30*, 1168-1174.
8. Stirling, M. J.; Mwansa, J. M.; Sweeney, G.; Blacker, A. J.; Page, M. I. *Org. Biomol. Chem.* **2016**, *14*, 7092-7098.
9. Jerphagnon, T.; Gayet, A. J. A.; Berthiol, F.; Ritleng, V.; Mršić, N.; Meetsma, A.; Pfeffer, M.; Minnaard, A. J.; Feringa, B. L.; de Vries, J. G. *Chem. Eur. J.* **2009**, *15*, 12780-12790.
10. Sato, Y.; Kayaki, Y.; Ikariya, T. *Chem. Asian. J.* **2016**, *11*, 2924-2931.
11. (a) Dunina, V. V. *Curr. Org. Chem.* **2011**, *15*, 3415-3440; (b) Dunina, V. V.; Kazakova, M. Y.; Grishin, Y. K.; Malyshev, O. R.; Kazakova, E. I. *Russ. Chem. Bull.* **1997**, *46*, 1321-1330.
12. Sortais, J.-B.; Pannetier, N.; Holuigue, A.; Barloy, L.; Sirlin, C.; Pfeffer, M.; Kyritsakas, N. *Organometallics* **2007**, *26*, 1856-1867.
13. Attar, S.; Nelson, J. H.; Fischer, J.; de Cian, A.; Sutter, J.-P.; Pfeffer, M. *Organometallics* **1995**, *14*, 4559-4569.
14. (a) Jiang, X.; Tang, W.; Xue, D.; Xiao, J.; Wang, C. *ACS Catal.* **2017**, *7*, 1831-1835; (b) Michon, C.; MacIntyre, K.; Corre, Y.; Agbossou-Niedercorn, F. *ChemCatChem* **2016**, *8*, 1755-1762; (c) Matsunami, A.; Kuwata, S.; Kayaki, Y. *ACS Catal.* **2016**, *6*, 5181-5185; (d) Corre, Y.; Iali, W.; Hamdaoui, M.; Trivelli, X.; Djukic, J. P.; Agbossou-Niedercorn, F.; Michon, C. *Catal. Sci. Technol.* **2015**, *5*, 1452-1458.

15. (a) Zimbron, J. M.; Passador, K.; Gatin-Fraudet, B.; Bachelet, C.-M.; Plażuk, D.; Chamoreau, L.-M.; Botuha, C.; Thorimbert, S.; Salmain, M. *Organometallics* **2017**, *36*, 3435-3442; (b) Mukhopadhyay, S.; Gupta, R. K.; Paitandi, R. P.; Rana, N. K.; Sharma, G.; Koch, B.; Rana, L. K.; Hundal, M. S.; Pandey, D. S. *Organometallics* **2015**, *34*, 4491-4506; (c) Liu, Z.; Romero-Canelón, I.; Qamar, B.; Hearn, J. M.; Habtemariam, A.; Barry, N. P. E.; Pizarro, A. M.; Clarkson, G. J.; Sadler, P. J. *Angew. Chem. Int. Ed.* **2014**, *53*, 3941-3946.

16. (a) Pannetier, N.; Sortais, J.-B.; Issenhuth, J.-T.; Barloy, L.; Sirlin, C.; Holuigue, A.; Lefort, L.; Panella, L.; de Vries, J. G.; Pfeffer, M. *Adv. Synth. Catal.* **2011**, *353*, 2844-2852; (b) Jerphagnon, T.; Haak, R.; Berthiol, F.; Gayet, A. J. A.; Ritleng, V.; Holuigue, A.; Pannetier, N.; Pfeffer, M.; Voelklin, A.; Lefort, L.; Verzijl, G.; Tarabiono, C.; Janssen, D. B.; Minnaard, A. J.; Feringa, B. L.; de Vries, J. G. *Top. Catal.* **2010**, *53*, 1002-1008.

CHAPTER 4

Structures of Cycloiridated Complexes
A Structural Examination of Cycloiridated 1-Arylalkylamine and Imine Complexes

ABSTRACT

A comparative study of half sandwich cyclometalated iridium(III) complexes with 1-arylalkyl framework was performed. Although slight deviations in bond distances and angles within these complexes were apparent across functional groups, they were found to be similar in nature. Substituents on the organometallic ring were seen to extend the carbon-metal bond slightly across all examined species. Steric interactions between the bidentate framework and the spectator Cp* ligand also played a role in larger cyclometalating systems.

Keywords: Cyclometalation / Cycloiridated Complexes / *ortho*-Iridated Compounds / 1-Arylalkylamine and Imine Complexes / Structural Analysis

1 INTRODUCTION

The easy access to *pseudo*-tetrahedral cycloiridated compounds through either facile carboxylate-assisted C–H bond activation of cyclometalating ligands,[1] or similar bond activation of the same ligand *via* activated cationic metal center,[2] have led to an increase in output of these complexes within cycloiridation chemistry.[3]

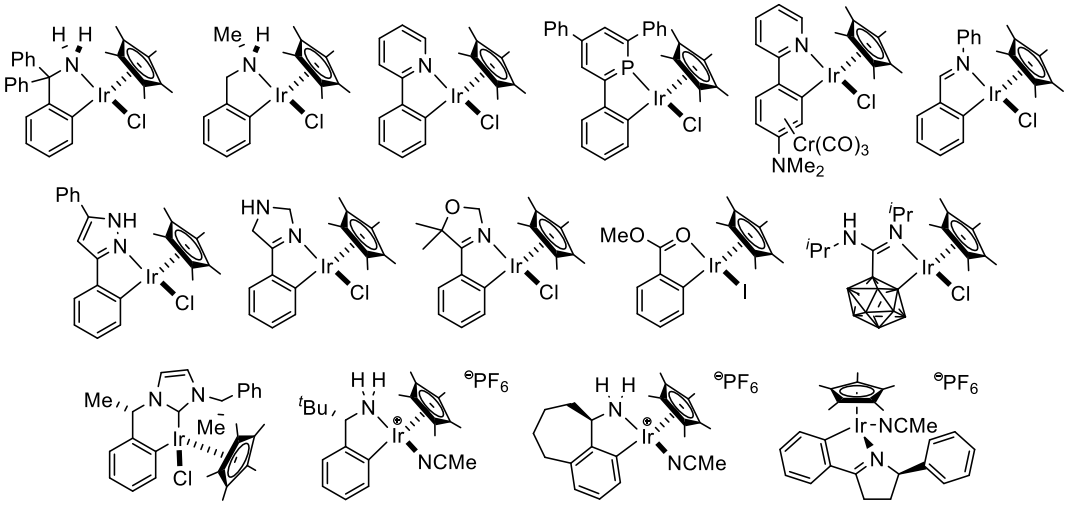

Figure 4.1. Myriad of piano-stool cycloiridated complexes in literature.

Whilst newer cycloiridated systems continue to develop, much effort is placed into defining the structure of the novel iridacycles and/or into the activity of its applications.[4] Although the importance of these investigations cannot be undermined, the study into their parent cyclometalated variants are of utmost importance since they form the groundwork within the field.

With several of these cycloiridated species at hand, our intentions were to perform a comparative analysis between the complexes. Moreover, the motifs of these compounds represented the fundamental frameworks to numerous classes of Cp*-based iridium(III) cyclometalated complexes. The piano-stool systems of these compounds have often been compared against its *pseudo*-tetrahedral η^6-aryl ruthenium(II) twin. As such, comparative studies into the basic framework of these compounds are scarce.[5] It should be noted that while the metallacycles are structurally analogous, selective formation of the former complexes were more prevalent.[2a, 6] In addition, these systems were found to be more active in applications than its ruthenium derivatives.[7]

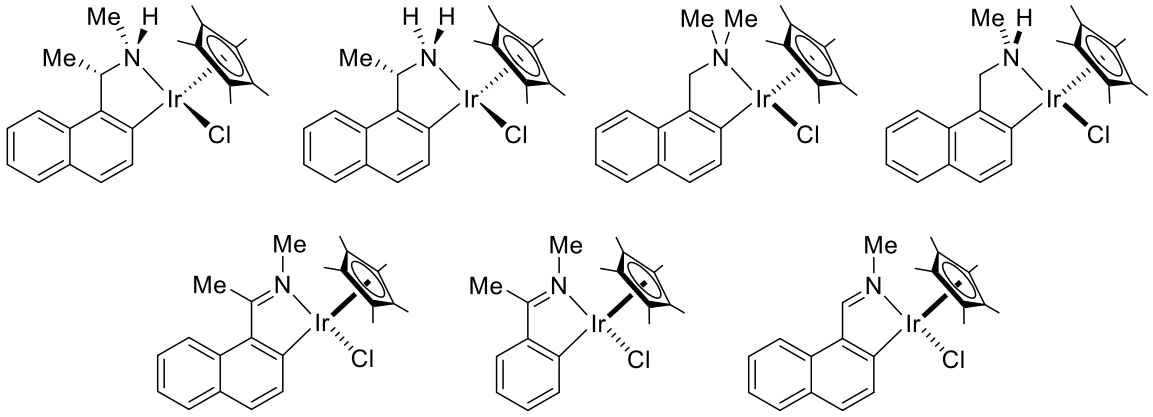

Figure 4.2. *Pseudo*-tetrahedral cycloiridated complexes involved in the structural study.

2 RESULTS AND DISCUSSION

2.1 A Comparison between Cycloiridated 1-Naphthylalkylamine Complexes

The dominant bidentate ligand employed for cyclometalation involves the 1-arylalkylamine motif.[8] The framework is easily tunable and is known to undergo the cyclization procedure with ease. Moreover, its optically-active variants are either commercially-available or can be readily synthesized in several steps to generate its chiral counterparts. Lastly, whilst the study should involve the phenyl derivative, we were, disappointingly, unable to obtain either of its chiral or achiral complexes for comparison.

Examination into the coordination of the Cp* moiety to the iridium center reflected similar bonding nature of the ligand between the four compounds, as indicated by the minute deviations in bond lengths. Since the ligand is *trans* to all other coordinating groups (*i.e.* the amine donor, the aromatic carbanion and the chloride) within the coordination sphere of the metal center, electronic effects projected by the Cp* moiety onto the latter ligands should be consistent and comparable across the complexes. Moreover, the same ligand would impose similar steric effects to the coordinative spaces about the iridium center.

Table 4.1. Selected bond lengths (Å), bond angles (deg) and torsion angles (deg) of structurally analogous cycloiridated 1-naphthylalkylamines complexes.

	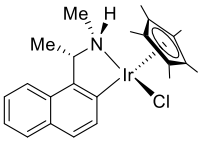	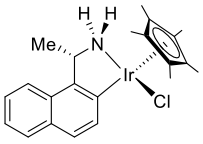	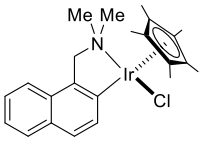	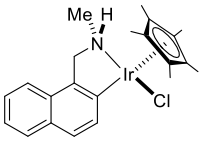
	(S_C,S_N,R_{Ir})-**1**	(S_C,R_{Ir})-**11**	*rac*-**7**	*rac*-**13**
		bond length (Å)		
Ir–C_{Ar}	2.040(9)	2.060(9)	2.043(6)	2.046(4)
Ir–$C_{Cp(avg)}$	2.209	2.209	2.209	2.198
Ir–N	2.151(8)	2.122(8)	2.192(5)	2.127(3)
Ir–Cl	2.425(3)	2.431(3)	2.438(2)	2.414(1)
		bond angle (deg)		
N–Ir–C_{Ar}	76.7(3)	76.8(3)	78.5(2)	76.8(1)
N–Ir–Cl	82.5(2)	82.5	85.9(1)	84.1(1)
C_{Ar}–Ir–Cl	86.6(3)	86.8	87.8(2)	87.1(1)
		torsion angle (deg)		
C_{Ar}–C_{Ar}–C–N	28.5	19.2	29.5	26.1
C_{Ar}–C_{Ar}–Ir–N	11.1	14.3	10.1	20.7

Whilst the Ir–C_{Ar} and Ir–Cl bond lengths between the complexes were comparable, a significant disparity was observed for the Ir–N bond distance. Analysis across the compounds revealed an increase in separation between iridium and nitrogen for every additional group at the nitrogen atom ((*S*C,*S*N,*R*Ir)-**1** *vs* (*S*C,*R*Ir)-**11**, and *rac*-**7** *vs rac*-**13**). Given that substituents about the nitrogen center would bring about greater steric hindrance between the two atoms leading to an extended bond, the result was not surprising. Substituents about the *α*-carbon was also shown to impact the Ir–N bond distances ((*S*C,*S*N,*R*Ir)-**1** *vs rac*-**13**), though the effect was less pronounced.

Bond angles about the coordination sphere between (*S*C,*S*N,*R*Ir)-**1** and (*S*C,*R*Ir)-**11** were found to be almost identical. It was, hence, postulated that the conformationally rigid ligands were strictly confined to their coordinative spaces on the basis of significant variance between that of complexes *rac*-**7** and *rac*-**13**. That being said, deviation between the former two structures lie outside the bite angle of the bidentate ligands, as depicted by their interior bond angles about the organometallic ring. In addition, torsion angles between the aromatic ring with the C–N, and Ir–N, bonds portrayed obvious difference in the internal structure of these compounds.

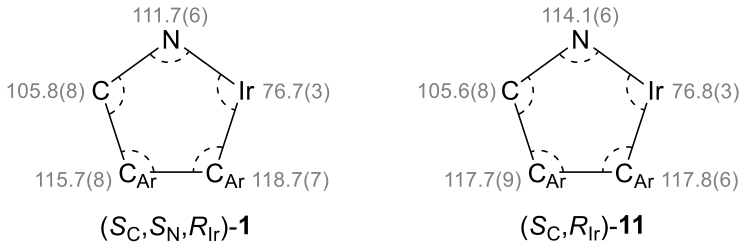

Figure 4.3. Interior angles about the five-membered organometallic ring of cycloiridated complexes (*S*C,*S*N,*R*Ir)-**1** and (*S*C,*R*Ir)-**11**.

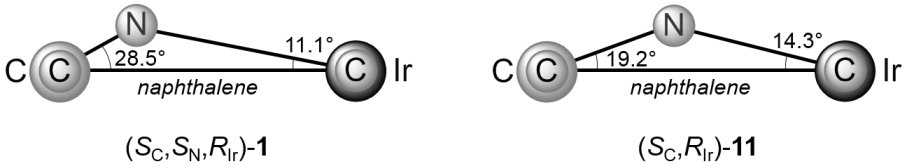

Figure 4.4. Torsion angles about the five-membered organometallic ring of cycloiridated complexes (*S*C,*S*N,*R*Ir)-**1** and (*S*C,*R*Ir)-**11**.

With regards to torsion angles, the {C_{Ar}–C_{Ar}–C–N} and {C_{Ar}–C_{Ar}–Ir–N} dihedral angles had an inverse relationship among the complexes. The more substituted amine donors were found to have smaller torsion angles between the aromatic ring and the Ir–N bond ((*S*C,*S*N,*R*Ir)-**1** *vs* (*S*C,*R*Ir)-**11**, and *rac*-**7** *vs rac*-**13**). Justification for the differences could be rationalized from the longer N–Ir bonds due to steric effects between the higher substituted nitrogen center and iridium as described earlier. The opposite was also true for the {C_{Ar}–C_{Ar}–C–N} torsion angles, although a larger than expected increase of the angle (*ca.* 9.3°), despite similar C–N bond distances, was observed for iridacycle (*S*C,*S*N,*R*Ir)-**1**. The abnormal increment was proposed to be attributable to 1,2-diaxial η^5-Cp*–*N*-methyl interaction.

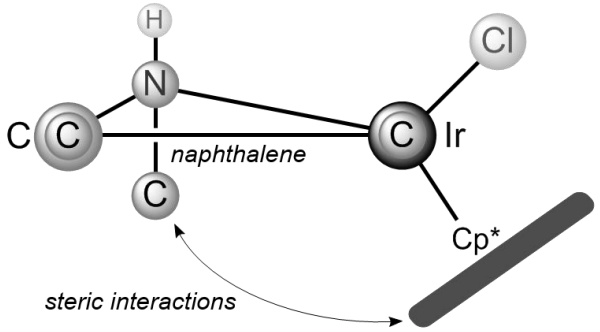

Figure 4.5. 1,2-Diaxial η^5-Cp*–*N*-methyl interaction in cycloiridated complex (*S*C,*S*N,*R*Ir)-**1**.

2.2 A Comparison between Cycloiridated 1-Arylalkylimine Complexes

The *imino* class cycloiridated systems present one of the more typical variants of half sandwich iridacyclic complexes due to its enhanced activity in applications.[7] If required, electronic effects can be easily tuned either through substituents at the imine moiety or, more commonly, on the aromatic ring. Steric projections, on the other hand, plays a smaller role in these metallacycles (due to the planar framework of the cyclometalating ligand), although bulky substituents or chiral groups may be constructed onto the ligand motif.

Among the three *imino*-type *ortho*-iridated complexes we had synthesized, dative bonding between the Cp* ligand and the iridium center, like its 1-naphthylalkylamine counterparts, were found to have little deviations in their Ir–$C_{Cp(avg)}$ bond distances. As such, we could assume similar electronic and steric effects imposed by the Cp* moiety onto the *trans* ligands and the coordination sphere respectively, as described in the earlier section.

Table 4.2. Selected bond lengths (Å), bond angles (deg) and torsion angles (deg) of structurally analogous cycloiridated 1-arylalkylimines complexes.

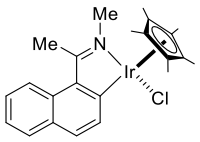

rac-**4**

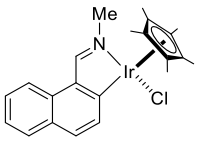

rac-**7**

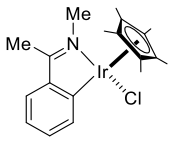

rac-**9**

bond length (Å)			
Ir–C_{Ar}	2.028(8)	2.025(10)	2.030(3)
Ir–$C_{Cp(avg)}$	2.198	2.195	2.202
Ir–N	2.070(7)	2.056(8)	2.082(3)
Ir–Cl	2.405(2)	2.398(3)	2.400(1)
bond angle (deg)			
N–Ir–C_{Ar}	77.7(3)	77.9(4)	77.6(1)
N–Ir–Cl	82.8(2)	83.5(2)	84.4(1)
C_{Ar}–Ir–Cl	90.5(2)	87.5(3)	87.5(1)
C_{Ar}–C–N	114.3(12)	116.0(10)	114.5(3)
torsion angle (deg)			
C_{Ar}–C_{Ar}–C–N	14.2	4.4	3.8
C_{Ar}–C_{Ar}–Ir–N	4.5	2.3	0.7
C_{Ar}–C_{Ar}–C–C_{Me}	22.2	-	4.0

With all complexes having the same *N*-methyl substituent, it would appear that alkyl groups at the carbon center of Schiff base decreased the coordinative ability of the imine moiety, as indicated by the elongated Ir–N bond in *rac*-**4** (compared to *rac*-**7**). Based on the C_{Ar}–C–N bond angle, the additional methyl substituent supplemented a minor reduction of the angle by 1.7° (*rac*-**4** *vs rac*-**7**), although reflection of the effect was not obvious from the smaller deviation in the bite angle between the bidentate ligands. Whilst it seemed that steric effects may have influenced the bonding mode, closer examination into the crystallographic data revealed the methyl group directing away from the coordination sphere. No visible Cp*–*C*-methyl interactions were also observed.

Increased conjugation within the aromatic ring also brought about a shorter Ir–N bond (*rac*-**4** *vs rac*-**9**), although a direct comparison was difficult since bond angles about the coordination sphere at iridium differ significantly across the two complexes. Perhaps the most obvious deviation lies with the torsion angles within the complex. It would seem that the replacement of the phenyl system to a naphthalene ring moiety brought about steric effects with an evident difference in the {C_{Ar}–C_{Ar}–C–N} and {C_{Ar}–C_{Ar}–C–C_{Me}} dihedral angles. Whilst iridacycles *rac*-**7** and *rac*-**9** maintained a somewhat planar structure along the hydrocarbon motif, the naphthylketimine framework in *rac*-**4** was found to be slightly twisted due to spatial interactions between the two substituents at the imine moiety. The effect strongly resembled the stereogenic locking mechanism in the 1-naphthylethylamine systems described in Chapter 3 of the thesis, albeit the twist was towards the direction where steric hindrance was minimal (unlike the conformational lock which fixated the methyl substituent in the unfavorable axial position).

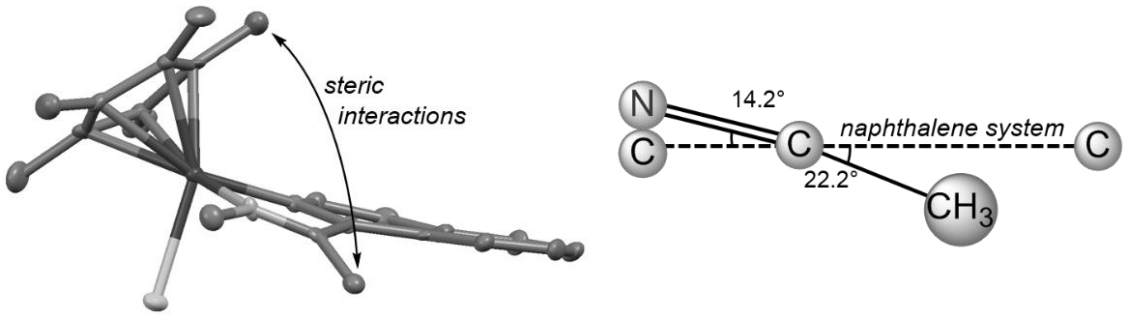

Figure 4.6. Deviation from planarity in the ligand framework of cycloiridated complex *rac*-**4**.

2.3 A Comparison between Cycloiridated 1-Naphthylalkylamine and Imine Complexes

Finally, we completed the study by analyzing cycloiridated complexes across functional groups.

On the basis of similar electronic effects from the *trans* Cp* ligand, coordination of the lone electron pair from the donor to the metal center was more effective in the imine complexes than its amine counterparts, as represented by the shorter Ir–N bond distances (*rac*-**4** *vs* (S_C,S_N,R_{Ir})-**1**, and *rac*-**7** *vs rac*-**13**). While the observation may seem counter-intuitive (due to the higher basicity of amines to imines), steric hindrance about the nitrogen atom was more prevalent in substituted amines than imines. As such, steric crowd about the former functionality limits the σ donation of its lone electron pair to the metal center. On the other hand, the planar imine moiety has less steric hindrance about the nitrogen center allowing it to share its lone electron pair more effectively with the electron-deficient iridium center.

Table 4.3. Selected bond lengths (Å), bond angles (deg) and torsion angles (deg) of structurally analogous cycloiridated 1-naphthylalkylamines and imine complexes.

	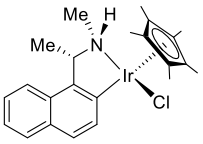 (S_C,S_N,R_{Ir})-**1**	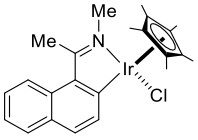 *rac*-**4**	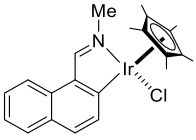 *rac*-**7**	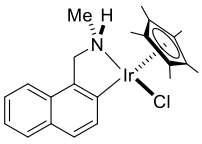 *rac*-**13**
		bond length (Å)		
Ir–C_{Ar}	2.040(9)	2.028(8)	2.025(10)	2.046(4)
Ir–$C_{Cp(avg)}$	2.209	2.198	2.195	2.198
Ir–N	2.151(8)	2.070(7)	2.056(8)	2.127(3)
Ir–Cl	2.425(3)	2.405(2)	2.398(3)	2.414(1)
		bond angle (deg)		
N–Ir–C_{Ar}	76.7(3)	77.7(3)	77.9(4)	76.8(1)
N–Ir–Cl	82.5(2)	82.8(2)	83.5(2)	84.1(1)
C_{Ar}–Ir–Cl	86.6(3)	90.5(2)	87.5(3)	87.1(1)
		torsion angle (deg)		
C_{Ar}–C_{Ar}–C–N	28.5	14.2	4.4	26.1
C_{Ar}–C_{Ar}–Ir–N	11.1	4.5	2.3	20.7

With respect to the carbon-metal bond, the iridacycles differ somewhat across the functional groups with slightly shorter Ir–C_{Ar} bond for the imine complexes compared to their amine analogues (*rac*-**4** *vs* (S_C,S_N,R_{Ir})-**1**, and *rac*-**7** *vs* *rac*-**13**). It is worth recalling that the Ir–C_{Ar} bond distances do not differ significantly within cycloiridated complexes of same donor type. As such, the data presented interesting findings since the compounds consist of the same ligands, other than the bidentate cyclometalating agent. An explanation for the observation could lie with the non-innocent nature of the *imino*-type cyclometalating ligand in which the imine moieties could be reduced to some extent.

As described in an earlier section, the cycloiridated *imino* complexes exhibited mainly planar structures about their organic framework, as denoted by their small torsion angles within the five-membered organometallic ring system. Despite the fact that iridacycle *rac*-**4** displayed slight abnormally from the other imine-type metallacycles with respect to its {C_{Ar}–C_{Ar}–C–N} and {C_{Ar}–C_{Ar}–Ir–N} dihedral angles, deviation in its torsion angles to its structurally analogous amine complexes ((S_C,S_N,R_{Ir})-**1** and *rac*-**13**) remained significantly different. The *ortho*-iridated imine complexes were also found to have slightly larger N–Ir–C_{Ar} bond angles (as compared to its amine variants) within the coordination sphere of iridium, although this was attributable to less flexibility within the chelate ring in these compounds.

Lastly, we review the coordinative ability of the ligands within the *pseudo*-tetrahedral cycloiridated complexes. Assuming that the Cp* ligand exerts similar electronic influence onto its *trans* ligands (as indicated by similar Ir–$C_{Cp(avg)}$ bond lengths across all synthesized iridacycles), it can be determined that the coordinative strength of the ligands was bounded in order of the aromatic carbanion, imine moiety, amine donor and, finally, the *chlorido* anion. It should, however, be noted that the order is reflective of a combination of electronic and steric effects, and not purely on the basis of basicity.

3 SUMMARY AND CONCLUSION

In this chapter, we have examined and compared the crystallographic structures of several cycloiridated complexes synthesized in the thesis. The study involved parent cyclometalating groups, specifically the 1-arylalkylamine ligands and its imine derivatives, which could act as references for other structurally analogous *pseudo*-tetrahedral iridacycles. The analysis also presented the consequences to bond lengths and angles within the molecule upon minor additions or modifications to the cyclometalating motif. Lastly, we explained how the spectator ligand may have influenced the structure of the complex through steric interactions.

With greater understanding into the nature of bonding within these cycloiridated complexes, we hope that the investigation would provide chemists with further information on these classes of compounds. It is also within our intentions that the groundwork could be applied in rational design of novel Cp*-based iridacyclic complexes or its related systems.

REFERENCES

1. (a) Ackermann, L. *Chem. Rev.* **2011**, *111*, 1315-1345; (b) Davies, D. L.; Donald, S. M. A.; Al-Duaij, O.; Macgregor, S. A.; Pölleth, M. *J. Am. Chem. Soc.* **2006**, *128*, 4210-4211; (c) Davies, D. L.; Al-Duaij, O.; Fawcett, J.; Giardiello, M.; Hilton, S. T.; Russell, D. R. *Dalton Trans.* **2003**, 4132-4138.
2. (a) Barloy, L.; Issenhuth, J.-T.; Weaver, M. G.; Pannetier, N.; Sirlin, C.; Pfeffer, M. *Organometallics* **2011**, *30*, 1168-1174; (b) Jerphagnon, T.; Gayet, A. J. A.; Berthiol, F.; Ritleng, V.; Mršić, N.; Meetsma, A.; Pfeffer, M.; Minnaard, A. J.; Feringa, B. L.; de Vries, J. G. *Chem. Eur. J.* **2009**, *15*, 12780-12790.
3. Han, Y.-F.; Jin, G.-X. *Chem. Soc. Rev.* **2014**, *43*, 2799-2823.
4. (a) Arthurs, R. A.; Horton, P. N.; Coles, S. J.; Richards, C. J. *Eur. J. Inorg. Chem.* **2017**, 229-232; (b) Sato, Y.; Kayaki, Y.; Ikariya, T. *Organometallics* **2016**, *35*, 1257-1264; (c) Sato, Y.; Kayaki, Y.; Ikariya, T. *Chem. Asian. J.* **2016**, *11*, 2924-2931; (d) Sabater, S.; Baya, M.; Mata, J. A. *Organometallics* **2014**, *33*, 6830-6839; (e) Féghali, E.; Barloy, L.; Issenhuth, J.-T.; Karmazin-Brelot, L.; Bailly, C.; Pfeffer, M. *Organometallics* **2013**, *32*, 6186-6194; (f) Djukic, J.-P.; Iali, W.; Pfeffer, M.; Le Goff, X.-F. *Chem. Eur. J.* **2012**, *18*, 6063-6078.
5. Sortais, J.-B.; Pannetier, N.; Holuigue, A.; Barloy, L.; Sirlin, C.; Pfeffer, M.; Kyritsakas, N. *Organometallics* **2007**, *26*, 1856-1867.
6. Arthurs, R. A.; Ismail, M.; Prior, C. C.; Oganesyan, V. S.; Horton, P. N.; Coles, S. J.; Richards, C. J. *Chem. Eur. J.* **2016**, *22*, 3065-3072.
7. (a) Wang, C.; Xiao, J. *Chem. Commun.* **2017**, *53*, 3399-3411; (b) Michon, C.; MacIntyre, K.; Corre, Y.; Agbossou-Niedercorn, F. *ChemCatChem* **2016**, *8*, 1755-1762.
8. (a) Cerón-Camacho, R.; Morales-Morales, D.; Hernandez, S.; Le Lagadec, R.; Ryabov, A. D. *Inorg. Chem.* **2008**, *47*, 4988-4995; (b) Meneghetti, M. R.; Grellier, M.; Pfeffer, M.; Dupont, J.; Fischer, J. *Organometallics* **1999**, *18*, 5560-5570; (c) Rietveld, M. H. P.; Nagelholt, L.; Grove, D. M.; Veldman, N.; Spek, A. L.; Rauch, M. U.; Herrmann, W. A.; van Koten, G. *J. Organomet. Chem.* **1997**, *530*, 159-167; (d) Pfeffer, M.; Urriolabeitia, E. P.; de Cian, A.; Fischer, J. *J. Organomet. Chem.* **1995**, *494*, 187-193; (e) Abbenhuis, H. C. L.; Pfeffer, M.; Sutter, J. P.; de Cian, A.; Fischer, J.; Ji, H. L.; Nelson, J. H. *Organometallics* **1993**, *12*, 4464-4472; (f) Vicente, J.; Chicote, M. T.; Bermúdez, M. D. *J. Organomet. Chem.* **1984**, *268*, 191-195; (g) Longoni, G.; Fantucci, P.; Chini, P.; Canziani, F. *J. Organomet. Chem.* **1972**, *39*, 413-425; (h) Cope, A. C.; Siekman, R. W. *J. Am. Chem. Soc.* **1965**, *87*, 3272-3273.

EXPERIMENTAL

1 GENERAL CONSIDERATIONS

Reactions involving air- or moisture-sensitive compounds were carried out by means of conventional Schlenk techniques under a positive pressure of nitrogen gas. Unless stated otherwise, chemicals and solvents were used as received from commercial vendors without further purification. When required, anhydrous solvents were freshly distilled and dried according to standard procedures prior to use.

Nuclear magnetic resonance (NMR) spectroscopy were recorded at Nanyang Technological University Division of Chemistry and Biological Chemistry Central Facilities Laboratory on the Bruker Avance III 400 (BBFO 400) spectrometers at 400 MHz for ^{1}H NMR, 100 MHz for ^{13}C NMR and 161 MHz for ^{31}P{^{1}H} NMR. Chemical shifts (δ) are quoted in ppm, and referenced to chemical shifts of residual solvent peaks for ^{1}H and ^{13}C NMR. 85% H_3PO_4/D_2O mixture was utilized as the external standard for ^{31}P{^{1}H} NMR.

High resolution mass spectrometry *via* electrospray ionization (ESI) was performed on the Waters Q-Tof Premier spectrometer. Unless stated otherwise, acetonitrile was used as the solvent for the dissolution of compounds.

Elemental analysis was performed on the EuroVector Euro EA elemental analyzer at Nanyang Technological University Division of Chemistry and Biological Chemistry Central Facilities Laboratory.

Optical rotation studies were measured on the Jasco P-1030 polarimeter in a 0.1 dm polarimetry cell at the specified temperature using the D-line of sodium (589 nm) as the source of light. Unless stated otherwise, dichloromethane was used as the solvent for the dissolution of compounds.

2 CHAPTER 2: CHALLENGES TO CYCLOMETALATION

2.1 The Iridation Reaction of (*R*)-*N*,*N*-Dimethyl-1-naphthylethylamine (*R*)-L1

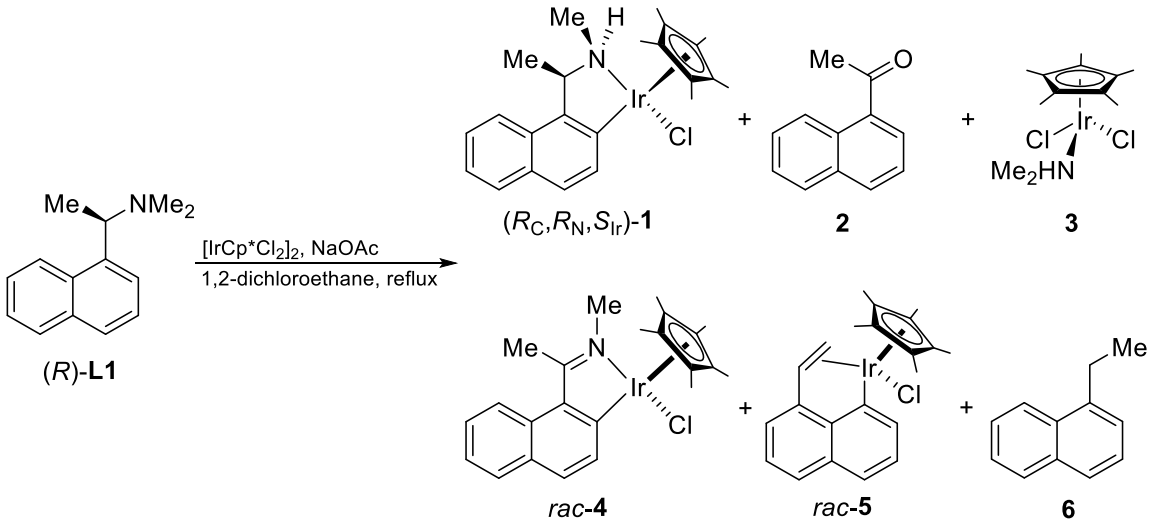

$[IrCp^*Cl_2]_2$ (100 mg, 0.125 mmol) and NaOAc (41 mg, 0.50 mmol) were added to a stirring solution of (*R*)-*N*,*N*-dimethyl-1-naphthylethylamine (*R*)-**L1** (50 mg, 0.25 mmol) in 1,2-dichloroethane (5 mL). The reaction mixture was then reflux for the desired time period. The crude reaction mixture was evaporated to dryness and purified directly by column chromatography on silica gel (*refer to* Chapter 2, Section 2.1 *on eluent system for column chromatography*).

(S_C,S_N,R_{Ir})-(1,2,3,4,5-Pentamethylcyclopentadienyl){(κ^2-C,N)-1-[1-(N-methylamino)-ethyl]naphthyl}iridium(III) chloride, (S_C,S_N,R_{Ir})-1

Yield: 5.5 mg (4%; *two-day reaction*); $[\alpha]_D$ (22 °C, *c* 0.5) = +102.1°; ^{1}H NMR (400 MHz, CD_2Cl_2): δ 1.24 (d, $^3J_{HH}$ = 6.5 Hz, 3H, ArCH(C*H*$_3$)), 1.67 (s, 15H, Cp(C*H*$_3$)), 3.02 (d, $^3J_{HH}$ = 6.4 Hz, 3H, NH(C*H*$_3$)), 4.69 (dq, $^3J_{HH}$ = 4.2 Hz and 6.4 Hz, 1H, ArC*H*(CH$_3$)), 5.02 (br s, 1H, N*H*(CH$_3$)), 7.20-7.74 (m, 6H, Ar*H*); ^{13}C NMR (100 MHz, CD_2Cl_2): δ 9.36 (C_5(*C*H$_3$)$_5$), 17.39 (ArCH(*C*H$_3$)N), 39.57 (N*C*H$_3$), 66.89 (Ar*C*H(CH$_3$)N), 87.35 (*C*$_5$(CH$_3$)$_5$), 122.66 (aromatic carbon), 123.41 (aromatic carbon), 125.41 (aromatic carbon), 126.05 (aromatic carbon), 127.92 (aromatic carbon), 128.38 (aromatic carbon), 131.07 (aromatic carbon), 136.07 (aromatic carbon), 144.65 (aromatic carbon), 153.10 (aromatic carbon); HRMS (ESI) *m*/*z* [*negative mode*] calcd for $C_{23}H_{29}ClIrN$ 547.1618, found 547.1619; Anal. calcd for $C_{23}H_{29}ClIrN$: C, 50.49; H, 5.34; N, 2.56. Found: C, 50.02; H, 5.56; N, 2.31.

1-Acetonaphthone, 2

Yield: 20.4 mg (48%; *two-day reaction*); ^{1}H NMR (400 MHz, $CDCl_3$): δ 2.75 (s, 3H, Ar(C=O)C*H*$_3$), 7.48-8.74 (m, 7H, Ar*H*); ^{13}C NMR (100 MHz, $CDCl_3$): δ 29.93 (C(=O)*C*H$_3$), 124.29 (aromatic carbon), 126.00 (aromatic carbon), 126.41 (aromatic carbon), 128.01 (aromatic carbon), 128.37 (aromatic carbon), 128.58 (aromatic carbon), 130.15 (aromatic carbon), 132.97 (aromatic carbon), 133.98 (aromatic carbon), 135.52 (aromatic carbon), 201.76 (*C*(=O)CH$_3$); HRMS (ESI) *m*/*z* $[(M+H)]^+$ calcd for $C_{12}H_{11}O$ 171.0810, found 170.0814; Anal. calcd for $C_{12}H_{10}O$: C, 84.68; H, 5.92. Found: C, 84.93; H, 5.59.

Dichloro(dimethylamino)-1,2,3,4,5-pentamethylcyclopentadienyl iridium(III), 3

Yield: 24.4 mg (22%; *two-day reaction*); ^{1}H NMR (400 MHz, $CDCl_3$): δ 1.64 (s, 15H, Cp(C*H*$_3$)), 2.89 (d, $^3J_{HH}$ = 5.4 Hz, 6H, HN(C*H*$_3$)$_2$), 3.90 (br s, 1H, *H*N(CH$_3$)$_2$); ^{13}C NMR (100 MHz, $CDCl_3$): δ 9.20 (C_5(*C*H$_3$)$_5$), 43.94 (N*C*H$_3$), 84.76 (*C*$_5$(CH$_3$)$_5$); HRMS (ESI) *m*/*z* [*negative mode*] calcd for $C_{12}H_{22}ClIrN$ 443.0759, found 443.0747.

(1,2,3,4,5-Pentamethylcyclopentadienyl){(κ²-C,N)-1-[1-(N-methylimino)ethyl]naphthyl}iridium(III) chloride, rac-4

Yield: 2.7 mg (2%; *two-day reaction*); ^{1}H NMR (400 MHz, $CDCl_3$): δ 1.73 (s, 15H, Cp(C*H*$_3$)), 2.98 (s, 3H, C(=NMe)(C*H*$_3$)Ar)), 3.98 (s, 3H, NC*H*$_3$), 7.32-8.22 (m, 6H, Ar*H*); ^{13}C NMR (100 MHz, $CDCl_3$): δ 9.16 ($C_5(CH_3)_5$), 20.65 (C(=N)*C*H$_3$), 45.68 (N*C*H$_3$)), 89.34 ($C_5(CH_3)_5$), 122.11 (aromatic carbon), 122.46 (aromatic carbon), 125.92 (aromatic carbon), 129.57 (aromatic carbon), 130.95 (aromatic carbon), 131.17 (aromatic carbon), 132.80 (aromatic carbon), 134.49 (aromatic carbon), 140.83 (aromatic carbon), 174.92 ((*C*(=N)CH$_3$)), 180.39 (aromatic carbon); HRMS (ESI) *m*/*z* [*negative mode*] calcd for $C_{23}H_{27}ClIrN$ 545.1461, found 545.1451; Anal. calcd for $C_{23}H_{27}ClIrN$: C, 50.68; H, 4.99; N, 2.57. Found: C, 50.50; H, 5.07; N, 2.73.

(1,2,3,4,5-Pentamethylcyclopentadienyl){(κ²-C,[η²-ethylene])-1-naphthylethene}iridium(III) chloride, rac-5

Yield: 2.6 mg (2%; *two-day reaction*); ^{1}H NMR (400 MHz, $CDCl_3$): δ 1.63 (s, 15H, Cp(C*H*$_3$)), 4.04 (d, $^{3}J_{HH}$ = 11.3 Hz, 1H, ArCHCH*H*), 4.10 (d, $^{3}J_{HH}$ = 8.8 Hz, 1H, ArCHC*H*H), 5.32 (dd, $^{3}J_{HH}$ = 8.9 Hz and 11.2 Hz, ArC*H*CH$_2$), 7.02-7.49 (m, 6H, Ar*H*); ^{13}C NMR (100 MHz, $CDCl_3$): δ 8.29 ($C_5(CH_3)_5$), 56.16 (ArCH=*C*H$_2$), 80.82 (Ar*C*H=CH$_2$), 99.36 ($C_5(CH_3)_5$), 121.11 (aromatic carbon), 121.43 (aromatic carbon), 124.84 (aromatic carbon), 125.38 (aromatic carbon), 127.98 (aromatic carbon), 131.70 (aromatic carbon), 133.83 (aromatic carbon), 143.47 (aromatic carbon), 146.03 (aromatic carbon), 148.17 (aromatic carbon); HRMS (ESI) *m*/*z* [*negative mode*] calcd for $C_{22}H_{24}ClIr$ 516.1196, found 516.1188; Anal. calcd for $C_{22}H_{24}ClIr$: C, 51.20; H, 4.69. Found: C, 51.45; H, 4.11.

1-Ethylnaphthalene, 6

Yield: 0.3 mg (<1%; *two-day reaction*); ^{1}H NMR (400 MHz, $CDCl_3$): δ 1.40 (t, $^{3}J_{HH}$ = 7.5 Hz, 3H, $ArCH_2CH_3$), 3.13 (q, $^{3}J_{HH}$ = 7.5 Hz, 2H, $ArCH_2CH_3$), 7.34-8.08 (m, 7H, Ar*H*); ^{13}C NMR (100 MHz, $CDCl_3$): δ 15.03 ($ArCH_2CH_3$), 25.88 ($ArCH_2CH_3$), 123.72 (aromatic carbon), 124.83 (aromatic carbon), 125.37 (aromatic carbon), 125.65 (aromatic carbon), 126.37 (aromatic carbon), 128.73 (aromatic carbon), 131.77 (aromatic carbon), 133.81 (aromatic carbon), 140.27 (aromatic carbon); HRMS (ESI) *m*/*z* $[(M+H)]^+$ calcd for $C_{12}H_{13}$ 157.1017, found 157.1017; Anal. calcd for $C_{12}H_{12}$: C, 92.26; H, 7.74. Found: C, 92.57; H, 7.50.

2.2 The Iridation Reaction of *rac*-*N*,*N*-Dimethyl-1-naphthylethyl-*α*-*d*-amine *rac*-L1'

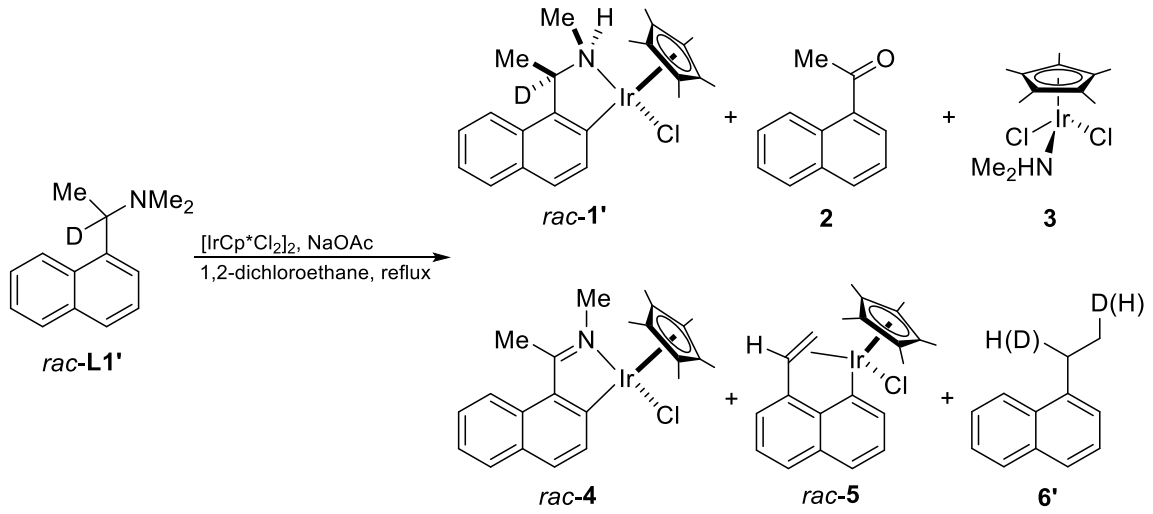

$[IrCp^*Cl_2]_2$ (100 mg, 0.125 mmol) and NaOAc (41 mg, 0.50 mmol) were added to a stirring solution of *rac*-*N*,*N*-dimethyl-1-naphthylethyl-*α*-*d*-amine *rac*-**L1'** (50 mg, 0.25 mmol) in 1,2-dichloroethane (5 mL). The reaction mixture was then reflux for 48 h. The crude reaction mixture was evaporated to dryness and purified directly by column chromatography on silica gel (*eluent system of deuterated products is similar to that of its non-deuterated counterparts; refer to* Chapter 2, Section 2.1 *on eluent system for column chromatography*).

(1,2,3,4,5-Pentamethylcyclopentadienyl){(κ²-C,N)-1-[1-(N-methylamino)ethyl]naphthyl}-iridium(III) chloride, rac-1'

^{1}H NMR (400 MHz, CD_2Cl_2): δ 1.25 (s, 3H, ArCD(CH_3)), 1.68 (s, 15H, Cp(CH_3)), 3.02 (d, $^3J_{HH}$ = 6.3 Hz, 3H, NH(CH_3)), 5.03 (br s, 1H, NH(CH$_3$)), 7.21-7.75 (m, 6H, ArH); ^{2}H NMR (400 MHz, CD_2Cl_2): δ 4.72 (ArCD(CH$_3$)); ^{13}C NMR (100 MHz, CD_2Cl_2): δ 9.37 (C_5(CH$_3$)$_5$), 17.28 (ArCD(CH$_3$)N), 39.54 (NCH$_3$), 66.51 ($^1J_{CD}$ = 20.5 Hz, ArCD(CH$_3$)N), 87.35 (C_5(CH$_3$)$_5$), 122.66 (aromatic carbon), 123.41 (aromatic carbon), 125.41 (aromatic carbon), 126.05 (aromatic carbon), 127.95 (aromatic carbon), 128.39 (aromatic carbon), 131.09 (aromatic carbon), 136.09 (aromatic carbon), 144.64 (aromatic carbon), 153.13 (aromatic carbon); HRMS (ESI) *m*/*z* [*negative mode*] calcd for $C_{23}H_{28}DClIrN$ 548.1681, found 548.1675.

1-Acetonaphthone, 2

^{1}H NMR (400 MHz, $CDCl_3$): δ 2.75 (s, 3H, Ar(C=O)CH_3), 7.48-8.74 (m, 7H, Ar*H*); ^{13}C NMR (100 MHz, $CDCl_3$): δ 29.93 (C(=O)*C*H_3), 124.29 (aromatic carbon), 126.00 (aromatic carbon), 126.41 (aromatic carbon), 128.01 (aromatic carbon), 128.37 (aromatic carbon), 128.58 (aromatic carbon), 130.15 (aromatic carbon), 132.97 (aromatic carbon), 133.98 (aromatic carbon), 135.52 (aromatic carbon), 201.76 (*C*(=O)CH_3); HRMS (ESI) *m*/*z* $[(M+H)]^+$ calcd for $C_{12}H_{11}O$ 171.0810, found 170.0814; Anal. calcd for $C_{12}H_{10}O$: C, 84.68; H, 5.92. Found: C, 84.93; H, 5.59.

Dichloro(dimethylamino)-1,2,3,4,5-pentamethylcyclopentadienyl iridium(III), 3

^{1}H NMR (400 MHz, $CDCl_3$): δ 1.64 (s, 15H, Cp(CH_3)), 2.89 (d, $^{3}J_{HH}$ = 5.4 Hz, 6H, HN(CH_3)$_2$), 3.90 (br s, 1H, *H*N(CH_3)$_2$); ^{13}C NMR (100 MHz, $CDCl_3$): δ 9.20 (C_5(*C*H_3)$_5$), 43.94 (N*C*H_3), 84.76 (*C*$_5$(CH_3)$_5$); HRMS (ESI) *m*/*z* [*negative mode*] calcd for $C_{12}H_{22}ClIrN$ 443.0759, found 443.0747.

(1,2,3,4,5-Pentamethylcyclopentadienyl){(κ^2-C,N)-1-[1-(N-methylimino)ethyl]naphth-yl}iridium(III) chloride, rac-4

^{1}H NMR (400 MHz, $CDCl_3$): δ 1.73 (s, 15H, Cp(CH_3)), 2.98 (s, 3H, C(=NMe)(CH_3)Ar)), 3.98 (s, 3H, NCH_3), 7.32-8.22 (m, 6H, Ar*H*); ^{13}C NMR (100 MHz, $CDCl_3$): δ 9.16 (C_5(*C*H_3)$_5$), 20.65 (C(=N)*C*H_3), 45.68 (N*C*H_3)), 89.34 (*C*$_5$(CH_3)$_5$), 122.11 (aromatic carbon), 122.46 (aromatic carbon), 125.92 (aromatic carbon), 129.57 (aromatic carbon), 130.95 (aromatic carbon), 131.17 (aromatic carbon), 132.80 (aromatic carbon), 134.49 (aromatic carbon), 140.83 (aromatic carbon), 174.92 ((*C*(=N)CH_3)), 180.39 (aromatic carbon); HRMS (ESI) *m*/*z* [*negative mode*] calcd for $C_{23}H_{27}ClIrN$ 545.1461, found 545.1451; Anal. calcd for $C_{23}H_{27}ClIrN$: C, 50.68; H, 4.99; N, 2.57. Found: C, 50.50; H, 5.07; N, 2.73.

(1,2,3,4,5-Pentamethylcyclopentadienyl){(κ²-C,[η²-ethylene])-1-naphthylethene}iridium (III) chloride, rac-5

^{1}H NMR (400 MHz, $CDCl_3$): δ 1.63 (s, 15H, Cp(C*H*$_3$)), 4.04 (d, $^3J_{HH}$ = 11.3 Hz, 1H, ArCHCH*H*), 4.10 (d, $^3J_{HH}$ = 8.8 Hz, 1H, ArCHC*H*H), 5.32 (dd, $^3J_{HH}$ = 8.9 Hz and 11.2 Hz, ArC*H*CH_2), 7.02-7.49 (m, 6H, Ar*H*); ^{13}C NMR (100 MHz, $CDCl_3$): δ 8.29 (C_5(*C*H_3)$_5$), 56.16 (ArCH=*C*H_2), 80.82 (Ar*C*H=CH_2), 99.36 (*C*$_5$(CH_3)$_5$), 121.11 (aromatic carbon), 121.43 (aromatic carbon), 124.84 (aromatic carbon), 125.38 (aromatic carbon), 127.98 (aromatic carbon), 131.70 (aromatic carbon), 133.83 (aromatic carbon), 143.47 (aromatic carbon), 146.03 (aromatic carbon), 148.17 (aromatic carbon); HRMS (ESI) *m*/*z* [*negative mode*] calcd for $C_{22}H_{24}ClIr$ 516.1196, found 516.1188; Anal. calcd for $C_{22}H_{24}ClIr$: C, 51.20; H, 4.69. Found: C, 51.45; H, 4.11.

1-Ethylnaphthalene, 6 and 6'

^{1}H NMR (400 MHz, $CDCl_3$): δ 1.40 (t, $^3J_{HH}$ = 7.5 Hz, 2.86H, $ArCH_2CH_3$), 3.13 (q, $^3J_{HH}$ = 7.5 Hz, 1.62H, ArC*H*$_2$$CH_3$), 7.34-8.08 (m, 7H, Ar*H*); ^{2}H NMR (400 MHz, $CDCl_3$): δ 1.41 ($ArCH_2CH_2$*D*), 3.13 (ArCH*D*CH_3); ^{13}C NMR (100 MHz, $CDCl_3$): δ 14.73 ($^1J_{CD}$ = 20.6 Hz, $ArCH_2$*C*H_2D) 15.01 ($^1J_{CD}$ = 19.3 Hz, $ArCH_2$*C*H_3), 25.55 (Ar*C*HDCH_3), 25.87 (Ar*C*H_2CH_3), 123.72 (aromatic carbon), 124.83 (aromatic carbon), 125.36 (aromatic carbon), 125.65 (aromatic carbon), 126.36 (aromatic carbon), 128.72 (aromatic carbon), 131.78 (aromatic carbon), 133.83 (aromatic carbon), 140.27 (aromatic carbon); HRMS (ESI) *m*/*z* $[(M–H)]^+$ calcd for $C_{12}H_{11}D$ 156.0924, found 156.0919.

2.3 The Iridation Reaction of *N*,*N*-Dimethyl-1-naphthylmethylamine L3

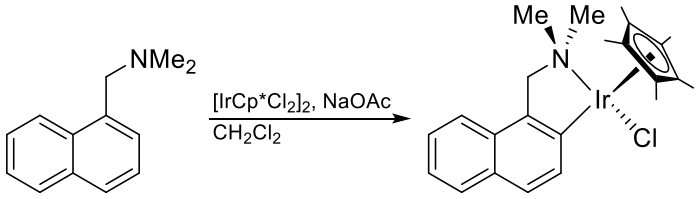

$[IrCp^*Cl_2]_2$ (40 mg, 0.05 mmol) and NaOAc (10 mg, 0.12 mmol) were added to a stirring solution of *N*,*N*-dimethyl-1-naphthylmethylamine **L3** (0.10 mmol) in dichloromethane (3 mL). The reaction mixture was then stirred at room temperature for 24 h. The crude reaction mixture was evaporated to dryness and purified by column chromatography on silica gel with dichloromethane as the eluent.

(1,2,3,4,5-Pentamethylcyclopentadienyl){(κ²-C,N)-(N,N-dimethylamino)methylnaphthyl}iridium(III) chloride, rac-7

Yield: 40 mg (73%); ^{1}H NMR (400 MHz, CD_2Cl_2): δ 1.65 (s, 15H, Cp(C*H*$_3$)), 2.96 (s, 3H, ArCH$_2$NMe(C*H*$_3$)), 3.11 (s, 3H, ArCH$_2$N(C*H*$_3$)Me), 3.99 (d, $^2J_{HH}$ = 13.1 Hz, 1H, ArC*H*HNMe$_2$), 4.48 (d, $^2J_{HH}$ = 13.0 Hz, 1H, ArCH*H*NMe$_2$), 7.24-7.84 (m, 6H, Ar*H*); ^{13}C NMR (100 MHz, CD_2Cl_2): δ 9.11 (C$_5$(*C*H$_3$)$_5$), 51.83 (N*C*H$_3$), 57.90 (N*C*H$_3$), 70.92 (Ar*C*H$_2$N), 87.85 (*C*$_5$(CH$_3$)$_5$), 122.56 (aromatic carbon), 123.18 (aromatic carbon), 124.74 (aromatic carbon), 125.06 (aromatic carbon), 128.09 (aromatic carbon), 129.82 (aromatic carbon), 130.72 (aromatic carbon), 134.48 (aromatic carbon), 141.10 (aromatic carbon), 150.86 (aromatic carbon); HRMS (ESI) *m*/*z* [*negative mode*] calcd for $C_{23}H_{29}ClIrN$ 547.1618, found 547.1608; Anal. calcd for $C_{23}H_{29}ClIrN$: C, 50.49; H, 5.34; N, 2.56. Found: C, 50.52; H, 5.15; N, 2.59.

2.4 The Iridation Reaction of (*R*)-*N*,*N*-Dimethyl-1-phenylethylamine (*R*)-L4

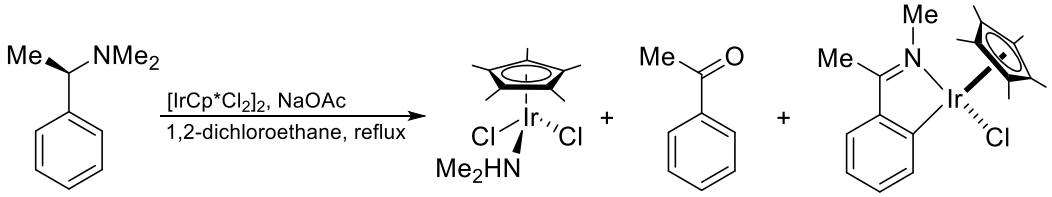

$[IrCp^*Cl_2]_2$ (100 mg, 0.125 mmol) and NaOAc (41 mg, 0.50 mmol) were added to a stirring solution of (*R*)-*N*,*N*-dimethyl-1-phenylethylamine (*R*)-**L4** (50 mg, 0.25 mmol) in 1,2-dichloroethane (5 mL). The reaction mixture was then reflux for 2 days. The crude reaction mixture was evaporated to dryness and purified directly by column chromatography on silica gel with hexane/ethyl acetate as the eluent.

Dichloro(dimethylamino)-1,2,3,4,5-pentamethylcyclopentadienyl iridium(III), 3

Yield: 18.8 mg (17%); ^{1}H NMR (400 MHz, $CDCl_3$): δ 1.64 (s, 15H, Cp(C*H*$_3$)), 2.89 (d, $^3J_{HH}$ = 5.4 Hz, 6H, HN(C*H*$_3$)$_2$), 3.90 (br s, 1H, *H*N(CH$_3$)$_2$); ^{13}C NMR (100 MHz, $CDCl_3$): δ 9.20 (C$_5$(*C*H$_3$)$_5$), 43.94 (N*C*H$_3$), 84.76 (*C*$_5$(CH$_3$)$_5$); HRMS (ESI) *m*/*z* [*negative mode*] calcd for $C_{12}H_{22}ClIrN$ 443.0759, found 443.0747.

Acetophenone, 8

Yield: 12.3 mg (41%); ^{1}H NMR (400 MHz, $CDCl_3$): δ 2.61 (s, 3H, C*H*$_3$), 7.44-7.97 (m, 5H, Ar*H*); ^{13}C NMR (100 MHz, $CDCl_3$): δ 26.57 (C(=O)*C*H$_3$), 128.27 (aromatic carbon), 128.54 (aromatic carbon), 133.07 (aromatic carbon), 137.12 (aromatic carbon), 198.12 (*C*(=O)*C*H$_3$); HRMS (ESI) *m*/*z* [(M+H)]$^+$ calcd for C_8H_8O 121.0653, found 121.0649; Anal. calcd for C_8H_8O: C, 79.97; H, 6.71. Found: C, 80.13; H, 6.78.

(1,2,3,4,5-Pentamethylcyclopentadienyl){(κ^2-C,N)-1-[1-(N-methylimino)ethyl]phenyl}-iridium(III) chloride, rac-9

Yield: 16.1 mg (13%); ^{1}H NMR (400 MHz, $CDCl_3$): δ 1.67 (s, 15H, Cp(C*H*$_3$)), 2.51 (s, 3H, Ar(CN)C*H*$_3$), 3.84 (s, 3H, N(C*H*$_3$)), 6.95-7.76 (m, 4H, Ar*H*); ^{13}C NMR (100 MHz, $CDCl_3$): δ 8.99 (C_5(*C*H$_3$)$_5$), 14.65 (C(=N)*C*H$_3$), 45.09 (N*C*H$_3$), 88.67 (*C*$_5$(CH$_3$)$_5$), 121.07 (aromatic carbon), 127.34 (aromatic carbon), 130.77 (aromatic carbon), 135.10 (aromatic carbon), 148.18 (aromatic carbon), 167.89 (aromatic carbon), 180.04 (Ar*C*(=N)CH$_3$); HRMS (ESI) *m*/*z* [*negative mode*] calcd for $C_{19}H_{25}ClIrN$ 495.1305, found 495.1292; Anal. calcd for $C_{19}H_{25}ClIrN$: C, 46.10; H, 5.09; N, 2.83. Found: C, 45.62; H, 5.38; N, 2.83.

3 CHAPTER 3: STEREOGENIC LOCK IN CYCLOIRIDATED COMPLEXES

3.1 General Procedure to the Cycloiridation of 1-Arylalkylamines

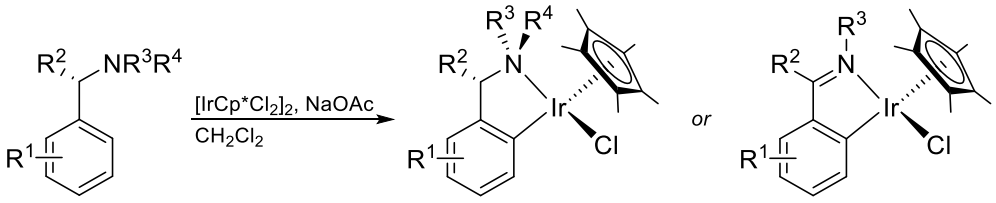

$[IrCp^*Cl_2]_2$ (40 mg, 0.05 mmol) and NaOAc (10 mg, 0.12 mmol) were added to a stirring solution of 1-arylalkylamine (0.10 mmol) in dichloromethane (3 mL). The reaction mixture was then stirred at room temperature until full conversion or over three days, whichever is shorter. The crude reaction mixture was evaporated to dryness and purified by column chromatography on silica gel with hexane/ethyl acetate as the eluent.

(S_C,S_N,R_{Ir})-(1,2,3,4,5-Pentamethylcyclopentadienyl){(κ^2-C,N)-1-[1-(N-methylamino)-ethyl]naphthyl}iridium(III) chloride, (S_C,S_N,R_{Ir})-1

Yield: 53 mg (97%); $[\alpha]_D$ (22 °C, *c* 0.5) = +102.1°; ^{1}H NMR (400 MHz, CD_2Cl_2): δ 1.24 (d, $^3J_{HH}$ = 6.5 Hz, 3H, ArCH(C*H*$_3$)), 1.67 (s, 15H, Cp(C*H*$_3$)), 3.02 (d, $^3J_{HH}$ = 6.4 Hz, 3H, NH(C*H*$_3$)), 4.69 (dq, $^3J_{HH}$ = 4.2 Hz and 6.4 Hz, 1H, ArC*H*(CH$_3$)), 5.02 (br s, 1H, N*H*(CH$_3$)), 7.20-7.74 (m, 6H, Ar*H*); ^{13}C NMR (100 MHz, CD_2Cl_2): δ 9.36 (C_5(*C*H$_3$)$_5$), 17.39 (ArCH(*C*H$_3$)N), 39.57 (N*C*H$_3$), 66.89 (Ar*C*H(CH$_3$)N), 87.35 (*C*$_5$(CH$_3$)$_5$), 122.66 (aromatic carbon), 123.41 (aromatic carbon), 125.41 (aromatic carbon), 126.05 (aromatic carbon), 127.92 (aromatic carbon), 128.38 (aromatic carbon), 131.07 (aromatic carbon), 136.07 (aromatic carbon), 144.65 (aromatic carbon), 153.10 (aromatic carbon); HRMS (ESI) *m*/*z* [*negative mode*] calcd for $C_{23}H_{29}ClIrN$ 547.1618, found 547.1619; Anal. calcd for $C_{23}H_{29}ClIrN$: C, 50.49; H, 5.34; N, 2.56. Found: C, 50.02; H, 5.56; N, 2.31.

***rac*-1,2,3,4,5-pentamethylcyclopentadienyl-(κ^2-*C*,*N*)-1-[1-(*N*-methylimino)ethyl]phenyl-iridium(III) chloride, *rac*-9**

Yield: 21 mg (42%); ^{1}H NMR (400 MHz, $CDCl_3$): δ 1.67 (s, 15H, Cp(C*H*$_3$)), 2.51 (s, 3H, Ar(CN)C*H*$_3$), 3.84 (s, 3H, N(C*H*$_3$)), 6.95-7.76 (m, 4H, Ar*H*); ^{13}C NMR (100 MHz, $CDCl_3$): δ 8.99 (C_5(*C*H$_3$)$_5$), 14.65 (C(=N)*C*H$_3$), 45.09 (N*C*H$_3$), 88.67 (*C*$_5$(CH$_3$)$_5$), 121.07 (aromatic carbon), 127.34 (aromatic carbon), 130.77 (aromatic carbon), 135.10 (aromatic carbon), 148.18 (aromatic carbon), 167.89 (aromatic carbon), 180.04 (Ar*C*(=N)CH$_3$); HRMS (ESI) *m*/*z* [*negative mode*] calcd for $C_{19}H_{25}ClIrN$ 495.1305, found 495.1292; Anal. calcd for $C_{19}H_{25}ClIrN$: C, 46.10; H, 5.09; N, 2.83. Found: C, 45.62; H, 5.38; N, 2.83.

***(S*$_C$,*R*$_{Ir}$)-(1,2,3,4,5-Pentamethylcyclopentadienyl){(κ^2-*C*,*N*)-1-[1-aminoethyl]naphthyl}-iridium(III) chloride, (*S*$_C$,*R*$_{Ir}$)-11**

Yield: 48 mg (90%); [α]$_D$ (22 °C, *c* 0.5) = +110.3°; ^{1}H NMR (400 MHz, CD_2Cl_2): 1.32 (d, $^3J_{HH}$ = 6.6 Hz, 3H, ArCH(C*H*$_3$)), 1.74 (s, 15H, Cp(C*H*$_3$)), 3.70 (br s, 1H, N*H*), 4.78 (br s, 1H, N*H*), 5.06 (m, 1H, ArC*H*(CH$_3$)), 7.21-7.74 (m, 6H, Ar*H*); ^{13}C NMR (100 MHz, CD_2Cl_2): δ 10.77 (C_5(*C*H$_3$)$_5$), 23.95 (ArC(*C*H$_3$)N), 60.92 (Ar*C*(CH$_3$)N), 88.44 (*C*$_5$(CH$_3$)$_5$), 124.08 (aromatic carbon), 124.93 (aromatic carbon), 126.82 (aromatic carbon), 127.39 (aromatic carbon), 129.61 (aromatic carbon), 129.82 (aromatic carbon), 132.59 (aromatic carbon), 137.72 (aromatic carbon), 147.15 (aromatic carbon), 155.07 (aromatic carbon); HRMS (ESI) *m*/*z* [*negative mode*] calcd for $C_{22}H_{27}ClIrN$ 533.1461, found 533.1456; Anal. calcd for $C_{22}H_{27}ClIrN$: C, 49.56; H, 5.10; N, 2.63. Found: C, 49.46; H, 5.29; N, 2.79.

***rac*-1,2,3,4,5-Pentamethylcyclopentadienyl-(κ^2-*C*,*N*)-1-[(*N*-methylamino)methyl]naphthyliridium(III) chloride, *rac*-13**

Yield: 17 mg (31%); ^{1}H NMR (400 MHz, CD_2Cl_2): δ 1.58 (s, 15H, Cp(C*H*$_3$)), 3.08 (d, $^3J_{HH}$ = 6.3 Hz, 3H, N(C*H*$_3$)), 3.89 (m, 1H, ArCH*H*), 4.34 (br s, 1H, N*H*), 4.71 (dd, $^3J_{HH}$ = 13.3 Hz, $^2J_{HH}$ = 4.28 Hz, 1H, ArC*H*H), 7.14-7.68 (m, 6H, Ar*H*); ^{13}C NMR (100 MHz, CD_2Cl_2): δ 9.17 (C_5(*C*H$_3$)$_5$), 43.21 (N*C*H$_3$), 63.95 (Ar*C*H$_2$N), 87.17 (*C*$_5$(CH$_3$)$_5$), 122.72 (aromatic carbon), 123.44 (aromatic carbon), 125.35 (aromatic carbon), 126.07 (aromatic carbon), 128.23 (aromatic carbon), 128.60 (aromatic carbon), 130.85 (aromatic carbon), 135.95 (aromatic carbon), 138.58 (aromatic carbon), 156.07(aromatic carbon).

rac-1,2,3,4,5-Pentamethylcyclopentadienyl-(κ²-C,N)-1-[(N-methylimino)methyl]naphthyliridium(III) chloride, rac-14

Yield: 32 mg (61%) (*heating to 60 °C in 1,2-dichloroethane required*), 16 mg (94%) (*from stirring complex rac-**13** at room temperature in open environment*); ^{1}H NMR (400 MHz, CD_2Cl_2): δ 1.76 (s, 15H, Cp(C*H*$_3$)), 3.99 (s, 3H, N(C*H*$_3$)), 7.32-8.10 (m, 6H, Ar*H*), 9.07 (s, 1H, *H*C(=N)); ^{13}C NMR (100 MHz, CD_2Cl_2): δ 9.05 ($C_5(CH_3)_5$), 49.71 (NCH_3), 89.57 ($C_5(CH_3)_5$), 121.79 (aromatic carbon), 123.35 (aromatic carbon), 126.87 (aromatic carbon), 128.82 (aromatic carbon), 129.95 (aromatic carbon), 130.55 (aromatic carbon), 132.81 (aromatic carbon), 134.33 (aromatic carbon), 139.61 (aromatic carbon), 171.64 (H*C*(=N)Ar), 174.53 (aromatic carbon); HRMS (ESI) *m*/*z* [*negative mode*] calcd for $C_{22}H_{25}ClIrN$ 531.1305, found 531.1297; Anal. calcd for $C_{22}H_{25}ClIrN$: C, 49.75; H, 4.74; N, 2.64. Found: C, 49.59; H, 5.21; N, 2.91.

3.2 Iridation of (*R*)-1-Phenylethylamine (*R*)-L7

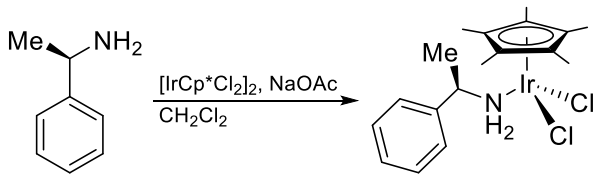

$[IrCp^*Cl_2]_2$ (40 mg, 0.05 mmol) and NaOAc (10 mg, 0.12 mmol) were added to a stirring solution of 1-phenylethylamine (12 mg, 0.10 mmol) in dichloromethane (3 mL). The reaction mixture was then stirred at room temperature for 16 h. The crude reaction mixture was evaporated to dryness and purified by column chromatography on silica gel with hexane/ethyl acetate as the eluent.

(R)-1,2,3,4,5-Pentamethylcyclopentadienyl-1-(1-aminoethyl)phenyliridium(III) chloride, (R)-12

Yield: 47 mg (90%); ^{1}H NMR (400 MHz, $CDCl_3$): δ 1.58 (d, 3H, ArCH(C*H*$_3$)), 1.60 (s, 15H, Cp(C*H*$_3$)), 3.96 (br s, 1H, N*H*H), 4.03 (br s, 1H, NH*H*), 4.36 (m, 1H, ArC*H*(CH_3)), 7.32-7.40 (m, 5H, Ar*H*); ^{13}C NMR (100 MHz, $CDCl_3$): δ 9.18 (C_5(*C*H_3)$_5$), 23.95 (ArC(*C*H_3)N), 55.85 (Ar*C*(CH_3)N), 85.02 (*C*$_5$(CH_3)$_5$), 126.09 (aromatic carbon), 128.32 (aromatic carbon), 129.18 (aromatic carbon), 143.05 (aromatic carbon).

3.3 Procedure for the Determination of Stereostability at Nitrogen

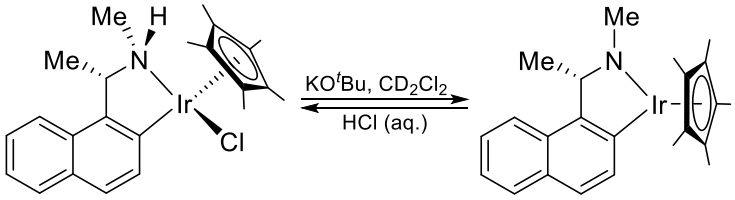

KO^{t}Bu (3.4 mg, 0.03 mmol) was added to a stirring mixture of complex (S_C,S_N,R_{Ir})-**1** (11 mg, 0.02 mmol) in d_2-dichloromethane (1.5 mL). The reaction mixture was stirred at room temperature for 24 h. The crude reaction mixture was then filtered and characterized by ^{1}H NMR spectroscopy. Dilute aqueous HCl (1 M, 1.5 mL) was added to the dark red solution and left to stir for 1 h. The organic phase of biphasic solution was collected and the aqueous partition was further extracted with dichloromethane. The organic extracts were then combined, dried over anhydrous $MgSO_4$, filtered and evaporated to dryness affording orange powder.

(S)-1,2,3,4,5-pentamethylcyclopentadienyl-(κ^2-C,N)-1-[1-(N-methylamido)ethyl]naphthyliridium(III) complex, (S)-15

^{1}H NMR (400 MHz, CD_2Cl_2): δ 1.45 (d, $^3J_{HH}$ = 6.4 Hz, ArCH(CH_3), 1.94 (s, 15H, Cp(CH_3)), 2.80 (q, $^3J_{HH}$ = 6.4 Hz, ArCH(CH$_3$)), 3.48 (d, $^4J_{HH}$ = 0.6 Hz, 3H, N(CH_3)), 7.19-8.19 (m, 6H, ArH); ^{13}C NMR (100 MHz, CD_2Cl_2): δ 10.00 (C_5(CH$_3$)$_5$), 19.96 (ArCH(CH$_3$)N), 54.57 (NCH$_3$), 82.01 (ArCH(CH$_3$)N), 87.57 (C_5(CH$_3$)$_5$), 122.65 (aromatic carbon), 124.12 (aromatic carbon), 124.78 (aromatic carbon), 124.89 (aromatic carbon), 127.46 (aromatic carbon), 128.25 (aromatic carbon), 130.89 (aromatic carbon), 135.10 (aromatic carbon), 155.37 (aromatic carbon), 160.26 (aromatic carbon).

3.4 Procedure for the Determination of Stereostability at Iridium

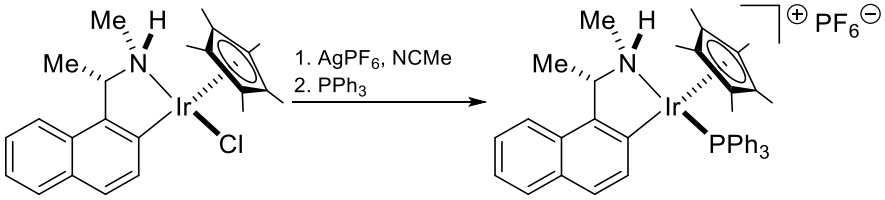

$AgPF_6$ (7.6 mg, 0.03 mmol) was added to a stirring acetonitrile solution (3 mL) of complex (S_C,S_N,R_{Ir})-**1** (11 mg, 0.02 mmol) in the dark. The reaction mixture was stirred at room temperature for 1 h. PPh_3 (5.2 mg, 0.02 mmol) was subsequently added to the reaction mixture and left to stir for another 2 h. The crude mixture was filtered over Celite®, evaporated to dryness and recrystallized from a solvent mixture of hexane and ethyl acetate.

1,2,3,4,5-Pentamethylcyclopentadienyl-{(κ²-C,N)-1-[1-(N-methylamino)ethyl]naphth-yl}(triphenylphosphino)iridium(III) hexafluorophosphate, rac-16

Yield: 9.7 mg (53%) (*recrystallized*); ^{1}H NMR (400 MHz, $CDCl_3$): δ 1.14 (d, $^3J_{HH}$ = 6.6 Hz, 3H, ArCH(C*H*$_3$)), 1.65 (d, 15H, Cp(C*H*$_3$)), 2.94 (d, $^3J_{HH}$ = 6.3 Hz, 3H, NH(C*H*$_3$)), 3.92 (m, 1H, ArC*H*(CH$_3$)), 4.38 (br s, 1H, N*H*(CH$_3$)), 7.11-7.74 (m, 21H, Ar*H*); ^{13}C NMR (100 MHz, $CDCl_3$): δ 9.48 (C$_5$(*C*H$_3$)$_5$), 16.83 (ArCH(*C*H$_3$)N), 41.15 (N*C*H3), 68.86 (Ar*C*H(CH$_3$)N), 96.15 (d, (*C*$_5$(CH$_3$)$_5$)), 123.47 (aromatic carbon), 123.99 (aromatic carbon), 126.32 (aromatic carbon), 126.54 (aromatic carbon), 128.27 (aromatic carbon), 128.49 (aromatic carbon), 128.92 (d, $^1J_{CP}$ = 10.2 Hz, aromatic carbon), 131.20 (aromatic carbon), 132.01 (aromatic carbon), 133.93 (br s, aromatic carbon), 134.44 (d, $^4J_{CP}$ = 2.4 Hz, aromatic carbon), 136.79 (aromatic carbon), 136.91 (aromatic carbon), 146.69 (aromatic carbon); ^{31}P{^{1}H} NMR (161 MHz, $CDCl_3$): δ –144.32 (sep, *P*F_6^-), 16.03 (s, *P*Ph$_3$); HRMS (ESI) *m*/*z* [*negative mode*] calcd for $C_{41}H_{44}F_6IrNP_2$ 919.2483, found 919.2482; Anal. calcd for $C_{41}H_{44}F_6IrNP_2$: C, 53.59; H, 4.83; N, 1.52. Found: C, 53.39; H, 4.78; N, 1.29.

3.5 General Procedure for Catalytic Asymmetric Hydrogen Transfer Reactions

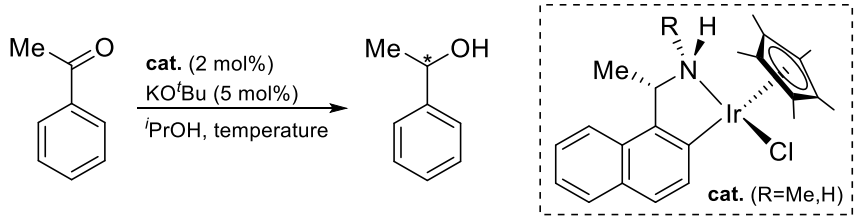

Acetophenone (58.3 μL, 60 mg, 0.5 mmol), 1,4-dimethoxybenzene (69 mg, 0.5 mmol) and KO^{t}Bu (2.8 mg, 0.025 mmol) was added sequentially into a stirring solution of cycloiridated complex (0.01 mmol) in dry 2-propanol (10 mL) at the desired temperature. The reaction mixture was stirred at the temperature for the indicated time. The pale brown mixture was then diluted with water (10 mL), extracted with ethyl acetate (10 mL × 3), washed with brine (20 mL), dried over anhydrous $MgSO_4$, filtered and evaporated to dryness. The crude mixture was then purified by column chromatography on silica gel with hexane/ethyl acetate as the eluent to afford colourless oil.

1-Phenylethanol

^{1}H NMR (400 MHz, $CDCl_3$): δ 1.49 (d, $^3J_{HH}$ = 6.4 Hz, 3H, PhCH(C*H*$_3$)), 1.88 (d, $^3J_{HH}$ = 3.4 Hz, 1H, O*H*), 4.89 (dq, $^3J_{HH}$ = 3.3 Hz and 6.4 Hz, 1H, PhC*H*(CH_3)), 7.25-7.38 (m, 5H, Ar*H*); ^{13}C NMR (100 MHz, $CDCl_3$): δ 25.12 (PhCH(*C*H_3)(OH)), 70.39 (Ph*C*H(CH_3)(OH)), 125.35 (aromatic carbon), 127.45 (aromatic carbon), 128.48 (aromatic carbon), 145.78 (aromatic carbon); HRMS (ESI) *m*/*z* [*negative mode*] calcd for $C_8H_{10}O$ 112.0732, found 122.0726; Anal. calcd for $C_8H_{10}O$: C, 78.65; H, 8.25. Found: C, 78.69; H, 8.44.

APPENDICES

APPENDIX I

Nuclear Magnetic Resonance (NMR) Data

Nuclear magnetic resonance (NMR) spectroscopy were recorded at Nanyang Technological University Division of Chemistry and Biological Chemistry Central Facilities Laboratory on the Bruker Avance III 400 (BBFO 400) spectrometers at 400 MHz for ^{1}H NMR, 100 MHz for ^{13}C NMR and 161 MHz for $^{31}P\{^{1}H\}$ NMR. Chemical shifts (δ) are quoted in ppm, and referenced to chemical shifts of residual solvent peaks for ^{1}H and ^{13}C NMR. 85% H_3PO_4/D_2O mixture was utilized as the external standard for $^{31}P\{^{1}H\}$ NMR.

(1,2,3,4,5-Pentamethylcyclopentadienyl){(κ^2-*C*,*N*)-1-[1-(*N*-methylamino)ethyl]naphthyl}iridium(III) chloride

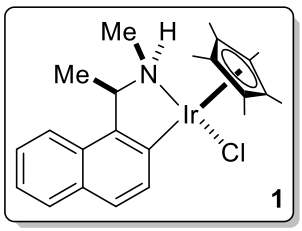

^{1}H NMR spectrum (400 MHz, CD_2Cl_2)

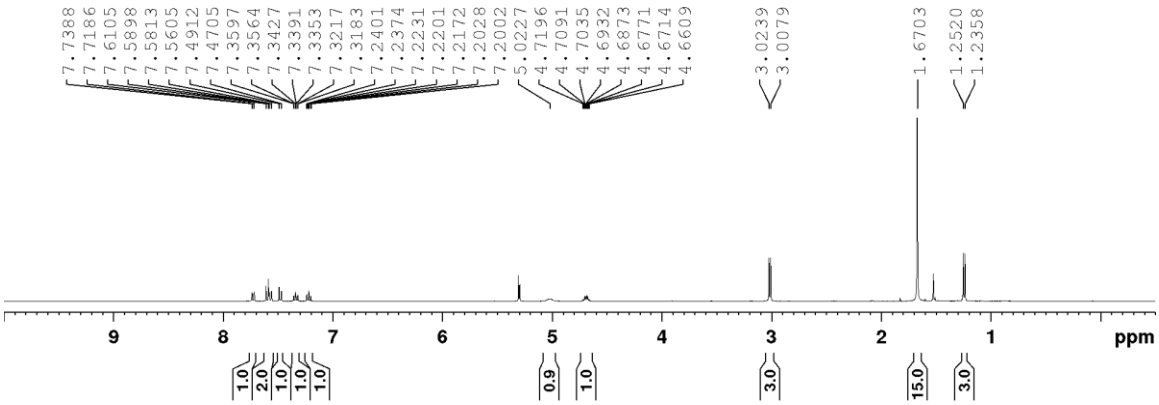

^{13}C NMR spectrum (100 MHz, CD_2Cl_2)

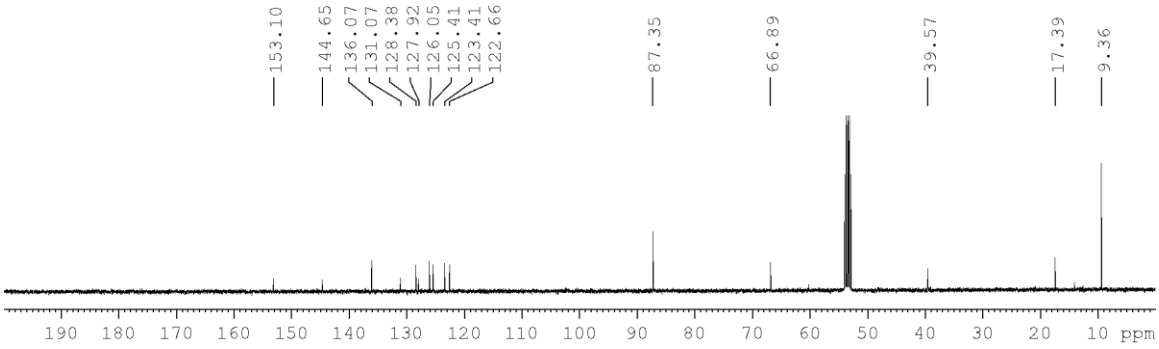

***d*$_1$-(1,2,3,4,5-Pentamethylcyclopentadienyl){(κ^2-*C*,*N*)-1-[1-(*N*-methylamino)ethyl]naphthyl}iridium(III) chloride**

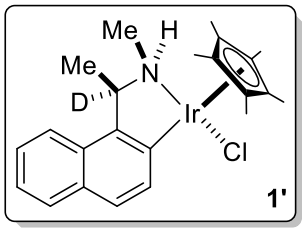

^{1}H NMR spectrum (400 MHz, CD_2Cl_2)

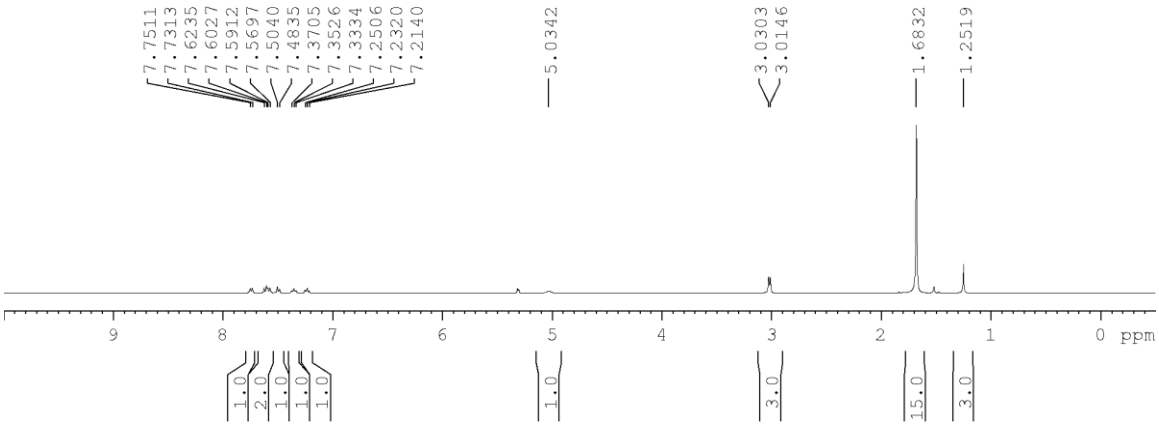

^{2}H NMR spectrum (400 MHz, CD_2Cl_2)

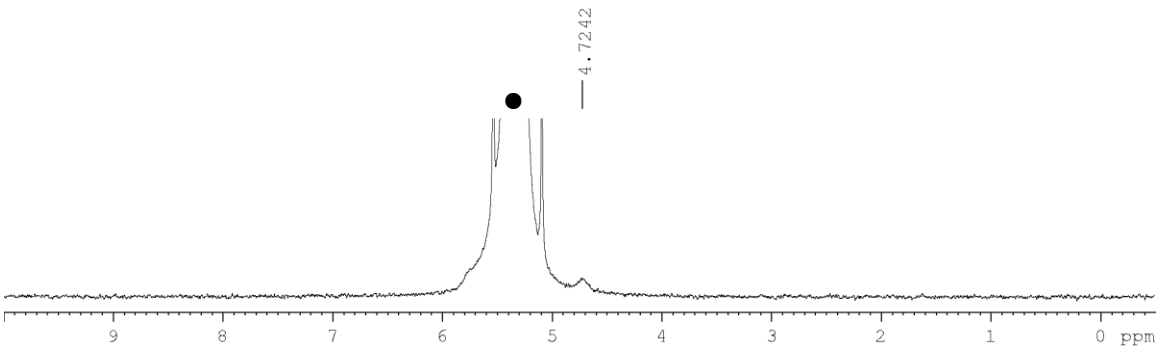

Note: The spectrum has been enlarged for clarity (● (*5.32 ppm*): *CD_2Cl_2*).

^{13}C NMR spectrum (100 MHz, CD_2Cl_2)

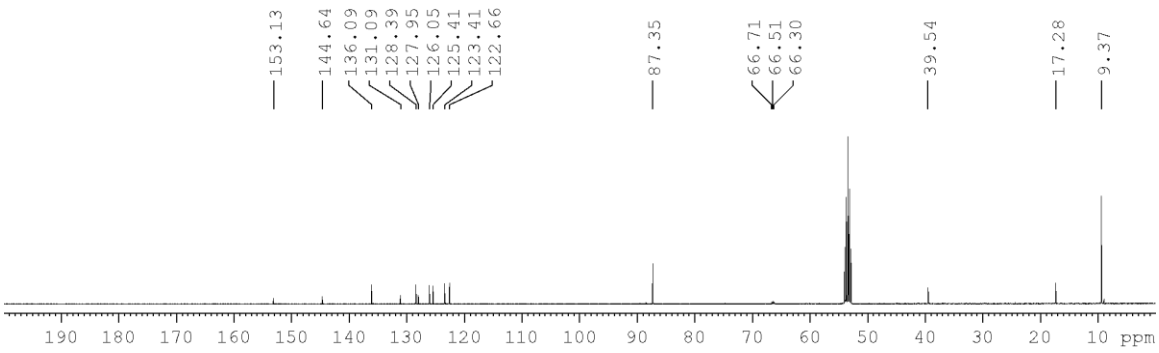

1-Acetonaphthone

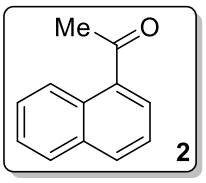

^{1}H NMR spectrum (400 MHz, $CDCl_3$)

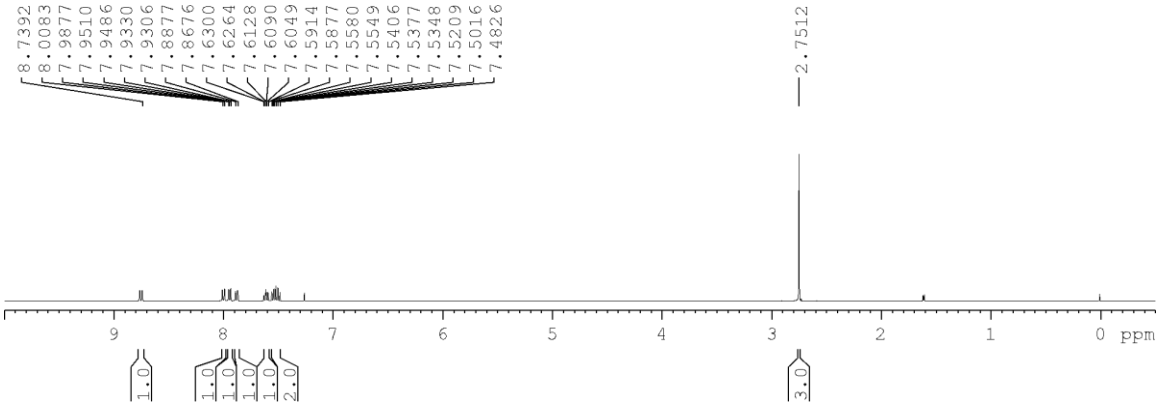

^{13}C NMR spectrum (100 MHz, $CDCl_3$)

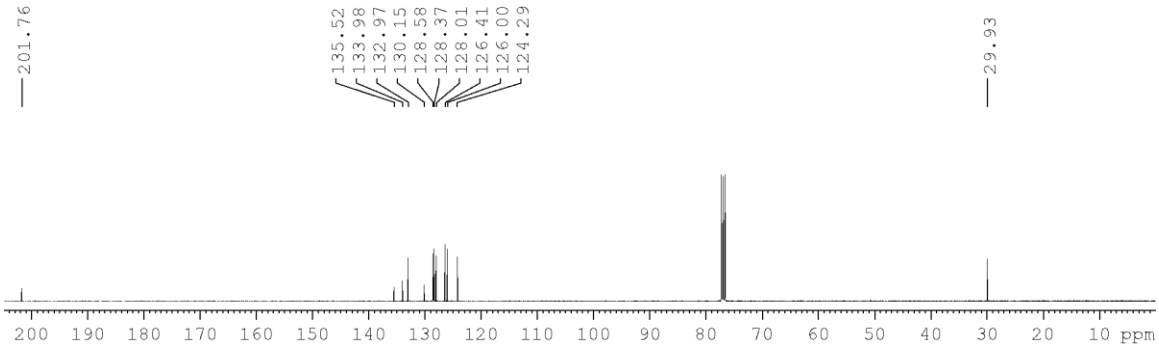

Dichloro(dimethylamino)-1,2,3,4,5-pentamethylcyclopentadienyl iridium(III)

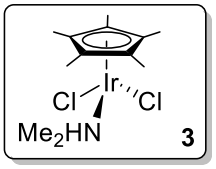

^{1}H NMR spectrum (400 MHz, $CDCl_3$)

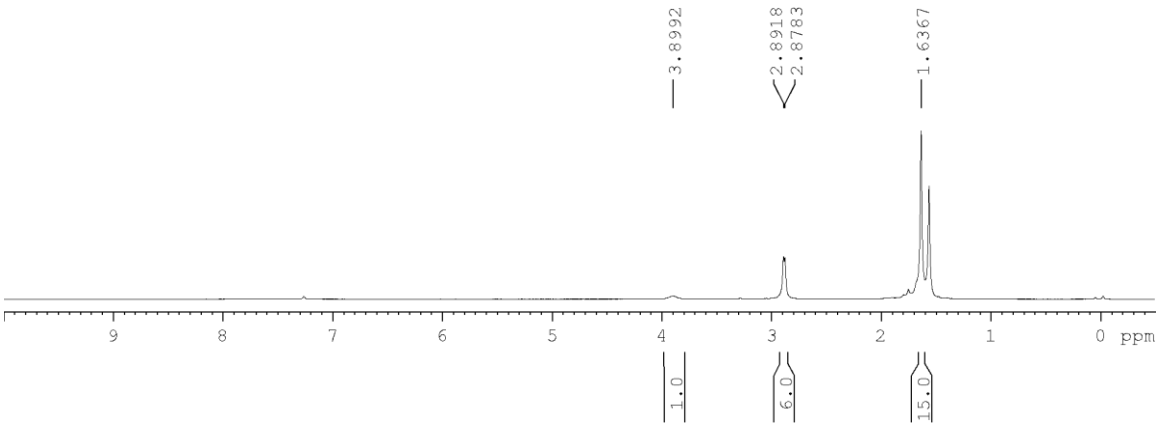

^{13}C NMR spectrum (100 MHz, $CDCl_3$)

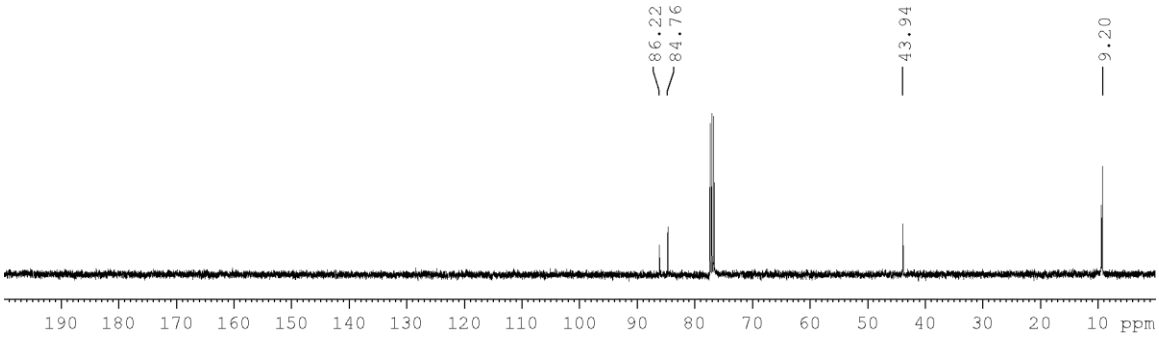

(1,2,3,4,5-Pentamethylcyclopentadienyl){(κ^2-*C*,*N*)-1-[1-(*N*-methylimino)ethyl]naphthyl}iridium(III) chloride

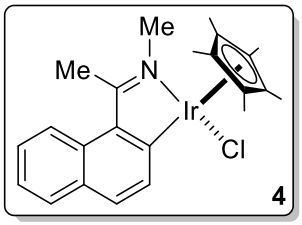

^{1}H NMR spectrum (400 MHz, $CDCl_3$)

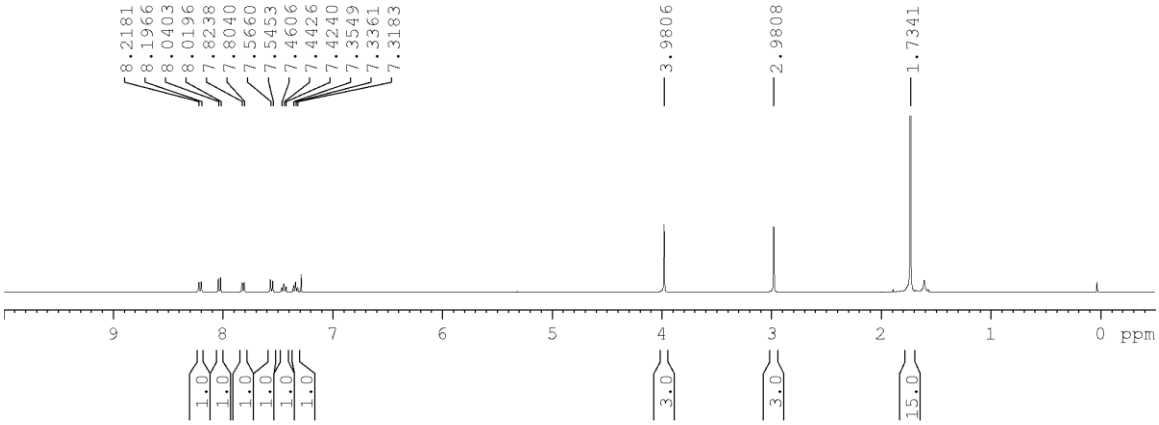

^{13}C NMR spectrum (100 MHz, $CDCl_3$)

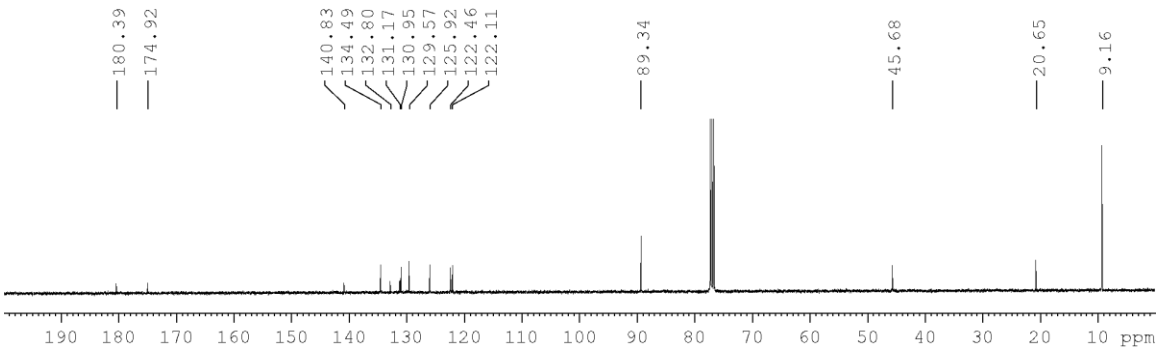

(1,2,3,4,5-Pentamethylcyclopentadienyl){(κ^2-*C*,[η^2-ethylene])-1-naphthylethene}iridium(III) chloride

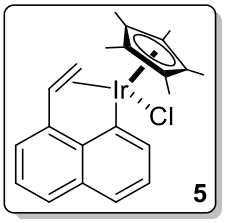

^{1}H NMR spectrum (400 MHz, $CDCl_3$)

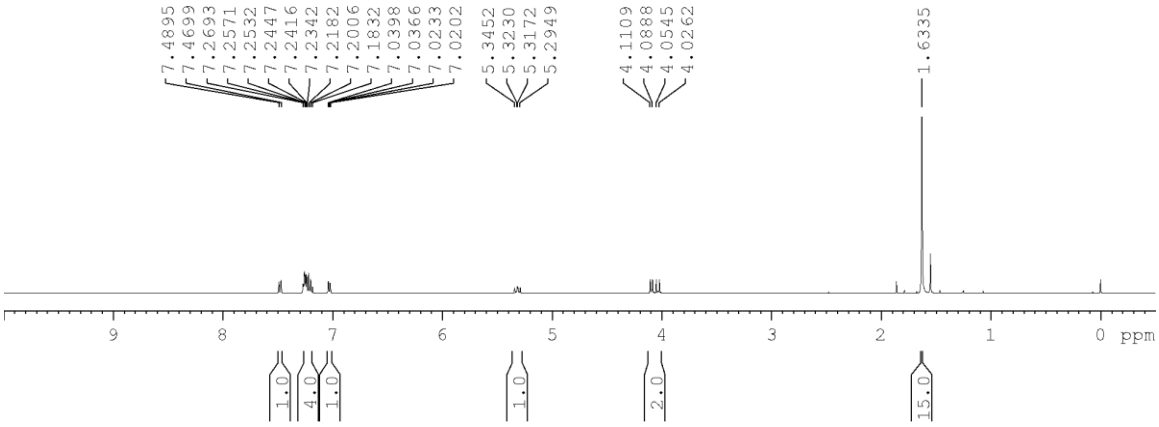

^{13}C NMR spectrum (100 MHz, $CDCl_3$)

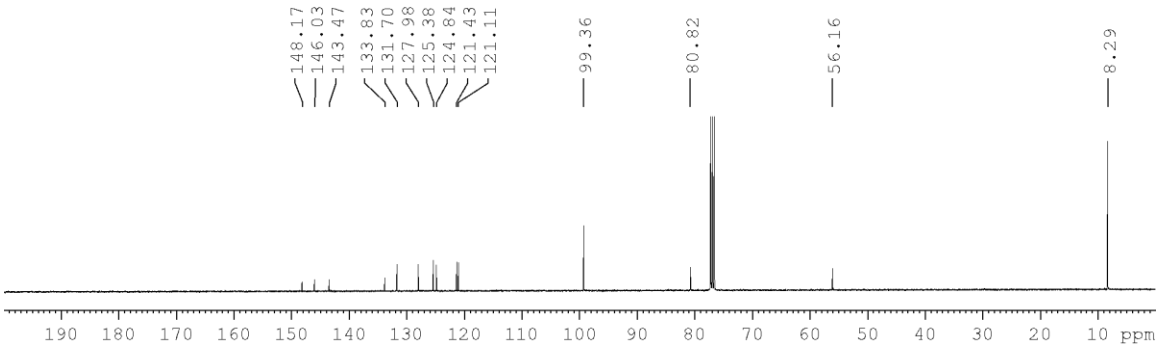

1-Ethylnaphthalene

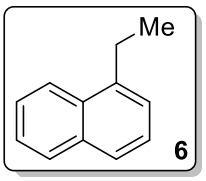

^{1}H NMR spectrum (400 MHz, $CDCl_3$)

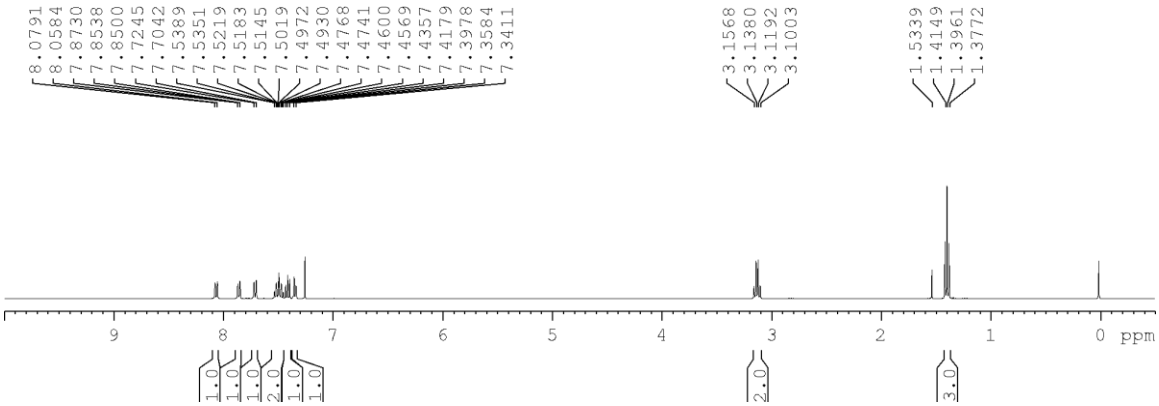

^{13}C NMR spectrum (100 MHz, $CDCl_3$)

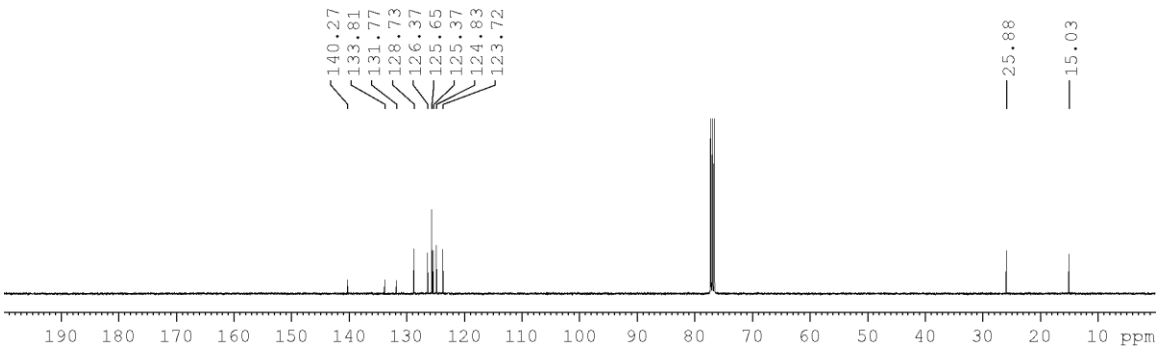

1-Ethylnaphthalene mixture

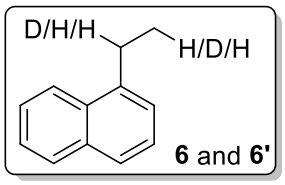

^{1}H NMR spectrum (400 MHz, $CDCl_3$)

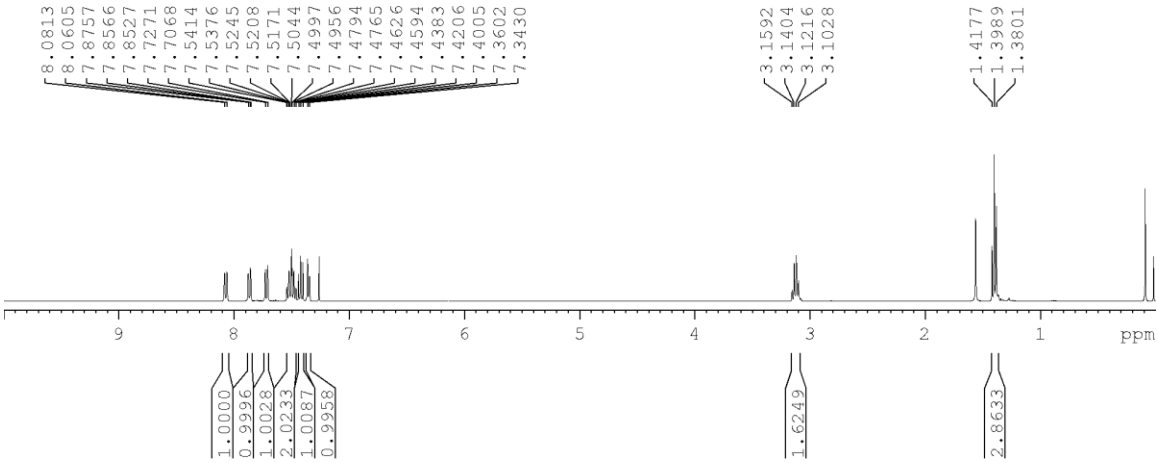

^{2}H NMR spectrum (400 MHz, $CDCl_3$)

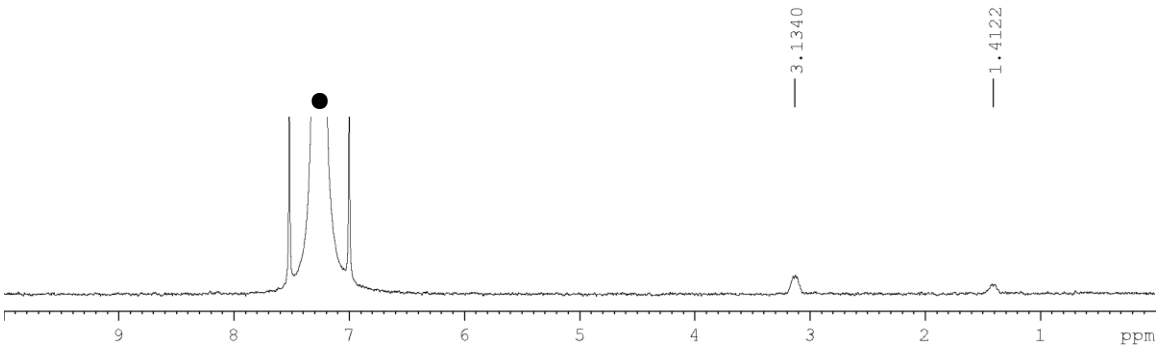

Note: The spectrum has been enlarged for clarity (● (*7.26 ppm*): *$CDCl_3$*).

^{13}C NMR spectrum (100 MHz, $CDCl_3$)

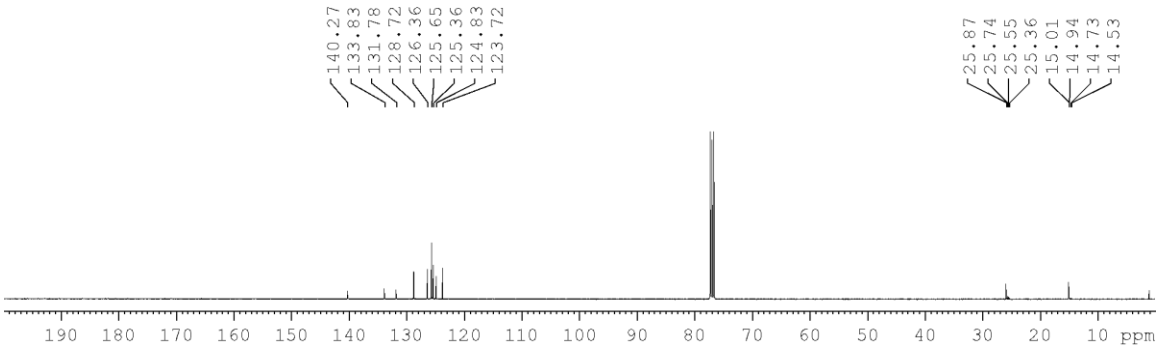

(1,2,3,4,5-Pentamethylcyclopentadienyl){(κ^2-*C*,*N*)-(*N*,*N*-dimethylamino)methylnaphthyl}iridium(III) chloride

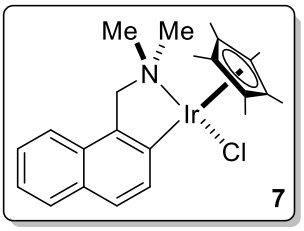

^{1}H NMR spectrum (400 MHz, CD_2Cl_2)

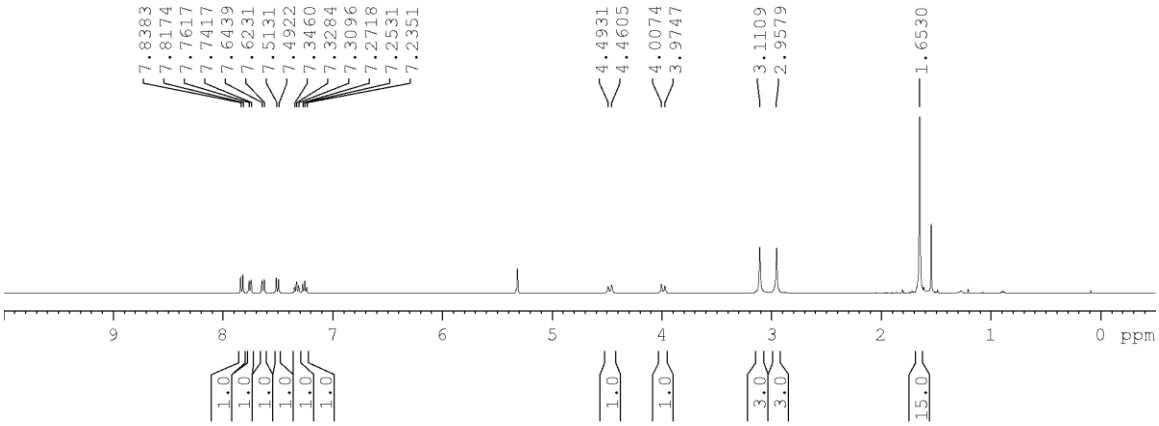

^{13}C NMR spectrum (100 MHz, CD_2Cl_2)

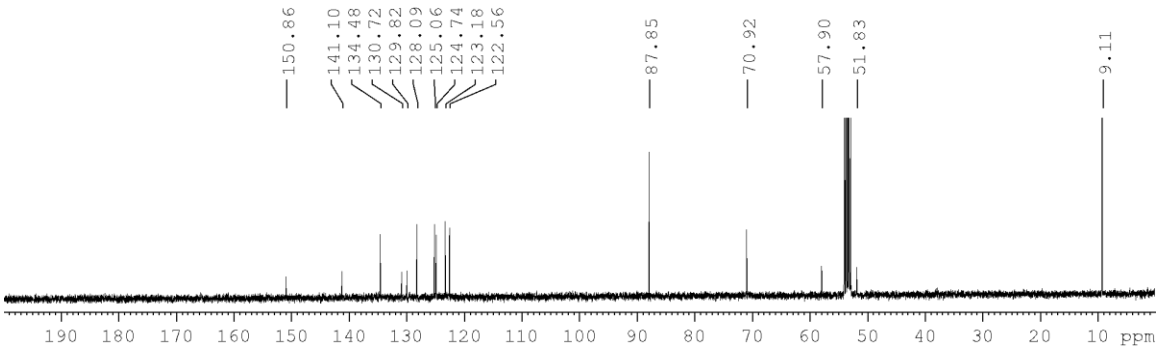

Acetophenone

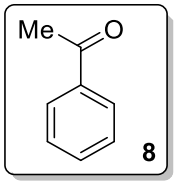

^{1}H NMR spectrum (400 MHz, $CDCl_3$)

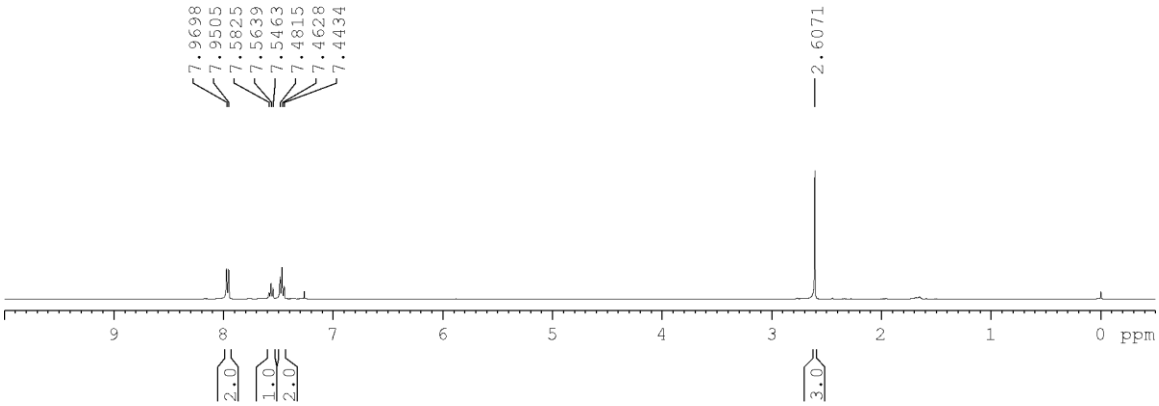

^{13}C NMR spectrum (100 MHz, $CDCl_3$)

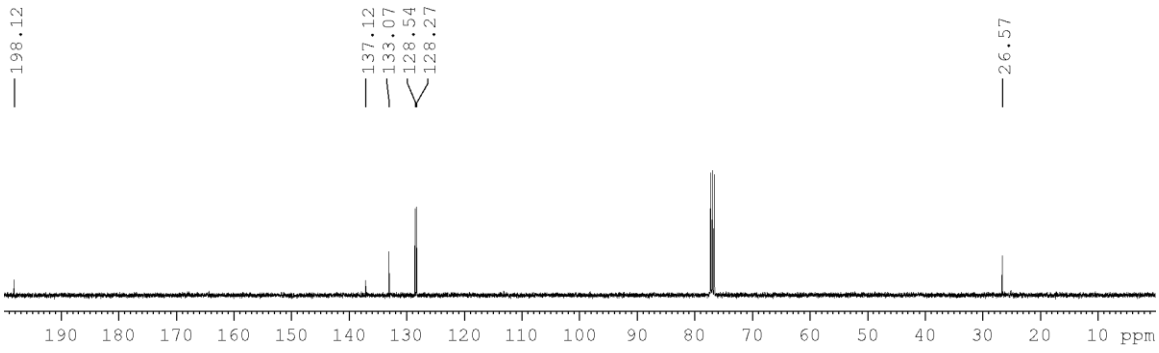

(1,2,3,4,5-Pentamethylcyclopentadienyl){(*κ*^{2}-*C*,*N*)-1-[1-(*N*-methylimino)ethyl]phenyl}iridium(III) chloride

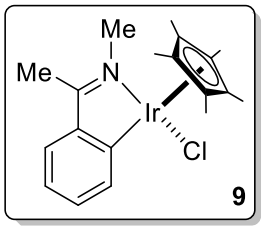

^{1}H NMR spectrum (400 MHz, CD_2Cl_2)

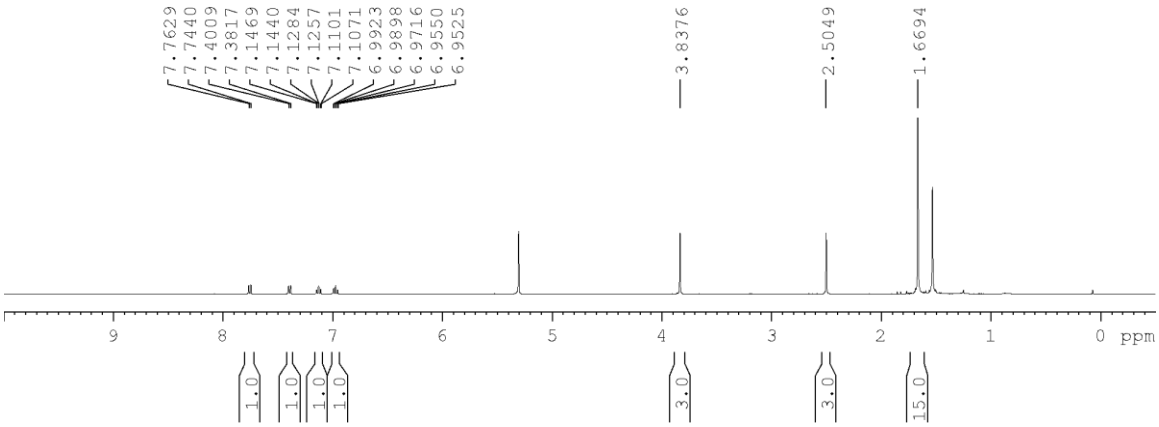

^{13}C NMR spectrum (100 MHz, CD_2Cl_2)

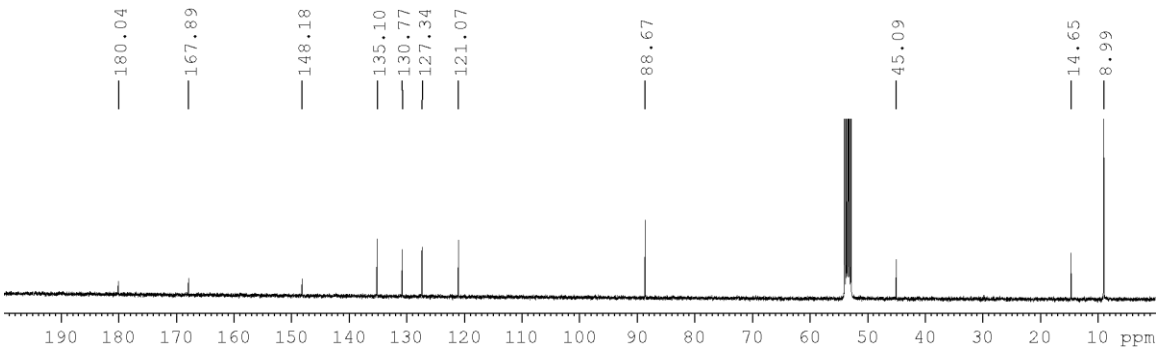

(1,2,3,4,5-Pentamethylcyclopentadienyl){(κ^2-*C*,*N*)-1-[1-aminoethyl]naphthyl}iridium(III) chloride

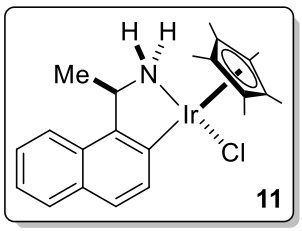

^{1}H NMR spectrum (400 MHz, CD_2Cl_2)

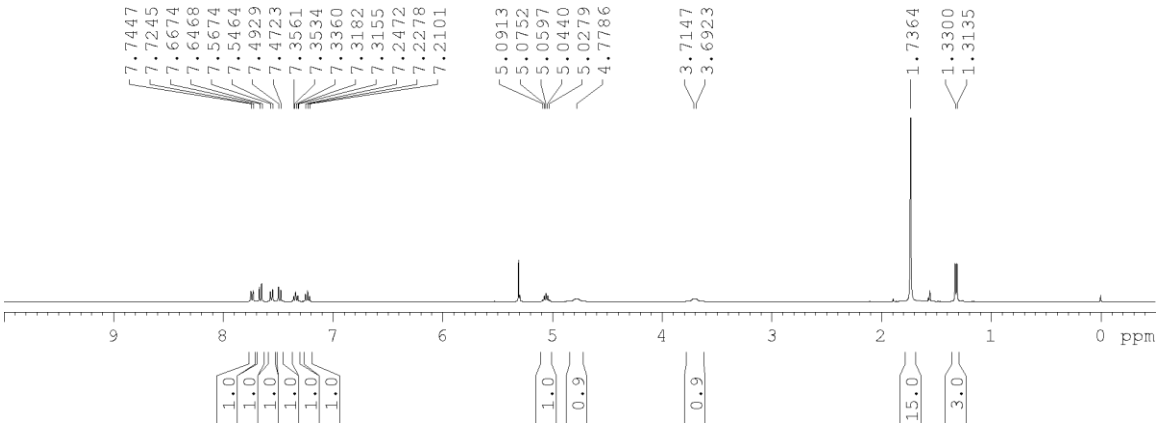

^{13}C NMR spectrum (100 MHz, CD_2Cl_2)

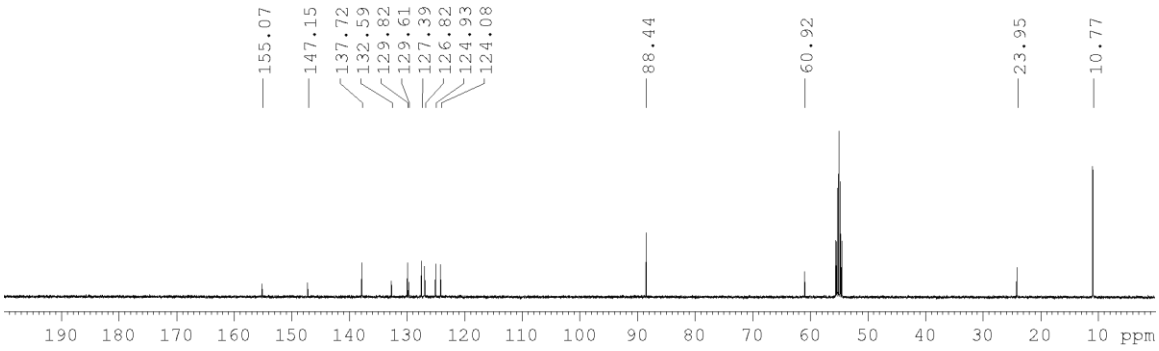

1,2,3,4,5-Pentamethylcyclopentadienyl-1-(1-aminoethyl)phenyliridium(III) chloride

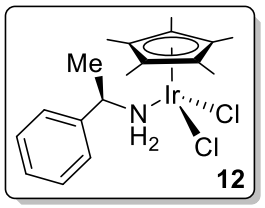

^{1}H NMR spectrum (400 MHz, $CDCl_3$)

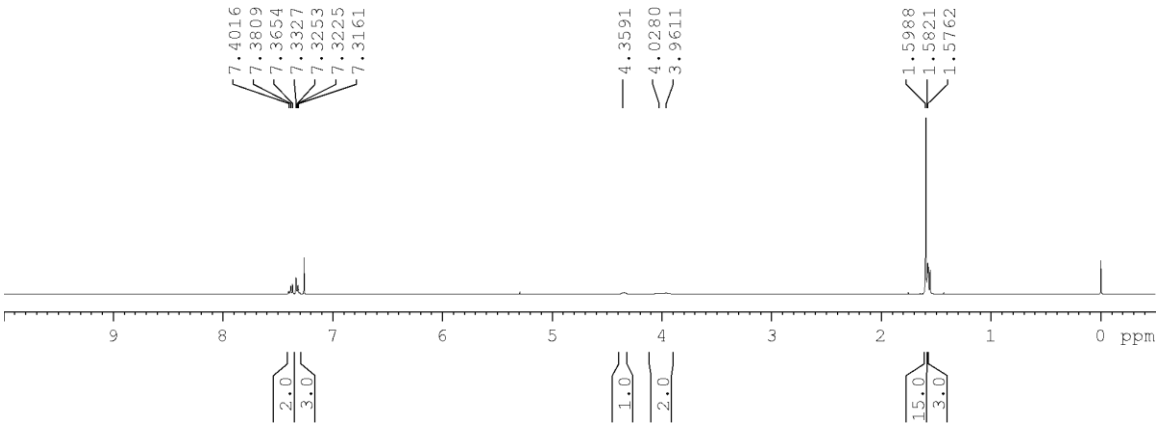

^{13}C NMR spectrum (100 MHz, $CDCl_3$)

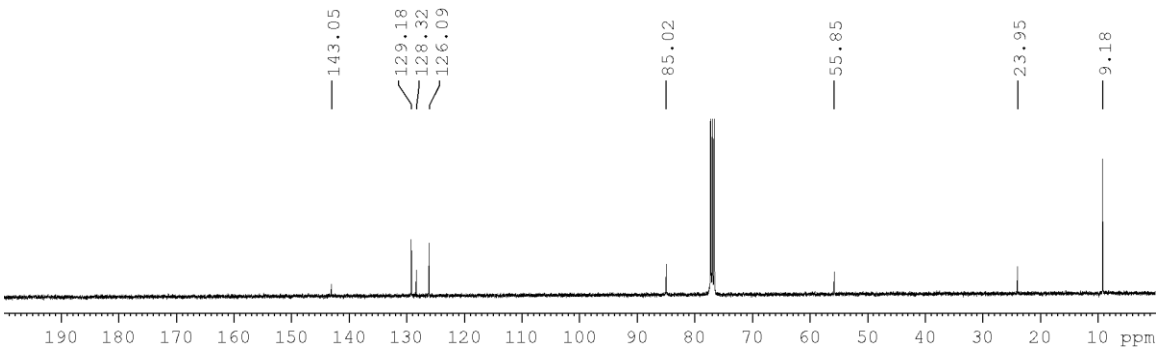

1,2,3,4,5-Pentamethylcyclopentadienyl-(κ^2-*C*,*N*)-1-[(*N*-methylamino)methyl]naphthyliridium(III) chloride

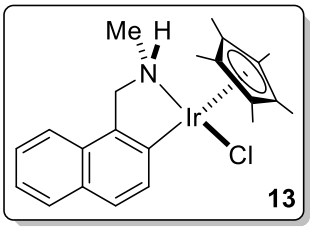

^{1}H NMR spectrum (400 MHz, CD_2Cl_2)

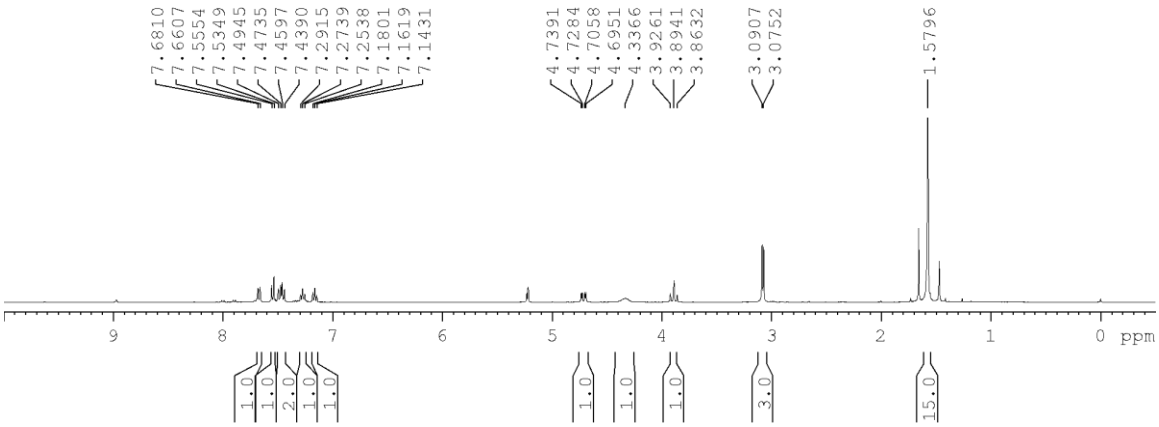

^{13}C NMR spectrum (100 MHz, CD_2Cl_2)

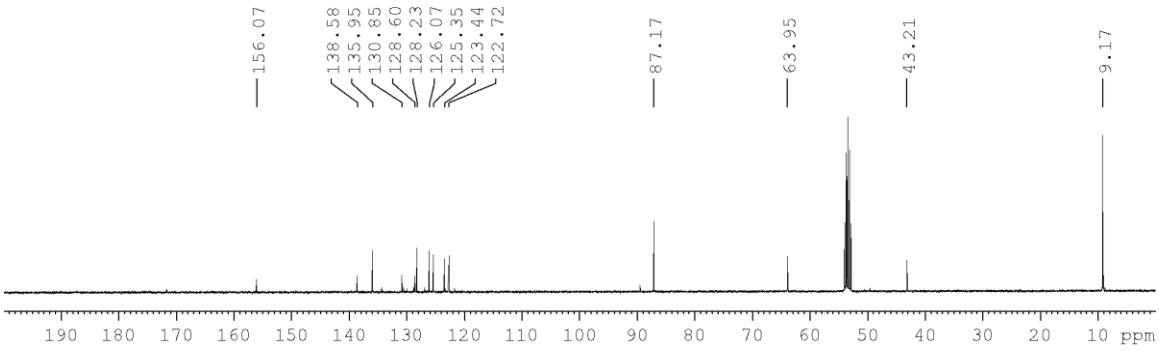

1,2,3,4,5-Pentamethylcyclopentadienyl-(κ^2-*C*,*N*)-1-[(*N*-methylimino)methyl]naphthyliridium(III) chloride

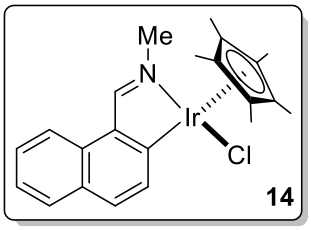

^{1}H NMR spectrum (400 MHz, CD_2Cl_2)

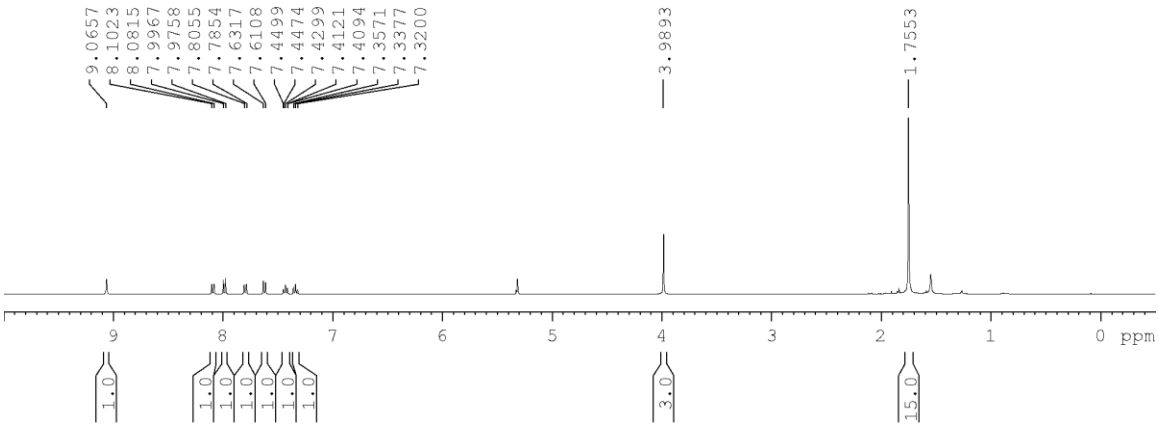

^{13}C NMR spectrum (100 MHz, CD_2Cl_2)

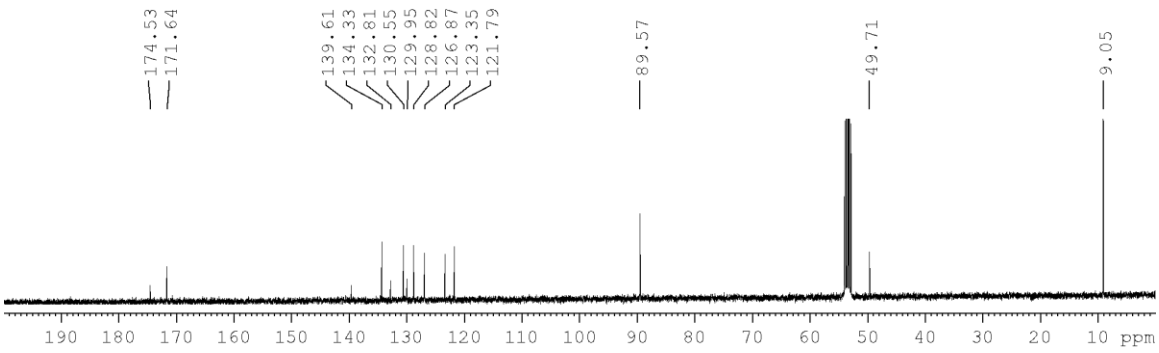

1,2,3,4,5-Pentamethylcyclopentadienyl-(κ^2-*C*,*N*)-1-[1-(*N*-methylamido)ethyl]naphthyliridium(III) complex,

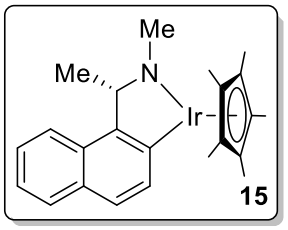

^{1}H NMR spectrum (400 MHz, CD_2Cl_2)

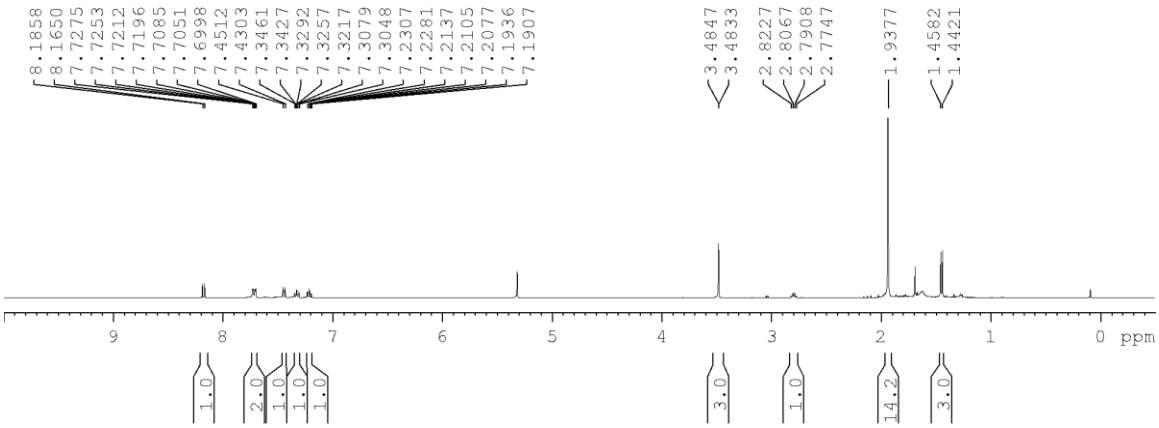

^{13}C NMR spectrum (100 MHz, CD_2Cl_2)

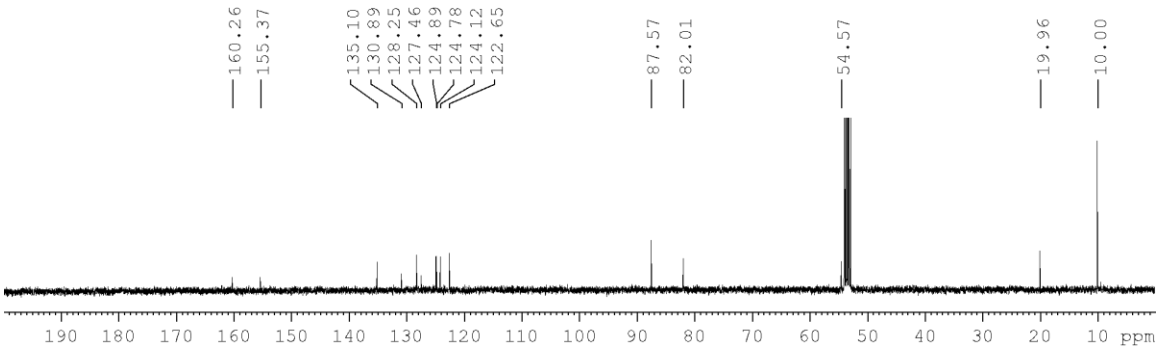

1,2,3,4,5-Pentamethylcyclopentadienyl-{(κ^2-*C*,*N*)-1-[1-(*N*-methylamino)ethyl]naphthyl}(triphenylphosphino)iridium(III) hexafluorophosphate

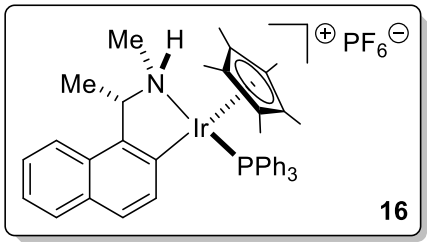

^{1}H NMR spectrum (400 MHz, $CDCl_3$)

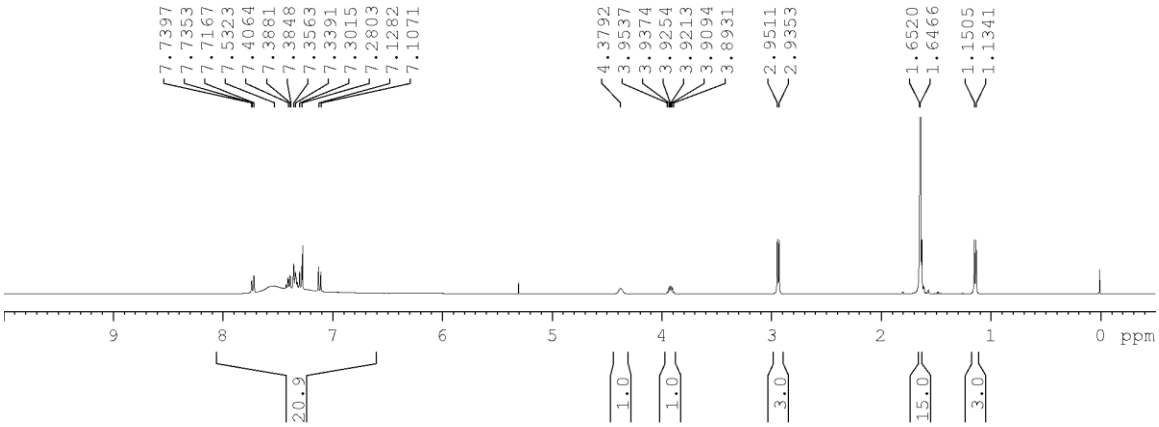

^{13}C NMR spectrum (100 MHz, $CDCl_3$)

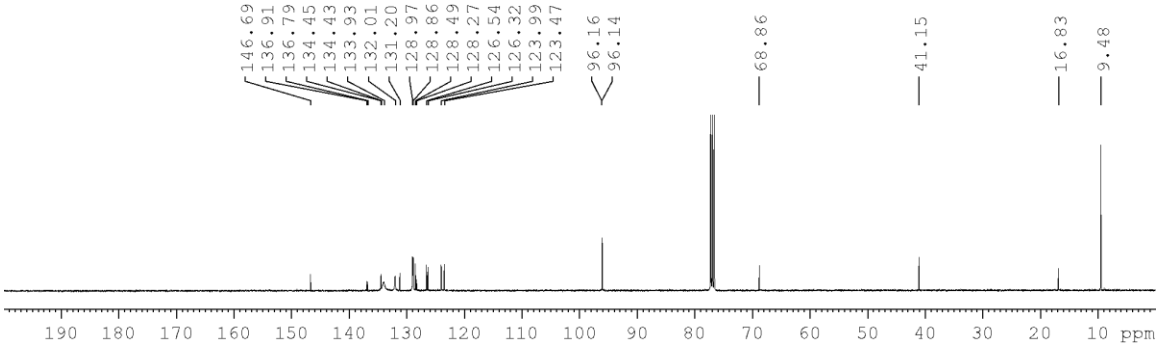

$^{31}P\{^{1}H\}$ NMR spectrum (161 MHz, $CDCl_3$)

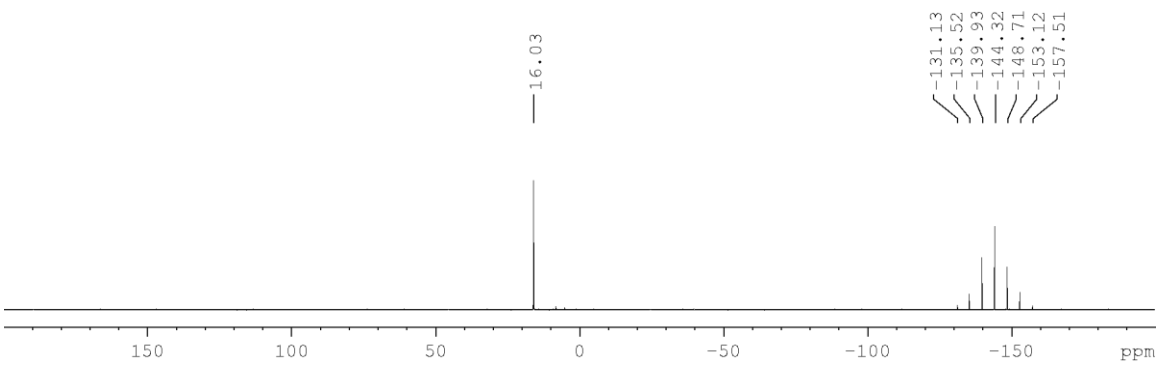

APPENDIX II

Crystallographic Data

The x-ray structural analyses were kindly performed by Dr. Li Yongxin of Nanyang Technological University Division of Chemistry and Biological Chemistry Central Facilities Laboratory. All relevant crystallographic data have been uploaded to the Cambridge Crystallographic Data Center (CCDC) database and are available for download from *www.ccdc.cam.ac.uk/data_request/cif*, or by emailing *data_request@ccdc.cam.ac.uk*.

X-Ray Crystallographic Data for Cycloiridated Complex (R_C,R_N,S_{Ir})-1

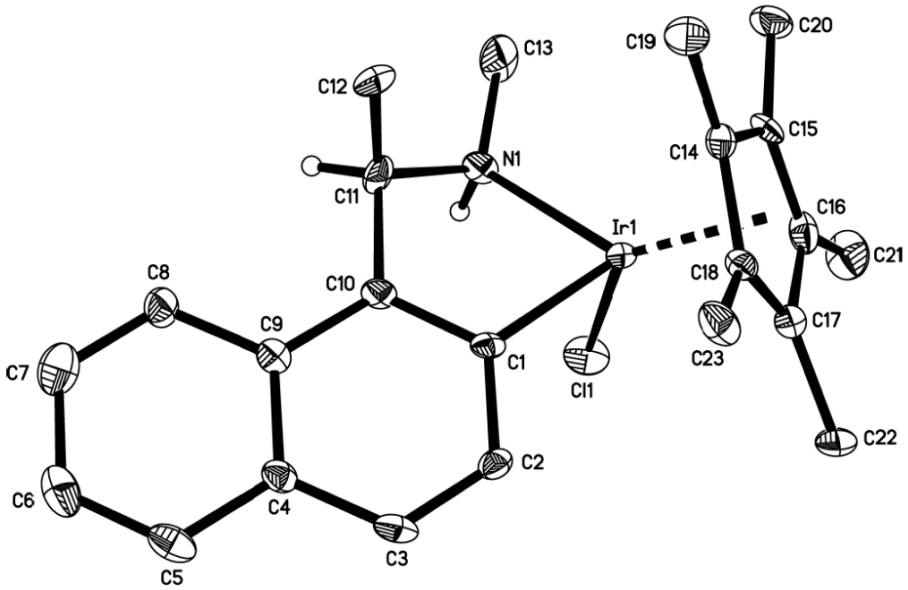

Molecular structure of cycloiridated complex (R_C,R_N,S_{Ir})-**1** with thermal ellipsoids shown at 50% probability. Hydrogen atoms except H(C11) and H(N1) are omitted for clarity.

Depository Number	
CCDC Number	1815863
Crystal Data	
Chemical Formula	$C_{23}H_{29}ClIrN$
Formula Weight (FW), g mol^{-1}	547.12
Crystal System	orthorhombic
Space Group	P 21 21 21
Temperature (K)	103(2)
a,*b*,*c* (Å)	7.8309(9), 18.449(2), 28.858(3)
α,*β*,*γ* (°)	90, 90, 90
V (Å^3)	4169.2(8)
Z	8
F(000)	2144
Radiation Type (Wavelength)	Mo (0.71073 Å)
Absorption Coefficient (mm^{-1})	6.539
Crystal Size (mm)	0.260 × 0.340 × 0.400
Data Collection	
Theta Range for Data Collection	5.10° to 31.08°
Index Ranges	$-8 \le h \le 11$, $-26 \le k \le 22$, $-37 \le l \le 41$
Reflections Collected	35193
Independent Reflections	13198 [R(int) = 0.0516]
T_{min}, T_{max}	0.1800, 0.2810

Refinement	
Refinement Method	Full-matrix least-squares on F^2
Refinement Program	SHELXL-2013 (Sheldrick, 2013)
Function Minimized	$\Sigma\, w(F_o^2 - F_c^2)^2$
No. of Reflections	13198
No. of Restraints	595
No. of Parameters	570
Goodness-of-Fit on F^2	0.986
Δ/σ_{max}	0.004
Final R Indices	11509 data; $I>2\sigma(I)$
	(R1 = 0.0379, wR2 = 0.0626)
	all data
	(R1 = 0.0475, wR2 = 0.0649)
Weighting Scheme	$w = 1 / [\sigma^2(F_o^2) + (0.0120P)^2]$,
	where $P = (F_o^2 + 2F_c^2) / 3$
Absolute Structure Parameter	0.0(0)
r_{max}, r_{min} (e Å^{-3})	2.378, -1.500
R.M.S. Deviation from Mean (e Å^{-3})	0.166

X-Ray Crystallographic Data for Cycloiridated Complex (S_C,S_N,R_{Ir})-1

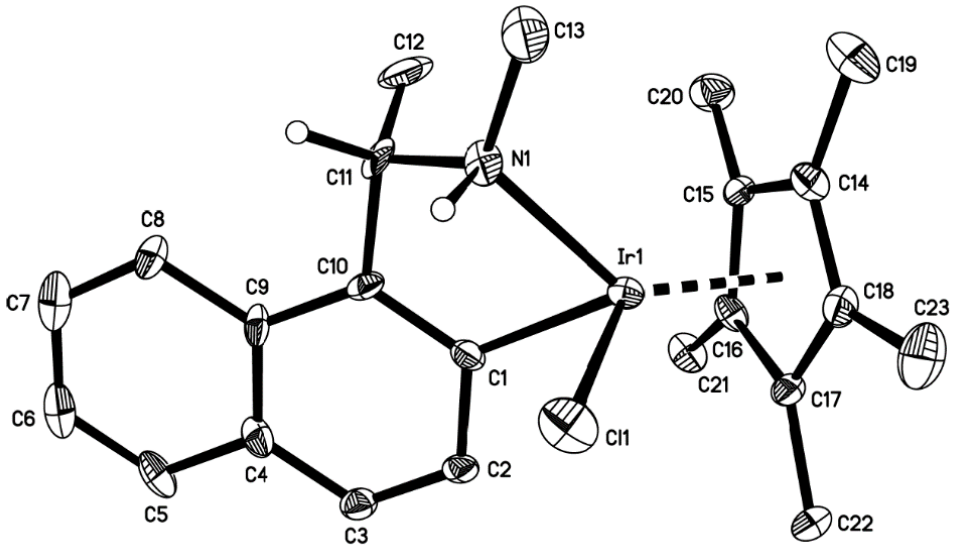

Molecular structure of cycloiridated complex (S_C,S_N,R_{Ir})-**1** with thermal ellipsoids shown at 50% probability. Hydrogen atoms except H(C11) and H(N1) are omitted for clarity.

Depository Number	
CCDC Number	1577410
Crystal Data	
Chemical Formula	$C_{23}H_{29}ClIrN$
Formula Weight (FW), g mol^{-1}	547.12
Crystal System	orthorhombic
Space Group	P 21 21 21
Temperature (K)	103(2)
a,b,c (Å)	7.8215(4), 18.4976(5), 28.7859(13)
α,β,γ (°)	90, 90, 90
V (Å^3)	4164.7(3)
Z	8
F(000)	2144
Radiation Type (Wavelength)	Mo (0.71073 Å)
Absorption Coefficient (mm^{-1})	6.546
Crystal Size (mm)	0.200 × 0.220 × 0.380
Data Collection	
Theta Range for Data Collection	1.79° to 31.11°
Index Ranges	$-10 \le h \le 11$, $-19 \le k \le 26$, $-41 \le l \le 41$
Reflections Collected	40445
Independent Reflections	13341 [R(int) = 0.0989]
T_{min}, T_{max}	0.1900, 0.3540

Refinement	
Refinement Method	Full-matrix least-squares on F^2
Refinement Program	SHELXL-2014/6 (Sheldrick, 2014)
Function Minimized	$\Sigma\, w(F_o^2 - F_c^2)^2$
No. of Reflections	13341
No. of Restraints	932
No. of Parameters	579
Goodness-of-Fit on F^2	0.964
Δ/σ_{max}	0.002
Final R Indices	10877 data; $I>2\sigma(I)$ (R1 = 0.0490, wR2 = 0.0950) all data (R1 = 0.0662, wR2 = 0.1024)
Weighting Scheme	$w = 1 / [\sigma^2(F_o^2)]$, where $P = (F_o^2 + 2F_c^2) / 3$
Absolute Structure Parameter	0.0(0)
r_{max}, r_{min} (e Å^{-3})	1.957, -1.522
R.M.S. Deviation from Mean (e Å^{-3})	0.207

X-Ray Crystallographic Data for Cycloiridated Complex *rac*-4

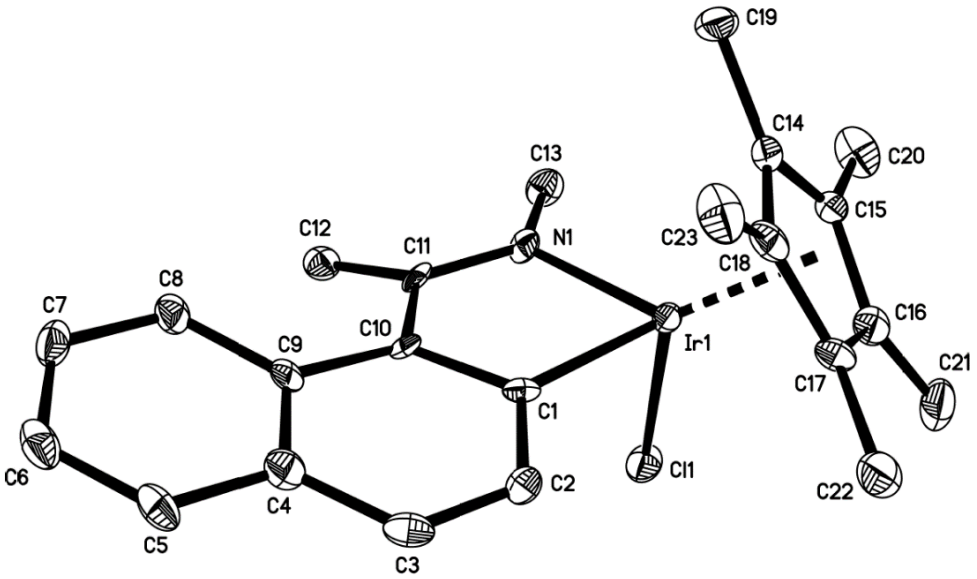

Molecular structure of cycloiridated complex *rac*-**4** with thermal ellipsoids shown at 50% probability. Hydrogen atoms are omitted for clarity.

Depository Number	
CCDC Number	1578300

Crystal Data	
Chemical Formula	$C_{23}H_{27}ClIrN$
Formula Weight (FW), g mol^{-1}	545.10
Crystal System	monoclinic
Space Group	P 1 21 1
Temperature (K)	103(2)
a,*b*,*c* (Å)	8.0397(2), 15.4800(5), 8.1193(2)
α,*β*,*γ* (°)	90, 96.7264(17), 90
V (Å^3)	1003.53(5)
Z	2
F(000)	532
Radiation Type (Wavelength)	Mo (0.71073 Å)
Absorption Coefficient (mm^{-1})	6.792
Crystal Size (mm)	0.020 × 0.220 × 0.320

Data Collection	
Theta Range for Data Collection	2.87° to 30.57°
Index Ranges	$-11 \le h \le 11$, $-22 \le k \le 22$, $-11 \le l \le 11$
Reflections Collected	16928
Independent Reflections	6116 [R(int) = 0.0573]
T_{min}, T_{max}	0.2200, 0.8760

Refinement	
Refinement Method	Full-matrix least-squares on F^2
Refinement Program	SHELXL-2016/6 (Sheldrick, 2016)
Function Minimized	$\Sigma\, w(F_o^2 - F_c^2)^2$
No. of Reflections	6116
No. of Restraints	1
No. of Parameters	243
Goodness-of-Fit on F^2	1.071
Final R Indices	5310 data; $I>2\sigma(I)$ (R1 = 0.0404, wR2 = 0.0688) all data (R1 = 0.0503, wR2 = 0.0713)
Weighting Scheme	$w = 1 / [\sigma^2(F_o^2) + (0.129P)^2 + 0.7736P]$, where $P = (F_o^2 + 2F_c^2) / 3$
r_{max}, r_{min} (e Å^{-3})	1.842, -2.835
R.M.S. Deviation from Mean (e Å^{-3})	0.206

X-Ray Crystallographic Data for Cycloiridated Complex *rac*-5

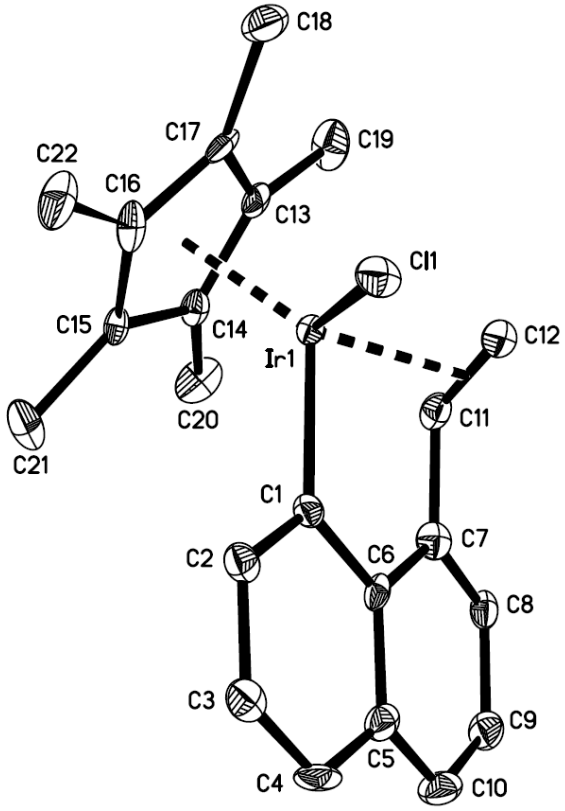

Molecular structure of cycloiridated complex *rac*-**5** with thermal ellipsoids shown at 50% probability. Hydrogen atoms are omitted for clarity.

Depository Number	
CCDC Number	1830655

Crystal Data	
Chemical Formula	$C_{22}H_{24}ClIr$
Formula Weight (FW), g mol^{-1}	516.06
Crystal System	orthorhombic
Space Group	P n a 2 1
Temperature (K)	100(2)
a,b,c (Å)	17.0801(5), 7.2442(2), 14.5460(5)
α,β,γ (°)	90, 90, 90
V (Å^3)	1799.80(10)
Z	4
F(000)	1000
Radiation Type (Wavelength)	Mo (0.71073 Å)
Absorption Coefficient (mm^{-1})	7.567
Crystal Size (mm)	0.060 × 0.080 × 0.100

Data Collection	
Theta Range for Data Collection	2.38° to 34.00°
Index Ranges	$-26 \leq h \leq 26$, $-11 \leq k \leq 11$, $-22 \leq l \leq 22$
Reflections Collected	26362
Independent Reflections	7323 [R(int) = 0.0562]
T_{min}, T_{max}	0.5180, 0.6600

Refinement	
Refinement Method	Full-matrix least-squares on F^2
Refinement Program	SHELXL-2016/6 (Sheldrick, 2016)
Function Minimized	$\Sigma\, w(F_o^2 - F_c^2)^2$
No. of Reflections	7323
No. of Restraints	1
No. of Parameters	223
Goodness-of-Fit on F^2	1.069
Final R Indices	5966 data; $I>2\sigma(I)$
	(R1 = 0.0328, wR2 = 0.0558)
	all data
	(R1 = 0.0490, wR2 = 0.0604)
Weighting Scheme	$w = 1 / [\sigma^2(F_o^2) + 1.6661P]$,
	where $P = (F_o^2 + 2F_c^2) / 3$
r_{max}, r_{min} (e Å^{-3})	1.934, -1.385
R.M.S. Deviation from Mean (e Å^{-3})	0.178

X-Ray Crystallographic Data for Cycloiridated Complex *rac*-7

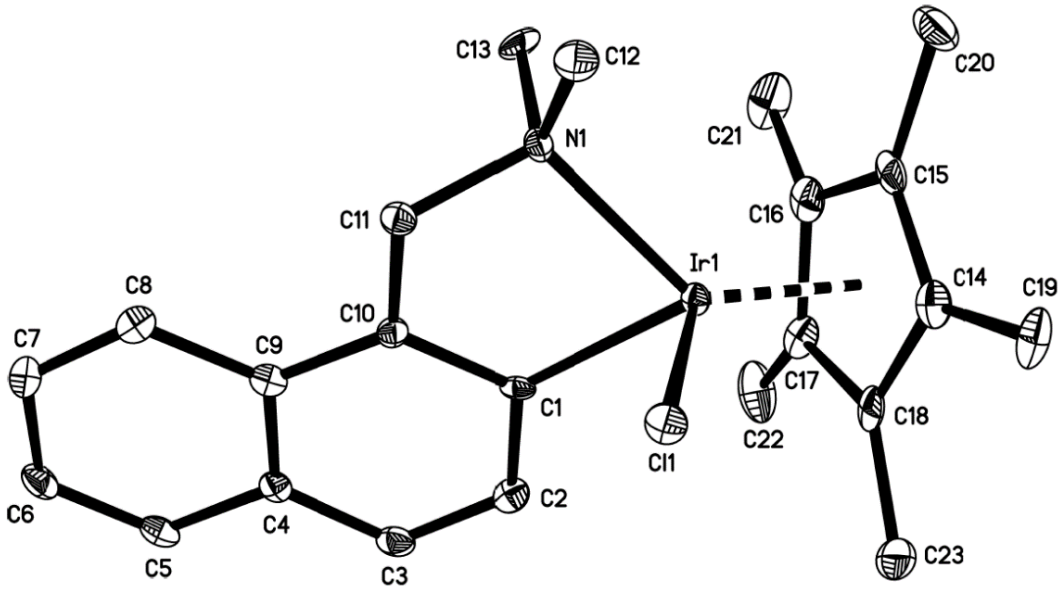

Molecular structure of cycloiridated complex *rac*-**7** with thermal ellipsoids shown at 50% probability. Hydrogen atoms are omitted for clarity.

Depository Number	
CCDC Number	1815864
Crystal Data	
Chemical Formula	$C_{23}H_{29}ClIrN$
Formula Weight (FW), g mol^{-1}	547.12
Crystal System	monoclinic
Space Group	P 1 21 1
Temperature (K)	103(2)
a,b,c (Å)	8.5640(5), 13.4034(8), 9.7175(6)
α,β,γ (°)	90, 114.7655(8), 90
V (Å^3)	1012.85(11)
Z	2
F(000)	536
Radiation Type (Wavelength)	Mo (0.71073 Å)
Absorption Coefficient (mm^{-1})	6.730
Crystal Size (mm)	0.120 × 0.180 × 0.200
Data Collection	
Theta Range for Data Collection	2.76° to 30.50°
Index Ranges	$-12 \le h \le 12$, $-19 \le k \le 19$, $-13 \le l \le 13$
Reflections Collected	5788
T_{min}, T_{max}	0.3460, 0.4990

Refinement	
Refinement Method	Full-matrix least-squares on F^2
Refinement Program	SHELXL-2013 (Sheldrick, 2013)
Function Minimized	$\Sigma\, w(F_o^2 - F_c^2)^2$
No. of Reflections	5788
No. of Restraints	1
No. of Parameters	243
Goodness-of-Fit on F^2	0.894
Final R Indices	5524 data; $I>2\sigma(I)$ (R1 = 0.0253, wR2 = 0.0533) all data (R1 = 0.0267, wR2 = 0.0538)
Weighting Scheme	$w = 1 / [\sigma^2(F_o^2)]$, where $P = (F_o^2 + 2F_c^2) / 3$
r_{max}, r_{min} (e Å^{-3})	1.447, -1.865
R.M.S. Deviation from Mean (e Å^{-3})	0.145

X-Ray Crystallographic Data for Cycloiridated Complex *rac*-9

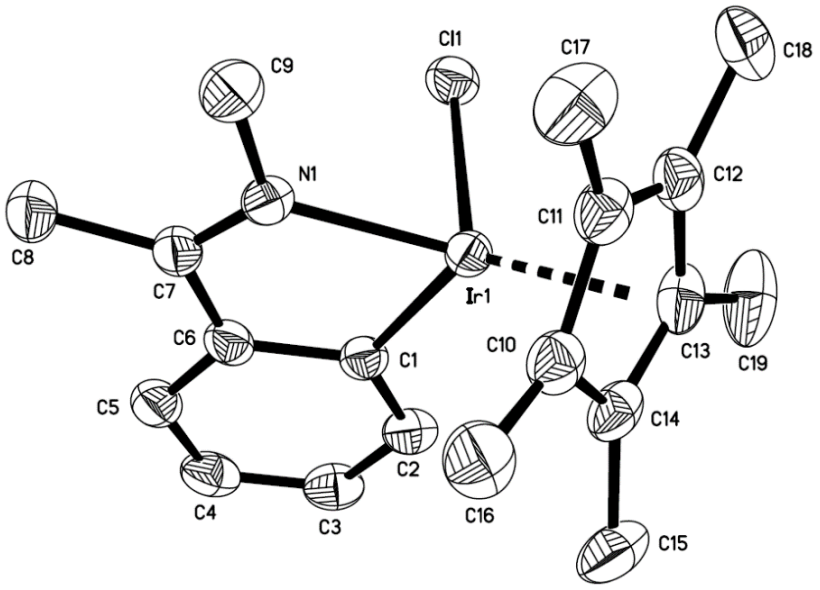

Molecular structure of cycloiridated complex *rac*-**9** with thermal ellipsoids shown at 50% probability. Hydrogen atoms are omitted for clarity.

Depository Number	
CCDC Number	1815868
Crystal Data	
Chemical Formula	$C_{19}H_{25}ClIrN$
Formula Weight (FW), g mol^{-1}	495.05
Crystal System	triclinic
Space Group	P -1
Temperature (K)	100(2)
a,b,c (Å)	7.8549(2), 8.5214(3), 14.1000(4)
α,β,γ (°)	77.7995(12), 77.9991(12), 68.3521(12)
V (Å^3)	848.58(4)
Z	2
F(000)	480
Radiation Type (Wavelength)	Mo (0.71073 Å)
Absorption Coefficient (mm^{-1})	8.021
Crystal Size (mm)	0.060 × 0.120 × 0.220
Data Collection	
Theta Range for Data Collection	2.60° to 29.00°
Index Ranges	$-10 \leq h \leq 10$, $-11 \leq k \leq 11$, $-19 \leq l \leq 19$
Reflections Collected	27663
Independent Reflections	4511 [R(int) = 0.0513]
T_{min}, T_{max}	0.2710, 0.6450

Refinement	
Refinement Method	Full-matrix least-squares on F^2
Refinement Program	SHELXL-2016/6 (Sheldrick, 2016)
Function Minimized	$\Sigma\, w(F_o^2 - F_c^2)^2$
No. of Reflections	4511
No. of Restraints	2
No. of Parameters	206
Goodness-of-Fit on F^2	1.056
Δ/σ_{max}	0.003
Final R Indices	4218 data; $I>2\sigma(I)$ (R1 = 0.0230, wR2 = 0.0549) all data (R1 = 0.0257, wR2 = 0.0563)
Weighting Scheme	$w = 1 / [\sigma^2(F_o^2) + (0.0219P)^2 + 1.2143P]$, where $P = (F_o^2 + 2F_c^2) / 3$
r_{max}, r_{min} (e Å^{-3})	2.587, -0.812
R.M.S. Deviation from Mean (e Å^{-3})	0.120

X-Ray Crystallographic Data for Cycloiridated Complex (S_C,R_{Ir})-11

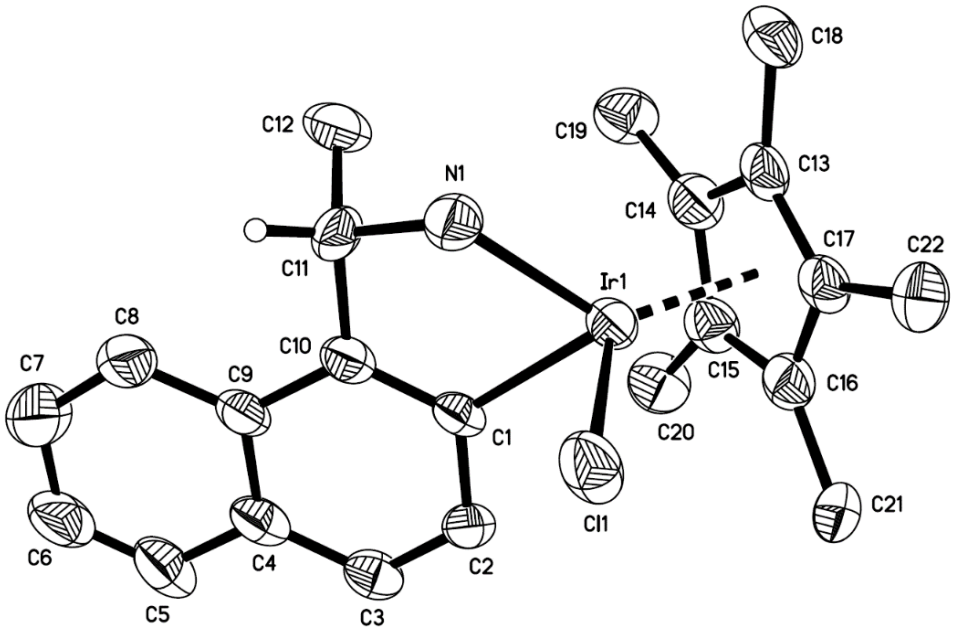

Molecular structure of cycloiridated complex (S_C,R_{Ir})-**11** with thermal ellipsoids shown at 50% probability. Hydrogen atoms except H(C11) are omitted for clarity.

Depository Number	
CCDC Number	1578840

Crystal Data	
Chemical Formula	$C_{22}H_{27}ClIrN$
Formula Weight (FW), g mol^{-1}	533.09
Crystal System	hexagonal
Space Group	P 65
Temperature (K)	103(2)
a,*b*,*c* (Å)	17.2092(4), 17.2092(4), 14.5483(4)
α,*β*,*γ* (°)	90, 90, 120
V (Å^3)	3731.3(2)
Z	6
F(000)	1560
Radiation Type (Wavelength)	Mo (0.71073 Å)
Absorption Coefficient (mm^{-1})	5.478
Crystal Size (mm)	0.240 × 0.200 × 0.040

Data Collection	
Theta Range for Data Collection	2.367° to 31.025°
Index Ranges	$-24 \leq h \leq 24$, $-24 \leq k \leq 20$, $-21 \leq l \leq 21$
Reflections Collected	51041
Independent Reflections	7932 [R(int) = 0.0977]

Refinement	
Refinement Method	Full-matrix least-squares on F^2
No. of Reflections	7932
No. of Restraints	490
No. of Parameters	328
Absorption Correction	None
Goodness-of-Fit on F^2	1.016
Final R Indices	$I>2\sigma(I)$
	(R1 = 0.0436, wR2 = 0.0775)
	all data
	(R1 = 0.0831, wR2 = 0.0897)
Absolute Structure Parameter	0.087(9)
Extinction Coefficient	not applicable
r_{max}, r_{min} (e $Å^{-3}$)	1.010, -1.245

X-Ray Crystallographic Data for Cycloiridated Complex *rac*-13

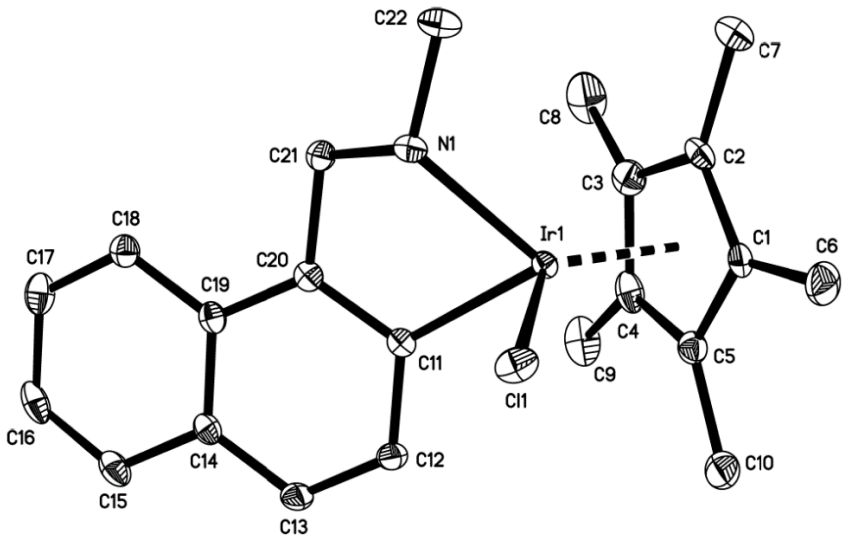

Molecular structure of cycloiridated complex *rac*-**13** with thermal ellipsoids shown at 50% probability. The structure presented in the figure has stereochemistry of *S* and *R* at nitrogen and iridium respectively. Hydrogen atoms are omitted for clarity.

Depository Number	
CCDC Number	1577413

Crystal Data	
Chemical Formula	$C_{22}H_{27}ClIrN$
Formula Weight (FW), g mol^{-1}	533.09
Crystal System	monoclinic
Space Group	C1 2/c 1
Temperature (K)	103(2)
a,*b*,*c* (Å)	35.1113(11), 8.3422(3), 28.2340(9)
α,*β*,*γ* (°)	90, 103.5499(11), 90
V (Å^3)	8039.7(5)
Z	16
F(000)	4160
Radiation Type (Wavelength)	Mo (0.71073 Å)
Absorption Coefficient (mm^{-1})	6.780
Crystal Size (mm)	0.220 × 0.280 × 0.340

Data Collection	
Theta Range for Data Collection	2.51° to 31.05°
Index Ranges	$-32 \le h \le 50$, $-11 \le k \le 12$, $-40 \le l \le 39$
Reflections Collected	62894
Independent Reflections	12843 [R(int) = 0.0484]
T_{min}, T_{max}	0.2060, 0.3170

Refinement	
Refinement Method	Full-matrix least-squares on F^2
Refinement Program	SHELXL-2013 (Sheldrick, 2013)
Function Minimized	$\Sigma\, w(F_o^2 - F_c^2)^2$
No. of Reflections	12843
No. of Restraints	0
No. of Parameters	463
Goodness-of-Fit on F^2	1.138
Δ/σ_{max}	0.004
Final R Indices	11378 data; $I>2\sigma(I)$ (R1 = 0.0336, wR2 = 0.0697) all data (R1 = 0.0415, wR2 = 0.0718)
Weighting Scheme	$w = 1 / [\sigma^2(F_o^2) + (0.0244P)^2 + 39.0991P]$, where $P = (F_o^2 + 2F_c^2) / 3$
r_{max}, r_{min} (e Å^{-3})	3.339, -1.956
R.M.S. Deviation from Mean (e Å^{-3})	0.181

X-Ray Crystallographic Data for Cycloiridated Complex *rac*-14

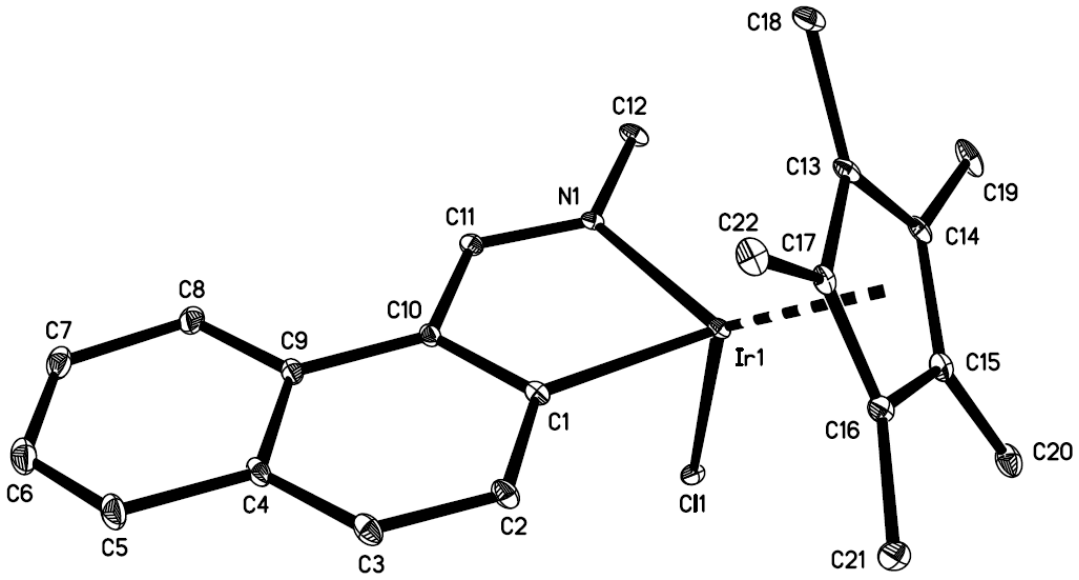

Molecular structure of cycloiridated complex *rac*-**14** with thermal ellipsoids shown at 50% probability. Hydrogen atoms are omitted for clarity.

Depository Number	
CCDC Number	1815867

Crystal Data	
Chemical Formula	$C_{22}H_{25}ClIrN$
Formula Weight (FW), g mol^{-1}	531.08
Crystal System	monoclinic
Space Group	P 1 21/n 1
Temperature (K)	100(2)
a,*b*,*c* (Å)	8.6626(11), 16.239(3), 14.0831(19)
α,*β*,*γ* (°)	90, 96.412(4), 90
V (Å^3)	1968.7(5)
Z	4
F(000)	1032
Radiation Type (Wavelength)	Mo (0.71073 Å)
Absorption Coefficient (mm^{-1})	6.921
Crystal Size (mm)	0.020 × 0.040 × 0.120

Data Collection	
Theta Range for Data Collection	2.68° to 26.42°
Index Ranges	$-10 \le h \le 10$, $-20 \le k \le 20$, $-17 \le l \le 17$
Reflections Collected	25545
Independent Reflections	4039 [R(int) = 0.1559]
T_{min}, T_{max}	0.4910, 0.8740

Refinement	
Refinement Method	Full-matrix least-squares on F^2
Refinement Program	SHELXL-2016/6 (Sheldrick, 2016)
Function Minimized	$\Sigma\, w(F_o^2 - F_c^2)^2$
No. of Reflections	4039
No. of Restraints	336
No. of Parameters	232
Goodness-of-Fit on F^2	1.003
Δ/σ_{max}	0.001
Final R Indices	2716 data; $I>2\sigma(I)$ (R1 = 0.0498, wR2 = 0.0902) all data (R1 = 0.0937, wR2 = 0.1081)
Weighting Scheme	$w = 1 / [\sigma^2(F_o^2) + (0.0313P)^2 + 6.3294P]$, where $P = (F_o^2 + 2F_c^2) / 3$
r_{max}, r_{min} (e Å^{-3})	1.253, -1.264
R.M.S. Deviation from Mean (e Å^{-3})	0.210

X-Ray Crystallographic Data for Cycloiridated Complex *rac*-16

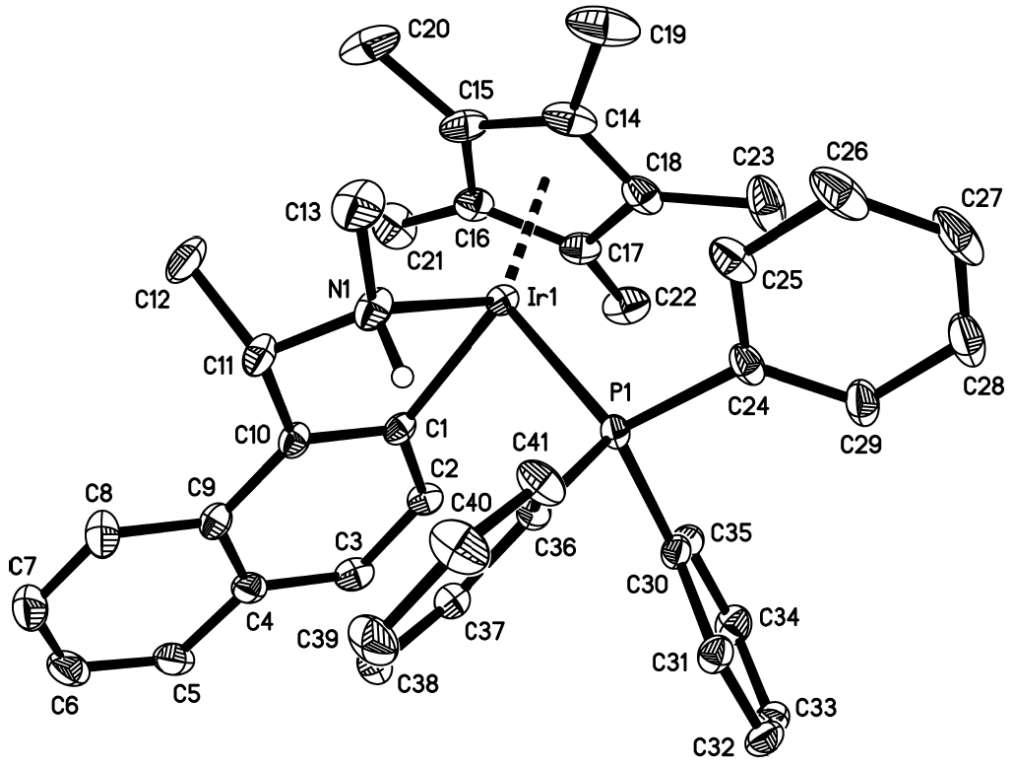

Molecular structure of cycloiridated complex *rac*-**16** with thermal ellipsoids shown at 50% probability. The structure presented in the figure has stereochemistry of *S*, *S* and *R* at carbon, nitrogen and iridium respectively. The hexafluorophosphate anion and hydrogen atoms except H(N1) are omitted for clarity.

Depository Number	
CCDC Number	1577411

Crystal Data	
Chemical Formula	$C_{41}H_{44}IrNP_2$
Formula Weight (FW), g mol^{-1}	918.91
Crystal System	monoclinic
Space Group	P 1 21/n 1
Temperature (K)	103(2)
a,*b*,*c* (Å)	13.0905(8), 16.2793(10), 17.4626(10)
α,*β*,*γ* (°)	90, 98.7763(14), 90
V (Å^3)	3677.8(4)
Z	4
F(000)	1832
Radiation Type (Wavelength)	Mo (0.71073 Å)
Absorption Coefficient (mm^{-1})	3.779
Crystal Size (mm)	0.180 × 0.240 × 0.420

Data Collection	
Theta Range for Data Collection	3.63° to 37.09°
Index Ranges	$-22 \leq h \leq 22$, $-27 \leq k \leq 27$, $-29 \leq l \leq 29$
Reflections Collected	126153
Independent Reflections	18740 [R(int) = 0.1006]
T_{min}, T_{max}	0.3000, 0.5490

Refinement	
Refinement Method	Full-matrix least-squares on F^2
Refinement Program	SHELXL-2014/6 (Sheldrick, 2014)
Function Minimized	$\Sigma\, w(F_o^2 - F_c^2)^2$
No. of Reflections	18740
No. of Restraints	369
No. of Parameters	531
Goodness-of-Fit on F^2	1.003
Δ/σ_{max}	0.001
Final R Indices	13327 data; $I>2\sigma(I)$ (R1 = 0.0394, wR2 = 0.0725) all data (R1 = 0.0730, wR2 = 0.0826)
Weighting Scheme	$w = 1 / [\sigma^2(F_o^2) + (0.0280P)^2 + 2.0506P]$, where $P = (F_o^2 + 2F_c^2) / 3$
r_{max}, r_{min} (e Å^{-3})	2.393, -1.991
R.M.S. Deviation from Mean (e Å^{-3})	0.176